

11th SOLEIL USERS' MEETING

JANUARY 21st and 22nd, 2016

Ecole Polytechnique (Palaiseau) & SOLEIL (Saint-Aubin)



SCIENTIFIC COMMITTEE

d'ANGELO Marie (Institut des Nanosciences de Paris)
BOUDON Vincent (Lab. Interdisciplinaire Carnot
de Bourgogne - Dijon)
BROUTIN Isabelle (Lab. de cristallographie
et RMN biologiques - Paris)
CARMONA TEJERO Noemi (Lab. de Physique des Matériaux,
Université Complutense - Madrid)
DATCHI Frédéric (IMPMC - Paris)
GIRARDON Jean-Sébastien (Unité de Catalyse et
de Chimie du Solide - Lille)
GOHON Yann (Institut Jean-Pierre Bourgin - Versailles)
GUILLON Emmanuel (Institut de Chimie Moléculaire - Reims)
LYONNARD Sandrine (INAC/SPRAM - CEA - Grenoble)
PENENT Francis (Lab. de Chimie Physique Matière et
Rayonnement - Paris)
PROVOST Karine (Institut de Chimie et des Matériaux
de Paris-Est - Thiais)
TEJEDA Antonio (Lab. de Physique des Solides - Orsay)

Satellite Workshop

**Hi-SPEAR: Hi-resolution SPECTroscopy
for Applied Research**

January 19th and 20th, 2016

Information and registration:
www.synchrotron-soleil.fr/Workshop/2016/SUM16





Welcome

The 11th SOLEIL Users' Meeting takes place on January 21st and 22nd, 2016 at Polytechnique (Palaiseau) and at SOLEIL.

The meeting provides an invaluable forum for the synchrotron radiation user community, presenting an important opportunity to obtain the latest information on beamline performance at SOLEIL, to hear about the latest and most exciting results obtained at SOLEIL and to share scientific, technical and practical issues about the synchrotron radiation use. The meeting takes the form of 3 plenary lectures:

- *Biology / Health,*
- *Surfaces / Interfaces*
- *Chemistry*

Technical workshops are organized on the following topics:

- Temporal resolution and dynamics
- Spatial resolution
- Multi beamline Measurements

Half-day parallel sessions in which scientific presentations, selected from submitted abstracts, are presented.

In addition, the draftsman Aurélie Bordenave is present both at Polytechnique and at SOLEIL from 9 am to 7:30 pm. Through her drawings, she gives her vision of the event in a humoristic and unusual way

A social programme with a buffet dinner is organized at SOLEIL on the afternoon of January 21st in conjunction with the poster session, commercial exhibitions and visits of the Facility.

The Roger Fourme Prize awarded to the student best poster will be given on Thursday, January 21st at about 7:30 p.m. just before the buffet dinner.

Bienvenue

Le 11ème Colloque des Utilisateurs de SOLEIL se tiend les jeudi 21 et vendredi 22 janvier 2016, à l'Ecole Polytechnique et à SOLEIL.

Ce rendez-vous incontournable pour la communauté des utilisateurs du rayonnement synchrotron est l'occasion de recueillir les dernières informations sur la machine, sur les performances des lignes, et d'échanger ensemble sur les aspects scientifiques, techniques et pratiques de l'utilisation du synchrotron.

Il est constitué de 3 conférences plénières couvrant différents thèmes de recherche de la communauté des utilisateurs de SOLEIL :

- *Biologie / Santé,*
- *Surfaces / Interfaces*
- *Chimie*

Des ateliers techniques transversaux sont organisés sur les thèmes suivants :

- Résolution temporelle et aspects dynamiques
- Résolution spatiale
- Mesures multi-lignes

Les sessions parallèles sont composées d'exposés scientifiques originaux, sélectionnés à partir de résumés soumis par les participants.

Par ailleurs, la dessinatrice Aurélie Bordenave sera présente sur les sites de Polytechnique et du synchrotron SOLEIL de 9h00 à 19h30. A travers son coup de crayon, elle apportera sa vision de l'évènement de manière et décalée'.

Un temps de convivialité et de discussion est organisé à SOLEIL le jeudi 21 janvier après-midi avec la session posters, les stands d'entreprises, la visite des installations et le buffet d'inoire.

Le Prix Roger Fourme décerné au meilleur poster étudiant sera remis le jeudi 21 janvier vers 19h30 au démarrage du buffet d'inoire.

SOLEIL Users' Meeting 2016

January 21st – 22nd, 2016

École Polytechnique, Palaiseau – France

&

Synchrotron SOLEIL, Saint-Aubin - France

Summary

- Programme
- Plenary Session
- Parallel Sessions:
 - Biology – Health
 - Chemistry & Physico-Chemistry, In Situ Reactivity, Soft Matter
 - Cultural Heritage, Archaeology, Environment, Geosciences
 - Diluted Matter
 - Electronic & Magnetic Property of Matter, Surfaces and Interfaces
 - Matter & Material Properties: Structure, Organization, Characterization, Elaboration
- Technical Workshops
- Posters Session
 - List of Student Posters
 - List of other posters
- List of Commercial Exhibitors
- Companies Advertisements



École Polytechnique, Palaiseau – France
&
Synchrotron SOLEIL, Saint-Aubin - France

Programme

Thursday, January 21st

ECOLE POLYTECHNIQUE – POINCARÉ AUDITORIUM

- 09:00 - 10:00 Registration & coffee
- 10:00 - 10:15 Welcome / Introduction
Antonio Tejeda - *ORGUES Chairperson*
- 10:15 - 10:30 The word of SOLEIL General Director
Jean Daillant
- 10:30 - 10:50 Last improvements of the Machine
Amor Nadji
- 10:50 - 11:20 Scientific highlights and prospective of SOLEIL
Paul Morin / Andy Thompson
- 11:20 - 12:05 Probing carriers and molecules on oxide surfaces by X-ray
Susumu Yamamoto - *Institute for Solid State Physics - University of Tokyo (Japan)*
- 12:05 - 12:50 X-ray spectroscopic studies of biological dinitrogen reduction
Serena DeBeer - *Max Planck Institute (Germany)*
- 12:50 - 14:30 *Lunch*

Transfer to SOLEIL (14h30)



Technical Workshops :

Temporal resolution and dynamics

Auditorium Main Building - SOLEIL

Contributors:

- Marie-Agnès Tordeux : "Storage ring operation modes for time-resolved experiments"
- Claire Laulhé : "Studies on photoinduced sub-ns and sub-ps structural dynamics: pump-probe X-ray diffraction setup at CRISTAL beamline"
- Fausto Sirotti: "Time-resolved experiments with soft x-rays"
- Ferenc Borondics : "Opportunities in dynamics studies on biological systems at the SMIS beamline."

Spatial resolution

Auditorium Reception Building - SOLEIL

Contributors:

15:00 - 16:30

- Clotilde Policar, ENS Paris: "M(CO) compounds imaged at different energies (IR, classical fluorescence, X-fluorescence) and different scales (sub-cellular, tissue)."
- Dominique Bazin, LPS, CNRS, Univ. Paris Sud: "Interest of microbeam for the study of pathological calcifications".
- Delphine Vantelon (Lucia beam line, SOLEIL)
- Andrea Somogyi (Nanoscopium beam line, SOLEIL)

Multi beamline Measurements

Auditorium BLOCH - CEA

Contributors:

- Jean-Paul Itié, SOLEIL
- Amélie Bordage, Univ. Paris Sud
- Charlotte Martineau, Univ. Versailles-Saint Quentin.
- Mathieu Kociak, Univ. Paris Sud

16:30 – 17:00 *Coffee break*

17:00 - 19:30 Posters session / Commercial exhibition / Users' questions Booth

18:00 - 19:30 Visit of DIFFABS, ODE, PSICHE & SMIS Beamlines

19:30 - 21:00 *Buffet / Award of the best student poster*



Friday, January 22nd

9:00 - 11:00 Parallel sessions (see detailed programme here after)

11:00 - 11:30 *Coffee break*

11:30 - 13:00 Parallel sessions (see detailed programme here after)

13:00 - 14:30 *Lunch*

14:30 - 15:15 Structural and functional studies of the translation initiation factor e/alf2
Emmanuelle Schmitt - *Ecole Polytechnique, Palaiseau (France)*

15:15 - 16:15 Synthesis of technical workshops and discussion with SOLEIL management

16:15 - 16:30 Conclusions



Parallel Sessions Schedule

Biology – Health

Chairpersons: Yann GOHON and Isabelle BROUTIN
ECOLE POLYTECHNIQUE – MONGE Auditorium

- 09:00 - 09:30
(25'+5')
- Solution studies of Suppressor of Fused reveal features undetected by crystal structures
Valérie Biou - IBPC, Paris, France
- 09:30 - 09:50
(15'+5')
- New structural insights into the final steps of methanogenesis*
Tristan Wagner - MPI for Terrestrial Microbiology, Marburg, Germany
- 09:50 - 10:10
(15'+5')
- Time-resolved WAXS of swelling and deformation of hydrogel fibers for soft-tissue reconstruction
Laurent Corté - Mines ParisTech, Evry, France
- 10:10 - 10:30
(15'+5')
- Structural and biochemical study of bacterial FIC toxins
Simon Veyron - LBPA, Cachan, France
- 10:30 - 10:50
(15'+5')
- Biomass hydrolysis: A time lapse localization of enzyme and modifications of plant cell walls by autofluorescence and infrared imaging
Marie-Françoise Devaux - BIA, Nantes, France
- 10:50 - 11:10
- Coffee break
- 11:10 - 11:40
(25'+5')
- Synchrotron IR and DUV fluorescent microscopy study of PB1-F2 amyloid structures: From the cell to the animal model
Christophe Chevalier - VIM, Jouy-en-Josas, France
- 11:40 - 12:00
(15'+5')
- Two different centered monoclinic crystals of the E. Coli outer-membrane protein OmpF originate from the same building block
Vincent Chaptal - IBCP, Lyon, France
- 12:00 - 12:20
(15'+5')
- Structural models of intrinsically disordered and calcium-bound folded states of a protein adapted for secretion by SAXS, raman and HDX-MS
Darragh P. O'Brien - Institut Pasteur, Paris, France
- 12:20 - 12:40
(15'+5')
- Chaperoning 5S RNA assembly
Clément Madru - LCRB, Paris, France
- 12:40 - 13:00
(15'+5')
- Coping with polyproline stalling: Structural insights to hypusine-induced protein synthesis by the eukaryotic ribosome
Justine Mailliot - IGBMC, Strasbourg, France



Parallel Sessions Schedule

Chemistry & Physico-Chemistry, In Situ Reactivity, Soft Matter

Chairpersons: Jean-Sébastien GIRARDON and Sandrine LYONNARD
ECOLE POLYTECHNIQUE – BECQUEREL Auditorium

- 09:00 - 09:30
(25'+5')
- Study of the reduction of TiO₂ supported molybdenum oxide catalysts by combining in-situ XANES spectroscopy at K, L_{2,3} edge and DFT calculation
Asma Tougeri - UCCS, Lille, France
- 09:30 - 09:50
(15'+5')
- Oxidation and reactivity of small supported Pt-based nanoparticles under near-ambient pressure exposures to O₂ and CO
Ahmed Naitabdi – LCPMR, Paris, France
- 09:50 - 10:10
(15'+5')
- In situ characterization of hydrogen-evolving cobalt electrocatalysts by X-Ray absorption spectroscopy
Benedikt Lassalle-Kaiser – Synchrotron SOLEIL, Gif-sur-Yvette, France
- 10:10 - 10:30
(15'+5')
- In situ XAS investigations of butene oligomerization under industrially relevant conditions
Joerg Radnick - Leibniz Institute for Catalysis, Rostock, Germany
- 10:30 - 10:50
(15'+5')
- Chemical speciation determined by multivariate curve resolution optimized with alternating least square fitting of quick EXAFS data
Valérie Briois – Synchrotron SOLEIL, Gif-sur-Yvette, France
- 10:50 - 11:10
- Coffee break
- 11:10 - 11:40
(25'+5')
- In-situ SAXS studies of the alignment of colloidal suspensions in electric and magnetic fields
Patrick Davidson - LPS, Orsay, France
- 11:40 - 12:00
(15'+5')
- Colloidal crystal : Correlation between atomic and mesoscopic ordering scale
Nicolas Goubet – MONARIS Paris and LPS, Orsay, France
- 12:00 - 12:20
(15'+5')
- Time resolved infrared spectroelectrochemistry studies at the diffraction limit
Ferenc Borondics - Synchrotron SOLEIL, Gif-sur-Yvette, France
- 12:20 - 12:40
(15'+5')
- 2D inorganic mixed phase templated by organic layer at the air-water interface
Sophie Cantin – LPPI, Cergy-Pontoise, France
- 12:40 - 13:00
(15'+5')
- High resolution spectroscopy of SOCl₂ and its isotopologues: From the microwave to the far-infrared
Anthony Roucou – LPCA, Dunkerque, France



Parallel Sessions Schedule

Cultural heritage, Archaeology, Environment, Geosciences

Chairpersons: Emmanuel GUILLON and Noemi CARMONA-TEJERO
ECOLE POLYTECHNIQUE – SAUVY Auditorium

- 10:00 - 10:30
(25'+5') Metal contaminated soils and phytoremediation
Marie-Pierre Isaure - IPREM, Pau, France
- 10:30 - 10:50
(15'+5') Copper binding to nitrogen functional groups in tomato and wheat root apoplasts
Armand Masion - CEREGE, Aix-en-Provence, France
- 10:50 - 11:10 *Coffee break*
- 11:10 - 11:40
(25'+5') X-ray micro imaging in cultural heritage studies
Koen Janssens - University of Antwerp, Belgium
- 11:40 - 12:00
(15'+5') Development of manganese-rich patinas on the building sandstones from Luneville Castle: From initial bearing phases towards final phases
Laure Gatuingt - LGE, Marne la Vallée, France
- 12:00 - 12:20
(15'+5') The role of microbes in the geochemical cycle of P in lake Pavin
Karim Benzerara - IMPMC, Paris, France



Parallel Sessions Schedule

Diluted Matter

Chairpersons: Vincent BOUDON and Francis PENENT
ECOLE POLYTECHNIQUE – CARNOT Auditorium

- 09:00 - 09:30
 (25'+5') Combining Synchrotron Radiation with low temperature and long optical paths: IR signatures of halogen-containing atmospheric trace molecules
Laurent Manceron - Synchrotron SOLEIL, Gif-sur-Yvette and MONARIS, Paris, France
- 09:30 - 09:50
 (15'+5') Photoelectron diffraction observed in the ionization of the 2a₁ orbital of methane
Saikat Nandi - Synchrotron SOLEIL, Gif-sur-Yvette, France
- 09:50 - 10:10
 (15'+5') Hard X-ray induced multi-step ultrafast dissociation
Oksana Travnikova - LCPMR, Paris, France
- 10:10 - 10:30
 (15'+5') First high-resolution analysis of phosgene ³⁵Cl₂CO and ³⁵Cl³⁷ClCO fundamentals in the 250 - 480 cm⁻¹ spectral region
Moustafa Ndao – LISA, Créteil, France
- 10:30 - 10:50
 (15'+5') Probing the VUV photoionisation of methyl radicals produced in a pyrolysis and a reactor sources
Christian Alcaraz – LCP, Orsay, France
- 10:50 - 11:10
 Coffee break
- 11:10 - 11:40
 (25'+5') Threshold photoelectron spectra (TPES) applied to the OH + propene and OH + isoprene reactions
Jean-Christophe Loison – ISM, Talence, France
- 11:40 - 12:00
 (15'+5') Multiple Photoionization processes of alkali vapors
Jerome Palaudoux - LCPMR, Paris, France
- 12:00 - 12:20
 (15'+5') Frequency analysis of the ν_2 band of SO₂F₂ using the C_{2v} Top Data System
Fadoua Hmida – GSMA, Reims, France and LDMMP, Tunis, Tunisia
- 12:20 - 12:40
 (15'+5') Electron-nuclear dynamics in resonant X-ray Raman scattering of CO molecule
Loïc Journel - LCPMR, Paris, France
- 12:40 - 13:00
 (15'+5') Photoionisation VUV de molécules prébiotiques : Spectroscopie et réactivité
Ayad Bellili – MSME, Marne-la-Vallée, France



Parallel Sessions Schedule

Electronic & Magnetic Property of Matter, Surfaces and Interfaces

Chairpersons: Marie d'ANGELO and Antonio TEJEDA
ECOLE POLYTECHNIQUE – FAURE Auditorium

- 09:00 - 09:30
(25'+5')
- Multimagnetic core-shell nanoparticles: Towards a fine control of the magnetic anisotropy
Vincent Dupuis - *laboratoire PHENIX, Paris, France*
- 09:30 - 09:50
(15'+5')
- Probing magnetization dynamics by time-resolved X-ray holography with extended references
Feodor Y. Ogrin - *School of Physics and Astronomy, Exeter, UK*
- 09:50 - 10:10
(15'+5')
- Symmetry of the Fermi surface and evolution of the electronic structure across the paramagnetic-helimagnetic transition in MnSi/Si(111)
Alessandro Nicolaou - *Synchrotron SOLEIL, Gif-sur-Yvette, France*
- 10:10 - 10:30
(15'+5')
- k dependence of the spin polarization in Mn₅Ge₃/Ge(111) thin films
Waly Ndiaye – *LPMS, Cergy-Pontoise and DSM, IRAMIS,CEA Saclay, Gif-sur-Yvette, France*
- 10:30 - 10:50
(15'+5')
- Calculation of XMCD and XNCD at the K-edge from first principles
Nadejda Mas – *IMPMC, Paris, France*
- 10:50 - 11:10
Coffee break
- 11:10 - 11:40
(25'+5')
- Interfaces between strongly correlated oxides : Controlling charge transfer and induced magnetism by hybridization
Manuel Bibes - *Unité Mixte de Physique CNRS/Thales, Palaiseau, France*
- 11:40 - 12:00
(15'+5')
- Structure and growth mechanisms of silicene layers on silver surfaces
Geoffroy Prevot – *INP, Paris, France*
- 12:00 - 12:20
(15'+5')
- Bandgap and structural periodicities of buffer layer graphene
Maya Narayanan Nair - *Synchrotron SOLEIL, Gif-sur-Yvette, France*
- 12:20 - 12:40
(15'+5')
- Studying chemical bonding between NTCDA and noble metal surfaces by photoelectron spectroscopy and scanning tunneling microscopy
Yong Feng Tong - *Synchrotron SOLEIL, Gif-sur-Yvette and ISMO, Orsay, France*
- 12:40 - 13:00
(15'+5')
- Mueller ellipsometer with Synchrotron light
Enric Garcia-Caurel – *LPICM, Palaiseau, France*



Parallel Sessions Schedule

Matter & Material Properties : Structure, Organization, Characterization, Elaboration

Chairpersons: Frédéric DATCHI and Karine PROVOST
ECOLE POLYTECHNIQUE – POINCARÉ Auditorium

- | | |
|---------------------------|--|
| 09:00 - 09:30
(15'+5') | High pressure single crystal X-ray diffraction on CRISTAL beamline
Jerôme Rouquette – <i>Institut Charles Gerhardt, Montpellier, France</i> |
| 09:30 - 09:50
(15'+5') | Structure of Lu phthalocyanine thin films deposited on Au(111)
Mattia Farronato – <i>INSP, Paris, France</i> |
| 09:50 - 10:10
(15'+5') | High resolution three dimensional structural microscopy by single angle Bragg ptychography
Marc Allain - <i>Institut Fresnel, Marseille, France</i> |
| 10:10 - 10:30
(15'+5') | Effect of myoglobin crowding on the dynamics of water: An infrared study
Sophie Le Caër - <i>LIONS, NIMBE, Gif-sur-Yvette, France</i> |
| 10:30 - 10:50
(15'+5') | Water in carbon nanotubes: the original hydrogen bonds network revealed by infrared spectroscopy
Pascale Launois – <i>LPS, Orsay, France</i> |
| 10:50 - 11:10 | <i>Coffee break</i> |
| 11:10 - 11:40
(25'+5') | Mn ₂ Ru _x Ga - A zero moment half metal that could change spintronic
Karsten Rode - <i>Trinity College, Dublin, Ireland</i> |
| 11:40 - 12:00
(15'+5') | Pressure-induced spin transitions in chiral magnet MnGe
Nicolas Martin - <i>Laboratoire Léon Brillouin, Gif-sur-Yvette, France</i> |
| 12:00 - 12:20
(15'+5') | The photomagnetism of CoFe PBAs nanoparticles investigated by an in situ XAS study
Amélie Bordage – <i>ICMMO, Orsay, France</i> |
| 12:20 - 12:40
(15'+5') | Terahertz spectroscopy study of low energy excitations in Tb ₂ Ti ₂ O ₇
Evan Constable - <i>Institut Néel, Grenoble, France</i> |
| 12:40 - 13:00
(15'+5') | Evidence of charge density wave ability to slide in a 3D metal
Vincent L.R. Jacques – <i>LPS, Orsay, France</i> |

PLENARY SESSION

PLENARY SESSION

21/01/2016

- PT-01 Probing carriers and molecules on oxide surfaces by X-ray
S. Yamamoto
- PT-02 X-ray spectroscopic studies of biological dinitrogen reduction
S. DeBeer

22/01/2016

- PT-03 Structural and functional studies of the translation initiation factor e/alf2
E. Schmitt

Probing Carriers and Molecules on Oxide Surfaces by X-ray

S. Yamamoto

*The Institute for Solid State Physics, The University of Tokyo,
5-1-5, Kashiwanoha, Kashiwa, Chiba, 277-8581, Japan.*

ABSTRACT

Transition-metal oxides exhibit many remarkable physical properties such as superconductivity, ferroelectricity, or large magnetoresistance, resulting from a subtle interplay between the charge, spin, and orbital degrees of freedom. In addition to the fundamental interest in these phenomena, oxides have been playing a central role in many practical applications such as photocatalysis and photovoltaics. The real oxide surfaces in these applications are complex; oxide surfaces are often covered with atoms and molecules, or form heterointerfaces with metal particles or organic materials. Information on the dynamics of carrier and molecules at these complex oxide surfaces is quite limited. In this talk, I will introduce our researches on oxide surfaces which aim to clarify the dynamics of photo-excited carriers and the influence of atomic and molecular adsorption at oxide surfaces using the state-of-the-art X-ray photoelectron spectroscopy (PES) techniques.

First, as an example of intriguing physical properties of oxides surfaces, I will show that the metallization of the insulating SrTiO₃ surface can be induced by the adsorption of atomic hydrogen [1, 2]. Surface metallization of the H-adsorbed SrTiO₃ surface was demonstrated by metallic states observed by angle-resolved PES and an increase of surface conductivity in surface transport measurements.

Secondly, I will describe the time-resolved PES (tr-PES) system developed at SPring-8 BL07LSU [3, 4]. By the pump-probe method using a femtosecond-pulse laser and brilliant soft X-ray, we have studied the dynamics of the photo-excited carriers at various oxide surfaces and interfaces of TiO₂ [5], ZnO [6], C₆₀/TiO₂ [7] after generation of the surface photovoltage. I will discuss the relaxation process of photo-excited carriers at oxide surfaces, and its relation to the activity of oxides in photocatalysis and photovoltaics.

Thirdly, I will introduce our research efforts towards operando spectroscopy. Recently, we have developed ambient-pressure PES (AP-PES) system [8], which allows one to study electronic structures and chemical states of adsorbate and substrate under gas atmosphere. Examples of AP-XPS studies on oxide surfaces and future development of AP-XPS system will be given.

REFERENCES

1. M. D'Angelo, R. Yukawa, K. Ozawa, S. Yamamoto, T. Hirahara, S. Hasegawa, M.G. Silly, F. Sirotti, I. Matsuda, *Phys. Rev. Lett.* **108**, 116802 (2012).
2. R. Yukawa, S. Yamamoto, K. Ozawa, M. D'Angelo, M.G. Silly, F. Sirotti, I. Matsuda, *Phys. Rev. B* **87**, 115314 (2013).
3. S. Yamamoto, I. Matsuda, *J. Phys. Soc. Jpn.* **82**, 021003 (2013).
4. M. Ogawa, S. Yamamoto, Y. Kousa, F. Nakamura, R. Yukawa, A. Fukushima, A. Harasawa, H. Kondoh, Y. Tanaka, A. Kakizaki, I. Matsuda, *Rev. Sci. Instrum.* **83**, 023109 (2012).
5. K. Ozawa, M. Emori, S. Yamamoto, R. Yukawa, Sh. Yamamoto, R. Hobara, K. Fujikawa, H. Sakama, I. Matsuda, *J. Phys. Chem. Lett.* **5**, 1953-1957 (2014).
6. R. Yukawa, S. Yamamoto, K. Ozawa, M. Emori, M. Ogawa, Sh. Yamamoto, K. Fujikawa, R. Hobara, S. Kitagawa, H. Daimon, H. Sakama, I. Matsuda, *Appl. Phys. Lett.* **105**, 151602 (2014).
7. K. Ozawa, S. Yamamoto, R. Yukawa, K. Akikubo, M. Emori, H. Sakama, I. Matsuda, submitted (2015).
8. T. Koitaya, S. Yamamoto, Y. Shiozawa, K. Takeuchi, R.-Y. Liu, K. Mukai, S. Yoshimoto, K. Akikubo, I. Matsuda, J. Yoshinobu, *Topics in Catalysis*, in press (2016).

X-ray Spectroscopic Studies of Biological Dinitrogen Reduction

S. DeBeer

*Max Planck Institute for Chemical Energy Conversion,
Stiftstr. 34-36, 45470 Mülheim an der Ruhr, Germany*

serena.debeer@cec.mpg.de

ABSTRACT

The conversion of dinitrogen to ammonia is a challenging, energy intensive process, which is enabled biologically by the nitrogenase family of enzymes. By far the most studied nitrogenases are the Mo-dependent forms, which contain a $\text{MoFe}_7\text{S}_9\text{C}$ cluster, the so-called FeMoco active site, where N_2 to NH_3 conversion occurs. The presence of a central carbon in this cluster was revealed by a combination of valence-to-core X-ray emission spectroscopy (VtC XES), high-resolution crystallography and pulsed EPR methods. However, numerous questions about the electronic structure of this cluster and how it enables such remarkable reactivity remain. Herein, a brief overview of the recent contributions of X-ray spectroscopy to our understanding of biological nitrogen reduction will be given. This will include high-resolution Mo X-ray absorption (XAS) studies, which have revealed the presence of an unusual spin-coupled Mo(III) site in the FeMoco cluster. In addition, Mössbauer and high-resolution Fe XAS studies, which have been used to establish the oxidation state distribution of the iron atoms will be presented. Finally, very recent VtC XES and high-resolution Fe XAS studies of the vanadium-dependent nitrogenases will be presented. While the molybdenum-dependent forms of the enzymes are far better nitrogenases, the vanadium-dependent enzymes have been shown to effectively enable carbon-carbon bond coupling. The differences in the FeMoco and FeVco electronic structures will be discussed, with an emphasis on the potential role of the heterometal in modifying the enzymatic selectivity.

Structural and Functional Studies of the Translation Initiation Factor e/alf2

E. Schmitt, P-D. Coureux, E. Dubiez, A. Monestier, M. Panvert,
C. Lazennec-Schurdevin and Y. Mechulam

*Laboratoire de Biochimie, Unité mixte de Recherche 7654, Ecole Polytechnique,
Centre National de la Recherche Scientifique, F-91128 Palaiseau cedex, France*

ABSTRACT

Translation of messenger RNAs (mRNAs) into proteins is a key step in decoding genetic information. This allows a four-letter code to be translated into a twenty-letter code, the amino acids that make up proteins. Many studies have recently shown that initiation of translation is a critical step in controlling many cellular processes, i.e. response to nutrient deprivation, cell differentiation, synaptic response or even cancer. Understanding the molecular mechanisms that govern this step is therefore of particular importance for both basic biology and its therapeutic applications.

Eukaryotic and archaeal translation initiation complexes have in common a functional core containing mRNA, the ternary initiation complex (e/alf2, GTP, Met-tRNA_i^{Met}), e/alf1 and e/alf1A bound to the small ribosomal subunit. In eukaryotes, the functional core is made more complex by many additional factors, most of them being involved in a long-range scanning of mRNA, necessary to decipher the initiation codon. In archaea, long-range scanning does not occur thanks to the occurrence of Shine-Dalgarno sequences or of very short 5' untranslated regions on mRNA. Concomitantly, archaeal translation initiation only requires the core complexes. Within the core complex, e/alf2, in its GTP-bound form, is responsible for selecting the methionylated initiator tRNA and bringing it to the small ribosomal subunit. The establishment of the connection between the start codon on the mRNA and the anticodon of the initiator tRNA is also coupled to the release of one molecule of phosphate resulting from the hydrolysis of GTP bound to eIF2. The function of the e/alf2 protein in eukaryotes and archaea is therefore a key to translation initiation. We have been studying factor e/alf2 for the last few years. In particular, using eukaryotic or archaeal versions of this factor, many data have been accumulated to help understand how it operates. Finally, using purified versions of the archaeal translation initiation complexes, we recently solved the structure of two stages of archaeal translation initiation by Cryo-EM. The two snapshots highlight a new network of interactions crucial for translation initiation in archaea. According to the conservation of the core complex in eukaryotes, this network of interactions is also anticipated to be relevant for the eukaryotic translation initiation process.

PARALLEL SESSIONS

PARALLEL SESSION

Biology - Health

ECOLE POLYTECHNIQUE – MONGE Auditorium

Chairpersons: Yann GOHON and Isabelle BROUTIN

- IT-01 Solution studies of Suppressor of Fused reveal features undetected by crystal structures
V. Biou
- OC-01 New structural insights into the final steps of methanogenesis
T. Wagner
- OC-02 Time-resolved WAXS of swelling and deformation of hydrogel fibers for soft-tissue reconstruction
L. Corté
- OC-03 Structural and biochemical study of bacterial FIC toxins
S. Veyron
- OC-04 Biomass hydrolysis: A time lapse localization of enzyme and modifications of plant cell walls by autofluorescence and infrared imaging
M-F. Devaux
- IT-02 Synchrotron IR and DUV fluorescent microscopy study of PB1-F2 amyloid structures: From the cell to the animal model
C. Chevalier
- OC-05 Two different centered monoclinic crystals of the E. Coli outer-membrane protein OmpF originate from the same building block
V. Chaptal
- OC-06 Structural models of intrinsically disordered and calcium-bound folded states of a protein adapted for secretion by SAXS, raman and HDX-MS
D.P. O'Brien
- OC-07 Chaperoning 5S RNA assembly
C. Madru
- OC-08 Coping with polyproline stalling: Structural insights to hypusine-induced protein synthesis by the eukaryotic ribosome
J. Mailliot

Solution Studies of Suppressor of Fused Reveal Features Undetected by Crystal Structures

S. Makamte & V. Biou

*Laboratoire de Biologie Physico-Chimique des Protéines Membranaires
UMR 7099 CNRS/Univ. Paris Diderot P7, Institut de Biologie Physico-Chimique
13 rue Pierre et Marie Curie, 75005 Paris - France*

ABSTRACT

Suppressor of Fused (SUFU) is a highly conserved protein that acts as a negative regulator of the Hedgehog signalling pathway, a major determinant of cell differentiation and proliferation. Therefore, SUFU deletion in mammals has devastating effects on embryo development. SUFU is part of a multi-protein cytoplasmic signal-transducing complex. Its partners include the Gli family of transcription factors that function either as a repressor, or as a transcription activator, according to the HH activation state. Moreover, SUFU removal has very contrasted effects. In drosophila, it is almost featureless, whereas SUFU deficient mice die before birth. The crystal structure of SUFU [1, 2] revealed a two-domain arrangement, which undergoes a closing movement upon binding a peptide from Gli1.

There remains however, much to be discovered about SUFU's behaviour. To this end, we expressed recombinant, full-length SUFU from drosophila, Zebrafish and human, and characterised them using Synchrotron Radiation Circular Dichroism and Small angle X-ray scattering combined with molecular modelling simulations. We have disclosed structural differences between human, zebrafish and drosophila proteins that may be relevant to their phenotypic differences.

Furthermore, sequence analysis revealed a conserved metal binding site, and we discovered that SUFU binds zinc. This binding was found to occur with a nanomolar affinity to SUFU from all three species. Molecular modelling supports this finding, showing that the conserved site can indeed accommodate a zinc ion. Together, these results reveal new structural and metal binding affinity characteristics about SUFU that could be of importance for its regulatory function in HH.

REFERENCES

- [1] A.L. Cherry, C. Finta, M. Karlstrom, Q. Jin, T. Schwend, J. Astorga-Wells, R.A. Zubarev, M. Del Campo, A.R. Criswell, D. de Sanctis, L. Jovine, R. Toftgard, Structural basis of SUFU-GLI interaction in human Hedgehog signalling regulation, *Acta Crystallographica Section D* 69 (2013) 2563-2579.
- [2] Y. Zhang, L. Fu, X. Qi, Z. Zhang, Y. Xia, J. Jia, J. Jiang, Y. Zhao, G. Wu, Structural insight into the mutual recognition and regulation between Suppressor of Fused and Gli/Ci, *Nat Commun* 4 (2013) 2608.

New Structural Insights into the Final Steps of Methanogenesis

T. Wagner¹, J. Kahnt¹, U. Ermler², S. Shima¹

¹MPI für terrestrische Mikrobiologie, Karl-von-Frisch-Straße Marburg

²MPI für biophysik, Max-von-Laue-Straße 3, Frankfurt am Main

ABSTRACT

Global warming threat stimulates research about methane releasing in the atmosphere. Since half of the global methane amount comes from the methanogens, we have to understand at the molecular level how these archaea are able to produce methane (1).

The last reaction of methanogenesis is catalyzed by methyl-coenzyme M reductase which uses methyl-Coenzyme M (CH₃-S-CoM) and Coenzyme B (HS-CoB) as substrates to release methane and forms heterodisulfide (CoM-S-S-CoB). The enzyme required Nickel containing cofactor F₄₃₀ and several post-translational modifications (e.g. thioglycine). MCR I isoenzyme has already been characterized (2) but the MCR II isoenzyme, which is upregulated in exponential phase, is still structurally unknown (3). We obtained the structure and observed some features defining MCR II class: an extra helix extension in the C-terminus of gamma subunit and a reorganization of the charge distribution. Most importantly, we discovered a new post-translational modification close to the active site, a didehydroaspartate. We confirm this modification by mass spectrometry and observed in the atomic structure of MCR I, which indicated that didehydroaspartate is common to MCR isoenzymes in this organism. Although this modification has already been described in antibiotic (4), this is first time a didehydroaspartate is discovered in a protein.

In the second part of the presentation, we will present the recycling step of methanogenesis (5). The CoM-S-S-CoB produced by MCR has to be regenerated by the hydrogenase/heterodisulfide reductase complex (Hdr/Mvh). The complex is using electrons from H₂ to reduce the heterodisulfide and in the same time, reduce ferredoxin to furnish electrons for the first reaction of methanogenesis. Reduction of ferredoxin with H₂ would be impossible without a chemical trick (6): the flavin based electron bifurcation. Hydrogenase transfers the electrons from H₂ (E⁰ = -414 mV) to the flavin; the reduced flavin can deliver one electron for the heterodisulfide reductase reaction (E⁰ = -140 mV). Then the semi-quinone flavin got enough reducing power to transfer the second electron to ferredoxin (E⁰ = -500 mV). We purified native Hdr/Mvh complex from five different methanogens and obtained low diffracting crystals for one of them. Thanks to crystal averaging, high symmetry and strong anomalous signals from iron-sulfur clusters, we obtained the first experimental map at 5.0 Å. Most of the subunits have been identified in the electron map and the first model of a dimer of heterohexamer has been build.

REFERENCES

1. R.K. Thauer, A.K. Kaster, H. Seedorf, W. Buckel and R. Hedderich, *Nat. Rev. Microbiol.*, 2008, pp. 579-91.
2. U. Ermler, W. Grabarse, S. Shima, M. Goubeaud and R.K. Thauer, *Science*, 1997, pp. 1457-62.
3. L. G. Bonacker, S. Baudner, R.K. Thauer, *Eur. J. Biochem.*, 1992, pp. 87-92.
4. J.S. Grimley, A.M. Sawayama, H. Tanaka, M.M. Stohlmeyer, T.F. Woiwode, T.J. Wandless, *Angew. Chem. Int. Ed. Engl.*, 2007, pp. 8157-9.
5. R.K. Thauer, *Proc. Natl. Acad. Sci.*, 2012, pp. 15084-5
6. W. Buckel and R.K. Thauer, *Biochim. Biophys. Acta.*, 2012, pp. 94-113

Time-resolved WAXS of Swelling and Deformation of Hydrogel Fibers for Soft-tissue Reconstruction

J. Caroux^{1,2}, D. Moreau^{1,2}, S.Tencé-Girault², C. Mocuta³,
H. Proudhon^{1,3} and L. Corté^{1,2}

1. MINES ParisTech, PSL Research University, MAT - Centre des matériaux, CNRS UMR 7633, BP 87 91003 Evry, France

2. ESPCI ParisTech, PSL Research University, Laboratoire Matière Molle et Chimie, CNRS UMR 7167, 10 rue Vauquelin 75005 Paris, France

3. Synchrotron soleil, L'Orme des Merisiers, BP 48, 91192 Gif sur Yvette, France

ABSTRACT

Ligament ruptures are frequent injuries that require a surgical reconstruction using an autograft from a tendon sample. The use of an artificial substitute could alleviate several drawbacks of these autograft reconstructions¹. Implants have recently been designed from biocompatible hydrogel fibers that mimic closely the mechanical behavior of native ligaments.² Like for dry polymer fibers, the properties of these hydrogel fibers are strongly determined by the macromolecular organization. How is it affected upon water swelling and how can it be tuned? These are key questions to address to design fibers with suitable performances for tissue repair. Here, we devised WAXS experiments to quantify, in a time-resolved manner, the effect of deformation and water swelling on the macromolecular organization of one single hydrogel fiber, which has never been done hitherto.

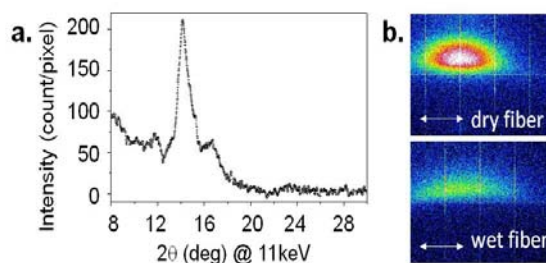


Fig. 1: WAXS measurements of single PVA fibers. **(a)** Diffraction profile along the normal of the fiber axis obtained on DiffAbs beamline ($E = 11$ keV) before swelling (3 seconds acquisition time). **(b)** 2D-WAXS showing the changes in the shape and intensity of the main peak from dry to wet (6 min. swelling time). Vertical direction is 2θ increasing going upward. Arrows indicate the fiber axis. (Same linear color scale)

The studied hydrogel fibers are composed of a water swollen network of PVA macromolecules that are cross-linked through the formation of crystallites.^{3,4} Most of the material characteristics can be inferred from the density, size and orientation of these crystallites. Thanks to the good collimation and the high photon flux of synchrotron beam, we measured these quantities in a time of the order of the second, despite the small scattering volume and the strong X-ray absorption by water. By this mean, we could follow the evolution of the macromolecular network during swelling or deformation of individual fibers.

REFERENCES

1. J. S. Bach, M. Cherkaoui, L. Corté, S. Cantournet and D. N. Ku, *Journal of Medical Devices* **6**, 045004 (2012).
2. J. S. Bach, F. Detrez, M. Cherkaoui, D. N. Ku and L. Corté, *Journal of Biomechanics* **46**, 1463-1470 (2013).
3. C. M. Hassan and N. A. Peppas. *Adv. Polym. Sci.* **153**, 37-64 (2000).
4. R. Ricciardi, F. Auriemma, C. De Rosa and F. Lauprêtre, *Macromolecules* **37**, 1921-1927(2004).

Structural and Biochemical Study of Bacterial FIC Toxins

S. Veyron¹, C.R. Roy², J. Cherfils¹

¹*Laboratoire de Biologie et de Pharmacologie Appliquée, Ecole Normale Supérieure,
CNRS, Cachan, France,*

²*Department of Microbial Pathogenesis, Yale University School of Medicine, New Haven, CT, USA*

ABSTRACT

FIC proteins are widespread in bacteria. They are characterized by a structurally conserved FIC domain, which carries a conserved motif that catalyzes the post-translational modification of target proteins with phosphate-containing groups as diverse as AMP or phosphocholine [1].

AnkX, a type IV effector from the *Legionella pneumophila* pathogen, is a member of the FIC family involved in pathogenesis [2]. It is comprised of a FIC domain, an ankyrin repeats domain and a C-terminal domain unrelated to any known structural domain. AnkX catalyzes the post-translational modification of small GTPases of the Rab subfamily by phosphocholine, which contributes to rewire cellular traffic in the infected host cell [2]. The structure of a truncated AnkX construct has been solved in our laboratory in the presence of CDP-choline, which partially uncovered the catalytic mechanism [3].

I will present our recent results that have focused on understanding how AnkX recognizes Rab proteins at the membrane interface, notably by using various AnkX constructs, peptides and artificial membranes.

This work was also extended to a FIC protein from another bacterial pathogen, in which we are investigating mechanisms of regulation.

REFERENCES

1. C. R. Roy and J. Cherfils, *Nat Rev Microbiol.* **10**, 631-40 (2015).
2. Mukherjee *et al.*, *Nature* **477**, 103-106 (2011).
3. Campanacci *et al.*, *EMBO J.* **32**, 1469-77 (2013).

Biomass Hydrolysis: A Time Lapse Localization of Enzyme and Modifications of Plant Cell Walls by Autofluorescence and Infrared Imaging

M-F. Devaux¹, F. Jamme², W. André², E. Bonnin¹, B. Bouchet¹,
C. Alvarado¹, S. Durand¹, P. Robert¹, L. Saulnier¹, F. Guillon¹

¹ UR1268 BIA. INRA Nantes. BP 71627. 44316 Nantes Cedex 03

² Synchrotron SOLEIL, BP 48 F- 91192 Gif-sur-Yvette.

ABSTRACT

The enzymatic conversion of lignocellulosic materials for the production of fine and bulk chemicals in place of the petroleum feedstock is a very promising approach due to high enzyme selectivity and mild use conditions. However, the complex architecture of plant cell walls makes them very resistant to degradation. Synchrotron SOLEIL facilities were used to follow simultaneously enzymes and changes in cell wall composition in maize stem during degradation by a cellulase cocktail.

Time-lapse multispectral autofluorescence imaging was performed at the DISCO beamline in the deep UV (Exc: 275 nm). Enzymes were localised by collecting autofluorescence of tryptophan between 320 and 350 nm and cell walls were observed by collecting autofluorescence of phenolic compounds in a separate channel between 420 and 480 nm¹ (Fig. 1). The biochemical evolution of polysaccharides in cell walls was followed by recording time lapse FT-IR spectra using the microfluidic device developed at the SMIS beamline².

Differences between cell types were evidenced (Fig. 1). Enzymes were excluded from sclerenchyma cell walls that were consequently not degraded. In degraded parenchyma, enzymes were concentrated on the cell walls. A separation between adjacent cells followed by a complete degradation of cell walls was observed. A huge heterogeneity was observed between and within cell types. The relation between this heterogeneity and the global degradation of maize stem cell walls will help to understand the resistance to degradation.

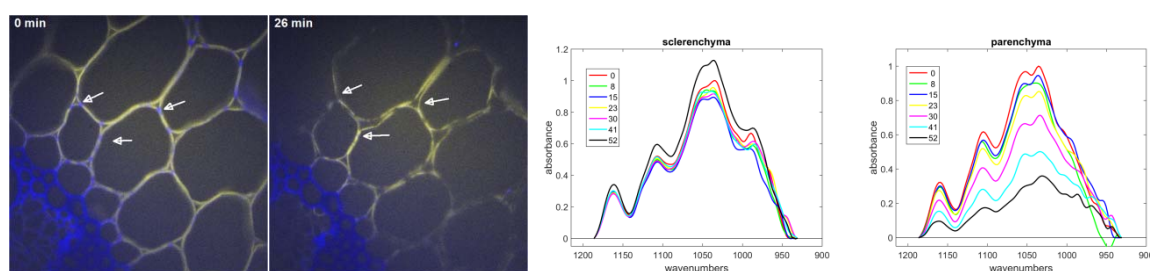


Fig. 1: Sclerenchyma and parenchyma cells. Multispectral autofluorescence images. Blue: cell wall fluorescence alone, white: enzymes + cell walls. Field of view: 320 x 320 μm^2 . Time-lapse FT-IR spectra. Sugar region: 1200-945 cm^{-1} . Left: recalcitrant sclerenchyma, right: degraded parenchyma

REFERENCES

1. F. Jamme, S. Kascakova, S. Villette, F. Allouche, S. Pallu, V. Rouam, M. Réfrégiers. *Biol. Cell*, **105**, 277-88 (2013).
2. C. Sandt, J. Frederick, P. Dumas. *J Biophotonics*, **6**, 60-72 (2013).

Synchrotron IR and DUV Fluorescent Microscopy Study of PB1-F2 Amyloid Structures: From the Cell to the Animal Model

C. Chevalier^{1*}, R. Le Goffic¹, F. Jamme², O. Leymarie¹,
M. Réfrégiers², B. Delmas¹

¹ *Unité de Virologie et Immunologie Moléculaires, EQUIPE INFLUENZA, UR 892 INRA,
UNIVERSITE PARIS-SACLAY, Jouy-en-Josas, France*

² *DISCO and SMIS Beamline, Synchrotron SOLEIL, L'Orme des Merisiers, Saint-Aubin, Gif-sur-Yvette, France*

ABSTRACT

Influenza A viruses (IAV) are responsible every year of seasonal epidemics resulting in considerable illness, death and important economic loss¹. IAV represent also a major pathogen of animals and cause devastating outbreaks in domestic poultry and massive culling in order to control the spread of the virus. Discovered in 2001, PB1-F2 is an accessory protein of the IAV, considered as a factor of virulence². PB1-F2 is a small protein of 87-90 a.a presenting a strong polymorphism in sequence and length depending on the viral strain³. First described as a proapoptotic protein targeting mitochondria, the function of PB1-F2 during the viral cycle is far to be elucidated yet. PB1-F2 has no structure in aqueous solution but is capable to change of conformation depending on the hydrophobicity of the environment from alpha helical conformation to beta sheet secondary structure. Moreover, PB1-F2 has a strong propensity to oligomerizes and form amyloid fibers⁶ in IAV-infected cells. In previous works, we developed biosensors to determine the kinetics of expression and oligomerization of PB1-F2 during the viral cycle using specific antibodies^{7,8,9}. We evidenced the presence of PB1-F2 soluble oligomers in a time and cell-dependent fashion. However, the putative role of the PB1-F2 beta aggregates (fibers and oligomers) in the virus cycle remains unclear and new techniques were needed to detect them properly in the viral context. In the present study, we evidenced the presence of PB1-F2 beta-aggregates in IAV-infected cells at the single cell level using synchrotron radiation. Fourier-transform infrared (FT-IR) and deep UV (DUV) microscopy are non-invasive techniques for monitoring biochemical changes in situ in cells and tissues. Human epithelial pulmonary cells (A549) and monocytic cells (U937) were infected with a wild-type IAV and its PB1-F2 knock-out mutant and harvested at different time post-infection. Infrared spectra were recorded in each condition, then compiled and processed to evaluate the change in the component band of the spectra corresponding to the amide I band (secondary structure changes) and the CH band (membranes and lipids). The data obtained were analyzed by component principal analysis (CPA) and confirmed the presence of an infrared specific beta aggregates signature only in IAV-infected cells expressing PB1-F2. Moreover, the detection of the fibers differs concerning epithelial and monocytic cells in a time-dependent fashion, confirming our previous observation. Taking advantage of the high frequency of tryptophan residues in the sequence of PB1-F2, we were able to correlate the increase of the auto-fluorescent signal recorded by DUV microscopy with the formation and the accumulation of the beta aggregates in IAV-infected cells. Furthermore, we also observed that PB1-F2 compromise the integrity of the cellular membranes in a cell-type dependent manner. Finally, we used the approach successfully developed at the single cells level in order to study the presence of such PB1-F2 amyloids in slices of lung tissues of IAV-infected mice. These combined studies should give us further insight into the structure-function relationship of PB1-F2 and to decipher its role in the pathogenicity of the virus.

REFERENCES

1. WHO (2014) Influenza GISR [internet]: http://www.who.int/influenza/gisrs_laboratory/en/.
2. W. Chen and PA Calvo, *Nat Med.* **7**, 1306-1312 (2001).
3. G Parisha and AC Mishra, *Influenza Other Respir Viruses.* **7**, 497-505.
4. O Leymarie and G Jouvion, *Plos One.* **8**, e57894.
5. R Le Goffic and O Leymarie, *Plos Pathogen.* **7**, e1002202.
6. C Chevalier and A Al Bazzal, *J Biol Chem.* **285**, 13233-13243.
7. J Vidc and R Le Goffic, *J Anal Bioanal Tech.* **4**, 10-11.
8. A Miodek and J Vidic, *Anal Chem.* **86**, 9098-105.
9. A Miodek and H Sauriat-Dorizon, *Biosens Bioelectron.* **59**, 6-13.

Two Different Centered Monoclinic Crystals of the *E. Coli* Outer-membrane Protein OmpF Originate from the Same Building Block

V. Chaptal^{1*}, A. Kilburg¹, D. Flot², B. Wiseman³, N. Aghajari⁴,
J.-M. Jault^{3,5} and P. Falson¹

¹*Drug Resistance Mechanism and Modulation team, Institut de Biologie et Chimie des Protéines (IBCP), UMR5086 CNRS/Université Lyon 1, 7 passage du Vercors, F-69367, Lyon, France.*

²*ESRF -The European Synchrotron 71, Avenue des Martyrs Grenoble, France.*

³*Université Grenoble Alpes, Institut de Biologie Structurale (IBS), 6 rue Jules Horowitz, Grenoble, F-38027 cedex-1, France; CEA, DSV, IBS, F-38000, Grenoble, France; CNRS UMR 5075, IBS, F-38000 Grenoble.*

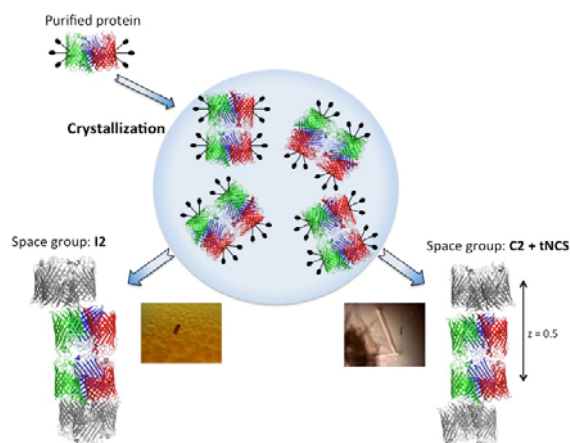
⁴*Biocrystallography and Structural Biology of Therapeutic Targets team, Institut de Biologie et Chimie des Protéines (IBCP), UMR5086 CNRS/Université Lyon 1, 7 passage du Vercors, F-69367, Lyon, France.*

⁵*Present address: Institut de Biologie et Chimie des Protéines (IBCP), UMR5086 CNRS/Université Lyon 1, 7 passage du Vercors, F-69367, Lyon, France.*

*Corresponding author, email : vincent.chaptal@ibcp.fr

ABSTRACT

Macromolecule crystal formation can be divided in two major steps: 1. the formation of a nucleus and 2. the growth of this nucleus into a full mature crystal. The latter is well described and understood, while the former remains elusive due to the difficulty to study it and is described by nucleation theories. Here we report the structure of the *E. coli* outer membrane porin OmpF in two centered monoclinic space groups. Strikingly, the two crystals originate from the same building block, made of two trimers of OmpF interacting *via* their rough side. The different crystallization conditions trigger the formation of distinct arrangement of these building blocks, leading to the formation of translational non-crystallographic symmetry (tNCS) in one case, made possible by the loose lateral packing mediated by detergents. In light of nucleation theories, these results allow us to speculate that these two crystals originate from nuclei made of either clusters of building blocks, or already forming columns that later associate laterally using detergents as glue.



Structural Models of Intrinsically Disordered and Calcium-bound Folded States of a Protein Adapted for Secretion by SAXS, Raman and HDX-MS

D.P. O'Brien¹, D. Durand², B. Hernandez³, V. Hourdel¹,
A.C. Sotomayor-Pérez¹, M. Ghomi³, J. Chamot-Rooke¹,
P. Vachette², D. Ladant¹, S. Brier¹, A. Chenal¹

¹Département de Biologie Structurale et Chimie, Institut Pasteur, Paris, France

²Département de Biochimie, Biophysique et Biologie Structurale, I2BC, CNRS, Orsay, France

³Groupe de Biophysique Moléculaire. UFR SMBH, Université Paris 13, Bobigny, France

ABSTRACT

The adenylate cyclase toxin (CyaA) is one of the primary virulence factors of *Bordetella pertussis*, the causative agent of whooping cough. We have shown that the C-terminal (aa 1006- 1706), receptor-binding Repeat-in-ToXin (RTX) Domain (RD) of CyaA is intrinsically disordered, and folds upon calcium binding [1]. We propose that this disorder-to-order transition is involved in bacterial toxin secretion. To obtain more details regarding protein conformations, we used SAXS in combination with Raman spectroscopy and Hydrogen/Deuterium eXchange Mass Spectrometry (HDX-MS). All three approaches indicated that apo-RD, although essentially unfolded, contained some residual secondary structure elements [2]. Calcium binding to RD induced a dramatic conformational rearrangement of the protein. Raman spectroscopy showed a major increase in β -sheet content, at the expense of structural disorder. HDX-MS revealed a massive masking effect around the calcium binding regions, proposed to be due to the compaction of the RTX motifs themselves. The flanking regions connecting the RTX motifs exhibited dynamic HDX events, suggesting that these regions are folded, but accessible inter-domain linkers. The SAXS pattern of apo-RD was analyzed in terms of statistical polymer chain with persistence length and thickness. This analysis was completed by an analysis in terms of an ensemble of conformations using EOM. The selected conformations illustrated the presence of residual local structure. Calcium-bound RD (holo-RD) appears to be in a compact, significantly folded and monomeric state. It adopts an elongated global conformation as shown by the program Gasbor that yields models looking like a curved elongated cylinder. Using the Webserver Phyre2, we obtained models for six protein regions that exhibited masking effects in HDX-MS. Their mutual arrangement was subsequently refined using the program Bunch. From the resulting models, we conclude that holo-RD is likely to adopt in solution an elongated conformation in which folded domains are linked by regions that are also significantly structured, part or all of which may exhibit some degree of limited flexibility, in agreement with the HDX-MS observations.

REFERENCES

1. Sotomayor-Pérez AC, Ladant D, Chenal A. Disorder-to-Order Transition in the CyaA Toxin RTX Domain: Implications for Toxin Secretion. *Toxins* (Basel). 2014 Dec 31;7(1):1-20.2. M. P. Brown and K. Austin, *Appl. Phys. Letters* **85**, 2503-2504 (2004).
2. O'Brien DP, Hernandez B, Durand D, Hourdel V, Sotomayor-Pérez AC, Vachette P, Ghomi M, Chamot-Rooke J, Ladant D, Brier S, Chenal A. Structural models of intrinsically disordered and calcium-bound folded states of a protein adapted for secretion. *Sci. Rep.* **5**, 14223; doi: 10.1038/srep14223 (2015)

Chaperoning 5S RNA Assembly

C. Madru

*Laboratoire de Cristallographie et RMN Biologiques, UMR CNRS 8015,
Université Paris Descartes, Sorbonne Paris Cité, Faculté de Pharmacie, 75006 Paris, France*

ABSTRACT

5S rRNA is an essential component of ribosome of all living organisms, contributing to ribosomal assembly, stability and function. In contrast to the 5,8S, 18S and 25S/28S rRNAs, the maturation of the 5S rRNA follows a totally different pathway before incorporation into pre-ribosome. The 5S rRNA, is transcribed by RNA polymerase III and is assembled into the 5S ribonucleoprotein particle (5S RNP), containing ribosomal proteins Rpl5 and Rpl11. Assembly of the 5S RNP requires two non-ribosomal proteins, Rpf2 and Rrs1. These two factors form a binary complex and interact with the 5S RNP to form the complex that is incorporated into pre-ribosome. In this work, we set out to elucidate the function of the Rrs1/Rpf2 complex in the 5S RNP incorporation, using a combination of structural approaches. We report here the structural characterisation of the Rrs1/Rpf2 complex alone, bound to 5S rRNA, and within pre-60S particles using X-ray crystallography, Small angle X-ray scattering, and fitting these structures to pre-60S cryo-electron microscopy envelopes. All these structural data, completed by in vivo and in vitro study of protein-RNA interactions enable us to propose a model for the function of Rrs1/Rpf2 in 5S RNP assembly.

REFERENCES

Madru C. *et al.* Chaperoning 5S RNA assembly. *Genes Dev.* 2015

Coping with Polyproline Stalling: Structural Insights to Hypusine-induced Protein Synthesis by the Eukaryotic Ribosome

J. Mailliot^{1,2*}, S. Melnikov^{1,2*}, B.-S. Shin³, L. Rigger⁴, G. Yusupova^{1,2},
R. Micura⁴, T.E. Dever³, M. Yusupov^{1,2}

¹ *Institut de Génétique et de Biologie Moléculaire et Cellulaire (IGBMC),
CNRS UMR7104, INSERM UMR964, Illkirch, France*

² *Université de Strasbourg, Strasbourg, France*

³ *Laboratory of Gene Regulation and Development, Eunice Kennedy Shriver National Institute of Child Health and Human Development, National Institutes of Health, Bethesda, MD, USA*

⁴ *Institute of Organic Chemistry, Leopold Franzens University, Innsrain 80/82,
A-6020, Innsbruck, Austria*

ABSTRACT

Many eukaryotic proteins harbor stretches of three and more consecutive prolines^{1,2}. Although these stretches help proteins to adopt functional folds¹, they also provoke ribosome stalling during protein synthesis³⁻⁵. Essential eukaryotic protein eIF5A resolves polyproline-induced stalling, relying on its unique amino acid hypusine^{5,6}. It is thought that hypusine interacts with the ribosomal active site⁷, augmenting the rate of peptide bond formation⁸⁻¹⁰ and alleviating stalling⁵. However, despite extensive studies, the hypusine binding site and the mechanism of its activity remain elusive. Here we report 3.1-3.5 Å-resolution crystal structures of the yeast 80S ribosome in complex with protein eIF5A and with a partial diprolyl-tRNA analog. The diprolyl peptide conformation in the ribosomal peptide tunnel suggests a mechanism of ribosome stalling. We find that the PII helix, a characteristic fold of polyproline peptides, creates an obstacle during nascent peptide elongation, leading to a clash between the nascent chain and the ribosomal peptide tunnel. Furthermore, we show that hypusine occupies the binding site of peptidyl-tRNA, suggesting that during protein synthesis hypusine distorts the polyprolyl-tRNA to alleviate stalling. Collectively, our study provides mechanistic insights into how hypusine enables cells to cope with the unique chemical structure of proline residues during protein synthesis.

REFERENCES

1. Adzhubei, A. A., Sternberg, M. J. & Makarov, A. A. Polyproline-II helix in proteins: structure and function. *JMB* 425, 2100-2132, (2013).
2. Morgan, A. A. & Rubenstein, E. Proline: the distribution, frequency, positioning, and common functional roles of proline and polyproline sequences in the human proteome. *PloS one* 8, e53785, (2013).
3. Doerfel, L. K. et al. EF-P is essential for rapid synthesis of proteins containing consecutive proline residues. *Science* 339, 85-88, (2013).
4. Ude, S. et al. Translation elongation factor EF-P alleviates ribosome stalling at polyproline stretches. *Science* 339, 82-85, (2013).
5. Gutierrez, E. et al. eIF5A promotes translation of polyproline motifs. *Mol. Cell* 51, 35-45, (2013).
6. Dever, T. E., Gutierrez, E. & Shin, B. S. The hypusine-containing translation factor eIF5A. *Crit. Rev. Biochem. Mol. Biol.* 49, 413-425, (2014).
7. Blaha, G., Stanley, R. E. & Steitz, T. A. Formation of the first peptide bond: the structure of EF-P bound to the 70S ribosome. *Science* 325, 966-970, (2009).
8. Cooper, H. L., Park, M. H., Folk, J. E., Safer, B. & Braverman, R. Identification of the hypusine-containing protein hy+ as translation initiation factor eIF-4D. *Proc. Nat. Acad. Sci. USA* 80, 1854-1857, (1983).
9. Park, M. H., Wolff, E. C. & Folk, J. E. Hypusine: its post-translational formation in eukaryotic initiation factor 5A and its potential role in cellular regulation. *BioFactors* 4, 95-104, (1993).
10. Saini, P., Eyster, D. E., Green, R. & Dever, T. E. Hypusine-containing protein eIF5A promotes translation elongation. *Nature* 459, 118-121, (2009).

PARALLEL SESSION

Chemistry & Physico-Chemistry, In Situ Reactivity, Soft Matter

ECOLE POLYTECHNIQUE – BECQUEREL Auditorium

Chairpersons: Jean-Sébastien GIRARDON and Sandrine LYONNARD

- IT-03 Study of the reduction of TiO₂ supported molybdenum oxide catalysts by combining in-situ XANES spectroscopy at K, L_{2,3} edge and DFT calculation
A. Tougeri
- OC-09 Oxidation and reactivity of small supported Pt-based nanoparticles under near-ambient pressure exposures to O₂ and CO
A. Naitabdi
- OC-10 In situ characterization of hydrogen-evolving cobalt electrocatalysts by X-Ray absorption spectroscopy
B. Lassalle-Kaiser
- OC-11 In situ XAS investigations of butene oligomerization under industrially relevant conditions
J. Radnick
- OC-12 Chemical speciation determined by multivariate curve resolution optimized with alternating least square fitting of quick EXAFS data
V. Briois
- IT-04 In-situ SAXS studies of the alignment of colloidal suspensions in electric and magnetic fields
P. Davidson
- OC-13 Colloidal crystal : Correlation between atomic and mesoscopic ordering scale
N. Goubet
- OC-14 Time resolved infrared spectroelectrochemistry studies at the diffraction limit
F. Borondics
- OC-15 2D inorganic mixed phase templated by organic layer at the air water interface
S. Cantin
- OC-16 High resolution spectroscopy of SOCl₂ and its isotopologues: From the microwave to the far-infrared
A. Roucou

Study of the Reduction of TiO₂ Supported Molybdenum Oxide Catalysts by Combining In-situ XANES Spectroscopy at K, L_{2,3} Edge and DFT Calculation

A.Tougerti[†], H. Hu[†], J-C. Morin[†], B. Lassalle[‡], D. Vantelon[‡],
V. Briois[‡] and S. Cristol[†],

[†]Unité de Catalyse et de Chimie du Solide, UMR CNRS 8181, Université Lille 1, France
[‡]Synchrotron SOLEIL L'Orme des Merisiers, Saint-Aubin - BP 48 91192 Gif-sur-Yvette Cedex, France

ABSTRACT

Supported Molybdenum catalysts are extensively investigated as they are active for numerous reactions like olefin metathesis and selective oxidation reactions. Furthermore this system (after sulfidation) is also widely used in the hydrotreating industrial processes, which represent 10% of the total world market for catalysts. Hence the improvement of the performance of this class of catalysts is of paramount economic and environmental importance. In recent works¹, with the combination of XANES spectra (Mo K edge), DFT calculation and modeling XANES spectra, we were able to draw a clear picture of the structure of the activated catalyst¹ ($[\text{Mo}_{14}\text{O}_{45}, n\text{Mo}_4\text{O}_{12}]^{6-}, 6(\text{HO-TiO}_2)^+$). However, electronic and geometric structure adopted by this catalyst during the catalytic reaction is still unknown. Indeed, drastic changes were observed upon reduction of the catalyst with methanol and it was rather complex to distinguish the changes in electronic structure and the changes in the geometry. In order to get more insights on the electronic structure of the system under *operando* conditions, the reducibility of this catalyst is studied by *in-situ* XANES at both Mo L_{2,3} edge (LUCIA beamline, Synchrotron SOLEIL) and Mo K edge (SAMBA beamline, Synchrotron SOLEIL).

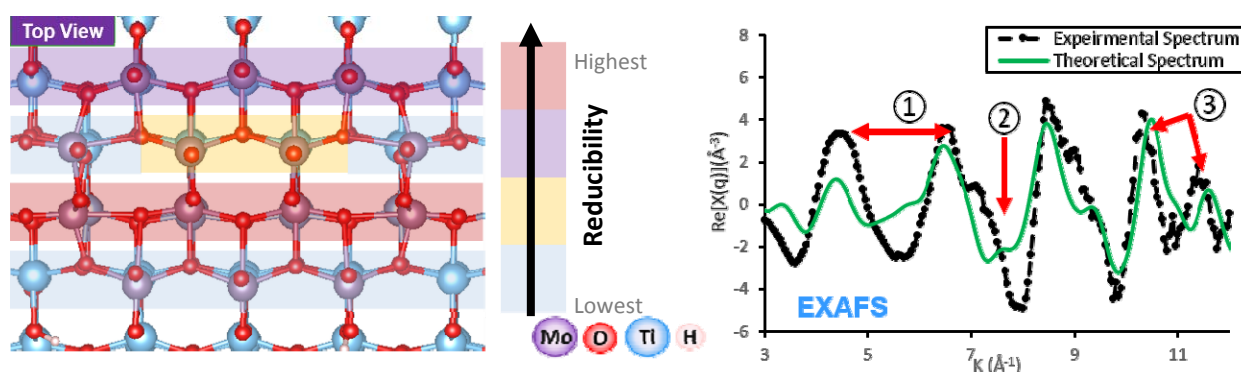


Figure (left) Reducibility of different sites of Molybdenum in Oxide cluster Structure (Mo14) (right) Experimental Mo K edge EXAFS spectra of 7.5wt% MoO₃/TiO₂ catalyst under 4% MeOH/N₂ flow (black). Theoretical Calculation of EXAFS spectrum of Oxide cluster reduced by 11 H atoms (green)

The reduction of the catalyst was carried out under two different reducing gases (CH₃OH and H₂). XAS spectra analysis reveals that under CH₃OH the catalyst is less reduced than under H₂ flow. DFT calculation shows that reducibility of supported oxomolybdates species depends on their configuration: oxo vs dioxo. Mo atoms showing one oxo bond are reduced. Meanwhile Mo atoms with dioxo bond are not reduced. Experimental spectra obtained under H₂/CH₃OH flow are reproduced by calculation, respectively, with 7 and 11 electrons. Spin density calculation however shows that a reduction under H₂ flow leads to the same number and type of reduced Mo atoms as under CH₃OH flow. However, the Mo atoms under H₂ flow carry a more important spin density than Mo atoms from CH₃OH reduction. Hence the degree of reduction is more related to the spin density on the reduced Mo atoms than to the number of reduced atoms.

REFERENCES

1. Tougerti, A. *et al. Angew. Chemie* **125**, 6568–6572 (2013).

Oxidation and Reactivity of Small Supported Pt-based Nanoparticles under Near-ambient Pressure Exposures to O₂ and CO

A. Naitabdi,¹ R. Fagiewicz,¹ A. Boucly,¹ G. Olivieri,¹⁻² F. Bournel,¹
H. Tissot,¹⁻² Y. Xu, R. Benbalagh,¹ J-J. Gallet,¹ M. Silly,²
F. Sirotti,² and F. Rochet¹

¹ Université Pierre et Marie Curie, Sorbonne Universités, Laboratoire de Chimie Physique Matière et Rayonnement, UMR 7614, 11, rue Pierre et Marie Curie, 75005 Paris

² Synchrotron SOLEIL, L'Orme des Merisiers, Saint-Aubin, 91192 Gif sur Yvette

ABSTRACT

The investigation of nanocatalysts under their working conditions of pressures and temperatures represents a real strategy toward a realistic understanding of their chemical reactivity and related issues. Additionally, the reduction of Pt load in the catalysts while maintaining their optimum performances is essential for large scale practical applications. Here, we show that small PtZn bimetallic nanoparticles (NPs) supported on the rutile and reduced TiO₂(110)-(1×1) surface can be prepared by a two steps consecutive deposition process where Pt was deposited first and followed by Zn.

Additionally, in situ Synchrotron-based Near Ambient Pressure Photoemission Spectroscopy experiments were used to monitor the evolution of the oxidation states and CO oxidation reaction of pure Pt and PtZn NPs under high exposure to O₂ and CO.¹ *Simultaneous monitoring of the chemical composition at the surface and in the near-surface gas phase, revealed the onset temperature of the CO oxidation reaction in both pure Pt and PtZn NPs at 1:4 CO:O₂ partial pressure ratio.* The formation of stable Pt surface oxide was evidenced for both pure Pt and PtZn NPs. While a sizeable encapsulation of pure Pt NPs by TiO_x was seen after annealing at 440 K under 1 mbar of O₂, no such effect was noticed for PtZn NPs. The formation of a zinc oxide layer on PtZn NPs enhances the stability of PtZn NPs. In addition, we show that the deposition of Zn leads to a substantial modification of the electronic properties of the TiO₂(110) surface which is expected to play an important role in the enhancement of the electronic conductivity of the TiO₂(110) surface. Spontaneous formation of a Pt-Zn alloy phase at room temperature was seen in PtZn NPs.

REFERENCES

¹ A. Naitabdi, R. Fagiewicz, A. Boucly, *et al.* *Topics in Catalysis* (2015) accepted.

In Situ Characterization of Hydrogen-evolving Cobalt Electrocatalysts by X-ray Absorption Spectroscopy

B. Lassalle-Kaiser,^a A. Zitolo,^a E. Fonda,^a
M. Robert^b and E. Anxolabéhère-Mallart.^b

^a *Synchrotron SOLEIL, L'Orme des Merisier, Saint-Aubin, 91191 Gif-sur-Yvette.*

^b *Université Paris Diderot, Laboratoire d'Electrochimie Moléculaire,
15 rue Jean-Antoine de Baïf, 75205 Paris.*

ABSTRACT

The development of catalysts for the Hydrogen Evolution Reaction (HER) on large scales require to use abundant and cheap materials. Research efforts have been directed in the last years to the preparation and study of transition metal-based inorganic catalysts for the HER. Cobalt-based systems have thrived as molecules, nanoparticles or amorphous materials. In particular, the cobaloxime class of compounds have been thoroughly studied in the recent years.¹ It has been recently shown, however, that these molecules suffer from reductive damage of their ligands under electrocatalytic conditions.^{2,3} This phenomenon leads to the formation of HER-active nanoparticles on the surface of the glassy carbon working electrode.

We have used Co K-edge X-ray absorption spectroscopy at the SAMBA beamline of SOLEIL to study the electrochemical formation and the structure of these nanoparticles *in situ*. We show that the particles formed are about 100 nm in size and consist of metallic cobalt. The Cobalt K-edge XANES together with the EXAFS fittings indicate that the cobalt particles formed are amorphous at the molecular level and does not present any order. We also studied their structure under electrocatalytic conditions and showed that the particles are covered with an oxide layer, which thickness decreases as the electrochemical potential applied to the system increases. The HER activity is correlated to the oxide thickness, although the layer does not completely disappear at high potentials. The oxide layer is not regenerated at lower potentials and the HER activity at lower potentials is increased after the oxide layer thickness has decreased. The role of the oxide layer is still under investigation.

With this study, we clearly describe the amorphous nature of these HER-active nanoparticles and suggest directions for the further understanding of their catalytic properties.

REFERENCES

1. M. Nguyen, A. Ranjbari, L. Catala, F. Brisset, P. Millet, A. Aukauloo, *Coordination Chemistry Reviews*, **256**, 2435-2444 (2012).
2. E. Anxolabéhère-Mallart, C. Costentin, M. Fournier, S. Nowak, M. Robert, J.-M. Savéant, *J. Am. Chem. Soc.* **134**, 6104-6107 (2012).
3. E. Anxolabéhère-Mallart, C. Costentin, M. Fournier, M. Robert, *J. Phys. Chem. C* **118**, 13377-13381 (2014).

In Situ XAS Investigations of Butene Oligomerization under Industrially Relevant Conditions

J. Radnik¹, J. Rabeah¹, V. Briois², D. Maschmeyer³ and A. Brückner¹

1 Leibniz Institute for Catalysis, Albert-Einstein-Str. 29a, 18059 Rostock, Germany

2 Synchrotron SOLEIL, L'Orme des Merisiers, Saint-Aubin, 91192 Gif-sur-Yvette, France

3 Evonik Industries AG, Paul-Baumann-Str. 1, 45772 Marl, Germany

ABSTRACT

X-ray absorption spectroscopy (XAS) allows structural investigations at catalytic systems, even if they are X-ray amorphous and contain a low amount of crucial components (< 1wt%). Furthermore, these investigations can be performed under industrial relevant conditions with e.g. elevated temperatures and high pressures. These benefits were exploited to examine the oligomerization of butenes (raffinate III) to industrially important C₈ – C₁₂ olefins in the OCTOL process at 25 – 35 bar using supported Ni/Si-Al catalysts with low Ni contents. Previous EPR studies stressed the importance of single Ni⁺ sites for this process, but a doubtless correlation to the activity could not be establish.¹ To obtain further information about other Ni valence states, especially the EPR silent bivalent Ni, XAS investigations were performed under flowing raffinate III at ≈12 bar at the SAMBA beamline at SOLEIL.

It could be shown that Ni⁺ single sites in the fresh catalyst are oxidized in the presence of 12 bar raffinate III at room temperature to Ni²⁺ single sites. Upon heating to the reaction temperature of 353 K, an average Ni valence state between +1 and +2 was observed, suggesting the action of a Ni²⁺/Ni⁺ redox shuttle under reaction conditions. EXAFS confirmed the existence of single Ni sites. Pre-edge evaluation revealed the changes of the coordination geometry from tetrahedral to octahedral under raffinate.

One striking result of this investigation was that a sufficiently high raffinate pressure was required to prevent clustering of the active Ni single sites to inactive metallic Ni particles during reaction, which was observed at a pressure of only 2 bar. This latter observation stresses the importance of such investigation under relevant conditions, e.g. high pressure and elevated temperature.

REFERENCE

1. A. Brückner, U. Bentrup, H. Zanthoff, D. Maschmeyer, J. Catal. 266, 120-128 (2009)

Chemical Speciation Determined by Multivariate Curve Resolution Optimized with Alternating Least Square Fitting of Quick-EXAFS Data

O. Roudenko, C. La Fontaine, S. Belin and V. Briois

SOLEIL ROCK beamline L'Orme des Merisiers BP48, 91192 Gif sur Yvette

ABSTRACT

With the advent of 3rd generation synchrotron radiation facilities allowing a sub-second time resolution in the monitoring of kinetics by X-ray Absorption Spectroscopy (XAS), the experimentalist can now access to a deeper and more accurate temporal description of the chemical species involved in such processes provided that the bottleneck of the data analysis has been overcome. Indeed, users at the time-resolved XAS beamlines have to face with a huge amount of data in a couple of minutes making the common strategy of data evaluation, reduction and analysis quite inefficient. New tools must be proposed to the users to interactively optimize the outcome of an experiment carried out at the beamline. In this framework, chemometric tools such as Multivariate Curve Resolution optimized with Alternating Least Square (MCR-ALS) fitting are emerging as a powerful method for getting more information from XAS spectra of evolving mixtures upon reaction [1-3]. At the ROCK beamline, it will be proposed in a near future a user-friendly interface to handle this high number of data into normalized matrices of absorption spectra directly suitable as input file for MCR-ALS analysis available on Matlab platform using free toolboxes developed by the Tauler's group [4].

In this presentation, a brief description of the MCR-ALS method will be given and examples of its application to Quick-EXAFS data acquired upon monitoring the activation of heterogeneous catalysts will illustrate the strength and limitation of the methodology.

REFERENCES

1. W. Cassinelli, L. Martins, A. R. Passos, S. H. Pulcinelli, C. V. Santilli, A. Rochet, V. Briois, *Cat. Today* **229**, 114-122 (2014).
2. J. Hong, E. Marceau, A. Khodakov, L. Gaberova, A. Griboval-Constant, Jean-Sebastien Girardon, C. La Fontaine, V. Briois, *ACS Catal.* **5**, 1273-1282 (2014).
3. H.W. P. Carvalho, S. H. Pulcinelli, C. V. Santilli, F. Leroux, F. Meneau, V. Briois, *Chem. Mater.* **25**, 2855-2867 (2013).
4. J. Jaumot, A. de Juan, R ; Tauler, *Chemom. Intell. Lab. Syst.* **140**, 1-12, (2015)

In-situ SAXS Studies of the Alignment of Colloidal Suspensions in Electric and Magnetic Fields

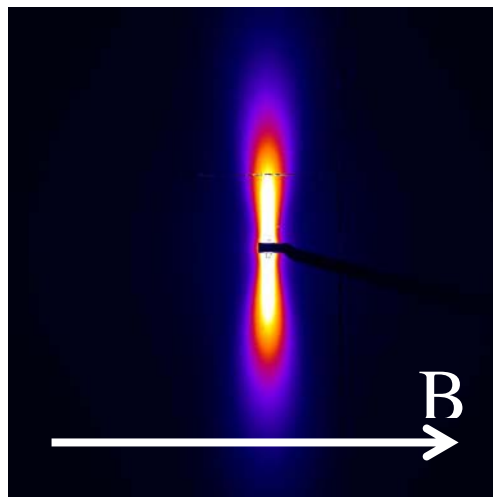
P. Davidson

*Laboratoire de Physique des Solides, CNRS, Univ. Paris-Sud,
Université Paris-Saclay, Orsay 91405, France.*

ABSTRACT

Colloidal suspensions of anisotropic nanoparticles, like nanorods and nanosheets, often display liquid-crystalline phases which are partially ordered states intermediate between the usual crystalline and liquid states. Liquid crystals are an important class of “soft matter” and, as such, they easily respond to small external stresses like the application of weak electric and magnetic fields. This feature provides a simple way of controlling the orientation of nanoparticles at the macroscopic scale.

In this communication, several examples will be given of how single domains of nematic and columnar liquid-crystalline phases can be easily grown by applying a magnetic or an electric field. Moreover, examples of field-induced phase transitions will also be shown. Furthermore, our experimental setups will be described in detail. These setups, which can easily be used at the Swing SAXS beamline of Soleil, are available on request to all members of the Soleil user community.



Anisotropic SAXS pattern of a single domain of a nematic suspension of GdPO₄ nanorods.

Colloidal Crystal: Correlation between Atomic and Mesoscopic Ordering Scale

N. Goubet^{1,2}; P.A. Albouy²; M.P. Pileni¹ and A. Thompson³

Université Pierre et Marie Curie, Paris 06, UMR 8233, Monaris, F-75005, Paris, France
 Laboratoire de Physique des Solides, Université Paris-Sud, 91405 Orsay, France
 Synchrotron Soleil, BP 48, Saint-Aubin, Gif sur Yvette 91192, France,

ABSTRACT

Colloidal crystals with submillimeter size are built by self-assembly of gold nanoparticles with nearly similar size but different nanocrystallinities.^{1,2} The high flux delivered by the synchrotron facility SOLEIL makes possible the collection, at PROXIMA1 beamline, of X-ray diffraction patterns from individual single-crystals covering a wide q -range. This allowed a highly-detailed reconstruction of the most relevant fraction of the reciprocal space including some diffuse scattering.

The external shape of the gold nanoparticles was characterized by electron microscopy and related to their nanocrystallinity. For 5 nm nanocrystals, X-ray diffraction demonstrates that colloidal crystals made of single-crystal nanoparticles belong to the body-centered cubic system while face-centered cubic single crystals are observed in case of polycrystalline particles; a remarkable feature is the preferential orientation of the symmetry axes of the single-crystal nanoparticles along those of the colloidal crystal; on the contrary polycrystalline nanoparticles display random orientation. These results show the importance of the nanocrystallinity on the nanocrystal packing.

By increasing the size of single nanocrystals to 12 nm,³ the quasi-spherical gold nanocrystal exhibit an unexpected marked orientational order.

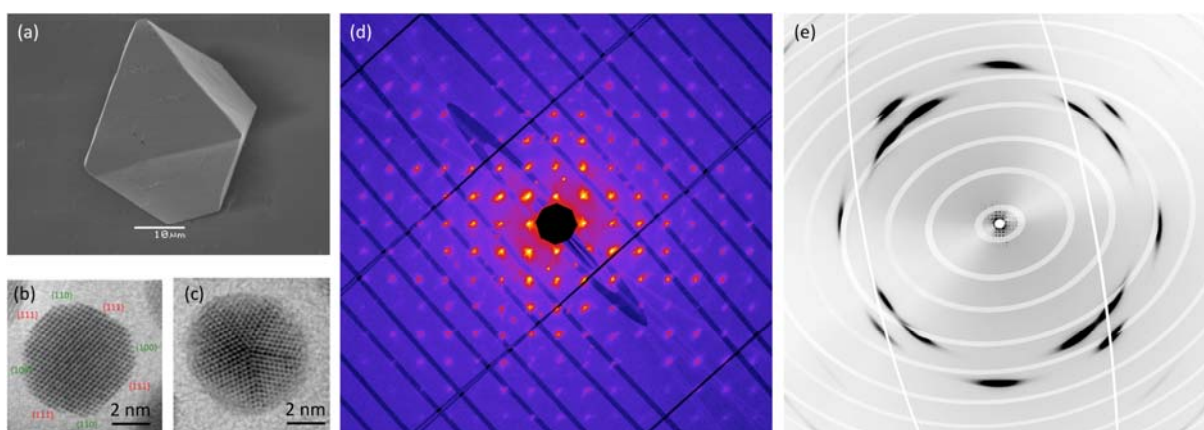


Fig. 1: (a) Colloidal crystal made of gold nanocrystals. (b) 5 nm gold single crystal. (c) 5 nm gold decahedron. (d) Planar cut of the reciprocal space perpendicular to a [100] axis at small q value, corresponding to the nanocrystals order ($q_{\max} = 7 \text{ nm}^{-1}$), of a single colloidal crystal made of 12 nm gold single crystal. (e) The same planar cut of the reciprocal space but on wider q values corresponding to the atomic order ($q_{\max} = 42 \text{ nm}^{-1}$).

REFERENCES

1. T. Hanrath, *Journal of Vacuum Science & Technology A: Vacuum, Surfaces, and Films* **30**, (3), 030802, (2012).
2. L. Motte, F. Billoudet and M.P. Pileni, *The Journal of Physical Chemistry* **99**, (44), 16425-16429, (1995).
3. N. Goubet, I. Tempira, J. Yang, G. Soavi, D. Polli, G. Cerullo and M.P. Pileni *Nanoscale* **7**, 3237–3246 (2015)

Time-resolved Infrared Spectroelectrochemistry Studies at the Diffraction Limit

F. Borondics¹, S. Rosendahl² and I. Burgess³

¹ SMIS Beamline, Soleil Synchrotron, BP48, L'Orme des Merisiers, Saint Aubin, France

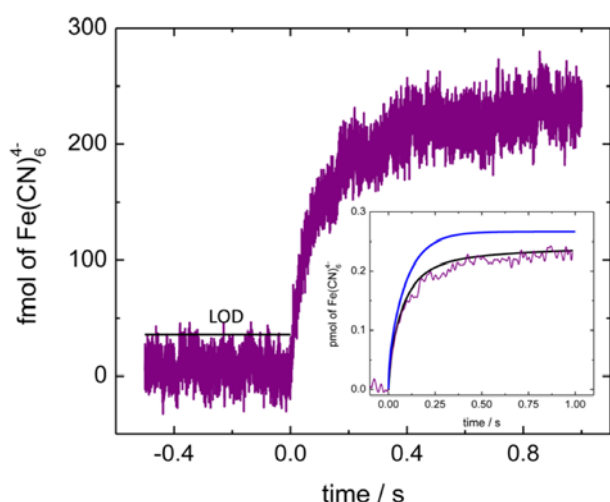
² Mid-IR beamline, Canadian Light Source Inc., 44 Innovation Boulevard, Saskatoon, SK Canada

³ Department of Chemistry, 110 Science Place, University of Saskatchewan, Saskatoon, SK Canada

ABSTRACT

A seldom exploited potential of time resolved dynamics experiments using synchrotron-based infrared spectromicroscopy will be introduced through the review of a series of electrochemical kinetics studies. The capabilities of the SMIS endstations allow dynamics investigations with as high as microsecond time resolution at the theoretically achievable far field diffraction limit.

In this series of experiments we have demonstrated the capabilities of extremely low



concentrations (36 fmol) of the ferro/ferricyanide system without surface enhancement effects with microsecond time resolution. The experimental results are in perfect agreement of the simulations.

Since the experimental techniques discussed in this presentation are generalizable and therefore applications from biology to solid state physics are possible with the proper sample geometry. The presented experiments will be implemented at the SMIS beamline in the near future.

REFERENCES

- 1 S.M. Rosendahl, F. Borondics, T.E. May, T.M. Pedersen, and I.J. Burgess, *Rev. Sci. Instrum.*, 82 [8] 083105 (2011).
- 2 S.M. Rosendahl, F. Borondics, T.E. May, T.M. Pedersen, and I.J. Burgess, *Anal. Chem.*, 83 [10] 3632–3639 (2011).
- 3 S.M. Rosendahl, F. Borondics, T.E. May, and I.J. Burgess, *Anal. Chem.*, 85 [18] 8722–8727 (2013).
- 4 M.J. Lardner, K. Tu, S.M. Rosendahl, F. Borondics, and I.J. Burgess, *Electrochim. Acta*, 162 [0] 72–78 (2015).

2D Inorganic Mixed Phase Templated by Organic Layer at the Air-water Interface

S. Cantin¹, A. El Haitami¹, P. Fontaine², M.-C. Fauré^{3,4},
and M. Goldmann^{2,3,4}

¹LPPI, Institut des Matériaux, Université de Cergy-Pontoise, 5 Mail Gay-Lussac, 95031 Cergy-Pontoise Cedex, France;

²SIRIUS Beamline, Synchrotron SOLEIL, L'Orme des Merisiers, Saint Aubin, BP48, 91192 Gif sur Yvette Cedex, France ;

³Institut des NanoSciences de Paris, Université Pierre et Marie Curie, 4 Place Jussieu, 75252 Paris Cedex 05, France ;

⁴Faculté des Sciences Fondamentales et Biomédicales, Université Paris Descartes, 45 rue des S^{ts}-Pères, 75006 Paris, France

ABSTRACT

Fatty acid Langmuir monolayers on aqueous solutions of divalent metal cations provide model systems for understanding bio-inspired materials.¹ The first category of ions (Mg^{2+} , Mn^{2+} ...) leads to a superstructure, i.e., a 2D inorganic lattice commensurate with the organic monolayer.² The second one (Cu^{2+} , Ca^{2+} ...) induces a change in the organic structure.³ Until now, the physicochemical conditions of the superstructure formation as well as its chemical composition are still fuzzy. We studied by GIXD the effect of aqueous solutions of $\text{Mg}^{2+}/\text{Mn}^{2+}$ mixtures on behenic acid monolayer. Superstructures were evidenced for all concentrations. We focused mainly on the diffraction peaks characteristic of the organic oblique cell. As the Mg^{2+} volume fraction x increases, one observes a continuous evolution of the oblique cell parameters, indicating a solubility process of Mg^{2+} in Mn^{2+} at the interface (Fig. 1). Then one detects the coexistence between two oblique phases signature of first-order transition. However, the lattice parameters still evolve continuously, meaning that two surface intensive parameters are simultaneously modified. Upon further increase in x , a single Mg^{2+} -rich phase is observed. The limit of solubility of Mn^{2+} in the Mg^{2+} lattice was thus determined. Surface X-rays fluorescence measurements also showed that Mn^{2+} surface concentration is driven by Mg^{2+} volume concentration. This first study of the 2D phase diagram of inorganic mixtures was possible thanks to the SIRIUS beamline high-resolution setup allowing resolving the drift of the peaks associated to each phases.

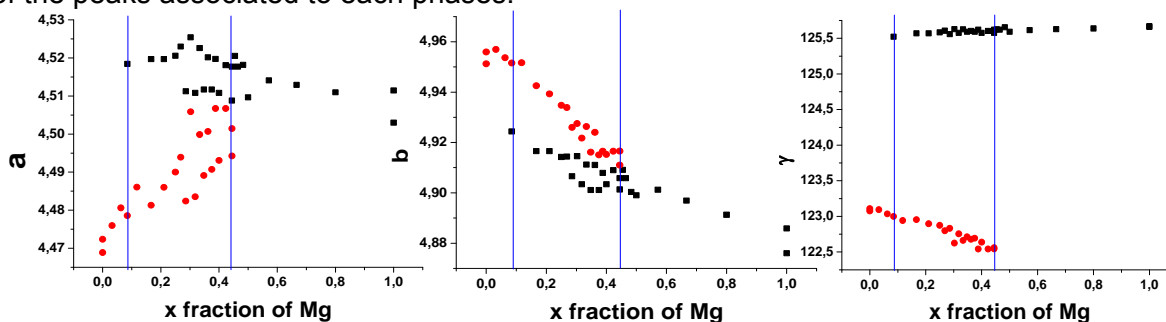


Fig. 1: Evolution of the oblique cell parameters (a, b, γ)

REFERENCES

1. Z. Tang, N. A. Kotov, S. Magonov and B. Ozturk, *Nature Materials* **2**, 413-418 (2003).
2. J. Daillant, J. Pignat, S. Cantin, F. Perrot, S. Mora and O. Kononov, *Soft Matter* **5**, 203-207 (2009).
3. S. Cantin, M.-C. Fauré, F. Perrot and M. Goldmann, *J. Phys. Chem. B* **117**, 16275-16282 (2013).

High Resolution Spectroscopy of SOCl₂ and its Isotopologues: From the Microwave to the Far-infrared

A. Roucou¹, A. Cuisset¹, G. Mouret¹, F. Hindle¹, M. A. Martin-Drumel², M. C. McCarthy², G. G. Brown³, S. Thorwirth⁴, O. Pirali⁵.

¹ *Laboratoire de Physico-Chimie de l'Atmosphère, Dunkerque, France.*

² *Harvard-Smithsonian Center for Astrophysics, Cambridge, USA.*

³ *Coker College, Hartsville, SC, USA.*

⁴ *I. Physikalisches Institut, Universität zu Köln, Germany.*

⁵ *AILES beamline, Synchrotron SOLEIL, Saint Aubin, France*

ABSTRACT

Thionyle chloride (SOCl₂) is a volatile inorganic compound used extensively in industry. Its monitoring in the gas phase is critical for both environmental and defense concerns. The high-resolution gas phase microwave spectrum (below 40 GHz) of the main isotopologue was recorded twenty years ago, however, due to high spectral congestion, no further study of the rotational and rovibrational spectra have been reported. In the present study, the pure rotational and rovibrational spectra of SOCl₂ and its isotopologues have been characterized from the microwave to the far-infrared, using three complementary experimental approaches:

- The rovibrational spectra of the symmetric ν_3 (344 cm⁻¹) and ν_2 (500 cm⁻¹) and asymmetric ν_6 (284 cm⁻¹) and ν_5 (460 cm⁻¹) fundamental bands of SO³⁵Cl₂, SO³⁵Cl³⁷Cl and SO³⁷Cl₂ have been resolved by means of FT-FIR spectroscopy on the AILES beamline of the SOLEIL synchrotron.¹
- Pure rotational transitions in the ground and selected vibrationally excited states of the same isotopologues have been recorded in absorption in the 70-660 GHz region using a frequency multiplication chain.
- The chirped-pulse Fourier transform microwave (CP-FTMW) spectrum of SOCl₂ has been recorded in the 7-19 GHz region, revealing pure rotational transitions of rare isotopologues, together with lines of the most abundant ones.

Fits of all these data have allowed an accurate determination of the molecular parameters (rotational and centrifugal distortion constants, vibrational band centers) and a refined geometry of the molecule has been derived. This presentation will be focused on the FT-FIR spectroscopy experiments at the AILES beamline of SOLEIL and on the analysis work to assign very congested high-resolution rovibrational spectra.

REFERENCES

1. doi:10.1016/j.jms.2015.02.001, M. A. Martin-Drumel, G. Mouret, O. Pirali, A. Cuisset, High-resolution synchrotron far infrared spectroscopy of thionyl chloride: Analysis of the ν_3 and ν_6 fundamental bands, *J. Mol. Spectrosc.* in press, (2015)

PARALLEL SESSION

Cultural Heritage, Archaeology, Environment, Geosciences

ECOLE POLYTECHNIQUE – SAUVY Auditorium

Chairpersons: Emmanuel GUILLON and Noemi CARMONA-TEJERO

- | | |
|--------|--|
| IT-05 | Metal contaminated soils and phytoremediation
<i>M-P. Isaure</i> |
| OC-17 | Copper binding to nitrogen functional groups in tomato and wheat root apoplasts
<i>A. Masion</i> |
| IT-06 | X-ray micro imaging in cultural heritage studies
<i>K. Janssens</i> |
| OC- 18 | Development of manganese-rich patinas on the building sandstones from Luneville Castle: From initial bearing phases towards final phases
<i>L. Gatuingt</i> |
| OC-19 | The role of microbes in the geochemical cycle of P in lake Pavin
<i>K. Benzerara</i> |

Metal Contaminated Soils and Phytoremediation

M-P. Isaure¹, S. Huguet¹, N. Trcera², S. Reguer³, C. Mocuta³,
H. Castillo-Michel⁴, O. Proux⁵, G. Sarret⁶, J-C.Cleyet-Marel⁷

¹ Université de Pau et des Pays de l'Adour, Laboratoire de Chimie Analytique Bio-Inorganique et Environnement, Institut des Sciences Analytiques et de Physico-chimie pour l'Environnement et les Matériaux (LCABIE/IPREM, UPPA/CNRS - UMR 5254), Hélioparc, 2 Av. Président Angot, 64053 Pau, France.

² Beamline LUCIA, Synchrotron SOLEIL, BP 48, 91192 Gif sur Yvette, France.

³ Beamline DIFFABS, Synchrotron SOLEIL, BP 48, 91192 Gif sur Yvette, France.

⁴ Beamline ID21, European Synchrotron Radiation Facility, BP 220, 38043 Grenoble, France.

⁵ Beamline FAME, European Synchrotron Radiation Facility, BP 220, 38043 Grenoble, France.

⁶ Institut des Sciences de la Terre (ISTerre, Université Joseph Fourier/CNRS/IRD - UMR 5275) BP 53, 38041 Grenoble, France.

⁷ Laboratoire des Symbioses Tropicales et Méditerranéennes (LSTM, INRA/Montpellier SupAgro/IRD/CIRAD /UM2 – UMR 113), Baillarguet TA A-82/J, 34398 Montpellier, France.

ABSTRACT

During the last century, contamination of soils with metals has increased due to intense anthropogenic activities. Conventional invasive physico-chemical techniques are mostly used to clean these soils but they generally lead to a loss of soil functionality. The concept of phytoremediation has emerged for two decades and represents an alternative sustainable remediation technique: the idea of agromining has been even recently proposed (1). In phytoremediation techniques, plants are used to extract (phytoextraction, agromining) or stabilize (phytostabilization) metals accumulated in soils. To promote these techniques, the ability of plants to cope with metal toxicity needs to be better understood, particularly the way they interact with the soil and the way they transfer and sequester metals in their tissues, cells and cell compartments. In this context, synchrotron radiation techniques are key tools to locate metals by chemical imaging (micro X-ray Fluorescence, μ XRF), to identify the metal speciation at the micrometer scale level (μ X-ray Absorption Near Edge Structure, μ XANES) or 'bulk' level (XANES and Extended X-ray Absorption Fine Structure, EXAFS), and to identify the crystallized phases in the heterogeneous rhizosphere (μ X Ray Diffraction, μ XRD) (2,3).

Two case studies will be presented. The first one is the accumulation of cadmium in a model hyperaccumulating plant, *Arabidopsis halleri* (4), originally candidate for phytoextraction, and the second one is behavior of cadmium and zinc in a phytostabilization process by a pioneer legume plant.

REFERENCES

1. A. Van der Ent et al., *Env. Sci. Technol.* **48**, 4773-4780 (2015).
2. E. Lombi and J. Susini, *Plant Soil* **320**, 1-35 (2009).
3. G. Sarret et al., *Adv. Agron.* **119**, 1-82 (2013).
4. M. P. Isaure et al., *J. Exp. Bot.* **66**, 3201-3214 (2015).

Copper Binding to Nitrogen Functional Groups in Tomato and Wheat Root Apoplasts

S. Guigues^{1,2}, M. Bravin³, A. Masion⁴, C. Garnier⁵, E. Doelsch¹

1: CIRAD, UPR Recyclage et risque, F-34398 Montpellier,

2: ADEME, BP-90406, Angers cedex;

3: CIRAD, UPR Recyclage et risque, F-97408 Saint-Denis, Réunion;

4: CNRS-CEREGE, Europole Arbois, BP8013545 Aix-en-Provence;

5: Université de Toulon, EA 3819, 83957 La Garde

ABSTRACT

Carboxylic groups located in plant cell walls (CW) are generally considered to be the main copper binding sites in plant roots, despite the presence of other functional groups. The aim of this study was to investigate sites responsible for copper binding in root apoplasts, i.e. CW and outer surface of the plasma membrane continuum. Binding sites in root apoplasts were investigated by comparing isolated cell walls of a monocotyledon and a dicotyledon crop, viz. wheat (*Triticum aestivum* L.) and tomato (*Solanum lycopersicum* L.) respectively, with their intact roots. Copper speciation was examined by X-ray absorption (XAS) and ¹³C-nuclear magnetic resonance spectroscopies. Homogeneous speciation and binding of copper was found in wheat and tomato root apoplasts. Only Cu-N and Cu-O bonds were detected in wheat and tomato root apoplasts. Nitrogen/oxygen ligands were identified in slightly higher proportions (40-70%) than single oxygen ligands. The high-affinity N functional groups embedded in root apoplasts participated in copper binding in the same magnitude than the low-affinity carboxylic groups.

X-ray Micro Imaging in Cultural Heritage Studies

K. Janssens

AXES Research Group, Department of Chemistry, University of Antwerp,
Groenenborgerlaan 171, B-2020 Antwerp, Belgium

ABSTRACT

Microscopic XANES currently is an almost routinely applied method when investigating the chemical transformations that cause discoloration (or other forms of macroscopically visible alteration) of artists' pigments/paint and equivalent cultural heritage materials.

Usually, these point-by-point investigations are combined with X-ray fluorescence (XRF)-based forms of imaging (either in 2D or 3D), for example to determine which sample positions are most promising/representative to answer the question at hand. In a second phase, at a (usually limited) series of locations, XAFS measurements can be performed by positioning the X-ray micro- or nanobeam at these locations and executing relevant energy-scans. In a third phase, a few energies are selected in the edge energy range just investigated to record a series of XRF maps of the central element studied. When the system being studied is sufficiently simple or the XAFS response of the species is sufficiently different from species to species, the E-stack of XRF maps can be converted into a series of species-specific maps. However, this is a process that only works well when the implicit assumptions made about the occurrence of (XAFS-distinct) species are correct.

Recently, a number of different approaches have been proposed that allow to efficiently record the complete (transmission or fluorescence) XANES response in all points of an area under investigation: some are based on the use of large, high-throughput XRF detectors, allowing fast spatial scanning of the area under investigation combined with slower E-scanning. Another approach involves the use of energy-dispersive X-ray camera's that allow to eliminate XY scanning. Finally, in transmission mode, Full-field XANES data recording can be done in parallel in all pixels of the field of view.

The advantages and limitations of these data collection modes will be outlined by discussing a number of cases studies, mostly dealing with the investigation of chemical alteration of artists' pigments such as *cadmium yellow* (CdS), a pigment employed by James Ensor and Henri Matisse and *chrome yellow* ($\text{PbCr}_{1-x}\text{S}_x\text{O}_4$, $0 < x < 0.8$), employed by Vincent Van Gogh. Time permitting, also the discolouration of other pigments such as minium (Pb_3O_4) [3] and other cultural heritage materials such as historical glass [4] will be discussed.

REFERENCES

1. E. Pouyet, M. Cotte, B. Fayard, M. Salome, F. Meirer, A. Mehta, E. Uffelman, A. Hull, F. Vanmeert, J. Kieffer, M. Burghammer, F. Sette, K. Janssens, J. Mass, *2D X-ray and FTIR micro-analysis of the degradation of cadmium yellow pigment in paintings of Henri Matisse*, Applied Physics A – Materials Science & Processing, **121**, 967-98 (2015).
2. L. Monico, K. Janssens, M. Alfeld, M. Cotte, F. Vanmeert, C.G. Ryan, G. Falkenberg, D.L. Howard, B.G. Brunetti and C. Miliani, *Full spectral XANES imaging using the Maia detector array as a new tool for the study of the alteration process of chrome yellow pigments in paintings by Vincent van Gogh*, Journal of Analytical Atomic Spectrometry, **30**, 613-626 (2015).
3. F. Vanmeert, G. Van der Snickt, K. Janssens, *Plumbonacrite Identified by X-ray Powder Diffraction Tomography as a Missing Link during Degradation of Red Lead in a Van Gogh Painting*, Angewandte Chemie-International Edition, **54** (2015) 3607-3610. 3
4. G. Nuyts, S. Cagno, S. Bugani, K. Janssens, *Micro-XANES study on Mn browning: use of quantitative valence state maps*, Journal of Analytical Atomic Spectrometry, **30**, 642-650 (2015).

Development of Manganese-rich Patinas on the Building Sandstones from Luneville Castle: From Initial Bearing Phases Towards Final Phases

L. Gatuingt^{1,2,5}, S. Rossano¹, J-D. Mertz², B. Lanson^{3,4}, O. Rozenbaum⁵

¹ Université Paris-Est, Laboratoire Géomatériaux et Environnement, EA4508, UPEM, 77454 Marne-la-Vallée, France

² Laboratoire de Recherche des Monuments Historiques, CRC-LRMH USR3224, 29 rue de Paris, 77420 Champs-sur-Marne, France

³ Université Grenoble Alpes, ISTERre, F-38041, France

⁴ CNRS, ISTERre, F-38041, France

⁵ Université d'Orléans, CNRS, BRGM, ISTO, UMR 7327, 1A rue de la Férollerie, 45071 Orléans cedex 2, France

ABSTRACT

Sandstones, used as building stones or in natural settings, are known to develop dark patinas at their surface when subjected to atmospheric conditions at a scale time of centuries^{1,2,3}. In January 2003, a violent fire affected the Luneville chateau (XVIIIth century), located in the east part of France and built with Triassic sandstones. The building materials were submitted to a huge amount of water, resulting from the firemen intervention. A few weeks after - i. e. very quickly - dark Mn-rich stains started developing on some stone blocks located in the burnt parts of the chateau. As they are not observed on all sandstones, their formation likely depends on the substrate and possibly results from the dissolution of Mn-bearing compounds in the stone core, followed by their transportation by their aqueous migration to the surface, through the porous network.

In order to investigate the patina formation mechanisms, two patinated stones have been sampled on site, in the burnt and unburnt zones respectively. Therefore, one patina dates from before 2003 and needed several years to appear, whereas the other one was formed in few weeks, after the 2003 fire. The aims of this work are (i) to characterize and compare the patinas developed in different conditions and different time range and (ii) to determine and compare the initial Mn-bearing phases in the sandstone bulks.

Optical and electronic microscopies, coupled with Energy-Dispersive X-ray Spectroscopy (EDS) allow establishing a correlation between the visual aspect of an area in the bulks and its Mn-enrichment. Moreover, these techniques permit to see the patinas are heterogeneous in thickness and colour, and cannot be described as a continuous coating onto the rock surfaces. The patina developed before the 2003 fire is darker and thicker than the other one. The Mn-enrichment of the patinas has also been confirmed. Quantitative chemical information was obtained using Inductively Coupled Plasma-Optical Emission Spectrometry (ICP-OES) and Particle-Induced X-ray Emission (PIXE) methods. Mn-speciations, in both the core and at the surface of the block, have been studied by X-ray diffraction (XRD) and X-ray absorption spectroscopy (XANES) at the SOLEIL synchrotron (France), with DiffAbs and LUCIA beamlines respectively.

REFERENCES

1. C. Thomachot, D. Jeannette, Effects of iron black varnish on petrophysical properties of building sandstone, *Environmental Geology* 47, (2004), 119-131
2. J-D. Mertz, Etat des lieux, diagnostic des pathologies et perspectives, In: *Un chantier, restauration des façades des monuments urbains*. Ministère de la Culture et de la Communication, OPPIC, (2010), 79p
3. A.G. Nord, T. Ericsson, Chemical analysis of thin black layers on building stone, *Studies in Conservation*, Vol. 38, (1993), pp. 25-35

The Role of Microbes in the Geochemical Cycle of P in Lake Pavin

K. Benzerara¹, S. Rivas-Lamelo¹, J. Miot¹, N. Trcera², D. Jezequel³,
E. Viollier³, F. Skouri-Panet¹, M. Poinot¹, C. Ferard¹,
C. Lefevre⁴, E. Duprat¹

¹IMPMC, CNRS UMR 7590, Sorbonne Universités, MNHN, UPMC, IRD UMR 206,
75005 Paris, France

² Synchrotron SOLEIL, L'Orme des Merisiers, St Aubin, BP 48, F-91192 Gif sur Yvette, France

³IPGP, Sorbonne Paris Cité, UMR 7154, Université Paris Diderot, CNRS, Paris, France

⁴CEA/CNRS/Aix-Marseille Université, UMR 7265, Laboratoire de Bioénergétique Cellulaire, Saint Paul les Durance, France

ABSTRACT

Phosphorus (P) is essential for life and a limiting nutrient in many ecosystems (Cosmidis et al., 2015). Microorganisms have developed all sorts of strategies to store P efficiently. Yet, the extent to which they control the geochemical cycle of P over abiotic processes remains poorly determined. Here we studied Lake Pavin (Massif Central) which is an exceptional environment of modern phosphogenesis (Cosmidis et al., 2014). Indeed, this lake is meromictic, i.e., its water column is permanently stratified and its deeper part is permanently anoxic providing a unique opportunity to track P speciation changes with oxygen fugacity. Using LUCIA beamline, we mapped the distribution and the speciation of P in particles collected at several depths (oxic and anoxic). Then we analyzed the particles at the exact same locations by FEG-SEM and epifluorescent microscopy. Overall, this correlative approach offered the opportunity to (1) localize, identify and quantify the major carriers of P in the particulate fraction of Lake Pavin at different depths, (2) assess their microbial origin and (3) distinguish between different species of P such as orthophosphates and polyphosphates. We show that P hotspots were systematically due to polyphosphate inclusions in a variety of microbial cells at oxic depths. At the oxic-anoxic transition, the highest P hotspots were due to Fe-phosphate precipitates encrusting microbial cells. Interestingly, several hotspots were due to polyphosphate inclusions growing within bacterial cells forming intracellular magnetites. At higher depth, Fe-phosphates, usually encrusting microbial cells become predominant (Benzerara et al., in prep). Overall, these observations highlight the major role of some microorganisms in P cycling and allow us to suggest a new picture of the P biogeochemical cycle in the water column of a meromictic lake.

REFERENCES

1. Cosmidis J., Benzerara K., Morin G., Busigny V., Lebeau O., Jézéquel D., Noël V., Dublet G., Othmane G. (2014) Biomineralization of iron-phosphates in the water column of Lake Pavin (Massif Central, France). *Geochim. Cosmochim. Acta*, 126, 78- 96.
2. Cosmidis J, Benzerara K, Guyot F, Skouri-Panet F, Férard C, Guigner JM, Babonneau F, Coelho C Calcium-phosphate biomineralization induced by alkaline phosphatase activity in *Escherichia coli*. *Frontiers in Earth Science*, in press
3. Benzerara K, Rivas-Lamelo S, Miot J, Trcera N, Jezequel D, Viollier E, Skouri-Panet F, Poinot M, Ferard C, Lefevre C, Duprat E. The diversity of microbial processes controlling the P geochemical cycle in the water column of Lake Pavin. In prep.

PARALLEL SESSION

Diluted Matter

ECOLE POLYTECHNIQUE – CARNOT Auditorium

Chairpersons: Vincent BOUDON and Francis PENENT

- IT-07 Combining Synchrotron Radiation with low temperature and long optical paths: IR signatures of halogen-containing atmospheric trace molecules
L. Manceron
- OC-20 Photoelectron diffraction observed in the ionization of the 2a₁ orbital of methane
S. Nandi
- OC-21 Hard X-ray induced multi-step ultrafast dissociation
O. Travnikova
- OC-22 First high-resolution analysis of phosgene ³⁵Cl₂CO and ³⁵Cl³⁷ClCO fundamentals in the 250 - 480 cm⁻¹ spectral region
M. Ndao
- OC-23 Probing the VUV photoionisation of methyl radicals produced in a pyrolysis and a reactor sources
C. Alcaraz
- IT-08 Threshold photoelectron spectra (TPES) applied to the OH + propene and OH + isoprene reactions
J.-C. Loison
- OC-24 Multiple Photoionization processes of alkali vapors
J. Palaudoux
- OC-25 Frequency analysis of the ν_2 band of SO₂F₂ using the C_{2v} Top Data System
F. Hmida
- OC-26 Electron-nuclear dynamics in resonant X-ray Raman scattering of CO molecule
L. Journal
- OC-27 Photoionisation VUV de molécules prébiotiques : Spectroscopie et réactivité
A. Bellili

Combining Synchrotron Radiation with Low Temperature and Long Optical Paths: IR Signatures of Halogen-containing Atmospheric Trace Molecules

L. Manceron

*Synchrotron SOLEIL, Beamline AILES, L'Orme des Merisiers, F-91192 Gif-sur-Yvette, France,
et MONARIS, CNRS UMR 8233, 4 Place Jussieu, F-75252 Paris Cedex, France*

ABSTRACT

For optical measurements of atmospheric or astrophysical systems, an accurate determination of molecular spectroscopic parameters (energies, rotational and distortion constants) is a necessary preliminary step for subsequent modeling and retrieval of concentration profiles. As a consequence, high resolution laboratory spectra are a prerequisite and line profile measurements with good signal-to-noise ratio at variable temperatures and pressures represent a crucial step. Also, it is worth noting that numerous molecular systems which have relatively weak transitions are important for modeling atmospheric absorptions; their observation in the laboratory requires long optical paths for proper analysis. Finally for systems having transitions in the mid-IR atmospheric windows, the knowledge of the rotational structure of lower energy states is essential for a proper modeling of hot bands: This requires preliminary measurements in the more difficult FIR region. For such studies, the use of synchrotron radiation (SR) as a broad band source for high resolution interferometry has become an important method. As a useful complement, a special instrumentation has been developed at SOLEIL in collaboration with the LISA laboratory combining SR with a new cell, designed especially for accurate spectroscopic measurements in the 80 to 400 K temperature range with variable path lengths from 3 to more than 141 m, able to accommodate the specific requirements of far infrared measurements [1] and fitted with a unique, homemade cryogenic pressure gauge [2].

Halogen-containing atmospheric traces gases are well known greenhouse gases or ozone-depleting substances, and possess in general numerous low energy vibrational levels. Even if these transitions are generally outside the atmospheric transparency windows useful for their remote sensing, a good description of these levels is an important step for the modelling of the atmospheric spectra. Several examples will be presented of the possibilities offered by this new instrumentation among the recent studies carried out on SF₆ [3], C₂H₄F₂ [4], SO₂F₂, COCl₂ [5] or CF₃I [6] on the AILES Beamline.

REFERENCES

1. F. Kwabia Tchana, F. Willaert, X. Landsheere, J. –M. Flaud, L. Lago, M. Chapuis, C. Herbeaux, P. Roy, and L. Manceron, *Rev. Sci. Instrum.* **84**, (2013) 0931101.
2. L. Lago, C. Herbeaux, M. Bol, P. Roy, and L. Manceron, *Rev. Sci. Instrum.* **85**, (2014) 015108.
3. V. Boudon, L. Manceron, F. Kwabia Tchana, M. Loëte, L. Lago, P. Roy. *Phys.Chem.Chem.Phys.*, 16,1415 (2014).
4. A. Wong, C. D. Thompson, D. R. T. Appadoo, R. Plathe, P. Roy, L. Manceron, J. Barros³, D. McNaughton. *Mol. Phys* 111 (14-15) 2198 (2013).
5. F. Kwabia Tchana, W. J. Lafferty, J. M. Flaud, L. Manceron and M. Ndao, *Mol. Phys.* **15** (2015) 1-6.
6. F. Willaert, P. Roy, L. Manceron, A. Perrin, F. Kwabia Tchana, D. Appadoo, D. McNaughton, C. Medcraft and J.Demaison, *J. Mol. Spec.* 315 (2015) 16-23.

Photoelectron Diffraction Observed in the Ionization of the $2a_1$ Orbital of Methane

S. Nandi^{*}, E. Plésiat[†], M. Patanen^{*}, C. Miron^{*}, J. D. Bozek^{*}, F. Martín[†],
D. Toffoli[‡] and P. Decleva[‡]

^{*}Synchrotron SOLEIL, Saint Aubin - BP 48, 91192, Gif-sur-Yvette CEDEX, France

[†]Universidad Autónoma de Madrid, Cantoblanco 28049, Madrid, Spain

[‡]Università di Trieste, Via L. Giorgieri 1, 34127 Trieste, Italy

ABSTRACT

Following ionization from a core level molecular orbital, the ionized electron often gets scattered in the molecular potential leading to photoelectron diffraction. The influence of this potential on valence electrons is thought to be smaller than on the core level electrons, due to the higher degree of delocalization in the former. Usually, the photoionization cross section decreases rapidly with increase in photon energy. As a result, direct observation of such modulations is very difficult when measuring the absolute cross sections. However, they can be revealed in an efficient way by measuring the photon energy dependence of the appropriate branching ratios of partial cross sections. One such possibility is to study the cross section ratios of different vibrational levels ("v-ratios") in the same electronic state of the molecule. According to the Franck-Condon principle, in absence of any diffraction and interference effects due to the molecular potential, the v-ratios should essentially be an energy independent constant. However, a significant departure from the Franck-Condon value has been noted in the photon energy dependence of the v-ratios in the case of diatomic [1-4] and polyatomic molecules [5-8].

Here, we have measured the vibrationally resolved photoelectron spectra of the symmetric stretch mode of the $2a_1^{-1}$ state of the methane molecule over a broad range of photon energies [9]. The measurements were carried out at the ultra-high resolution PLÉIADES beamline of the Synchrotron SOLEIL using a VG-Scienta R4000 spectrometer [10]. The oscillations in the experimental v-ratios are found to be qualitatively very well reproduced by the theoretical calculations. Also, we have compared the photon energy dependence of the v-ratios between the photoionization of the delocalized inner-valence $2a_1$ orbital and the localized $1a_1$ core orbital of methane. Unexpectedly, both experimental and theoretical v-ratios for photoionization of the $2a_1$ orbital exhibit a different pattern compared to that for the $1a_1$ orbital, indicating that the oscillations in the former case are modulated by other effects in addition to the diffraction of an electron from a localized emitter [9].

REFERENCES

1. D. Akoury *et al*, *Science*, **318**, 949 (2007).
2. B. Zimmermann *et al*, *Nat. Phys.*, **4**, 649 (2008).
3. S. E. Canton *et al*, *Proc. Nat. Acad. Sci. USA*, **110**, 15201 (2013).
4. M. Ilchen *et al*, *Phys. Rev. Lett.*, **112**, 023001 (2014).
5. E. Plésiat *et al*, *Phys. Rev. A*, **85**, 023409 (2012).
6. K. Ueda *et al*, *J. Chem. Phys.*, **139**, 124306 (2013).
7. M. Patanen *et al*, *J. Phys. B: At. Mol. Opt. Phys.*, **47**, 12432 (2014).
8. D. Ayuso *et al*, *J. Phys. Chem. A*, **119**, 6148 (2015).
9. S. Nandi *et al*, submitted.
10. <http://www.synchrotron-soleil.fr/Recherche/LignesLumiere/PLEIADES>

Hard X-ray Induced Multi-step Ultrafast Dissociation

O. Travnikova^a, T. Marchenko^a, R. Guillemin^a, L. Journal^a, G. Goldsztejn^a,
D. Céolin^b, K. Jänkälä^c, R. Püttner^d, H. Iwayama^e, E. Shigemasa^e,
S. Carniato^a, M.N. Piancastelli^{a,f} and M. Simon^{a,b}

^aLaboratoire de Chimie Physique-Matière et Rayonnement, UPMC & CNRS, UMR7614,
75231 Paris Cedex 05, France;

^bSynchrotron SOLEIL, Saint-Aubin, France;

^cDepartment of Physics, University of Oulu, Oulu, Finland,

^dInstitut für Experimentalphysik, Freie Universität Berlin, Berlin, Germany;

^eUltraviolet Synchrotron Orbital Radiation Facility, Institute for Molecular Science, Okazaki, Japan;

^fDepartment of Physics and Astronomy, Uppsala University, Uppsala, Sweden

ABSTRACT

Creation of deep core holes leads to extensive nuclear dynamics on a few femtosecond timescale despite the very short ($\tau \leq 1$ fs) lifetime of such states. This is because the 1st steps of the relaxation processes (*i.e.* both radiative and non-radiative decays) generate intermediate states with one and multiple holes in shallower core orbitals. As an example, ultrafast dissociation is observed in three well-distinguishable LVV Auger decay channels for HCl following Cl1s $\rightarrow\sigma^*$ excitation.

Hard X-ray photons (>1 keV) may reach deeper-lying core electrons. The electronic relaxation dynamics of deep-core-hole states is very rich. At variance with that, the very short lifetimes ($\tau \leq 1$ fs) of these states do not allow for extensive nuclear dynamics to take place before electronic relaxation occurs. However, in interpreting the hard X-ray data it is important to consider that creation of deep electron vacancies triggers a chain of relaxation events. In the HCl molecule, the leading relaxation decays of the Cl1s $\rightarrow\sigma^*$ state are Auger KLL and radiative $K\alpha$ channels, which create Cl $2p^2\sigma^*$ and Cl $2p^1\sigma^*$ intermediate states, respectively. The latter one can be created by direct soft X-ray absorption and has been well characterized [1]. It is known to undergo ultrafast dissociation (UFD) within the Cl $2p^1$ lifetime of ~ 8 fs. [1,2] The former double core-hole Cl $2p^2\sigma^*$ states are yet exotic and can be also created as “super”-shake-up satellites [3,4] of direct $2p^2$ double core-hole ionization. Recent theoretical studies show that the energy gradients of the $core^2V$ states can be very large (3 times larger compared to the $core^1V$ state in the case of H₂O [4]). Therefore, nuclear dynamics is correspondingly faster in $core^2V$ “super”-satellites.

Our experimental measurements reveal UFD phenomena in Cl $2p^2\sigma^*$ state of HCl with τ only about 3 fs. The measured LVV Auger decay spectrum of HCl clearly shows 3 possible decay channels following Cl 1s $\rightarrow\sigma^*$ excitation. Ultrafast dissociation is observed in every step of these LVV decay channels before the next electronic relaxation takes place.

The measurements were performed at GALAXIES beamline using hard X-ray photoelectron spectroscopy (HAXPES) end-station [5,6].

The observed results are supported by *ab initio* theoretical calculations.

Multi-step ultrafast nuclear dynamics induced by hard X-rays is predicted to be a rather general phenomenon.

REFERENCES

- [1] O. Björneholm *et al.* 1997 *Phys. Rev. Lett.* **79**, 3150
- [2] O. Travnikova *et al.* 2013 *J. Phys. Chem. Lett.* **4**, 2361
- [3] F. Penent *et al.* 2015 *J. Electron Spectrosc. Relat. Phenom.* **204B**, 303
- [4] S. Carniato *et al.* 2015 *J. Chem. Phys.* **142**, 014307
- [5] D. Céolin *et al.* 2013 *J. Electron Spectrosc. Relat. Phenom.* **190**, 188 □
- [6] M. Simon *et al.* 2014 *Nat. Comm* **5**, 4069

First High-resolution Analysis of Phosgene $^{35}\text{Cl}_2\text{CO}$ and $^{35}\text{Cl}^{37}\text{ClCO}$ Fundamentals in the 250 - 480 cm^{-1} Spectral Region

M. Ndao^a, F. Kwabia Tchana^a, L. Manceron^b, A. Perrin^a,
J. M. Flaud^a, L. Coudert^a, W.J. Lafferty^c

^aLaboratoire Interuniversitaire des Systèmes Atmosphériques (LISA), UMR CNRS 7583, Universités Paris Est Créteil et Paris Diderot, Institut Pierre Simon Laplace, 61 Avenue du Général de Gaulle, 94010 Créteil Cedex, France

^bLigne AILES, Synchrotron SOLEIL, L'Orme des Merisiers, F-91192 Gif-sur-Yvette, France, et MONARIS, CNRS UMR 8233, 4 Place Jussieu, F-75252 Paris Cedex, France

^cSensor Science Division, National Institute of Standards and Technology (NIST), Gaithersburg, MD 20899-8440, USA

ABSTRACT

Monitoring the abundance and distribution of dominant chemical compounds is critical for understanding the photochemistry and dynamics of planetary atmospheres. Phosgene (COCl_2) is relatively more abundant in the stratosphere, where it has a lifetime of several years, but is also present in the troposphere in spite of a shorter lifetime (seventy days). Thus, monitoring its concentration by remote sounding of the upper atmosphere is of importance, all the more so that some of its strong infrared absorptions, occurring in the important 8-12 μm atmospheric window, hinder the correct retrieval of Freon-11 concentration profiles [1]. Indeed, the useful infrared absorptions of this compound, a reference for ozone depleting substances, occur in the same spectral region.

Phosgene, presents two fundamentals in the 250 - 480 cm^{-1} spectral region, with the lowest (ν_3) near 285 cm^{-1} . These are responsible for hot bands, not yet analysed but of great importance for accurate modeling of the 5.47 and 11.75 μm spectral regions (that correspond to the absorptions of the ν_1 and ν_5 bands of phosgene) and the correct retrieval of Freon-11 atmospheric absorption profiles.

For this purpose high-resolution absorption spectra of phosgene has been recorded at 0.00102 cm^{-1} resolution in the 250–480 cm^{-1} region by Fourier transform spectroscopy at synchrotron SOLEIL. Due to the spectral congestion, the spectra have been recorded at low temperature (197 K) using a 93.15 m optical path length cryogenic cell [2]. This enables the first detailed far-infrared analyzes of the ν_3 and ν_6 bands of the $^{35}\text{Cl}_2\text{CO}$ and $^{35}\text{Cl}^{37}\text{ClCO}$ isotopologues of phosgene. Using a Watson-type Hamiltonian, it was possible to reproduce the upper state rovibrational infrared energy levels to within the experimental accuracy [3,4].

REFERENCES

- [1] G. Toon, J.F. Blavier, B. Sen and B.J. Drouin, *Geophys. Res. Lett.*, **28/14** (2001) 2835.
 [2] F. Kwabia Tchana, F. Willaert, X. Landsheere, J.-M. Flaud, L. Lago, M. Chapuis, P. Roy and L. Manceron, *Rev. Sci. Inst.*, **84** (2013) 093101.
 [3] J.-M. Flaud, F. Kwabia Tchana, W.J. Lafferty, L. Manceron and M. Ndao, *Journal of Molecular Spectroscopy*, **in press** (2015).
 [4] M. Ndao, A. Perrin, F. Kwabia Tchana, L. Manceron, J.-M. Flaud and L. Coudert, *Journal of Molecular Spectroscopy*, **accepted** (2015).

Probing the VUV Photoionisation of Methyl Radicals Produced in a Pyrolysis and a Reactor Sources

F. Holzmeier¹, M. Lang¹, A. Röder¹, I. Fischer¹, J-C. Loison²
 C. Fittschen³, B. Gans⁴, J. Krüger⁵, G. Garcia-Macias⁵,
 B. Cunha de Miranda⁶, A. Lopes⁷, C. Romanzin⁷, C. Alcaraz⁷

¹IPTC, Julius-Maximilians Univ., Würzburg – Germany ;

²ISM, UMR5255 CNRS-Univ. Bordeaux 1, Talence;

³PC2A, UMR8522 CNRS-Univ. de Lille 1, Villeneuve d'Ascq;

⁴ISMO, UMR8214 CNRS-Univ. Paris-Sud & Paris-Saclay, Orsay;

⁵Synchrotron SOLEIL, L'Orme des merisiers, St Aubin;

⁶LCPMR, UMR7614 CNRS-Univ. Pierre et Marie Curie, Paris;

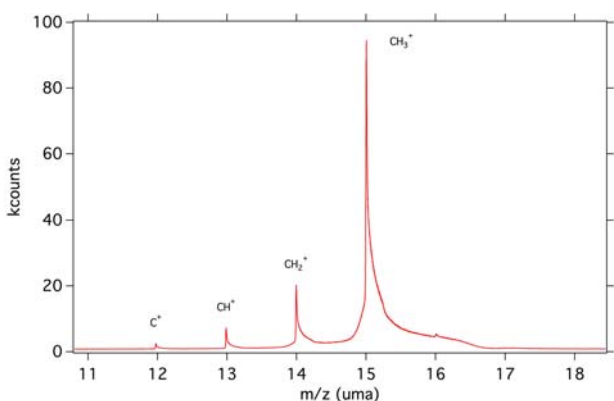
⁷LCP, UMR8000 CNRS-Univ. Paris-Sud & Paris-Saclay, Orsay

ABSTRACT

The methyl carbocation is a reactive species which has been detected in a lot of gaseous environments fed by high energy sources such as the interstellar medium, planetary ionospheres as well as laboratory plasmas for methane conversion into higher hydrocarbons for instance. His reactivity with several hydrocarbons is well-known for the ground state, whereas only few data about the reactivity of excited CH_3^+ ions are available in the literature although excited species are common in planetary atmospheres and plasmas.

Here, we report on the production of excited CH_3^+ ions via VUV photoionisation of methyl radicals in the 9.8-15 eV energy range on the DESIRS beamline, to characterize the vibrational [1] and electronic excitation of the methyl cation, with the motivation of studying its reactivity in future experiments. The goal was also to compare two complementary sources of the neutral methyl radicals which were formed in a beam either by: i. pyrolysis of CH_3NO_2

or CH_3NNCH_3 precursors in a heated SiC tube or ii. reaction of F atoms (produced in a F_2/He microwave discharge) with methane (CH_4) in a fast flow tube reactor (SYNCHROKIN project developed by J.-C. Loison et al [2]). We also wanted to take advantage of the new ion imaging capabilities of the DELICIOUS III spectrometer [3] to distinguish CH_3^+ ions formed either by photoionisation of CH_3 or by dissociative photoionisation of the remaining precursors and impurities. With the fast flow reactor source, we managed



to produce, in addition to the CH_3 radical, three very important radicals, C, CH and CH_2 as shown in Fig. 1.

Fig. 1: TOF mass spectrum of the C^+ , CH^+ , CH_2^+ and CH_3^+ cations formed by VUV photoionisation (in the 9.8-12 eV range) of C, CH, CH_2 and CH_3 radicals simultaneously produced by four successive H-abstractions on CH_4 by F atoms in the fast flow reactor ($\text{F} + \text{CH}_x \rightarrow \text{CH}_{x-1} + \text{HF}$).

Acknowledgments: For technical help from J.-F. Gil (DESIRS) and for financial support from ANR under the grant ANR-12-BS08-0020-02 (SYNCHROKIN project), RTRA “Triangle de la Physique” (RADICAUX project), and French Planetology Program (PNP).

REFERENCES

- 1 B.K. Cunha de Miranda, *et al.*, J. Phys. Chem. A **114**, 4818 (2010); B.K. Cunha de Miranda, Cotutelle PhD Thesis, Université Paris-Sud 11 (Orsay) et Université Fédérale Fluminense (Niteroi), 2011.
- 2 G.A. Garcia, *et al.*, J. Chem. Phys. **142** (2015); G.A. Garcia, *et al.*, J. Electron Spectrosc. Relat. Phenom. **203** 25-30 (2015).
- 3 G.A. Garcia, *et al.*, Rev. Sci. Instrum. **84** (5), 053112 (2013).

Threshold Photoelectron Spectra (TPES) Applied to the OH + Propene and OH + Isoprene Reactions

J-C. Loison

Institut des sciences moléculaires - Talence (France)

ABSTRACT

The OH reaction with alkenes is of great importance to atmospheric chemistry where the alkenes are removed by reactions with OH, NO₃ and O₃ radicals. The OH reaction with alkenes is thought to proceed mainly via OH radical addition to the double bond below 500K, the H atom abstraction is a minor channel at room temperature and only becomes the dominant channel above 700K. A critical aspect of the reactions of OH radicals with alkenes is the site-specific addition of OH radicals to the double bond as the different adducts will lead to different products in the atmospheric conditions. Some previous measurements have been performed to determine the branching ratio using the combination of a flow reactor technique in combination with molecular beam sampling mass spectrometry using 30 eV electron beam ionization method (Peeters *et al.* 2007) or 10.5 eV VUV photons (Loison *et al.* 2010). These study determined the primary hydroxy adduct distributions of the reaction of OH radicals with several alkenes by using the different fragmentation patterns of the site-specific adduct ions. However there remain large uncertainties due to ion fragmentation, and comparisons with previous measurements (associated with considerable uncertainties) for the OH + propene (Feltham *et al.* 2000) and OH + 1-butene (Hoyermann & Sievert 1983, Feltham *et al.* 2000) reactions are not entirely concordant. Moreover there is no such data for OH + Isoprene reaction, which is by far the most important reaction among the OH + alkenes ones in the atmosphere.

We present the results of the OH + propene and OH + Isoprene reaction obtained at SOLEIL using the recently built ANR SynchroKin apparatus. This apparatus consists in a microwave discharge flow tube coupled with a double imaging electron/ion coincidence device and vacuum ultraviolet (VUV) synchrotron radiation. The OH radicals were generated in a continuous manner by the F + H₂O reactions, F being generated through the microwave discharge of F₂ in He in an alumina tube, which will be subsequently mixed with the H₂O. The study of the photoelectron spectrum provides a high selectivity and yields isomer identification of the two reactions as a function of time. We were able to precisely identify the various adducts (two for OH + propene and four for OH + Isoprene) through the help of ab-initio calculations.

REFERENCES

- Feltham E.J., Almond M.J., Marston G., Wiltshire K.S., Goldberg N., 2000, Spectrochim. Acta A, 56, 2589
Hoyermann K., Sievert R., 1983, Ber. Bunsenges. Phys. Chem., 87, 1027
Loison J.C., Daranlot J., Bergeat A., Caralp F., Mereau R., Hickson K.M., 2010, J. Phys. Chem. A, 114, 13326
Peeters J., Boullart W., Pultau V., Vandenberg S., Vereecken L., 2007, J. Phys. Chem. A, 111, 1618

Multiple Photoionization Processes of Alkali Vapors

J. Palaudoux^{1,2}, P. Lablanquie^{1,2}, L. Andric^{1,2}, M. A. Khalal^{1,2},
F. Penent^{1,2}, J.-M. Bizau^{3,4}, D. Cubaynes^{3,4}, K. Jänkälä⁵ and M. Huttula⁵

¹ UPMC, Université Paris 06, LCPMR, 11 rue P. & M. Curie, 75231 Paris cedex 05, France

² CNRS, LCPMR (UMR 7614), 11 rue P. & M Curie, 75231 Paris Cedex 05, France

³ ISMO, CNRS UMR 8214, Université Paris-Sud, Bâtiment 350, F-91405 Orsay cedex, France

⁴ Synchrotron SOLEIL, L'Orme des Merisiers, Saint Aubin, F-91192 Gif-sur-Yvette cedex, France

⁵ Department of Physics, University of Oulu, P.O. Box 3000, 90014 Oulu, Finland

ABSTRACT

The study of multiple photoionization of isolated atoms and molecules by a single photon gives information on electron correlations and on involved mechanisms. After an extensive study of such processes in Ar and Kr rare gases, we have extended our investigations to K and Rb alkali atoms to understand the role of the additional electron: $K=[Ar]4s$: $Rb=[Kr]5s$, in multiple photoionization process.

The experiments were carried out at PLEIADES and SEXTANTS beam-lines. The HERMES (High Energy Resolution Multi Electron Spectrometer) setup [1-2] was used. It is a 2m long magnetic bottle time of flight electron spectrometer allowing the detection in coincidence of all the electrons (up to 5) emitted in multiple photoionization process (valence double ionization, core-valence DI, inner-shell ionization followed by Auger decay, ...).

An important difference between (K ; Rb) and (Ar ; Kr) is that inner-valence $K(3s)$ and $Rb(4s)$ ionization leads to Auger decay with a emission of a low energy Auger electron while this process is not accessible in Ar and Kr. We have investigated in details the $K 3s^{-1}$ decay and the peculiar PCI (Post Collision Interaction) arising close to the $3s$ threshold [3].

In K atom, direct or sequential paths following $2s^{-1}$ decay, and core-valence $2p^{-1}3l^{-1}$ double ionization present strong similarities with the similar process in Ar [2]. The coupling of the outer $4s$ electron multiplies however the number of possible states and makes the subsequent Auger decay more rich.

In both K and Rb atoms, the Auger spectra following inner-shell ionization does not result only from the decay of the inner-shell holes ($2p_{3/2,1/2}$ in K or $3d_{3/2,5/2}$ in Rb) because the outer electron ($4s$ in K and $5s$ in Rb) can be noticeably excited in the ionization process giving rise to multiple satellite states. The Auger decay of the main states and of all satellites can be filtered out very efficiently compared to other experiments [4]. Double Auger decay has also been observed as in Ar [5] and Kr atom [6].

The HERMES experiment was also modified for the last SEXTANTS beam-time (November 2015) in order to test a new configuration of magnet (hollow magnet) and an ion spectrometer, installed just behind the magnet. First results of coincidences between ions and electrons with our spectrometer will be presented in the Rb case.

REFERENCES

1. F. Penent *et al.*, PRL **95**, 083002, (2005).
2. S.-M. Huttula *et al.*, PRL **110**, 113002 (2013) ; P. Lablanquie *et al.*, PCCP **13**, 18355 (2011).
3. J. Palaudoux *et al.*, PRA **92**, 012510 (2015).
4. K. Jänkälä *et al.*, PRA **74**, 062704, (2006).
5. P. Lablanquie *et al.*, JESRP **156-158**, 51 (2007).
6. J. Palaudoux *et al.*, PRA **82**, 043419 (2010).

Frequency Analysis of the ν_2 Band of SO_2F_2 using the C_{2v} Top Data System

F. Hmida^{1,4}, M. Faye³, B. Grouiez¹, M. Rotger¹,
V. Boudon², L. Manceron³, H. Aroui⁴

¹GSMA, UMR CNRS 7331, Université de Reims Champagne Ardenne, Moulin de la Housse
B.P. 1039, F-51687 Reims Cedex 2, France

²Lab. ICB, UMR 6303 CNRS-Univ. Bourgogne Franche-Comté, 9 Av Alain Savary,
BP 47 870, F-21078 Dijon Cedex, France

³Synchrotron Soleil Ligne AILES, BP 48, 91192 Cedex Gif-sur-Yvette, France and MONARIS, UMR
8233 CNRS-UPMC, case 49, 4 place Jussieu, 75252 Cedex Paris, France

⁴LDMMP, Ecole Nationale Supérieure d'Ingénieurs de Tunis, 5 Av Taha Hussein, 1008 Tunis, Tunisia

ABSTRACT

Sulfuryl fluoride SO_2F_2 is a quasi-spherical top molecule, which can be considered as derived from tetrahedral SO_4^{2-} sulfate ion. For this reason, an oriented tensorial formalism adapted to almost tetrahedral XY_2Z_2 asymmetric tops with C_{2v} symmetry has been developed by Rotger *et al.*¹. This model has been already used to analyze the ground state² and the ($\nu_3 / \nu_7 / \nu_9$) bending triad³. We present here an application of this model to the analysis of the ν_2 band, in comparison with a previous study based on Watson's Hamiltonian⁴.

A new high resolution infrared spectrum of SO_2F_2 in the region of 830 – 865 cm^{-1} has been recorded at 165 K using a multi-pass cell⁵ coupled to a high-resolution Bruker IFS 125 interferometer with a spectral resolution of 0.00102 cm^{-1} located at the AILES beamline of the SOLEIL Synchrotron.

To calculate the high-resolution spectrum of the ν_2 band, an Hamiltonian operator based on the vibrational extrapolation has been developed respectively to the fourth and sixth order for the ground state and the excited ν_2 state. A total of 1715 lines corresponding to ν_2 have been assigned and fitted in frequency with a global root mean square deviation (RMS) of $0.199 \times 10^{-3} \text{ cm}^{-1}$.

REFERENCES

- [1] M. Rotger, V. Boudon and M. Loëte, *Journal of Molecular Spectroscopy* **216**, 297-307 (2002).
[2] M. Rotger, V. Boudon, M. Loëte, L. Margulès, J. Demaison, H. Mader, G. Winnewisser, H.S.P. Müller, *Journal of Molecular Spectroscopy*, **222**, 172–179 (2003).
[3] M. Rotger, V. Boudon, M. Loëte, N. Zvereva Loëte, L. Margulès, J. Demaison, I Merke, F. Hegelung, H. Bürger, *Journal of Molecular Spectroscopy*, **238**, 145–157 (2006).
[4] I. Merke *et al.*, *Journal of Molecular Structure* **795**, 185-189 (2006)
[5] F. Kwabia Tchana, F. Willaert, X. Landsheere, J.M. Flaud, L. Lago, M. Chapuis, P. Roy, L. Manceron, *Review of Scientific Instruments*, **84**, 093101 (2013)

Electron-nuclear Dynamics in Resonant X-ray Raman Scattering of CO Molecule

R. Couto^{1,2}, M. Guarise³, N. Alessandro⁴, N. Jaouen⁴, G. Chiuzbian⁵,
J. Luning⁵, V. Ekholm⁶, J.-E. Rubensson⁶, C. S  the⁷, F. Hennies⁷,
V. Kimberg¹, F. Guimar  es², H.   gren¹, F. Gel'mukhanov¹,
L. Journal⁵ and M. Simon⁵

¹Theoretical Chemistry & Biology, Royal Institute of Technology, Stockholm, Sweden

²Instituto de Quimica, Universidade Federal Goias, Campus Samambaia, -Gonia, Goias, Brazil

³Laboratorio Nacional Luz Sincrotron, 10000 Campinas, Brazil

⁴Synchrotron SOLEIL, l'Orme des Merisiers, Saint-Aubin, Gif-sur-Yvette Cedex, France

⁵Sorbonne Universit  s, UPMC Univ Paris 6, UMR7614, Laboratoire de Chimie Physique -
Mati  re et Rayonnement, Paris, France

⁶Department of Physics and Astronomy, Uppsala University, Uppsala, Sweden

⁷MAX IV Laboratory, Lund University, Lund, Sweden

ABSTRACT

High-resolution Resonant Inelastic Soft X-ray Scattering (RIXS) measurements with vibrational resolution of isolated CO molecules after O 1s \rightarrow 2 π photoexcitation are presented and analyzed using state of the art ab-initio calculations based on the wave packet propagation formalism and Potential Energy curves ab-initio calculations [1].

We observed new strong features in RIXS spectra in the spectral emission band around E₁-E₂ = 13 eV energy loss. The experimental spectrum exhibits a three-peak structure, varying with excitation energy E₁, which is reproduced satisfactory when two-electron one photon (TEOP) transitions and coupling between 'allowed' |4 $\sigma^{-1}2\pi^1$ > and 'forbidden' (|5 $\sigma^{-1}3p_\pi^1$ > and |5 $\sigma^{-1}3d_\pi^1$ >) states are taken into account. States are assigned from low resolution spectra previously published [2, 3]. One-electron-one-photon model only leads to a poor agreement with the experimental results. In this energy range, RIXS mechanism should be based on electron-nuclear dynamics where electronic and nuclear motions are coupled via vibronic coupling beyond the Born-Oppenheimer approximation [4] and opening TEOP decay channels.

Experimental high-resolution RIXS Spectra measurements were performed at the SEXTANTS beamline using the Soft X-ray emission spectrometer AEHRA end-station [5]. A gas cell has been used to maintain CO gas at a pressure of 1 bar while keeping the chamber in the high 10⁻⁸ mbar.

Experimental RIXS combined with accurate ab initio simulations allows deep understanding of the coupled electron-nuclear molecular dynamics in the excited states showing the large potential of RIXS technique for advanced study of highly excited states of neutral molecules.

REFERENCES

1. Rafael C. Couto et al., submitted.
2. Skytt, P., Glans, P., Gunnelin, K., Guo, J. & Nordgren, Phys. Rev. A 55, 146–154 (1997).
3. Skytt, P., Glans, P., Gunnelin, K., Guo, J. & Nordgren, Phys. Rev. A 55, 134–145 (1997).
4. Gel'mukhanov, F. &   gren, H. Resonant X-ray Raman Scattering. Phys. Rep. 312, 87–330 (1999).
5. S.G. Chiuzbaian, C.F. Hague, A. Avila, R. Delaunay, N. Jaouen, M. Sacchi, et al., Rev. Sci. Instrum., 85, (2014) 043108 (2014).

Photoionisation VUV de Molécules Prébiotiques : Spectroscopie et Réactivité

A. Bellili,¹ M. Schwell,² Y. Bénilan,² N. Fray,² M.-C. Gazeau,² M. Mogren Al-Mogren,³ J.-C. Guillemin,⁴ L. Poisson,⁵ et M. Hochlaf¹.

1. Laboratoire Modélisation et Simulation Multi Echelle, MSME UMR 8208 CNRS, Université Paris-Est, 5 bd Descartes, 77454 Marne-la-Vallée, France

2. Laboratoire Interuniversitaire des Systèmes Atmosphériques (LISA), UMR 7583 CNRS, Institut Pierre et Simon Laplace, Universités Paris-Est Créteil et Paris Diderot, 61 Avenue du Général de Gaulle, 94010 Créteil, France

3. Chemistry Department, Faculty of Science, King Saud University, P.O. Box 2455, Riyadh 11451, Kingdom of Saudi Arabia

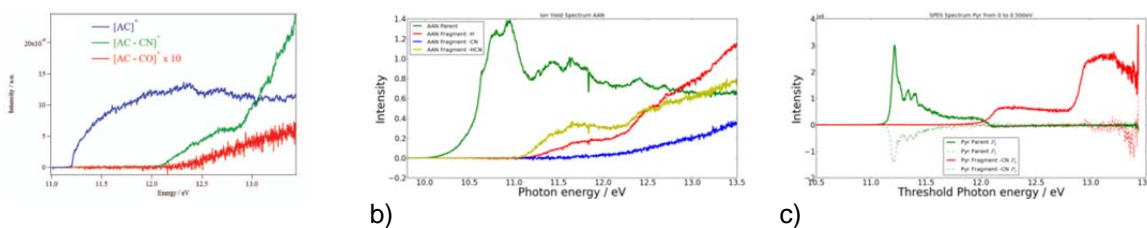
4. Institut des Sciences Chimiques de Rennes, Ecole Nationale Supérieure de Chimie de Rennes, CNRS, UMR 6226, Allée de Beaulieu, CS 50837, 35708 Rennes Cedex 7, France

5. Laboratoire Francis Perrin, CNRS URA 2453, CEA, IRAMIS, Laboratoire Interactions Dynamique et Lasers, Bât 522, F-91191 Gif/Yvette, France

ABSTRACT

Dans ce travail nous nous sommes intéressés à l'étude théorique et expérimentale de la photoionisation dissociative de molécules prébiotiques et à la spectroscopie des ions formés. On traitera le cas de Pyruvonnitrile (NC-C(O)CH_3) et de Aminoacétonitrile ($\text{H}_2\text{N-CH}_2\text{CN}$) [1]. Ces deux molécules ont un intérêt astrophysique, ces derniers sont inspirés de la réaction de Strecker [2] qui est à l'origine d'un scénario réaliste de formation d'acides aminés dans des conditions interstellaires. L'acétyl cyanure ($\text{H}_2\text{N-CH}_2\text{CN}$) a été détecté dans l'espace interstellaire et la Pyruvonnitrile (ou acétyl cyanure, AC, NC-C(O)CH_3) n'a pas été détectée encore.

La partie expérimentale a été effectuée en utilisant le rayonnement VUV de la ligne de lumière DESIRS du Synchrotron SOLEIL et le spectromètre DELICIOUS3 (électronique / imagerie d'ions). Les spectres PEPICO et SPES (spectroscopie de photoélectrons lents [3]) ont été mesurés. Les résultats sont présentés dans la figure ci-dessous.



a) Figure 1 : (a) spectre PEPICO de la Pyruvonnitrile [4] ; (b) Spectre PEPICO de de l'acétyl cyanure [5] ; (c) Spectre SPES de la Pyruvonnitrile

La seconde partie de ce travail consiste à analyser les spectres à l'aide de calculs ab-initio de la chimie quantique où on a déterminé la spectroscopie de l'état ionique, le spectre de ces états électroniques excités et les énergies d'apparence des fragments. Des travaux sont en cours afin d'interpréter les effets de la polarisation observés dans le spectre SPES de la Pyruvonnitrile (Figure1 (c)). Nous concluons sur la possibilité de réaliser des études résolues en temps pour sonder la dynamique de fragmentation des ions formés.

REFERENCES

- [1] A. Belloche, K.M. Menten, C. Comito, H.S.P. Müller, P. Schilke, J. Ott, S. Thorwirth, C. Hieret, *A&A*, 482, 179-196 (2008).
 [2] Danger et al, 2011 *Astrophys J* 735 (2011), A47, 1-9.
 [3] J.C. Pouilly, J.P. Schermann, N. Nieuwjaer, F. Lecomte, G. Grégoire, C. Desfrancois, G. A. Garcia, L. Nahon, D. Nandi, L. Poisson and M. Hochlaf, *Phys Chem Chem Phys*. 12 (2010) 3566.
 [4] A. Bellili, M. Schwell, Y. Bénilan, N. Fray, M.-C. Gazeau, M. Mogren Al-Mogren, J.C. Guillemin, L. Poisson, M. Hochlaf, *J. Chem Phys*. 141 (2014) 134311
 [5] A. Bellili, M. Schwell, Y. Bénilan, N. Fray, M.-C. Gazeau, M. Mogren Al-Mogren, J.C. Guillemin, L. Poisson, M. Hochlaf, *J. Mol. Spectrosc.*, 2015, in press, special issue: "Spectroscopy with Synchrotron Radiation"

PARALLEL SESSION

Electronic & Magnetic Property of Matter, Surfaces and Interfaces

ECOLE POLYTECHNIQUE – FAURE Auditorium

Chairpersons: Marie d'ANGELO and Antonio TEJEDA

- IT-09 Multimagnetic core-shell nanoparticles: Towards a fine control of the magnetic anisotropy
V. Dupuis
- OC-28 Probing magnetization dynamics by time-resolved X-ray holography with extended references
F.Y. Ogrin
- OC-29 Symmetry of the Fermi surface and evolution of the electronic structure across the paramagnetic-helimagnetic transition in MnSi/Si(111)
A. Nicolaou
- OC-30 k dependence of the spin polarization in Mn₅Ge₃/Ge(111) thin films
W. Ndiaye
- OC-31 Calculation of XMCD and XNCD at the K-edge from first principles
N. Mas
- IT-10 Interfaces between strongly correlated oxides : Controlling charge transfer and induced magnetism by hybridization
M. Bibes
- OC-32 Structure and growth mechanisms of silicene layers on silver surfaces
G. Prevot
- OC-33 Bandgap and structural periodicities of buffer layer graphene
M.N. Nair
- OC-34 Studying chemical bonding between NTCDA and noble metal surfaces by photoelectron spectroscopy and scanning tunneling microscopy
Y. Tong
- OC-35 Mueller ellipsometer with Synchrotron light
E. Garcia-Caure

Multimagnetic Core-shell Nanoparticles : Towards a Fine Control of the Magnetic Anisotropy

V. Dupuis¹, V. Gavrilov-Isaac¹, Y. Prado^{1,8}, N. Daffé^{1,2,4}, S. Neveu¹,
V. Cabuil¹, J. Fresnais¹, A. Gloter³, T. Georgelin^{5,6}, N. Yaacoub⁷,
J-M. Grenèche⁷, F. Choueikani⁴, E. Otero⁴, P. Ohresser⁴, D. Taverna²,
M-A. Arrio², P. Saintavit^{2,4}, C. Cartier-dit-Moulin^{8,9}, B. Fleury^{8,9},
L. Lisnard^{8,9}

1-Sorbonne Universités, UPMC Univ Paris 06, UMR 8234, PHENIX, F-75005, Paris, France.

2-Institut de Minéralogie, de Physique des Matériaux et de Cosmochimie, UMR 7590, CNRS, UPMC, IRD, MNHN, F-75005, Paris, France.

3-Laboratoire de Physique des Solides, CNRS UMR 8502, Université Paris-Sud 11, 91405 Orsay, France

4-Synchrotron SOLEIL, L'Orme des Merisiers, Saint-Aubin - BP 48, 91192 Gif-sur-Yvette, France

5-Sorbonne Universités, UPMC Univ Paris 06, UMR 7197, LRS, F-94200 Ivry-sur-Seine, France 6-CNRS, UMR 7197, Laboratoire de Réactivité de Surface, F-94200, Ivry-sur-Seine, France

7-LUNAM, Université du Maine, Institut des Molécules et Matériaux du Mans CNRS UMR-6283, F-72085, Le Mans, France

8-Sorbonne Universités, UPMC Univ Paris 06, UMR 8232, IPCM, F-75005, Paris, France

9-CNRS, UMR 8232, Institut Parisien de Chimie Moléculaire, F-75005, Paris, France.

ABSTRACT

Magnetic nanoparticles, thanks to their easy and cheap synthesis and their high sensitivity to magnetic fields are increasingly used in wide variety of applications such as permanent magnets, rotating seals, magnetic dampers, magnetic recording media and even nanomedicine (contrast agents in MRI, therapeutic agents in tumor hyperthermia and drug delivery). The optimization of existing applications, as well as the emergence of new ideas, requires an increased control of the magnetic properties such as the magnetic anisotropy.

In this presentation, I will report on our recent work to control the magnetic anisotropy at the nanoscale by combining different magnetic element/material within a magnetic nanoparticle. Two examples will be discussed: i) the coupling of magnetically 'hard' molecular complexes at the surface of a magnetically soft nanoparticle [1] and ii) the growth of nanoshells of hard and soft materials on the surface of a soft core nanoparticle [2]. In each case, I will show how the X ray magnetic circular dichroism (XMCD) technique available at the DEIMOS beamline, thank to its element sensitivity and combined with other characterization techniques, helps us to understand the behavior of such complex nanostructures.

REFERENCES

- [1] Y. Prado, N. Daffe, A. Michel, T. Georgelin, N. Yaacoub, J-M. Grenèche, F. Choueikani, E. Otero, P. Ohresser, M.-A. Arrio, C. Cartier-dit Moulin, P. Saintavit, B. Fleury, V. Dupuis, L. Lisnard, and J. Fresnais. Enhancing the magnetic anisotropy of maghemite nanoparticles via the surface coordination of molecular complexes. *Nat Commun*, 6, 12 2015.
- [2] Gavrilov-Isaac, V., Neveu, S., Dupuis, V., Taverna, D., Gloter, A. and Cabuil, V. (2015), Synthesis of Trimagnetic Multishell $\text{MnFe}_2\text{O}_4@ \text{CoFe}_2\text{O}_4@ \text{NiFe}_2\text{O}_4$ Nanoparticles. *Small*, 11: 2614–2618. doi:10.1002/sml.201402845.

Probing Magnetization Dynamics by Time-resolved X-ray Holography with Extended References

F.Y. Ogrin¹, E. Burgos Parra¹, N. Bukin¹, M. Dupraz², G. Beutier²,
S. Sani³, H. Popescu⁴, S.A. Cavill⁵, J. Åkerman^{6, 3}, N. Jaouen⁴,
and G. van der Laan⁷

1. School of Physics and Astronomy, University of Exeter, Exeter, Devon, United Kingdom.

2. SIMaP, Grenoble-INP, CNRS, Grenoble, France.

3. Material Physics, KTH- Royal Institute of Technology, Kista, Sweden.

4. SOLEIL synchrotron, Paris, France.

5. Department of Physics, University of York, York, North Yorkshire, United Kingdom.

6. The Physics Department, University of Gothenburg, Gothenburg, Västra Götaland, Sweden.

7. Diamond Light Source Ltd., Didcot, Oxfordshire, United Kingdom.

ABSTRACT

Vortex closure domains are fascinating nanoscopic magnetic structures. As well as being exemplary model objects – in many ways the vortices behave like classical harmonic oscillators – they are versatile elementary components, which can perform a number of functions ranging from non-volatile high-density data storage to microwave generation [1-3]. Here we demonstrate our recent studies of vortex structures in thin film permalloy elements and single layer spin transfer oscillator (SL-STO) [4] using a recently developed time-resolved soft x-ray imaging technique HERALDO [5-6], which can provide high spatial resolution as well as a high level of immunity to mechanical and thermal drifts. In particular, we imaged the magnetic states of nano-contact SL-STO produced by the applied DC current. The experiments were performed at the beamline SEXTANTS, where spatial resolution down to 15 nm could be achieved. The results showed that at currents above 20 mA a magnetic contrast indicative of vortex formation could be observed. The vortex chirality correlated with the current polarity. As well as the vortex structure a magnetic contrast coinciding with the rim of the aperture was also observed. We speculate that both types of contrast are related to the effect of the Oersted field generated by the current.

REFERENCES

1. J. Slonczewski, J., *MMM*, 159,1–2, L1–L7, (1996).
2. V.S. Pribiag et al., *Nature Physics*. 3, 498. (2007)
3. A. Dussaux et al., *Nature Communications*. 1 (2010).
4. D. Berkov *et al.*, *Phys. Rev. B*, **80**, no. 6, (2009) 064409.
5. T. Duckworth et al., *Optics Express*, 19, 16223 (2011).
6. T. Duckworth et al., *N. J. Phys.*, 15 023045 (2013)

Symmetry of the Fermi Surface and Evolution of the Electronic Structure across the Paramagnetic-helimagnetic Transition in MnSi/Si(111)

A. Nicolaou*¹, M. Gatti^{1,2,3}, E. Magnano⁴, P. Le Fèvre¹, F. Bondino⁴,
F. Bertrand¹, A. Tejada¹, M. Sauvage-Simkin¹, A. Vlad¹, Y. Garreau^{1,5},
A. Coati¹, N. Guérin⁶, F. Parmigiani^{7,8,9}, A. Taleb-Ibrahimi¹

¹ Synchrotron SOLEIL, L'Orme des Merisiers, Saint-Aubin, BP 48, 91192 Gif-sur-Yvette, FR

² Laboratoire des Solides Irradiés, École Polytech., CNRS-CEA/DSM, 91128 Palaiseau, FR

³ European Theoretical Spectroscopy Facility (ETSF)

⁴ CNR-IOM, Laboratorio TASC, S.S. 14 Km 163.5, 34149 Basovizza, Trieste, IT

⁵ MPQ, Université Denis Diderot Paris VII, Bât. Condorcet, 75205 Paris Cedex 13, FR

⁶ Department of Chemistry and Biochemistry, Univ. of Bern, Freiestrasse 3, 3012 Bern, CH

⁷ Elettra-Sincrotrone Trieste, Strada Statale 14, 34149 Basovizza, Trieste, IT

⁸ Università degli Studi di Trieste, Via A. Valerio 2, 34127 Trieste, IT

⁹ International Faculty - University of Cologne, DE

ABSTRACT

Among the family of transition metal monosilicides (MnSi, FeSi, CoSi), MnSi is a paradigmatic case for its exotic magnetic properties not accounted for by standard models of magnetism [1, 2]. At $T_C \sim 40$ K it shows a phase transition from a paramagnetic metal state to a helimagnetic order. The effective magnetic moment μ_{eff} of $2.27\mu_B/\text{Mn}$ drops to $\mu_{\text{sat}} = 0.4\mu_B/\text{Mn}$ in the saturated ferromagnetic phase, a value which is significantly smaller than the one of $1\mu_B/\text{Mn}$ predicted by local-density approximation (LDA) calculations [3]. Moreover, signatures of strong correlations are suggested by Haas-van Alphen experiments and by the non-Drude behavior of the optical conductivity [4,5].

By performing angle-resolved photoemission spectroscopy (ARPES) on high quality epitaxial MnSi/Si(111) crystals, we have disclosed the nesting properties of the Fermi surface (FS), not accounted for by the state-of-the-art band structure calculations, and the evolution of the electronic structure through the magnetic transition. This latter reveals the persistence of d-bands splitting in the paramagnetic phase and the appearance of sharp quasiparticles only below T_C [6].

Henceforth, we propose here that the nesting properties of the MnSi Fermi surface, by affecting the quasiparticles lifetime through the development of strong magnetic fluctuations, govern the magnetic interactions in this compound.

REFERENCES

1. N. Manyala *et al.* Nature 404, 581 (2000).
2. N. Manyala *et al.* Nature 454, 976 (2008).
3. S. Mühlbauer *et al.* Science 323, 915 (2009)
4. L. Taillefer *et al.* J. Magn. Magn. Mater. **54-57**, 957 (1986).
5. F. P. Mena *et al.* Phys. Rev. B **67**, 241101 (2003).
6. A. Nicolaou *et al.* Phys. Rev B **92**, 081110(R) (2015)

k Dependence of the Spin Polarization in Mn₅Ge₃/Ge(111) Thin Films

**W. Ndiaye¹, M. C. Richter^{1,5}, J.-M. Mariot^{2,3}, P. De Padova⁴, W. Wang^{1,6},
O. Heckmann^{1,5}, A. Taleb-Ibrahimi⁷, P. Le Fèvre⁸, F. Bertran⁸, C. Cacho⁹,
M. Leandersson¹⁰, T. Balasubramanian¹⁰, A. Stroppa^{11,12}, S. Picozzi^{11,12}
and K. Hricovini^{1,5}**

¹*Laboratoire de Physique des Matériaux et des Surfaces, Université de Cergy-Pontoise,
5 mail Gay-Lussac, 95031 Cergy-Pontoise, France*

²*Sorbonne Universités, UPMC Univ Paris 06, UMR 7614, Laboratoire de Chimie Physique–Matière
et Rayonnement, 75231 Paris Cedex 05, France*

³*CNRS, UMR 7614, Laboratoire de Chimie Physique–Matière et Rayonnement,
11 rue Pierre et Marie Curie, 75231 Paris Cedex 05, France*

⁴*CNR, Istituto di Struttura della Materia, via Fosso del Cavaliere, 00133 Roma, Italy*

⁵*DSM, IRAMIS, Service de Physique de l'Etat Condensé, CEA-Saclay, 91191 Gif-sur-Yvette, France*

⁶*Institute of Precision Optical Engineering, School of Physics Science and Engineering,
Tongji University, Shanghai 200092, People's Republic of China*

⁷*UR1-CNRS/Synchrotron SOLEIL, Saint-Aubin, B.P. 48, 91192 Gif-sur-Yvette Cedex, France*

⁸*Synchrotron SOLEIL, Saint-Aubin, B.P. 48, 91192 Gif-sur-Yvette Cedex, France*

⁹*Central Laser Facility, Rutherford Appleton Laboratory, Didcot, Oxon OX11 0QX, United Kingdom*

¹⁰*Lund University, MAX-lab, P.O. Box 118, 221 00 Lund, Sweden*

¹¹*CNR, Institute for Superconducting and Innovative Materials and Devices (CNR-SPIN),
67100 L'Aquila, Italy*

¹²*Dipartimento di Fisica, Università degli Studi dell'Aquila, Via Vetoio 10,
67010 Coppito (L'Aquila), Italy*

ABSTRACT

Mn₅Ge₃(001) thin films grown on Ge(111) were studied by angle- and spin-resolved photoemission using synchrotron radiation in the 17–40 eV photon energy range. The photoelectron spectra were simulated starting from a first-principles band-structure calculation for the ground state, using the free-electron approximation for the final states, taking into account photohole lifetime effects and k_{\perp} broadening plus correlation effects, but ignoring transition matrix elements. The measured spin polarizations for the various k points investigated in the Γ MLA plane of the Brillouin zone are found to be in fair enough agreement with the simulated ones, providing a strong support to the ground-state band-structure calculations. Possible origins for the departures between either simulations and experiments or previous and present experiments will be discussed in terms of the 3D nature of the sample and of correlation effects.

Calculation of XMCD and XNCD at the K-edge from First Principles

N. Mas^{1, 2}, N. J. Vollmers³, Ph. Saintavit^{1, 2}, Ch. Brouder¹,
F. Baudelet², M. Calandra¹, U. Gerstmann³ and A. Juhin¹.

¹ *Institut de Minéralogie, de Physique des Matériaux et de Cosmochimie, CNRS & UPMC, 75005 Paris, France*

² *Synchrotron SOLEIL, L'Orme des Merisiers, 91190 Saint Aubin, France*

³ *Lehrstuhl für Theor. Phys., Universität Paderborn, Warburger Str. 100, 33098 Paderborn, Germany*

ABSTRACT

X-ray Circular Dichroism is the difference between absorption spectra measured using right and left circularly polarized X-rays. It occurs when the symmetry is broken. In ferro- and ferrimagnetic samples, it is the breaking of time-reversal symmetry that leads to the existence of X-ray Magnetic Circular Dichroism (XMCD), while X-ray Natural Circular Dichroism (XNCD) is due to the breaking of inversion symmetry which occurs in non-centrosymmetric materials.

XMCD is a powerful tool for the study of the magnetic structure of complex systems as it gives element-specific information on the magnetic properties. When investigating systems under high pressure conditions, the use of hard X-rays is mandatory because diamond anvil cells are highly absorbing. Studying the properties of matter under pressure is important in geosciences and it is also a good way to test our understanding of the electronic structure as pressure changes the local environment of the atoms, giving rise to new bulk properties. For 3d transition elements, measurements of XMCD at the K-edge are the main way to probe magnetism under pressure. Nevertheless, unlike XMCD at the L_{2,3} absorption edges for which well-established sum rules allow to extract spin and orbital contributions, the quantitative analysis of K-edge XMCD spectra is far from straightforward. The crucial support of theoretical interpretation is, yet, required to understand the experimental results.

XNCD presents a fundamental interest as it gives access to stereochemical information; it can, for example, be used to identify enantiomeric crystals and chiral centers. Ab initio calculation of XNCD could be very useful to investigate the origin of chirality in new optically active materials that find applications as sensors/polarizers and therefore help to design highly chiral systems.

We will present the different operators that contribute to the XAS, XMCD and XNCD cross sections in a relativistic framework [1] and we will discuss in detail their physical meaning. In order to calculate the spectra ab initio, these different contributions have been implemented in a monoelectronic code [2] based on Density Functional Theory: the Xspectra package of the QUANTUM ESPRESSO distribution [3]. The theoretical XMCD spectra obtained for metals (Fe, Co, Ni) and XNCD spectra of the gyrotropic crystal LiIO₃ [4] will be carefully compared with experimental ones. The influence of pressure on the theoretical and experimental XMCD spectra will also be presented.

REFERENCES

1. Publication in preparation
2. Paolo Giannozzi et al., *Journal of Physics: Condensed Matter* 21, n° 39 (2009): 395502
3. Mathieu Tailliefumier et al., *Physical Review B* 66, n° 19 (novembre 2002)
4. C. R. Natoli et al., *The European Physical Journal B - Condensed Matter and Complex Systems* 4, no 1 (1 juillet 1998): 1 11
5. Roberta Sessoli et al., *Nature Physics* 11, n° 1 (janvier 2015): 69-74

Interfaces between Strongly Correlated Oxides : Controlling Charge Transfer and Induced Magnetism by Hybridization

M.N. Grisolia¹, J. Varignon¹, G. Sanchez-Santolino², A. Arora³, S. Valencia³,
M. Varela^{4,2}, R. Abrudan^{3,5}, E. Weschke³, E. Schierle³, J.E. Rault⁶,
J.-P. Rueff⁶, A. Barthélémy¹, J. Santamaria² and M. Bibes^{1*}

¹ *Unité Mixte de Physique CNRS/Thales, 1 avenue A. Fresnel, 91767 Palaiseau, France,
and Université Paris-Sud, 91405 Orsay, France.*

² *GFMC, Departamento Física Aplicada III, Universidad Complutense Madrid, 28040 Madrid, Spain,
and Laboratorio de Heteroestructuras con aplicación en Spintronica, Unidad Asociada CSIC/Universidad
Complutense de Madrid, Sor Juana Inés de la Cruz, 3, 28049 Madrid, Spain.*

³ *Helmholtz-Zentrum Berlin für Materialien & Energie, Albert-Einstein-Strasse 15, 12489 Berlin, Germany.*

⁴ *Materials Science & Technology Division, Oak Ridge National Laboratory, Oak Ridge, TN 37831, USA.*

⁵ *Institut für Experimentalphysik/Festkörperphysik, Ruhr-Universität Bochum, 44780 Bochum, Germany.*

⁶ *Synchrotron SOLEIL, L'Orme des Merisiers Saint-Aubin, BP 48, 91192 Gif-sur-Yvette, France*

ABSTRACT

At interfaces between conventional materials, band bending and alignment are classically controlled by differences in electrochemical potential. Applying this concept to oxides in which interfaces can be polar and cations may adopt a mixed valence has led to the discovery of novel two-dimensional states between simple band insulators such as LaAlO_3 and SrTiO_3 . However, many oxides have a more complex electronic structure, with charge, orbital and/or spin orders arising from correlations between transition metal and oxygen ions. Strong correlations thus offer a rich playground to engineer functional interfaces but their compatibility with the classical band alignment picture remains an open question. In this talk we will show that beyond differences in electron affinities and polar effects, a key parameter determining charge transfer at correlated oxide interfaces is the energy required to alter the covalence of the metal-oxygen bond. Using the perovskite nickelate (RNiO_3) family as a template, we have probed charge reconstruction at interfaces with gadolinium titanate GdTiO_3 using soft X-ray absorption spectroscopy and hard X-ray photoemission spectroscopy. We show that the charge transfer is thwarted by hybridization effects tuned by the rare-earth (R) size. Charge transfer results in an induced ferromagnetic-like state in the nickelate (observed by X-ray magnetic circular dichroism), exemplifying the potential of correlated interfaces to design novel phases. Further, our work clarifies strategies to engineer two-dimensional systems through the control of both doping and covalence.

Structure and Growth Mechanisms of Silicene Layers on Silver Surfaces

G. Prévot,¹ R. Bernard,¹ Y. Borensztein,¹ H. Cruguel,¹ A. Curcella,¹
M. Lazzeri² and L. Masson³

¹Institut des Nanosciences de Paris, CNRS UMR 7588 and UPMC, Paris, France

²Institut de Minéralogie, de Physique des Matériaux, et de Cosmochimie, UMR CNRS 7590, MNHN, IRD UMR 206 and UPMC, Paris, France

³Aix-Marseille Université, CNRS, CINaM UMR 7325, Marseille, France

ABSTRACT

The synthesis of bidimensional silicon films that would display electronic properties analog to those of graphene attracts today a considerable interest, in particular for applications in microelectronics. So-called silicene layers have been claimed to grow on various substrates such as MoS₂, ZrB₂, ZrC₂ or Ir(111), although, up to now, most of the studies have been performed on Ag(110) and Ag(111) substrates.^{1,2} Up to recently, it was thus assumed that Si should grow on Ag substrates with negligible interaction and that the structure would be a buckled hexagonal plane.

Using grazing incidence X-ray diffraction, scanning tunneling microscopy, Auger electron spectroscopy and surface differential reflectance spectroscopy, we have studied the structure of silicene single layers and multilayers and real-time followed up their growth on Ag(110) [3] and Ag(111) [4]. A strong interaction between silicon and the silver surface is observed. Ag(110) reconstructs upon Si adsorption, and Si atoms are found to be inserted in the Ag(111) surface even at room temperature. For both surfaces, the optical properties of the layers are far from what is expected for silicene. Moreover, Si multilayers have clearly a cubic diamond-like structure.

Using DFT simulations, we propose an energetical model that allows us to explain the growth mechanisms of Si on Ag(111).

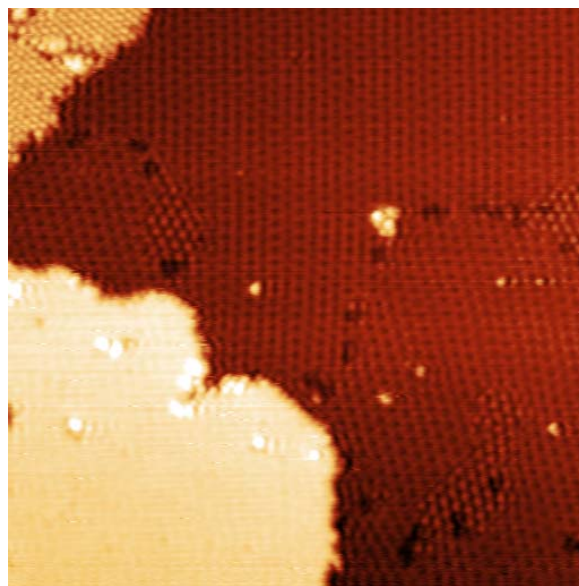


Fig. 1: STM image of silicene single and bilayers on Ag(111) (43 x 43 nm²)

REFERENCES

1. P. Vogt et al., *Phys. Rev. Lett.* 108 (2012) 155501.
2. H. Oughaddou et al., *Prog. Surf. Sci.* 90 (2015) 46.
3. R. Bernard et al., *Phys. Rev. B* 88 (2013) 121411(R), Y. Borensztein et al., *Phys. Rev. B* 89 (2014) 245410.
4. G. Prévot et al., *Appl. Phys. Lett.* 105 (2014) 213106., R. Bernard et al., *Phys. Rev. B* 92 (2015) 045415, Y. Borensztein et al., *Phys. Rev. B* 92 (2015) 155407

Bandgap and Structural Periodicities of Buffer Layer Graphene

M. N. Nair¹, A. Celis^{2,3}, J-P. Turmaud⁴, A. Zobelli³,
A. Gloter³, E. H. Conrad⁴, C. Berger⁴, W. A. de Heer⁴,
A. Taleb-Ibrahimi¹, and A. Tejada^{2,3}

¹UR1 CNRS/Synchrotron SOLEIL, Saint-Aubin, 91192 Gif sur Yvette, France

²Synchrotron SOLEIL, Saint-Aubin, 91192 Gif sur Yvette, France

³Laboratoire de Physique des Solides, Université Paris-Sud, CNRS, UMR 8502, Orsay Cedex, France

⁴School of Physics, The Georgia Institute of Technology, Atlanta, Georgia 30332-0430, USA

ABSTRACT

The main drawback of graphene for nanoelectronic applications stems from its inherent properties such as zero band gap in its electronic structure. Therefore, several methods have been proposed to open a band gap in monolayer graphene [1, 2]. Among all the growth methods, graphene grown on silicon carbide substrate has attracted much more attention as it is able to produce high quality graphene on a large wafer scale. Recently, for the first time, we have shown that on SiC(0001) substrate, under adequate growth conditions, a well ordered first single layer graphene (i.e. the buffer layer) exhibits a bandgap of more than 0.5eV [3], twice the previous value in epitaxial graphene samples [4]. The band gap opening of 0.5eV is extremely sensitive to the growth conditions. Using angle-resolved photoemission spectroscopy (ARPES), it was also shown that a temperature lower than 20°C in the growth lead to the disappearance of the π band.

Here, we focus on the structural characterization of these newly grown buffer layers by using scanning tunneling microscope (STM) and high-resolution scanning transmission electron microscope (HR-STEM). We have studied the effect of temperature on graphene growth on the substrate as it is the critical parameter giving rise to the buffer layer with 0.5eV bandgap. We have analyzed the different surface reconstructions associated to each growth stage, identified their surface states and their periodicities using ARPES [5]. We have identified a (6x6) SiC periodicity of the surface states from ARPES contours at constant binding energies which is in accordance with the observation of a (6x6) reconstruction observed by STM. Our explanation of the bandgap opening is the result of structural modulation of the buffer layer.

REFERENCES

1. R. Balog, B. Jørgensen, L. Nilsson, M. Andersen, E. Rienks, M. Bianchi, M. Fanetti, E. Laegsgaard, A. Baraldi, S. Lizzit, Z. Slijivancanin, F. Besenbacher, B. Hammer, T.G. Pedersen, P. Hofmann, and L. Hornekaer, *Nat. Mater.* **9**, 315-319 (2010)
2. E. Bekyarova, S. Sarkar, S. Niyogi, M.E. Itkis, and R.C. Haddon, *J. Phys. D: Appl. Phys.* **45**, 154009 (18pp) (2012).
3. M.S. Nevius, M. Conrad, F. Wang, A. Celis, M.N. Nair, A. Taleb-Ibrahimi, A. Tejada, and E.H. Conrad, *Phys.Rev. Lett.* **115**, 136802 (1-5) (2015)
4. S.Y. Zhou, G.-H. Gweon, a V Fedorov, P.N. First, W. A de Heer, D.-H. Lee, F. Guinea, A. H. Castro Neto, and A. Lanzara, *Nat. Mater.* **6**, 770-775 (2007).
5. M. N. Nair, A. Celis, J-P. Turmaud, A. Zobelli, A. Gloter, E. H. Conrad, C. Berger, W. A. de Heer, A. Taleb-Ibrahimi, and A. Tejada (in preparation)

Studying Chemical Bonding between NTCDA and Noble Metal Surfaces by Photoelectron Spectroscopy and Scanning Tunneling Microscopy

Y. Tong^{1,2}, T. Jiang^{1,2}, F. Nicolas¹, S. Kubsky¹, F. Sirotti¹,
V. Esaulov² and A. Bendounan¹

1. Synchrotron SOLEIL - L'Orme des Merisiers, Saint-Aubin - BP 48,
91192 Gif-sur-Yvette Cedex, France.

2. Institut des Sciences Moléculaires d'Orsay, Bâtiment 351, Université Paris-Sud,
91405 Orsay Cedex, France.

ABSTRACT

Organic molecules have been proved to be promising materials for electronic devices and thin films of such molecules on different metal surfaces have been widely studied over the last decades. Here we present a study on Naphthalene tetracarboxylic dianhydride (NTCDA) thin films deposited on Cu(100) and on Ag(110) single crystal surfaces. The bonding properties, the molecule orientation characteristics, as well as the surface crystalline structure were explored by photoemission (XPS, UPS), Near-edge X-ray absorption fine structure spectroscopy (NEXAFS) and STM/LEED, respectively. In both systems, at the molecule/metal interface, hybridization band develops, which indicates a large charge transfer from the substrate to the lowest unoccupied molecular orbital (LUMO). Thickness-dependence changes of the state binding energy were observed in high-resolution C1s and O1s core level spectra. One can conclude a strong covalent bonding at the interface and rapidly weakening of the molecular interaction upon the NTCDA coverage. Also significant differences in the C K-edge NEXAFS spectra were seen between 1ML and thick layer coverages, which signifies an evolution of the NTCDA orientation as function of thickness. This can be related to the competition between the molecule-molecule and the molecule-metal interactions. On the other hand, high ordered structures of the NTCDA monolayer with long-range scale and different domains have been observed by STM, in agreement with the LEED patterns. A brickwall-like structure of the molecule arrangement on both metal surfaces has been revealed.

PARALLEL SESSION

Matter & Material Properties: Structure, Organization, Characterization, Elaboration

ECOLE POLYTECHNIQUE – POINCARÉ Auditorium

Chairpersons: Frédéric DATCHI and Karine PROVOST

- IT-11 High pressure single crystal X-ray diffraction on CRISTAL beamline
J. Rouquette
- OC-36 Structure of Lu phthalocyanine thin films deposited on Au(111)
M. Farronato
- OC-37 High resolution three dimensional structural microscopy by single angle
Bragg ptychography
M. Allain
- OC-38 Effect of myoglobin crowding on the dynamics of water: An infrared study
S. Le Caër
- OC-39 Water in carbon nanotubes: the original hydrogen bonds network revealed
by infrared spectroscopy
P. Launois
- IT-12 Mn_2Ru_xGa - A zero moment half metal that could change spintronic
K. Rode
- OC-40 Pressure-induced spin transitions in chiral magnet MnGe
N. Martin
- OC-41 The photomagnetism of CoFe PBAs nanoparticles investigated by an in situ
XAS study
A. Bordage
- OC-42 Terahertz spectroscopy study of low energy excitations in $Tb_2Ti_2O_7$
E. Constable
- OC-43 Evidence of charge density wave ability to slide in a 3D metal
V.L.R. Jacques

High Pressure Single Crystal X-ray Diffraction on the CRISTAL Beamline

J. Rouquette¹, J. Haines¹, A. Van der Lee²

¹*Institu Charles Gehrardt Montpellier, UMR CNRS 5253 Université de Montpellier, France*

²*Institut Européen des membranes, UMR CNRS 5635, Université de Montpellier, France*

ABSTRACT

High pressure single crystal X-ray diffraction is a unique tool which permits to solve the crystallographic fine structure of complex materials and the associated structural modifications occurring at different pressure induced phase transitions. We will present here the general constraints of single crystal X-ray diffraction using a diamond anvil cell to generate hydrostatic pressure. Laboratory and synchrotron X-ray patterns will be compared. We will particularly present the interest to obtain the highest coverage and redundancy in reciprocal space in high pressure patterns of high-symmetry small unit-cell structures¹. Finally determination of complex structures for small crystal sizes and/or low Z-elements is also possible as a function of pressure by using synchrotron X-ray diffraction.

REFERENCES

1. A. Al-Zein*, P. Bouvier, A. Kania, C. Levelut, B. Hehlen, V. Nassif, T. C. Hansen, P. Fertey, J. Haines and J. Rouquette*, High pressure single crystal x-ray and neutron powder diffraction study of the ferroelectric–paraelectric phase transition in PbTiO₃, J. Phys. D: Appl. Phys. 48 (2015) 504008 (9 pages).

Structure of Lu Phtalocyanine Thin Films Deposited on Au(111)

M. Farronato^(a); A. Jones^(b); G. Prevot^(a,c); J. Simbrunner^(c);
R. Resel^(b); N. Witkowski^(a;c)

(a) UPMC Univ. Paris 6, UMR 7588, Institut de NanoSciences de Paris 75005 Paris, France

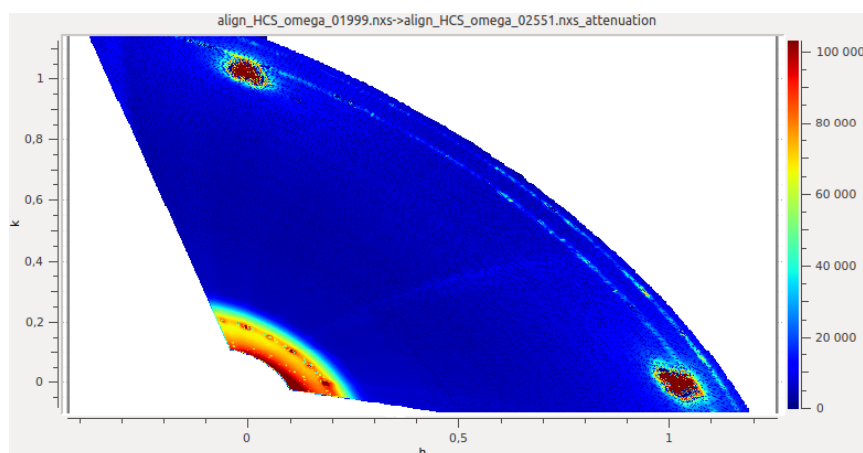
(b) Institute of Solid State Physics, Graz University of Technology, A-8010 Graz, Austria

(c) Laboratoire INSP, Universite Pierre et Marie Curie, 5 Place Jussieu, 75005 Paris, France

ABSTRACT

Lutetium bis-Phtalocyanine thin films are gaining attention as candidate for efficient gas sensing applications (1). Their peculiar electronic structure, and in particular the presence of a Single Occupied Molecular Orbital (SOMO) makes them ideal candidates for different gas sensing, as they are available for both oxidation and reduction. To better design this kind of devices more has to be understood about molecule-molecule and molecule-substrate interaction. To do this we studied the structure and the structure of LuPc2 thin films deposited on gold. Even if this is not the ideal substrate for gas sensing, Pcs are known to lie flat on the surface (2;3), posses long range order, and self organize at room temperature, making gold an ideal substrate to better understand fundamental properties of these molecules.

In this experiment we have deposited a thin film of LuPc2 under UHV conditions over (sqrt3x22) reconstructed Au(111) and we characterized it via Grazing Incidence X-ray Diffraction (GIXRD). We show how the molecules lie flat on the surface, arranged in a square lattice (beta structure) which is stabilized by the interaction with the gold substrate. No influence of the herringbone reconstruction was seen in the orientation of the molecular layer. Also we studied the stabilizing interaction, in the form of a charge transfer from the substrate to the molecules, via the relaxation of the herringbone reconstruction of gold.



REFERENCES

- (1) M. Passard; J.P. Blanc; C. Maleysson
- (2) K. Katoh, Y. Yoshida, M. Yamashita, H. Miyasaka, B. K. Breedlove, T. Kajiwara, S. Takaishi, N. Ishikawa, H. Isshiki, Y. F. Zhang, T. Komeda, M. Yamagishi, J. Takeya, *JACS* **131** 9967-9976 (2009)
- (3) M. Toader, M. Knupfer, D. R. T. Zahn, and M. Hietschold *JACS* **133** 5538-5544 (2011)

High Resolution Three Dimensional Structural Microscopy by Single Angle Bragg Ptychography

M. Allain³, S.O. Hruszkewycz¹, M.V. Holt¹, M.J. Highland¹,
A. Tripathi¹, G.B. Stephenson¹, S. Hong¹, P. Fuoss¹, C. Murray²,
J. Holt², V. Chamard³

¹ Materials Science Division, Argonne National Laboratory, Argonne, Illinois 60439, USA

² IBM T. J. Watson Research Center, Yorktown Heights, New York 10598, USA

³ Aix-Marseille Université, CNRS, Centrale Marseille, Institut Fresnel UMR 7249, Marseille, France

ABSTRACT

Hard X-ray lens-less microscopy has been proposed as an attractive alternative to image complex nanostructures. It makes use of far-field coherent intensity patterns produced by third generation synchrotron sources. Instead of lenses, numerical tools are employed to retrieve the lost phase and, hence, the 3D diffracted field at the sample position [1,2]. In *Bragg geometry*, this imaging technique provides sensitivity to the crystalline properties [3] of the probed material. This very promising approach can shed new light on a variety of outstanding questions in physics and biology. Finally, a “ptychographic” scan (a 2D scan of the sample surface performed with a finite-size beam spot) adds further flexibility, most importantly the capability to deal with crystalline objects of arbitrary extension [4].

Here, we will discuss the theory and application of our recently developed 3D Bragg Projection Ptychography (3DPP) approach in imaging strain fields in semiconductor materials [5]. This approach enables 3D imaging of materials structure using scanning probe coherent diffraction data measured at a single incident Bragg angle, *i.e. without any angle diversity*. The ability to image 3D crystals from 2D diffraction patterns is made possible by the Bragg geometry and by incorporating tomography operators into the ptychography reconstruction algorithm. By eliminating the need for angle diversity at every probe position, 3D Bragg Projection Ptychography substantially simplifies and expedites 3D imaging of extended crystals. We demonstrate our nondestructive, dose-efficient technique by imaging strain within a SiGe device stressor, and we show that our results agree with linear elastic strain predictions.

REFERENCES

- [1] J. Stangl, C. Moccuta, V. Chamard and D. Carbone, *Nanobeam X-ray Scattering*, Wiley (2013).
- [2] H. N. Chapman and K. A. Nugent, *Nature Photonics* 4, 833-839 (2010).
- [3] M. A. Pfeifer, *Nature* 442, 63-65 (2006).
- [4] P. Godard et al., *Nature Comm.* 2, 568 (2011)
- [5] S.O. Hruszkewycz, M. Allain, M.V. Holt, M.J. Highland, A. Tripathi, G.B. Stephenson, S. Hong, P. Fuoss, C. Murray, J. Holt and V. Chamard, “*High resolution three dimensional structural microscopy by single angle Bragg ptychography*”, Submitted to *Nat. Mat.*

Effect of Myoglobin Crowding on the Dynamics of Water: An Infrared Study

S. Le Caër,¹ G. Klein,¹ D. Ortiz,¹ M. Lima,² S. Devineau,¹ S. Pin,¹
J.-B. Brubach,³ P. Roy,³ S. Pommeret,¹ W. Leibl,⁴
R. Righini² and J. P. Renault¹

¹ LIONS, NIMBE, CEA, CNRS, Université Paris Saclay, CEA Saclay F-91191 Gif-sur-Yvette Cedex

² University of Florence, Polo Scientifico, Via Nello Carrara 1, I-50019 Sesto Fiorentino, Italy

³ SOLEIL, CNRS L'Orme des Merisiers, St-Aubin BP 48 F-91192 Gif-sur-Yvette Cedex

⁴ CEA SB2SM, iBiTec S, UMR 8221, F-91191 Gif Sur Yvette

ABSTRACT

Solutions containing 8% and 32% weight myoglobin fraction are studied by means of infrared spectroscopy, as a function of temperature (290 K and lower temperatures), in the mid- and far-infrared spectral range. Moreover, ultrafast time-resolved infrared measurements are performed at ambient temperature in the O-D stretching region. The results evidence that the vibrational properties of water remain the same in these myoglobin solution (anharmonicity, vibrational relaxation lifetime..) and in neat water. However, the collective properties of the water molecules are significantly affected by the presence of the protein: the orientational time increases, the solid-liquid transition is affected in the most concentrated solution and the dynamical transition of the protein is observed, from the point of view of water, even in the least concentrated solution, proving that the dynamics of water and of myoglobin are coupled [1].

REFERENCE

[1] S. Le Caër, G. Klein, D. Ortiz, M. Lima, S. Devineau, S. Pin, J.-B. Brubach, P. Roy, S. Pommeret, W. Leibl, R. Righini, J. P. Renault, *Phys. Chem. Chem. Phys.*, **16**, 22841 (2014).

Water in Carbon Nanotubes: The Original Hydrogen Bonds Network Revealed by Infrared Spectroscopy

S. Dalla Bernardina¹, E. Paineau², J. B. Brubach¹, P. Judeinstein³,
S. Rouzière², P. Launois² and P. Roy¹

¹ *Synchrotron SOLEIL, Gif-sur-Yvette, France*

² *Laboratoire de Physique des Solides, CNRS, Université Paris Saclay, Université Paris Sud, Orsay, France*

³ *Laboratoire Léon Brillouin, CNRS, CEA, Gif-sur-Yvette, France*

ABSTRACT

A groundbreaking discovery in the emerging field of nanofluidics was the demonstration of the tremendously enhanced water permeability of carbon nanotubes¹, which makes carbon nanotube membranes promising candidates for water treatment². The original behavior of water at the nanoscale is also of concern to biology, where the extreme permeability to water of aquaporins, those membrane proteins that form nanopores, is crucial for many physiological processes, as well as with respect to the unimpeded permeation of water through graphene-based membranes. Numerical calculations pointed towards the central role of hydrogen bonds network modifications to explain ultra-low friction properties of water in carbon nanotubes³. Infrared spectroscopy is a technique of choice to study the hydrogen bonds network⁴. Here, we will report the first infrared study, at controlled vapor pressures, of the water dynamics in single walled carbon nanotubes with diameters ranging from 0.7 to 2.1 nm (figure). It reveals a predominant contribution of OH dangling bonds even for fully hydrated states, irrespective to the nanotube size. While the dominating dangling bond signature is attributed to a one-dimensional chain structure for small diameter nanotubes, our results show that such feature also comes from a water layer with 'free' OH bonds facing the nanotube wall in larger diameter nanotubes. The specific thermodynamic and transport properties of water in nanotubes will be benchmarked against our experimental results.

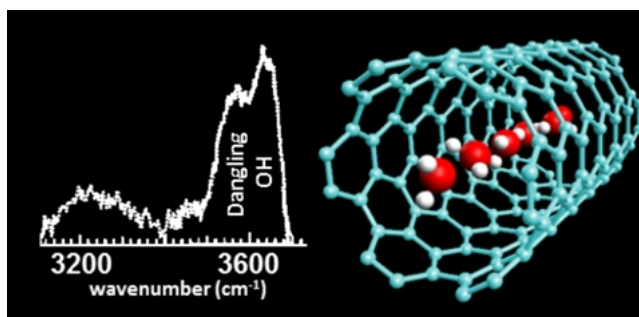


Figure: The O-H stretching band of nanoconfined water (ALES beamline, synchrotron SOLEIL) and single-file water inside smallest carbon nanotubes.

REFERENCES

1. M. Majumder et al., *Nature* **438**, 44 (2005); J.K. Holt et al., *Science* **312**, 1034 (2006)
2. H.Y. Yang et al., *Nature Comm.* **4**:2220 (2013) ; B. Lee et al., *Nature Comm.* **6**:7109 (2015)
3. G. Hummer et al., *Nature* **414**, 188 (2001) ; S. Joseph and N.R. Aluru, *Nano Lett.* **8**, 452 (2008)
4. J. Marti and M.C. Gordillo, *Phys. Rev. B* **63**, 165430 (2001); M. Sharma et al., *Nano Lett.* **8**, 2959 (2008)

Mn₂Ru_xGa – A Zero-Moment Half Metal That Could Change Spin Electronics

K. Rode¹, Y.-C. Lau¹, D. Betto¹, K. Borisov¹, N. Thiyagarajah¹, M. Zic¹,
T. Archer¹, E. Fonda², C. Piamonteze³, M.-A. Arrio⁴, K.J. O'Shea⁵,
C.A. Ferguson⁵, D.A. MacLaren⁵, A. Titova⁶, C. Fowley⁶, A.M. Deac⁶,
P. Stamenov¹, S. Sanvito¹ and J.M.D. Coey¹

¹CRANN, AMBER and School of Physics, Trinity College Dublin, Dublin 2, Ireland

²Synchrotron SOLEIL, L'Orme des Merisiers, Saint-Aubin, BP48, 91192 Gif-sur-Yvette Cedex, France

³Swiss Light Source, Paul Scherrer Institute, CH-5232 Villigen PSI, Switzerland

⁴IMPMC, F-75015 Paris, France

⁵SUPA, School of Physics and Astronomy, University of Glasgow, Glasgow G12 8QQ,
United Kingdom

⁶Helmholtz-Zentrum Dresden-Rossendorf, Institute of Ion Beam Physics and Materials Research,
Dresden, Germany

ABSTRACT

The zero-moment half metal is a material with a spin gap, and an electron occupancy that ensures compensation of two antiparallel sublattices. Unlike an antiferromagnet, the two sublattices are not related by a simple translation + time reversal symmetry operation, and the conduction electrons belong predominantly to one or other of the two sublattices. Although it was predicted as long ago as 1995 [1], the first example, a Heusler-type compound Mn₂Ru_xGa with $x \sim 0.5$ (MRG), was only reported in 2014 [2]. MRG can be stabilized in the cubic L2₁ structure on MgO, with an in-plane lattice parameter of 595 pm. Substrate-induced biaxial strain induces a slight tetragonal distortion such that the out-of-plane lattice parameter is ~ 607 pm, and a uniaxial anisotropy constant of about 40 kJm⁻³. On account of the different temperature dependence of the sublattice magnetizations, the compensation can be tuned by changing T , strain or composition. Evidence of half metallicity includes the linear variation of M with x , exceptionally large anomalous Hall effect (AHE), feeble magneto resistance, Andreev reflection as well as electronic structure calculations [2,3,4]. The coercivity diverges at compensation, and the AHE as well as the X-ray Magnetic Circular Dichroism signals change sign [3,5].

In this presentation, these and other properties will be reviewed, including the effect of crystalline defects on the magnetic and transport properties [4], as well as progress made towards incorporating MRG layers into spin valve and tunnel junction stacks [6]. Possible spin electronic applications of MRG, a zero-moment, highly spin-polarized material that has no demagnetizing field and is essentially immune to external magnetic fields include replacement of the synthetic antiferromagnets used in spin valves, field-insensitive memory cells with novel architectures, and near THz spin-transfer-torque oscillators.

REFERENCES

1. H. van Leuken and R.A. de Groot, Phys. Rev. Lett. 74, 1171 (1995)
2. H. Kurt, K. Rode, P. Stamenov, M. Venkatesan, Y.-C. Lau, E. Fonda, and J. M. D. Coey, Phys. Rev. Lett. 112, 027201, 2014
3. N. Thiyagarajah, Y.-C. Lau, D. Betto, K. Borisov, J. M. D. Coey, P. Stamenov and K. Rode, Appl. Phys. Lett. 106, 122402 (2015)
4. M. Zic et al, arXiv:1511.07923.
5. D. Betto, N. Thiyagarajah, Y.-C. Lau, C. Piamonteze, M.-A. Arrio, P. Stamenov, J. M. D. Coey, and K. Rode, Phys. Rev. B 91 094410 (2015)
6. K. Borisov et al, in preparation

Pressure-induced Spin Transitions in Chiral Magnet MnGe

N. Martin¹, I. Mirebeau¹, M. Deutsch², J.-P. Itié², J.-P. Rueff²,
U.K. Rößler³ and A.V. Tsvyashchenko⁴

¹Laboratoire Léon Brillouin, CEA, CNRS, Université Paris-Saclay, 91191 Gif-sur-Yvette, France

²Synchrotron SOLEIL, L'Orme des Merisiers, Saint-Aubin, 91192 Gif-sur-Yvette, France

³IFW Dresden, PO Box 270116, 01171 Dresden, Germany

⁴Vereshchagin Institute for High Pressure Physics, 142190 Troitsk, Moscow, Russia

ABSTRACT

MnGe belongs to the topical class of metals where the lack of inversion symmetry in the B20 crystal structure allows for relativistic Dzyaloshinskii-Moriya interaction. This leads to a long-wavelength twist of the otherwise ferromagnetic state and the system adopts a helimagnetic ground state below $T_N \approx 170$ K, with the largest ordered moment ($m_{\text{ord}} \approx 1.85 \mu_B/\text{Mn ion}$) of its family¹. A pressure-induced spin transition between the ambient pressure high spin (HS) state towards a pressure-induced low spin (LS) state, followed by the vanishing of the magnetic moment, has been predicted to occur in MnGe by means of *ab initio* density functional theory (DFT) calculations². The HS-LS transition was soon after observed in the magnetically *ordered* phase³ by neutron powder diffraction (NPD).

In order to get further insights into the mechanisms driving the two-step magnetic collapse in MnGe, we have made use of synchrotron-based x-ray techniques, namely powder diffraction (XRD) and emission spectroscopy (XES). Both allow working at much larger applied pressures than NPD. Additionally, XES is sensitive to the *local* spin state and permits a direct survey of the Mn moment even above T_N , therefore allowing a direct test of theoretical predictions. We have obtained an accurate (P,V) equation of state and monitored the collapse of local Mn moment beyond the LS phase at room temperature (see Fig. 1).

Our findings validate the DFT model and highlight the role of long-range elastic strains in the spin transition, with relevance to the physics of invar alloys⁴. Incidentally, our study underscores the invaluable complementarity of neutron and x-ray probes for the fine characterization of magnetic properties in condensed matter systems.

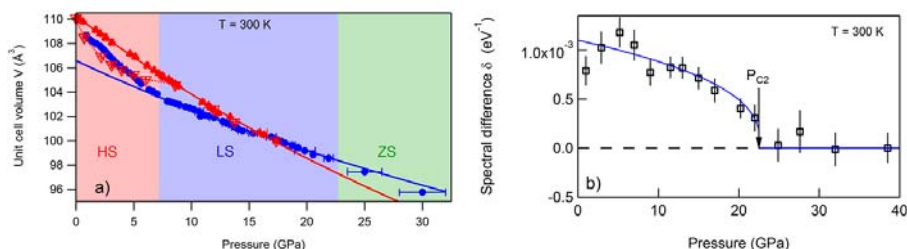


Fig. 1: **a)** (P,V) equation of state of MnGe determined by XRD. **b)** Pressure evolution of the XES intensity signaling magnetic collapse above ≈ 23 GPa.

REFERENCES

1. O. Makarova *et al.*, Phys. Rev. B **85**, 205205 (2012)
2. U.K. Rößler, J. Phys: Conf. Series **391**, 012104 (2015)
3. M. Deutsch *et al.*, Phys. Rev. B **89**, 180407(R) (2014)
4. N. Martin *et al.*, submitted to Phys. Rev. Lett. (2015)

The Photomagnetism of CoFe PBAs Nanoparticles Investigated by an In Situ XAS Study

A. Bordage, R. Moulin, G. Fornasieri and A. Bleuzen

ICMMO, Univ. Paris-Sud, UMR CNRS 8182, Bât. 420, rue du doyen G. Poitou, 91405 Orsay Cedex

ABSTRACT

Switchable molecular compounds have a significant potential for the elaboration of very high-density devices in the area of data storage systems. Switching properties observed in some of them are indeed reversible and intrinsically molecular, and are retained at a nanometric scale. With the idea to integrate such compounds into real applications, our group developed an original bottom-up approach, based on the use of the well-defined ordered porosity of mesoporous silica as a nanoreactor in order to control the size, the shape and the spatial organisation of the functional objects¹.

Prussian Blue analogues (PBA) are well-known candidates for such applications, and in particular the CoFe PBA family. The $\text{Co}_4[\text{Fe}(\text{CN})_6]_{2.7} \cdot 18\text{H}_2\text{O}$ PBA, called **CoFe**, is a ferrimagnetic compound ($T_c=16\text{K}$) with Co^{II} high-spin (HS)— Fe^{III} low-spin (LS) pairs. On the contrary, the $\text{Rb}_{1.8}\text{Co}_4[\text{Fe}(\text{CN})_6]_{3.3} \cdot 13\text{H}_2\text{O}$ PBA (called **RbCoFe**) is diamagnetic and mostly composed of $\text{Co}^{\text{III}}(\text{LS})$ - $\text{Fe}^{\text{II}}(\text{LS})$ pairs ($\text{Co}^{\text{III}}/\text{Co}^{\text{II}} = 80/20$). In addition, **RbCoFe** presents a photoinduced charge transfer within the CoFe pair at low temperature (10K)²: the Co^{III} - Fe^{II} ground state is transformed into a ferrimagnetic Co^{II} - Fe^{III} metastable state, with a long lifetime of several days and a T_c of 21 K. The photo-induced excited state relaxes to the initial Co^{III} - Fe^{II} state by heating above the thermal relaxation temperature ($T_R = 110\text{K}$). SQUID magnetometry measurements recently showed that these photomagnetic properties observed in **RbCoFe** persist in the corresponding nanocompound (called **nanoRbCoFe**), but differences were nevertheless observed between both compounds.

Therefore we investigated in details the two CoFe PBAs, both in the nanoconfined and powder (i.e. freely precipitated) forms, in order to characterize the electronic structure of Co and Fe ions in the different states as well as their local environment. Co and Fe K-edges X-ray absorption spectra were acquired in situ on the SAMBA beamline. While the white line at the Co K-edge consists of a single maximum for **RbCoFe**, it splits into two maxima for **nanoRbCoFe**, hence indicating the presence of both Co^{II} and Co^{III} ions in the nanocompound. Significant differences are also observed between the nanoconfined compounds and their powder references, in particular the spectral features in the edge rise, which demonstrates that confinement strongly modifies the local environment of the transition metal ions. However, despite these differences at room temperature between **RbCoFe** and **nanoRbCoFe**, the $\text{Co}^{\text{III}}\text{Fe}^{\text{II}} \rightarrow \text{Co}^{\text{II}}\text{Fe}^{\text{III}}$ charge transfer is observed and complete for both compounds.

REFERENCES

1. G. Fornasieri, M. Aouadi, P. Durand, P. Beaumier, E. Rivière and A. Bleuzen, *Chem. Commun.* **46**, 8061-8063 (2010).
2. A. Bleuzen, C. Lomenech, V. Escax, F. Villain, F. Varret, C. Cartier dit Moulin and M. Verdagner, *J. Am. Chem. Soc.* **122**, 6648-6652 (2000) ; C. Cartier dit Moulin, F. Villain, A. Bleuzen, M-A. Arrio, Ph. Sainctavit, C. Lomenech, V. Escax, F. Baudalet, E. Dartyge, J-J. Gallet, M. Verdagner, *J. Am. Chem. Soc.* **122**, 6653-6658R (2000).

Terahertz Spectroscopic Study of Low-energy Excitations in $\text{Tb}_2\text{Ti}_2\text{O}_7$

E. Constable¹, S. DeBrion¹, V. Simonet¹, J. Robert^{1,2}, R. Ballou¹,
S. Petit², C. Decorse³, J-B. Brubach⁴ and P. Roy⁴

¹*Institut Néel, CNRS et Université Joseph Fourier, BP166, F-38042 Grenoble Cedex 9, France*

²*Laboratoire Léon Brillouin, CEA Saclay, Bâtiment 563, 91191 Gif-sur-Yvette Cedex, France*

³*ICMMO, Université Paris-Sud, F-91400 Orsay, France*

⁴*Synchrotron SOLEIL, L'Orme des Merisiers Saint-Aubin, BP 48,
F-91192 Gif-sur-Yvette Cedex, France*

ABSTRACT

At the frontier of understanding quantum effects in magnetic materials is the study of frustrated magnetism. Materials that feature such effects are known to produce exotic magnetic states such as quantum spin liquids and spin ices. The rare earth pyrochlores ($\text{R}_2\text{Ti}_2\text{O}_7$), featuring corner-sharing tetrahedra of the rare earth ions are often considered the canonical example of geometric magnetic frustration [1]. Since the magnetic moments of the rare earth ions interact with six inequivalent nearest neighbors, a localized constraint is present restricting the magnetic ground state. When the dominant interaction is ferromagnetic as in $\text{Ho}_2\text{Ti}_2\text{O}_7$, the spins behave as classic Ising spins and the well-documented “two-in two-out” spin ice state is stabilized [2].

For $\text{Tb}_2\text{Ti}_2\text{O}_7$, the dominant antiferromagnetic (AFM) interaction should stabilize long-range AFM ordering yet no ordered phase is detected down to 20 mK [3]. Exotic quantum phases such spin-liquid [4] or Coulomb phases [5] have therefore been suggested as potential ground states. Evidence for these phases have involved the study of the particularly low energy crystal electric field (CEF) levels of the Tb^{3+} ions and suggest strong spin-lattice coupling is important. By inelastic neutron scattering, ground state doublets and magnetoelastic coupling consistent with an exotic magnetic phase have been observed for the CEF levels [5].

Here we present complementary terahertz spectroscopy of these low energy excitations in $\text{Tb}_2\text{Ti}_2\text{O}_7$ performed at SOLEIL on the AILES beamline. Our results give further confirmation to the presence of the level splitting and magnetoelastic coupling. Furthermore our results also reveal a new phonon like excitation at 0.67 THz (2.8 meV). The presence of this new mode below 100 K suggests structural distortions at higher temperatures than previously considered. Together our results highlight the potential importance of domain formation and dynamic spin lattice coupling in the observed magnetic state of $\text{Tb}_2\text{Ti}_2\text{O}_7$.

REFERENCES

1. J. S. Gardner, M. J. P. Gingras, and J. E. Greedan, *Rev. Mod. Phys.* **82**, 53-107 (2010). □
2. S. T. Bramwell, M. J. Harris, B. C. den Hertog, M. J. P. Gingras, J. S. Gardner, D. F. McMorrow, A. R. Wildes, A. L. Cornelius, J. D. M. Champion, R. G. Melko, and T. Fennell, *Phys. Rev. Lett.* **87**, 047205 (2001).
3. J. S. Gardner, S. R. Dunsiger, B. D. Gaulin, M. J. P. Gingras, J. E. Greedan, R. F. Kiefl, M. D. Lumsden, W. A. MacFarlane, N. P. Raju, J. E. Sonier, I. Swainson, □ and Z. Tun, *Phys. Rev. Lett.* **82**, 1012 (1999). □
4. S. Petit, P. Bonville, J. Robert, C. Decorse, and I. Mirebeau, *Phys. Rev. Lett.* **86**, 174403 (2012).
5. S. Guitteny, J. Robert, P. Bonville, J. Ollivier, C. Decorse, P. Steffens, M. Boehm, Hannu Mutka, I. Mirebeau and S. Petit, *Phys. Rev. Lett.* **111**, 087201 (2013).

Evidence of Charge Density Wave Ability to Slide in a 3D Metal

V.L.R. Jacques¹, C. Laulhé², N. Moisan¹, S. Ravy¹ and D. Le Bolloc'h¹

1. Laboratoire de Physique des Solides, CNRS, Univ. Paris-Sud, Université Paris-Saclay, 91405 Orsay Cedex, France

2. Synchrotron Soleil, L'Orme des Merisiers, Saint-Aubin, 91192 Gif-sur-Yvette, France

ABSTRACT

Charge density wave (CDW) systems are mostly found in low-dimensional materials, displaying strong anisotropy¹. Some incommensurate ones have the fascinating ability to slide over the atomic lattice when submitted to an external driving force, like a voltage^{2,3}. In that case, non-linear transport properties reveal that additional charges are brought to the contacts by the sliding CDW itself, and lead to a resistance drop. However, not only CDWs are scarcely found in 3D materials, but none has ever proved to display sliding properties⁴.

Chromium displays both a spin density wave and a CDW due to its peculiar Fermi surface topology. Here we used time-resolved x-ray diffraction, to probe the CDW out-of-equilibrium dynamics following a femtosecond laser excitation (Fig. 1). We show that the CDW first expands very rapidly, before contracting within 2ns. But surprisingly the CDW then rotates until 100ns, while the atomic lattice does not, which evidences that the CDW can decouple from the lattice after laser excitation. This is a sign that the CDW can slide over the atomic lattice, and should lead to new ways of apprehending the CDW state found in isotropic systems, both experimentally and theoretically⁵.

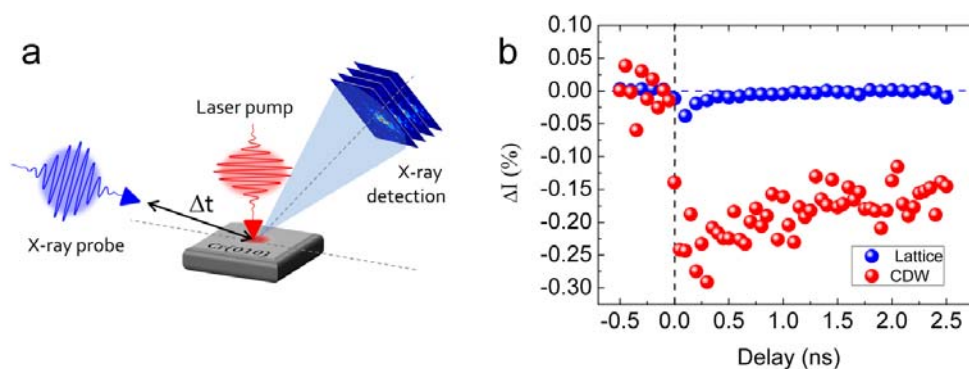


Fig. 1: **a**, laser pump x-ray probe setup. **b**, evolution of the diffracted intensity as a function of pump-probe delay for the (0 1 1) and (0 1-2 1) reflections associated to the atomic lattice and CDW respectively.

REFERENCES

1. G. Grüner, *Density Waves in Solids*, Addison Wesley, 1994.
2. J. Dumas et al., *Phys. Rev. Letters* **50**, 757 (1983).
3. P. Monceau et al., *Phys. Rev. Letters* **37**, 602 (1976)
4. E. Fawcett, *Rev. Mod. Phys.* **60**, 209 (1988)
5. V.L.R. Jacques et al., in preparation.

TECHNICAL WORKSHOPS

Technical Workshops

Spatial resolution

Auditorium Reception Building - SOLEIL

Contributors:

M(CO) compounds imaged at different energies (IR, classical fluorescence, X-fluorescence) and different scales (sub-cellular, tissue).

Clotilde Policar - ENS, Paris

Interest of microbeam for the study of pathological calcifications.

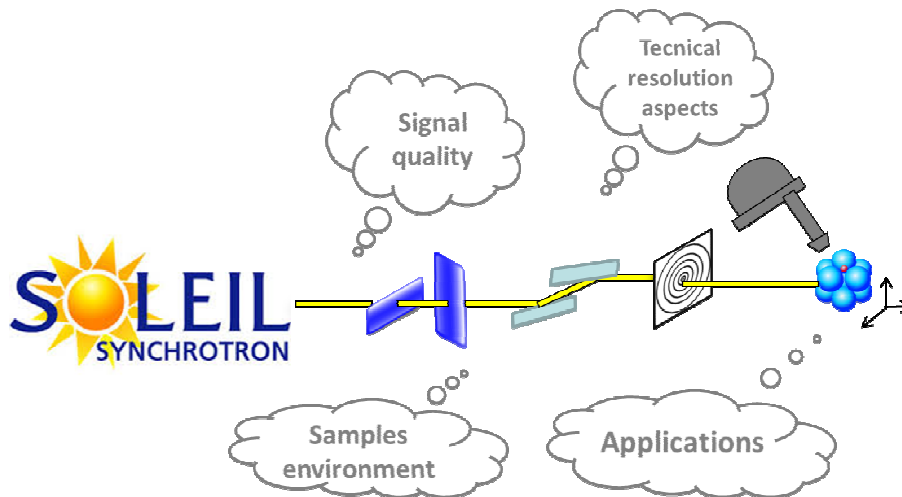
Dominique Bazin - LPS, CNRS, Université Paris Sud, Orsay

Delphine Vantelon - Synchrotron SOLEIL, Gif-sur-Yvette

Andrea Somogyi- Synchrotron SOLEIL, Gif-sur-Yvette

Technical workshop:

Spatial resolution at SOLEIL



10 beamlines at SOLEIL offer the possibility to perform experiments below the **10 μm** spatial resolution range: ANTARES, GALAXIES, HERMES, DISCO, LUCIA, PROXIMA, SEXTANTS, SMIS, and 2 new long beamlines especially dedicated to spatial resolution: NANOSCOPIUM and ANATOMIX.

This enhancement of SOLEIL capacities points out the importance of the beam size in certain experiments, makes real studies impossible to do before and bring an added value to the scientific community.

SUM 2016 is a good occasion for this workshop, where different possibilities of imaging and microanalysis using SR under extreme sensitivity conditions will be presented by beamtime scientists and users.

Afterwards, a **round table** will stimulate discussion between users and the SOLEIL management staff, in particular, in relation to possible applications, user needs and possibilities for exciting novel experiments.

Technical Workshops

Temporal resolution and dynamics

Auditorium Main Building – SOLEIL

Contributors:

Storage ring operation modes for time-resolved experiments

Marie-Agnès Tordeux - Synchrotron SOLEIL, Gif-sur-Yvette

Studies on photoinduced sub-ns and sub-ps structural dynamics: pump-probe X-ray diffraction setup at CRISTAL beamline

Claire Laulhé - Synchrotron SOLEIL, Gif-sur-Yvette

Time-resolved experiments with soft x-rays

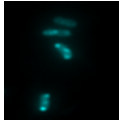
Fausto Sirotti - Synchrotron SOLEIL, Gif-sur-Yvette

Opportunities in dynamics studies on biological systems at the SMIS beamline

Ferenc Borondics - Synchrotron SOLEIL, Gif-sur-Yvette

Temporal resolution and dynamics

Antibiotic
accumulation
in bacteria



Catalysis



Phonons



Chemical reactions



1s

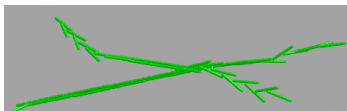
1ms

1 μ s

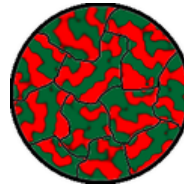
1ns

1ps

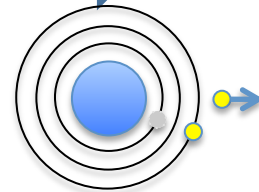
1fs



Fibrin
growth kinetics



Magnetization
dynamics



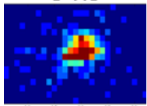
Auger
processes

Thanks to the different synchrotron filling modes and to the large amount of available technics, it is already possible to realize time resolved experiments and dynamic measurements at SOLEIL covering second to picosecond mechanisms.

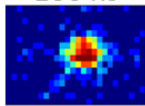
The purpose of this workshop is to present the actual possibilities and to discuss the future needs of users' community. Do we need further temporal resolution? Do we need to implement new time-resolved techniques such as Laue measurements?

In order to introduce the discussion, one presentation will be given on the machine operating modes, followed by examples from different communities.

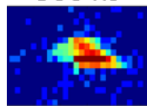
0 ns



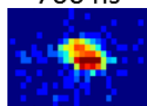
100 ns



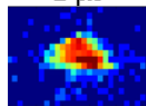
300 ns



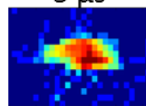
700 ns



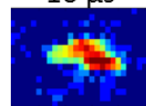
1 μ s



5 μ s



10 μ s



Technical Workshops

Multi beamline Measurements

Auditorium BLOCH – CEA

Contributors:

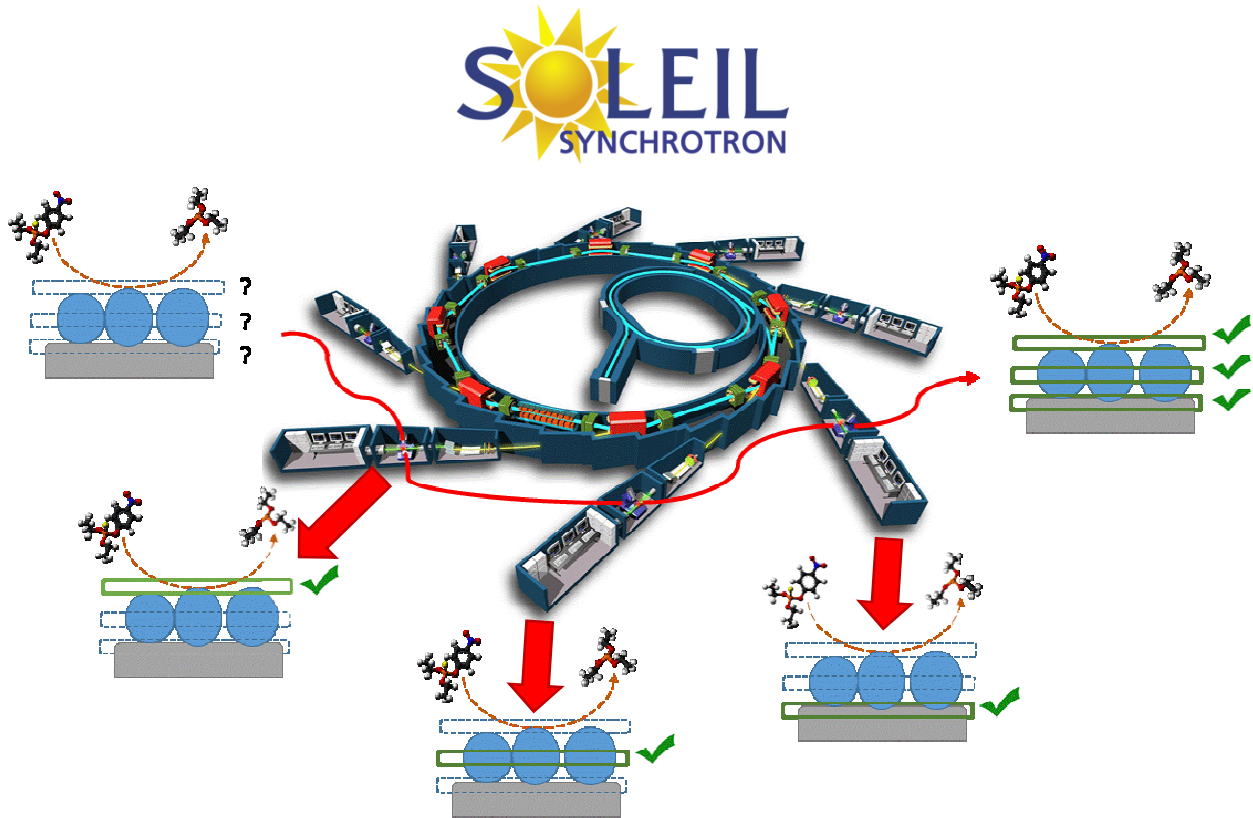
Jean-Paul Itié - Synchrotron SOLEIL, Gif-sur-Yvette

Amélie Bordage - Université Paris Sud, Orsay

Charlotte Martineau - Université Versailles-Saint Quentin

Mathieu Kociak - Université Paris Sud, Orsay

Technical workshop : Multi-beamline experiments at SOLEIL



With numerous beamlines, SOLEIL synchrotron offers a variety of techniques to explore a single question. When two or more techniques are required to reach the project objectives, users usually request beamtime separately for each beamline. In some cases though, it is necessary to collect data in a synchronous or consecutive manner, in order to cope with problems of sample stability, reproducibility of the experiment, constraints on sample conditioning, or to comply with time constraints of some research projects. In such cases, the synchronized or consecutive use of several beamlines during the same session appears to be a good solution, but so far not very developed. Indeed, the organization can raise logistical and practical difficulties for both the users and the beamline scientists.

This workshop is intended to address these questions. It will start with presentations dealing with feedback on synchronized experiments on multiple beamlines from both users and beamline scientists. This will be followed by a discussion among participants in order to highlight the difficulties and the needs of the user community.

POSTERS SESSION

List of Student Posters

- PO-BH-01** Structural Insights of Human Septin and *E. faecalis* Virulence Factor Transcriptional Regulator
M. De Groot
- PO-BH-02** Membrane – Interfacial Protein Interactions: Analysis of Dystrophin 3D Structure in the Presence of Membrane Lipids
R. Dos Santos Morais
- PO-BH-03** Suppressor of Fused, a Hedgehog Signalling Protein, Presents a Zn Binding Property and Different Oligomerization States
S. Makamé
- PO-BH-04** Towards the Analysis of Single Bacterial Cells in Aqueous Environment by Fourier Transform Infrared Spectroscopy
J. Meneghel
- PO-BH-05** Structural Insights into the Regulation of Competence in Streptococci
A. Talagas
- PO-BH-06** Structure and Interaction Network of the Long Form RNaseZ from *Saccharomyces Cerevisiae*
H. van Tilbeurgh
- PO-CP-07** Study of Self-assembled Block Copolymer Films Containing Gold Nanoparticles via GiSAXS Measurements
F. Aubrit
- PO-CP-08** Swelling of Hydroxylated Hectorite and Saponite Clays Monitored by NAP-XPS
A. Boucly
- PO-CP-09** 1s2p Resonant Inelastic X-ray Scattering (RIXS) of Cobalt based Catalysts
C. Desjacques
- PO-CP-10** Development of Bi-promoted (CoNiMoS) Hydrotreating Catalysts: An in-situ XAS Experiment for the Active Phase Formation Study
L. Plais
- PO-CH-11** Development of Manganese-rich Patinas on the Building Sandstones from Luneville Castle: From Initial Bearing Phases Towards Final Phases
L. Gatuingt
- PO-DM-12** High Resolution Analysis of the $\nu_2+\nu_4-\nu_5$ Band of SF₆ Leading to an Improvement of the ν_5 Raman Band Parameters
M. Faye
- PO-DM-13** Development of an Experimental Setup for Multi Electron-ion Coincidence Spectroscopy
M. A. Khalal
- PO-EM-14** Connected Semiconducting and Metallic Nanoribbons on a Graphene Layer
A. Celis
- PO-EM-15** Tailoring Band Gaps in Graphene by Substrate Nanostructuring
A. Celis

- PO-EM-16** L-edge XMCD Investigation of Photo-switchable Fe/Co Prussian Blue Molecular Magnets
S. Fatima
- PO-EM-17** Investigation of Orbital Excitations in TbMnO₃
J. Feng
- PO-EM-18** Investigate of Interface Annealing and Switching Polarization of the Pb_{1.1}(Zr_{0.52},Ti_{0.48})O₃/Ru/Pt by Operando (HAXPES) Analysis
I. Gueye
- PO-EM-19** *Exploring the Electronic Structure along Single Bi₂Te₃ Nanowires by Nano-angle-resolved Photoemission Spectroscopy*
J. Krieg
- PO-EM-20** Electronic Structure Change Associated with Re-emergence of Superconductivity in K_{0.8}Fe_{1.7}Se₂ and Tl_{0.6}Rb_{0.4}Fe_{1.67}Se₂ under Pressure
B. Lebert
- PO-EM-21** Photoemission Study of Irradiation Impact on Amorphous / Crystalline (a-Si:H/ c-Si) Silicon Heterojunction
M-I. Lee
- PO-EM-22** Two-dimensional Electron Systems at the Surface of Locally Doped Titanates Studied by ARPES
T. C. Rödel
- PO-EM-23** Universal Method for the Fabrication of Two-dimensional Electron Systems in Functional Oxides
T. C. Rödel
- PO-EM-24** Tailoring Electronic Properties in Long Range Ordered on Surface Synthesized Polymer
S. Xing
- PO-EM-25** Superconductivity, Pseudogap, and Stripe Correlations in High-Tc Cuprates
Z. Zhang
- PO-MM-26** Structure of Lu Phtalocyanine Thin Films Deposited on Au(111)
M. Farronato
- PO-MM-27** Local Environment Analysis of High-entropy Alloys with EXAFS Measurements
L. Liliensten
- PO-MM-28** XANES Analyses of Low Temperature Magnetic Transition of ε-Fe₂O₃ Nanoparticles Embedded in SiO₂ Sol-gel Films
J. Lopez-Sanchez
- PO-MM-29** Mechanical Behavior of Nanolayered Cu/W Thin Films under Cyclic and/or Monotonous Biaxial Solicitations: In-situ Study by X-ray Synchrotron Diffraction
N. Pouvreau

Structural Insights of Human Septin and *E. faecalis* Virulence Factor Transcriptional Regulator

M. De Groote, S. da Silva, R. Garrat, E. Horjales

Instituto de Física de São Carlos, Universidade de São Paulo-BR

ABSTRACT

In the first used beamline time only two projects (of three, in a bag) diffracted crystals. Human septin-9 and ElrR, an *Enterococcus faecalis* transcriptional regulator were diffracted.

Septins are GTP-binding proteins, that are involved in important cellular processes. Most of these biological functions are dependent on the intrinsic ability of septins to polymerize into filaments and its association with membranes (1-2). Most septins are composed of three domains; a variable N-terminal domain, a conserved GTP-binding domain and a C-terminal domain that encodes a coiled-coil. The hetero-filament is known to be stabilized by interactions which involve the GTP-binding domains (3) although a role for the C-terminal domain has also been implied (4). The individual septin-septin interfaces can be divided into two generic classes which alternate along the filament; the G-interfaces (where guanine nucleotide is bound) and the NC-interfaces (which involve the N- and C-terminal portions of the GTP-binding domain). NC-type interfaces is found between SEPT9-SEPT9 and generated when octameric core particles polymerized.

ElrR is a transcriptional regulator of the Rgg-like family, who are regulated by quorum sensors (6), that positively regulates a virulence factor of *Enterococcus faecalis* (7). Rgg and RNPP protein families are related to biofilm formation, virulence (6), DNA transference (8), etc, and have structural and regulatory similarity, but exclusive mechanisms of action. ElrR APO structure presents more dimeric contacts between N-terminal and central domain than the Rgg and RNPP families homologous structures registered on PDB. That strong contacts indicate a concerted movement in between the central domain and HTH domain position able to bind the DNA.

From the two structures of SEPT9 complexed with GDP and GTP obtained at high resolution, it was possible to get information of G and NC interfaces. This NC-interface, is responsible for the polymerization of protofilaments and therefore responsible for the observations of octamers electron microscopy. We diffracted 50 crystals of ElrR samples, in the presence of three proposed ligands and the DNA-binding fragment. Despite different crystals geometries any of the diffracted crystals presented ligands or DNA on the crystallographic cell. Data collections of supposed binary and ternary complexed crystals present different protein packing, in three different space groups, but still in APO form.

REFERENCES

1. M, Kinoshita, *Curr Opin Cell Biol* **18** 54–60 (2006)
2. ET, Spiliotis, WJ, Nelson, *J Cell Sci* **119** 4–10 (2006)
4. Sirajuddin, M. et al. *Nature* **449** 311–315 (2007)
5. I, Almeida Marques, et al *Cell Bioch. Bioph.* **62** 317–328 (2012)
6. J. Rocha-Estrada, et al, *Appl Microb Biotech* **87** 9213–3 (2010).
7. R. Dumoulin et al, *J of Bacteriology* **195** 3073–3083 (2013).
8. R. Grenha T. Wang, *PNAS* **110** 1047–1052 (2013).

Membrane – Interfacial Protein Interactions: Analysis of Dystrophin 3D Structure in the Presence of Membrane Lipids

R. Dos Santos Morais^{1, 2, 3}, E. Le Rumeur¹, O. Delalande¹,
A-E. Molza¹, C. Raguenes-Nicol¹, A. Cheron¹, T. Chenuel¹,
S. Combet², J. Perez³ and J-F. Hubert¹.

¹ IGDR (UMR6290, Rennes, France),

² LLB (UMR12, CEA-CNRS, Saclay, France),

³ Beamline SWING (Synchrotron SOLEIL, Saint-Aubin, France).

ABSTRACT

Protection of cell membrane against shearing stresses is ensured by cytoskeletal proteins. Amongst them, dystrophin¹ (Fig. 1) plays a key-role in muscle and its absence leads to the severe Duchenne Muscular Dystrophy (DMD), whereas its deficiency causes heterogeneous Becker Muscular Dystrophy (BMD). Exhaustive knowledge of dystrophin membrane interaction is needed to help for gene therapy strategies devoted to DMD and BMD, aiming to design a minimal functional protein. Dystrophin is a large, monomeric, amphipathic, and fibrous protein, whose structural analysis is not accessible by NMR and X-ray crystallography. Its three-dimensional structure is being elucidated through the combined use of SAXS and molecular modeling². Previous work of J.F. Hubert's team highlighted that the interfacial properties of dystrophin are modulated according to the region of the protein involved, the nature of lipids, as well as the membrane curvature, that play key-roles in the physiology of the muscle cell^{3, 4, 5}. To understand what may be the role of these properties *in vivo*, we aim to determine the structure and the interaction mode of dystrophin in the presence of membrane mimetic models. To carry out this project, SAXS and SANS data are coupled to molecular modelling (Fig. 2).

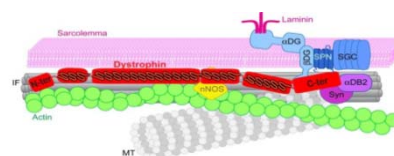


Fig 1: Schematic illustration of dystrophin (in red) interactions with its identified partners¹.

Dystrophin is a large, monomeric, amphipathic, and fibrous protein, whose structural analysis is not accessible by NMR and X-ray crystallography. Its three-dimensional structure is being elucidated through the combined use of SAXS and molecular modeling². Previous work of J.F. Hubert's team highlighted that the interfacial properties of dystrophin are modulated according to the region of the protein involved, the nature of lipids, as well as the membrane curvature, that play key-roles in the physiology of the muscle cell^{3, 4, 5}. To understand what may be the role of these properties *in vivo*, we aim to determine the structure and the interaction mode of dystrophin in the presence of membrane mimetic models. To carry out this project, SAXS and SANS data are coupled to molecular modelling (Fig. 2).

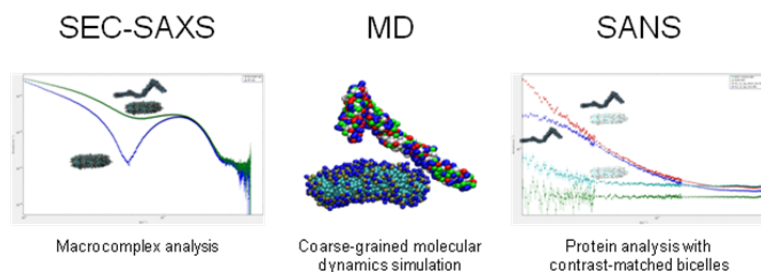


Fig 2: Graphical overview of the strategy employed. *Left:* SEC-SAXS intensity measured (SWING, SOLEIL) for bicelles with (green) or without (blue) R11-15 dystrophin fragment. *Middle:* R11-15/bicelle coarse-grained molecular dynamics simulation. *Right:* SANS intensity measured (D22, ILL) for buffer (green), contrast-matched deuterated bicelles (cyan), R11-15 dystrophin fragment with (red) or without contrast-matched deuterated bicelles (blue).

REFERENCES

1. Le Rumeur, E., Winder, S. J. & Hubert, J.-F., *Biochim. Biophys. Acta* **1804**, 1713–1722 (2010).
2. Molza, A.-E. *et al.*, *Faraday Discuss.* **169**, 45–62 (2014).
3. Legardinier, S. *et al.*, *J. Mol. Biol.* **389**, 546–558 (2009).
4. Sarkis, J. *et al.*, *J. Biol. Chem.* **286**, 30481–30491 (2011).
5. Sarkis, J. *et al.*, *FASEB J. Off. Publ. Fed. Am. Soc. Exp. Biol.* **27**, 359–367 (2013).

Suppressor of Fused, a Hedgehog Signalling Protein, Presents a Zn Binding Property and Different Oligomerization States

S. Makamté, V. Biou

Laboratoire de biologie physico-chimique des protéines membranaire, UMR 7099 CNRS univ Paris Diderot P7, 13 Rue Pierre et Marie Curie 75005 ,Paris – France

ABSTRACT

The Hedgehog (HH) signalling pathway was discovered during the 1980's. Since then, this pathway has been described to be involved in the development of many metazoans. The HH pathway is very conserved and its disruption causes many human diseases as holopresencephaly and some mutations of proteins in this pathway cause cancers. The HH pathway activation leads to the expression of some genes *via* the activation of its transcription factor, Cubitus interruptus (CI). On the other hand, when the pathway is switched off, CI is phosphorylated, partly degraded into a shorter, repressing form and inhibited by another protein, Suppressor of fused (SUFU). Recently, the structure of human and drosophila SUFU has been published in the PDB data bank. we performed solution studies to further characterise SUFU.

In fact, after expressing and purifying dSUFU, hSUFU and zSUFU, I have conducted ICP-AES and SAXS experiments. The data obtained reveal that SUFU has a Zn binding property. The analysis of its amino acid sequence reveals a conserved sequence H₇₁WH₇₃Y that may be associated with cation chelation. Indeed the mutation of the histidine 71 in dSUFU reveals a decrease in Zn binding. Furthermore, SAXS data obtained on all three proteins show that hSUFU and zSUFU present different oligomerization states than dSUFU in solution.

As the mutation of some residues in the Nterm of hSUFU is involved in some cancers and the mutation of the two histidines limits the stabilization of dSUFU, these findings can open new insights into SUFU structure and I intend to crystallise dSUFU associated with Zn to confirm the location of this cation in dSUFU.

REFERENCES

1. Nusslein-Volhard, C., and Wieschaus, E. (1980). Mutations affecting segment number and polarity in Drosophila. *Nature* 287, 795-801.
2. Ingham, P.W., and McMahon, A.P. (2001). Hedgehog signaling in animal development: paradigms and principles. *Genes Dev.* 15, 3059-3087.
3. Amy L. Cherry, Csaba Finta, Mikael Karlström, Qianren Jin, Thomas Schwend, Juan Astorga- Wells, Roman A. Zubarev, Mark Del Campo, Angela R. Criswell, Daniele de Sanctis, Luca Jovine and Rune Toftgard. Structural basis of SUFU–GLI interaction in human Hedgehog signalling regulation. *Acta Cryst.* (2013). D69, 2563–2579.
4. Taylor MD, Zhang X, Liu L, Hui CC, Mainprize TG, Scherer SW, Wainwright B, Hogg D, Rutka JT. Failure of a medulloblastoma-derived mutant of SUFU to suppress WNT signaling.

Towards the Analysis of Single Bacterial Cells in Aqueous Environment by Fourier Transform Infrared Spectroscopy

J. Meneghel^{1,2}, P. Dumas², S. Lefrançois², S. Passot¹, F. Fonseca¹

¹ INRA-AgroParisTech, UMR 782 GMPA, F-78850 Thiverval-Grignon

² Synchrotron SOLEIL, L'Orme des Merisiers, BP48, F-91191 Gif-sur-Yvette

ABSTRACT

FTIR spectroscopy is a sensitive and non invasive tool with great analytical potential in enabling the determination of the chemical composition of single eukaryotic cells, and thus *in situ* (1-2). Nowadays it remains very tricky to bring this analytical method to smaller biological cells, in particular bacteria in solution, due to the limited resolution (IR diffraction limit in the few microns range) and water absorption. Very recently our team pioneered the mapping of single bacteria (rod-shaped of approximately 1 x 6 μm in size) by FTIR in the dried state using high refractive index hemispheres (3) and the use of a synchrotron infrared source.

Trying to push the idea further and to achieve analysis of bacteria in solution, various strategies were investigated: FTIR spectroscopy in transmission using a microfluidics device as well as a static liquid chamber of both 2 μm in height: this mode appeared unsuccessful. Next, a new tailor-made inverted microscope was designed associating an ATR-mode FTIR spectrometer and the use of germanium hemispheres (4). A watertight chamber stands on top of the hemisphere on which a bacterial suspension is deposited. By using upstream apertures and germanium (refractive index: 4) as crystal material, a beam size of 2 x 2 μm was achieved at sample location. In such conditions we estimate the depth of penetration of the evanescent wave at < 1 μm , and therefore the number of probed bacterial cells in a crowded environment at 1 up to 3, giving rise to high quality FTIR spectra. Here we present the development of this new setup and its proof of principle with preliminary data obtained on two bacterial strains in physiological conditions.

This promising device has to be further exploited to analyze the effect of various stressful treatments on different micro-organisms *in situ* and with time evolved analysis by modulating environmental conditions directly in the liquid chamber. The goal is to map cellular responses to evaluate population heterogeneity and to better understand cellular damage mechanisms encountered during the production, stabilization or end-using processes of micro-organisms.

We are grateful to the SMIS beamline staff for its advice and technical support.

REFERENCES

1. M. J. Tobin, L. Puskar, R. L. Barber, E. C. Harvey, P. Heraud, B. R. Wood, K. R. Bambery, C. T. Dillon and K. L. Munro. *ib. Spectrosc.* **53**, 34–38 (2010).
2. L. Vaccari, G. Birarda, L. Businaro, S. Pacor and G. Greci. *Anal. Chem.* **84**, 4768–4775 (2012).
3. S. Passot, J. Gautier, F. Jamme, S. Cenard, P. Dumas and F. Fonseca. *Analyst* **140**, 5920-5928 (2015).
4. S. Lefrançois, F. Borondics and P. Dumas. Oral presentation at : *Instrumenter et Innover en Chimie Physique pour Préparer l'Avenir*, 22-23 Jan. 2015, Paris, France.

Structural Insights into the Regulation of Competence in Streptococci

A. Talagas¹, L. Fontaine², P. Hols², S. Nessler¹

¹*Institut de Biologie Intégrative de la Cellule (I2BC), Université Paris-sud, Orsay*

²*Institut des Sciences de la Vie, Université catholique de Louvain, Louvain-la-Neuve, Belgique*

ABSTRACT

Bacteria use a mode of communication, called quorum sensing (QS), to regulate gene expression in a population-density dependent manner. QS thus control processes such as sporulation, competence, or virulence, in a multicellular way. In Gram-positive bacteria, QS is mainly based on the production, secretion and detection of small signal peptides.

My PhD project focuses on the superfamily of quorum sensors from the RNPP family (for the first identified members Rap, NprR, PlcR and PrgX). RNPP proteins are characterized by a conserved TPR-type peptide-binding domain. Except for the Rap phosphatases, they also contain an N-terminal HTH-type DNA-binding domain and act as transcriptional regulators.

I will present my last results concerning a new member of the RNPP family, ComR, a transcriptional factor regulating competence in *Streptococcus thermophilus*. In presence of the octapeptide ComS (LPYFAGCL), the ComR/ComS complex is formed, leading to expression of the alternative sigma factor ComX controlling competence. I solved the crystal structure of the apo form of ComR as well as the ternary complex (ComR/ComS/DNA). Comparison of these structures allowed us to propose a unique molecular mechanism involving HTH-sequestration and peptide-induced dimerization.

This hypothesis was confirmed in solution, using SEC-MALLS for oligomerisation state analysis and ITC for protein-peptide interaction measurements, combined with *in vitro* and *in vivo* activity assays. Taken together, these results allowed us to identify essential residues directly involved in the activation mechanism.

Sequence alignment analysis demonstrated that these residues are conserved among ComR homologues, suggesting that the ComRS quorum sensing system could be used as a new target to impair pathogenic streptococci species to acquire and share genes encoding antibiotic resistance.

Structure and Interaction Network of the Long Form RNaseZ from *Saccharomyces Cerevisiae*

M. Ma^a, I. Gallay^a, N. Lazar^a, C. Condon^b and H. van Tilbeurgh^a

^a*Institut de Biologie Intégrative de la Cellule, Bât 430, Université de Paris-Sud, 91405 ORSAY CEDEX*

^b*Institut de Biologie Physico-Chimique, CNRS FRE3630, 75005 PARIS*

ABSTRACT

RNase Z cleaves precursors of transfer RNA lacking encoded CCA at 3'-end immediately after the discriminator nucleotide. RNase Z is highly conserved in all three kingdoms of life (bacteria, Archea, and eukaryotes). Two isoforms of RNase Z were identified, a short ubiquitous form (RNase Z^s); and a long form (RNase Z^L), which is approximately twice in length of short form and exists exclusively in eukaryotes. Mutations in ELAC2, the human ortholog of RNase Z^L, are found to be associated with the occurrence of prostate cancer and infantile hypertrophic cardiomyopathy. Apart from a few structures of RNase Z^s, we solved the first crystal structure of long form RNase Z from yeast. The structure shows RNase Z^L consists of amino- and carboxy- halves, which are structurally homologous. The carboxy domain is highly conserved with RNase Z^s (r.m.s.d 1.9 Å), except lacking the flexible arm which replaced by a short closed loop instead. Two zinc ions are observed in the conserved β -lactamase catalytic core, where 3'-end of tRNA inserts into and cleaved. The amino domain retains the typical flexible arm of RNase Z family which clamps tRNA substrates, but is enzymatically inactive. With above by superimpose with RNase Z^s/tRNA complex we proposed a model of tRNA complex with RNase Z^L: Although RNase Z^L monomer generally mimics the dimer of short form, unlike RNase Z^s dimer binds two tRNAs at the same time, the monomer RNase Z^L is only capable of binding one tRNA.

Yeast RNase ZL was detected to form a ternary complex with NUC1 and YMR099c. NUC1 is the homologue of human endonuclease G (EndoG) which involved in mitochondrial DNA recombination that relates to apoptosis. YMR099C encodes a D-hexose-6-phosphate mutarotase. We purified high quantities of recombinant RNase Z/Nuc1/ymr099c ternary complex, and characterized its assemblage by SEC-MALLS. The ternary complex is found to be hetero-hexamer in solution: RNase Z and mutarotase are mediated by Nuc1; due to dimerization of Nuc1, dimer of hetero-trimer constitutes the complex, implying a 2-2-2 /RNase Z-Nuc1-Mutarotase composition in the complex. Furthermore we established the activities of the complex towards the substrates of each enzyme. Compare to Nuc1 alone, the nuclease activity is remarkably suppressed in the ternary complex; whereas the tRnase and mutarotase activity remains unaffected. The determination of the complex structure will elucidate the mechanism of activity inhibition and will certainly aid the exploration of the biological function of the complex.

Key words: tRNA 3'-processing, crystal structure, RNase Z, Nuc1, ymr099c, enzyme activity

Study of Self-assembled Block Copolymer Films Containing Gold Nanoparticles via GiSAXS Measurements

F. Aubrit

*Laboratoire Interdisciplinaire sur l'Organisation Nanométrique et Supramoléculaire (LIONS)
DSM-IRAMIS-NIMBE CEA-Saclay, bât 12591191 GIF-sur-YVETTE, FRANCE*

ABSTRACT

In this work we have studied the organization of block copolymer polystyrene-b-poly(4-vinylpyridine) (PS-b-P4VP) in cylinder phases perpendicular to the substrate and the insertion of gold nanoparticles (AuNPs) and gold nanorods (AuNRs) into these cylinders via GiSAXS measurement.

Through the use of a non-specific solvent (mixture of toluene and tetrahydrofuran in ratio 80:20), we have achieved the deposition of PS-b-P4VP films formed by cylinders of P4VP into a PS matrix normal to the silicon substrate. GiSAXS measurements, performed on the SIRIUS beamline of SOLEIL, validated this organization and the perpendicular orientation across the whole film thickness.

Thanks to the affinity between gold and the P4VP, we have succeeded in forming and inserting AuNPs and AuNRs into these cylinders by various ways. The presence of gold into the copolymer have been studied and confirmed on the same beamline with diffraction measurements.

The materials created this way are expected to possess exceptional electromagnetic properties, leading the way to the creation of metamaterials and all the applications associated with them.

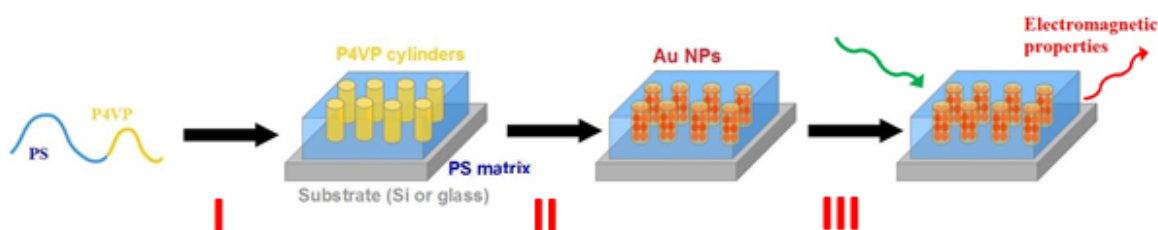


Figure 1 : Formation of a PS-b-P4VP film with AuNPs-containing P4VP cylinders into a PS matrix in three steps : I/the formation of the cylinders normal to the substrate, II/the insertion of gold nanoparticles inside the cylinders and III/the study of the electromagnetic properties of the material.

REFERENCES

- S. Park and J-Y. Wang, *Macromolecules* **40**, 9059-9063 (2007)
- J. Yin and X. Yao, *ACS Nano* **7**, 9961-9974 (2013)
- P. A. Mistark and S; Park, *ACS Nano* **12**, 3987-3992 (2009)

Swelling of Hydroxylated Hectorite and Saponite Clays Monitored by NAP-XPS

A. Boucly^{1,2*}, F. Bournel^{1,2}, E. Dubois³, J-J. Gallet^{1,2}, A. Koishi⁴,
V. Marry³, L. Michot³, F. Rochet^{1,2}, F. Sirotti² and S. Tesson³

¹Sorbonne universités, UPMC Univ paris 06, UMR 7614, Laboratoire de Chimie Physique Matière et Rayonnement (LCPMR), F-75005 Paris, France

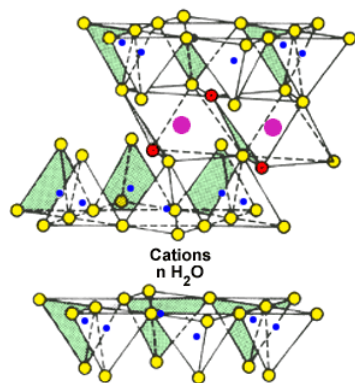
²Synchrotron SOLEIL, L'orme des Merisiers, Saint Aubin, Gif sur Yvette, France

³Sorbonne universités, UPMC Univ paris 06, UMR 8234, Laboratoire PHysicochimie des Electrolytes et Nanosystèmes Interfaciaux (PHENIX), F-75005 Paris, France

⁴Université Joseph-Fourier Grenoble I, UMR 5275, ISTERre, F-38041 Grenoble, France

ABSTRACT

This study deals with the hydration of swelling clays. Those clays are made of phyllosilicate sheets separated by an interlayer space. Depending on the smectite type, those sheets can have a negative charge localized at the surface (saponite) or in the middle (hectorite) of the lamella.¹ Those charges are compensated by the presence of cations in the interlayer space where water can penetrate, inducing the swelling of the clay. Understanding the role and behavior of the cation in the swelling process is vital to assess the impact of nuclear contamination in soils by predicting how radioactive elements move in confined water layers within the clays. In this regard, the study of the hydration of cesium-based smectites is of prime importance and the comparison with sodium-based smectites, highly relevant due to the much smaller size of the counter-ion.



● Hydroxyl ● Mg or Li
● Oxygen ● Si or Al

Figure 1 : Smectite Structure

the hydration properties of the clay. Interestingly, we have observed very different sheet/counter-ion interactions depending on the counter-ion size (Cs⁺ versus Na⁺), which has a huge impact on their mobility and on the retention capacity of the clays

While a number of studies have already been done on swelling clay minerals, most of them have been carried out via sorption and XRD methods.² Yet those methods do not give detailed information about the chemical environment of the counter-ions (i.e. the competition between the cation/sheet bonding and the formation of the solvation shell).

In this regard, the use of an NAP-XPS experimental station is extremely useful as it allows to follow *in situ* the evolution of the chemical environment of the various clay components with increasing pressure, until liquid water appears at the sample surface.

In this study we show that the core-level binding energies of the counter-ions and of the surface sheet element (Si) are affected by the penetration of water. We

REFERENCES

[1] Odom I. E., Philos. Trans. R. Soc. A, 311, 391 (1984)

[2] A) Michot, L et al., American Mineralogist., 90, 166, (2005). B) Ferrage, E. et al., J. Phys. Chem. C, 114, 4526 (2010)

1s2p Resonant Inelastic X-ray Scattering (RIXS) of Cobalt based Catalysts

C. Desjacques, A. Tougeri and S. Cristol

Univ. Lille, CNRS, ENSCL, Centrale Lille, Univ. Artois, UMR 8181 – UCCS –
Unité de Catalyse et de Chimie du Solide F-59000 Lille, France

ABSTRACT

Cobalt based catalysts supported on alumina are mainly used in the Fischer-Tropsch process, which consist of production of hydrocarbons from syngas ($\text{CO}+\text{H}_2$) [1]. In order to improve their catalytic performance, a detailed understanding of their active phase at a molecular scale is mandatory. To get more insights on the electronic structure of the system, we used the resonant inelastic X-ray spectroscopy (RIXS) at GALAXIES beamline at SOLEIL synchrotron [2]. 1s2p RIXS is two steps process in which a 1s electron is transferred to an intermediate d state, the final state being obtained by the filling of the 1s core-hole by a 2p electron (figure 1 left). Hence, 1s2p RIXS map provides us access to both the high resolution Co K edge and $L_{2,3}$ edge like spectra (figure 1 right). Another interesting feature of RIXS is the possibility to probe $L_{2,3}$ edges of 3d metals using hard X-Rays opening the way to *Operando* experiments. Thanks to the selectivity in energy of the RIXS maps, we are able to separate the different contributions of the different Co species. The first results of RIXS experiments at GALAXIES beamline show the ability of the technique to separate different spectroscopic signatures in a reference sample (e.g. Co^{2+} and Co^{3+} in Co_3O_4). Multiplet calculations of XANES spectra at $L_{2,3}$ edge (CTM4XAS software) for Co_3O_4 sample confirm the spin state of the different oxidation states of Co species (high spin for Co^{2+} and low spin for Co^{3+}), which are in agreement with the literature [3,4]. Modelling of 2D RIXS maps and K edge spectra are in progress.

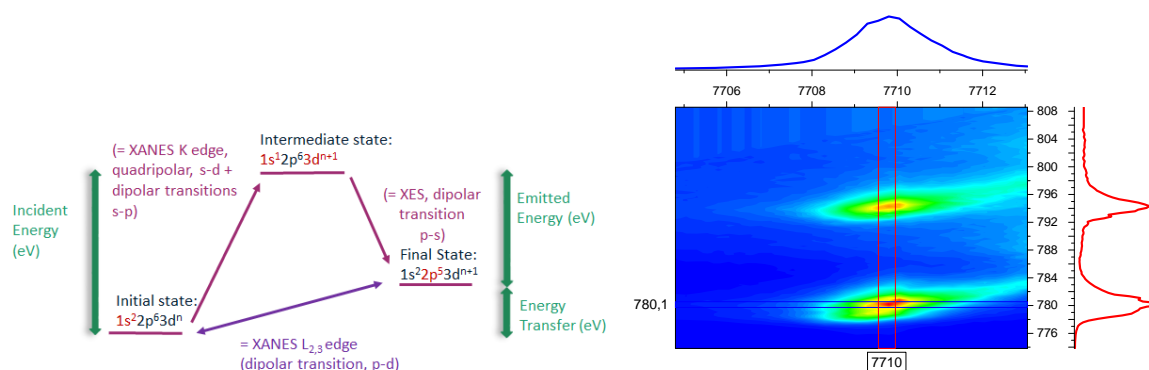


Figure 1: Left: RIXS process. Right: 2D RIXS map of $\text{Co}/\text{Al}_2\text{O}_3$ catalyst (Co loading $1.5 \text{ atom}/\text{nm}^2$). Horizontal cut: Co K edge spectrum in the pre-edge region, vertical cut: Co $L_{2,3}$ edge like spectrum.

REFERENCES

- [1] A.Y Khodakov, Catalysis Today **144**, 251-257 (2009)
- [2] J-P. Rueff, J.M. Ablett, D. Céolin, D. Prieur, Th. Moreno, V. Balédent, B. Lassall-Kaiser, J.E. Rault, M. Simon, J Synchrotron Rad **22**, 175- 179 (2015)
- [3] A.M. Hibberd, H.Q. Doan, E.N. Glass, F. M. F. de Groot, C. L. Hill, T. Cuk, J. Phys. Chem. C **119**, 4173-4179 (2015)
- [4] F. Morales, F. M. F. de Groot, P. Glatzel, E. Kleimenov, H. Bluhm, M. Hävecker, A. Knop-Gericke, B. M. Weckhuysen, J. Phys. Chem. B **108**, 16201-16207 (2004)

Development of Bi-promoted (CoNiMoS) Hydrotreating Catalysts: An *in-situ* XAS Experiment for the Active Phase Formation Study

L. Plais^{1,2}, C. Lancelot¹, V. Briois², C. Lamonier¹.

¹Unité de Catalyse et Chimie du Solide, Université de Lille 1, 59650 Villeneuve d'Ascq

²Synchrotron SOLEIL, L'Orme des Merisiers, 91190 Saint-Aubin

ABSTRACT

The treatment of heavy petroleum feedstock and the presence of environmental standards require a constant search for effective hydrotreating catalysts. Catalysts for hydrodesulfurization (HDS) processes can be described as supported MoS₂ slabs decorated at the corners and edges by cobalt and/or nickel atoms. Hydrotreating catalysts based on heteropolyanions (HPA) in which promoter (Co or Ni) and molybdenum are introduced at the oxidic level in the same molecular entity have shown a better hydrodesulfurization activity compared to catalysts prepared using co-impregnation of ammonium heptamolybdate and cobalt(II) nitrate.^{1,2} This work focuses on the preparation of bi-promoted hydrotreating catalysts (CoNiMoS) that contain at the nanoscale "CoMoS" active sites efficient for HDS together with "NiMoS" ones possessing hydrogenating properties required for deep HDS. As efficient bi-promoted catalysts appeared difficult to obtain,³ our approach consists in preparing catalysts using nickel and/or cobalt salts of Anderson HPA (figure 1a). After drying, *ex situ* Raman spectroscopy and EXAFS results indicate that the HPA structure is preserved on γ -alumina.

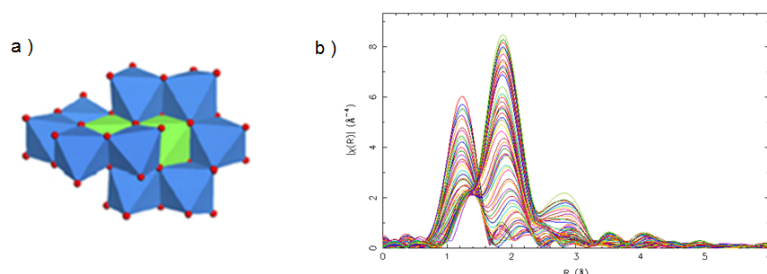


Figure 1 : a) Anderson Heteropolyanion and b) Mo K-edge R parameter of bi-promoted hydrotreating catalyst during *in-situ* sulfidation.

In situ sulfidation followed by time resolved X-ray absorption spectroscopy (Quick-XAS) has been done at the new ROCK beamline at SOLEIL synchrotron allowing to study in a same experiment Ni, Co and Mo local orders (figure 1b).⁴ The sulfidation was carried out on *ex-situ* dried samples, *in-situ* dried samples and calcined samples. Chemometric method based on multivariate curve regression with alternative least squares (MCR-ALS)^{5,6} is used to highlight the reaction intermediates during the genesis of the active phase when two promoters are simultaneously present in the sample and emphasize different sulfidation kinetics according to the pre-treatment of oxidic precursors.

REFERENCES

1. J. Mazurelle, C. Lamonier, C. Lancelot, E. Payen, C. Pichon and D. Guillaume, *Catalysis Today*, **130**, 41-49 (2008).
2. C.I. Cabello, F.M. Cabrerizo, A. Alvarez, and H.J. Thomas, *Journal of Molecular Catalysis A : Chemical*, **186**, 89-100 (2002).
3. T.K.T. Ninh, D. Laurenti, E. Leclercq, and M. Vrinat, *Applied Catalysis A : General*, **487**, 210-218 (2014).
4. C. La Fontaine, L. Barthe, A. Rochet, V. Briois, *Catalysis Today*, **205**, 148-158 (2013).
5. R. Tauler, *Chemometrics and Intelligent Laboratory Systems*, **30**, 133-146 (1995).
6. C. Ruckebush, L. Blanchet, *Analytica Acta*, **765**, 28-36 (2013).

Development of Manganese-rich Patinas on the Building Sandstones from Luneville Castle: From Initial Bearing Phases Towards Final Phases

L. Gatuingt^{1,2,5}, S. Rossano¹, J-D. Mertz², B. Lanson^{3,4}, O. Rozenbaum⁵

¹ Université Paris-Est, Laboratoire Géomatériaux et Environnement, EA4508, UPEM, 77454 Marne-la-Vallée, France

² Laboratoire de Recherche des Monuments Historiques, CRC-LRMH USR3224, 29 rue de Paris, 77420 Champs-sur-Marne, France

³ Université Grenoble Alpes, ISTerre, F-38041, France

⁴ CNRS, ISTerre, F-38041, France

⁵ Université d'Orléans, CNRS, BRGM, ISTO, UMR 7327, 1A rue de la Férollerie, 45071 Orléans cedex 2, France

ABSTRACT

Sandstones, used as building stones or in natural settings, are known to develop dark patinas at their surface when subjected to atmospheric conditions at a scale time of centuries^{1, 2, 3}. In January 2003, a violent fire affected the Luneville chateau (XVIIIth century), located in the east part of France and built with Triassic sandstones. The building materials were submitted to a huge amount of water, resulting from the firemen intervention. A few weeks after - i. e. very quickly - dark Mn-rich stains started developing on some stone blocks located in the burnt parts of the chateau. As they are not observed on all sandstones, their formation likely depends on the substrate and possibly results from the dissolution of Mn- and Fe-bearing compounds in the stone core, followed by their transportation by their aqueous migration to the surface, through the porous network.

In order to investigate the patina formation mechanisms, two patinated stones have been sampled on site, in the burnt and unburnt zones respectively. Therefore, one patina dates from before 2003 and needed several years to appear, whereas the other one was formed in few weeks, after the 2003 fire. The aims of this work are (i) to characterize and compare the patinas developed in different conditions and different time range and (ii) to determine the initial Mn-bearing phases in the sandstone bulks.

Optical and electronic microscopies, coupled with Energy-Dispersive X-ray Spectroscopy (EDS) allow establishing a correlation between the visual aspect of an area in the bulks and its Mn-enrichment. Moreover, these techniques permit to see the patinas are heterogeneous in thickness and colour, and cannot be described as a continuous coating onto the rock surfaces. The patina developed before the 2003 fire is darker and thicker than the other one. The Mn-enrichment of the patinas has also been confirmed. Quantitative chemical information was obtained using Inductively Coupled Plasma-Optical Emission Spectrometry (ICP-OES) and Particle-Induced X-ray Emission (PIXE) methods. Mn-speciations, in both the core and at the surface of the block, have been studied by X-ray diffraction (XRD) and X-ray absorption spectroscopy (XANES) at the SOLEIL synchrotron (France), with DiffAbs and LUCIA beamlines respectively.

REFERENCES

1. C. Thomachot, D. Jeannette, Effects of iron black varnish on petrophysical properties of building sandstone, *Environmental Geology* 47, (2004), 119-131
2. J-D. Mertz, Etat des lieux, diagnostic des pathologies et perspectives, In: *Un chantier, restauration des façades des monuments urbains*. Ministère de la Culture et de la Communication, OPPIC, (2010), 79p
3. A.G. Nord, T. Ericsson, Chemical analysis of thin black layers on building stone, *Studies in Conservation*, Vol. 38, (1993), pp. 25-35

High Resolution Analysis of the $\nu_2+\nu_4-\nu_5$ Band of SF_6 Leading to an Improvement of the ν_5 Raman Band Parameters

M. Faye¹, L. Manceron¹, P. Roy¹, V. Boudon² and M. Loete²

¹Synchrotron SOLEIL, AILES Beam line, Saint Aubin, France

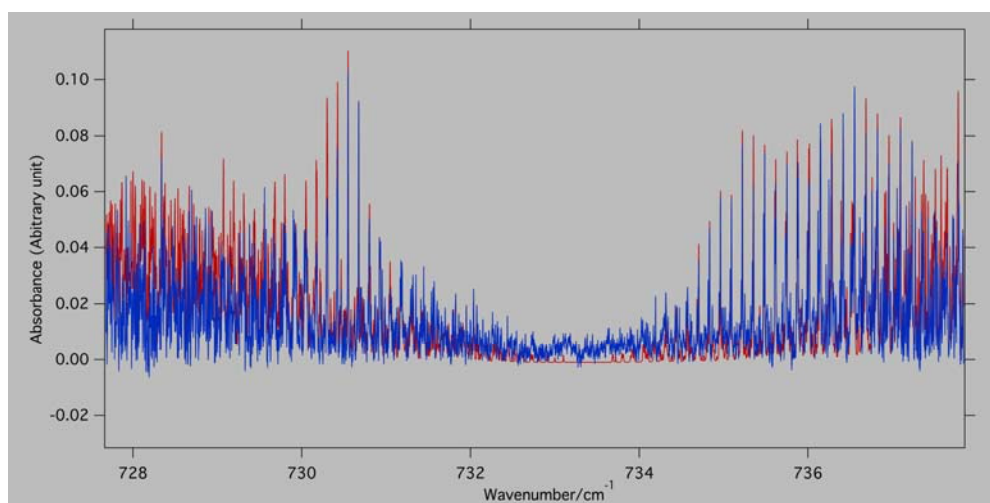
²Laboratoire Interdisciplinaire Carnot de Bourgogne, UMR 6303 CNRS-Université Bourgogne Franche-Comté, 9 Avenue Alain Savary, BP 47 870, F-21078 DIJON Cedex France

ABSTRACT

We recently performed measurements in infrared absorption of Sulfure Hexafluoride (SF_6) in the gas phase at the AILES beamline of the SOLEIL synchrotron facility, by using an IFS125HR interferometer coupled to a cryogenic multiple pass cell [1] and to a special home-made detector. The optical path length of the beam was adjusted to 141 m and the SF_6 sample was cooled down up to 243 K at a pressure of 10 mbar. Several bands have been recorded at a resolution of 0.00125 cm^{-1} in the $600\text{--}800 \text{ cm}^{-1}$ wave number range.

In this work, we present the analysis of the $\nu_2+\nu_4-\nu_5$ band (Figure below) performed tanks to the tensorial formalism [2].

This analysis has provided us more accurate parameters for the $\nu_5=1$ level of SF_6 which was previously analyzed at a less resolution, with only the R branch of the ν_5 Raman spectrum[3].



REFERENCES

1. F. Kwabia Tchana, F. Willaert, X. Landsheere, J.- M. Flaud, L. Lago, M. Chapuis, P. Roy, L. Manceron. *A new, low temperature long-pass cell for mid-IR to THz Spectroscopy and Synchrotron Radiation Use*. Rev. Sci. Inst. 84, 093101, (2013).
2. V. Boudon, L. Manceron, F. Kwabia Tchana, M. Loète, L. Lago, P. Roy, *Resolving the forbidden band of SF_6* . Phys.Chem.Chem.Phys.16,1415 (2014).
3. V. Boudon and D. Bermejo. *First High resolution Raman Spectrum and Analysis of the Bending Fundamental of SF_6* . Journal of Molecular Spectroscopy 213, 139-144 (2002).

Development of an Experimental Setup for Multi Electron-ion Coincidence Spectroscopy

M. A. Khalal¹, J. Palaudoux¹, P. Lablanquie¹, F. Penent¹, L. Andric¹,
M. Zitnik², K. Bucar², J-M. Bizau^{3,4}, D. Cubaynes^{3,4},
K. Jänkälä⁵ and M. Huttula⁵

¹ CNRS & UPMC, Université Paris 06, LCPMR, 11 rue P. & M. Curie, 75231 Paris cedex 05, France

² J. Stefan Institute, Jamova 39, 1000 Ljubljana, Slovenia

³ ISMO, CNRS UMR 8214, Université Paris-Sud, Bâtiment 350, F-91405 Orsay cedex, France

⁴ Synchrotron SOLEIL, L'Orme des Merisiers, Saint Aubin, F-91192 Gif-sur-Yvette cedex, France

⁵ Department of Physics, University of Oulu, P.O. Box 3000, 90014 Oulu, Finland

ABSTRACT

The study of multiple photoionization of isolated atoms by a single photon gives information on electron correlations and Auger decay mechanisms. For that purpose, a magnetic bottle time of flight spectrometer called HERMES (High Energy Resolution Multi Electron Spectrometer) has been used and a lot of results were obtained on atoms and molecules [1, 2]. Recently, a homemade oven has also allowed the study of alkali metal vapors (Rb and K) [3].

The experimental setup has been improved by adding an ion time of flight, so that we can detect both ions and electrons in coincidence. Electrons are sent on a 2 m long time of flight tube whereas an electric pulse repels ions, through a "hollow magnet", to the opposite side on a 30 cm tube.

The experiment was carried out at the SEXTANTS beamline. As a first test, Xe multiple photoionization was studied. Ions (Xe^{2+} , Xe^{3+} , Xe^{4+}) were successfully detected in coincidence with electrons with an efficiency of $\sim 10\%$. That allows us to filter and select electrons that come from double, triple or quadruple ionization. Figure 1 shows the spectra obtained at a photon energy of 220eV, where $4d^{-1}$ and $4p^{-1}$ Auger decays contribute.

A similar electron / ion coincidence apparatus was recently developed [4]. The advantage of our setup is that ions are detected through the hollow magnet, and not perpendicular to the magnetic bottle axis, thus allowing the use of an oven. First results of ions/electrons coincidences have been obtained on Rb vapor.

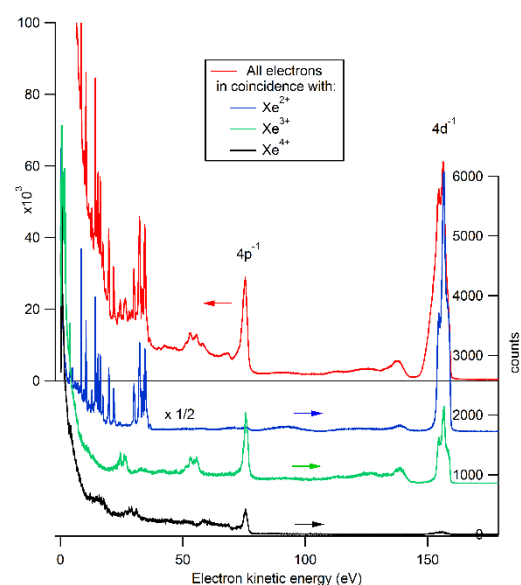


Figure 1: Spectra of electrons in coincidence with specific ions.

REFERENCES

1. F. Penent et al, Phys. Rev. Lett. **95**, 083002, (2005) ; F. Penent et al, Phys. Rev. Lett, **106**, 103002 (2011)
2. F. Penent et al, J Elect Spect Rel Phen. **204**, 303 (2015) and references included.
3. J. Palaudoux et al, Phys Rev A. **92**, 012510 (2015)
4. J H D Eland et al, J. Phys. B : At. Mol. Opt. Phys. **48** (2015) 2050

Connected Semiconducting and Metallic Nanoribbons on a Graphene Layer

A. Celis^{1,2}, I. Palacio², M. N. Nair², A. Gloter², A. Zobelli², M. Sicot⁴,
D. Malterre⁴, M. S. Nevius³, C. Berger³, W. de Heer³, E.H. Conrad³,
A. Taleb-Ibrahimi², A. Tejeda^{1,2}

¹Laboratoire de Physique des Solides, UMR CNRS 8502, Université Paris Sud. 91405 Orsay, France

²Synchrotron SOLEIL, Saint-Aubin, 91192 Gif-sur-Yvette, France

³School of Physics, The Georgia Institute of Technology, Atlanta, Georgia 30332-0430, USA

⁴Institut Jean Lamour, BP 70239, F-54506 Vandoeuvre-lès-Nancy, France

ABSTRACT

Armchair edged graphene nanoribbons are expected to present a controllable bandgap, suitable for graphene-based electronic devices. The gap relies on the fine control of the ribbon width and edge regularity at a level reaching a single atomic row, unattainable by state-of-the-art lithographic methods. We have studied graphene ribbons produced by combining lithography and thermal treatments to stabilize them on an array of artificial facets on a SiC(0001) surface^{1,2}. The ribbon array was then studied by Scanning Tunneling Microscopy (STM) and High Resolution cross-sectional Transmission Electron Microscopy (HR-XTEM) in order to correlate them to Angle Resolved Photoemission Spectroscopy (ARPES)^{3,4}. Our results indicate the presence of a continuous layer of graphene that exhibits both metallic and semiconducting behavior, depending on the graphene atomic local structure and interaction with the substrate. This dependence of the electronic properties is in agreement with DFT numerical simulations⁴.

REFERENCES

1. M. Sprinkle, M. Ruan, Y. Hu, J. Hankinson, M. Rubio-Roy, B. Zhang, X. Wu, C. Berger and W.A. de Heer. *Nature Nanotech.* **5**, 727 (2010)
2. W. de Heer, C. Berger, M. Ruan, M. Sprinkle, X. Li, Y. Hu, B. Zhang, J. Hankinson and E. Conrad. *Proceedings of the National Academy of Sciences of the United States of America*, **108**, 41 (2011)
3. J. Hicks, A. Tejeda, A. Taleb-Ibrahimi, M.S. Nevius, F. Wang, K. Shepperd, J. Palmer, F. Bertran, P. Le Fèvre, J. Kunc, W.A. de Heer, C. Berger and E. Conrad, . *Nature Physics*. Vol. **9**, 49 (2013)
4. I. Palacio, A. Celis, M. N. Nair, A. Gloter, A. Zobelli, M. Sicot, D. Malterre, M.S. Nevius, W.A. de Heer, C. Berger, E. Conrad, A. Taleb-Ibrahimi and A. Tejeda *Nanoletters*, **15**, 182 (2015)

Tailoring Band Gaps in Graphene by Substrate Nanostructuring

A. Celis^{1,2}, M. N. Nair², A. Taleb-Ibrahimi², A. Tejeda^{1,2}

¹Laboratoire de Physique des Solides, UMR CNRS 8502, Université Paris Sud, 91405 Orsay, France

²Synchrotron SOLEIL, Saint-Aubin, 91192 Gif-sur-Yvette, France

ABSTRACT

Nanostructuring is a successful way of tailoring the electronic properties of materials for devices [1]. One way of tuning electronic properties consists of exploiting the electronic confinement in artificial structures of nanometric size. Electronic confinement of metallic Shockley states has been demonstrated on noble metal surfaces by superperiodic potentials [2, 3]. Likewise, electronic confinement gaps have been observed on graphene nanoribbons of 1-2 nm width [4]. Here, we show how periodic nanostructures modify graphene's electronic properties. By using a nanostructured Pt substrate, we induce different superperiodicities on graphene triggering a band-gap opening in different energies and different regions of the reciprocal space. Our study correlates the mini gaps observed in Angle-Resolved Photoemission to the atomic structure observed by Scanning Tunneling Microscopy (STM).

REFERENCES

1. P. Lodahl, S. Mahmoodian and Soren Stobbe. *Reviews of Modern Physics*, **87**, 347 (2015)
2. A. Mugarza, A. Mascaraque, V. Pérez-Dieste, V. Repain, S. Rousset, F.J. Garcia de Abajo, and J.E. Ortega. *Physical Review Letters*, **87**, 107601 (2001)
3. C. Didiot, A. Tejeda, Y. Fagot-Revurat, V. Repain, B. Kierren, S. Rousset and D. Malterre. *Physical Review B*, **76**, 081404(R) (2007)
4. I. Palacio, A. Celis, M. N. Nair, A. Gloter, A. Zobelli, M. Sicot, D. Malterre, M.S. Nevius, W.A. de Heer, C. Berger, E. Conrad, A. Taleb-Ibrahimi and A. Tejeda *Nanoletters*, **15**, 182 (2015)

L-edge XMCD Investigation of Photo-switchable Fe/Co Prussian Blue Molecular Magnets

S. Fatima*¹, R. Moulin², M-A. Arrio¹, A. Juhin¹, A. Bordage², A. Bleuzen²
E. Otero³, P. Ohresser³, C. Cartier Dit Moulin⁴, P. Sainctavit^{1,3}

¹University of Pierre and Marie Curie, Institute of Mineralogy, Condensed Matter Physics and Cosmo-Chemistry (IMPMC), UMR 7590, Paris, France,

²University of Paris-Sud, Institute of Chemistry of Molecules and Materials (ICMMO), Orsay, France,
³Synchrotron Soleil, Saint Aubin, France,

⁴University of Pierre and Marie Curie, Paris Institute of Molecular Chemistry (IPCM), Paris, France.
Sadaf.fatima@impmc.upmc.fr

ABSTRACT

Molecular magnetic materials are potential candidates for energy efficient, photoswitchable molecule-based information storage. The family of Prussian Blue and its analogues, referred as Prussian Blue analogues (PBA), exhibit thermal and photomagnetic bistability which makes it well-suited for these applications [1]. 3D FeCo-PBA have been extensively investigated by conventional magnetometry and XMCD at the K-edges but never by XMCD at L_{2,3} edges [2]. In this study, we present L-edge XAS/XMCD results obtained on 3D Rb₂Co[Fe(CN)₆] PBA synthesized by Bleuzen and coworkers at ICMMO (Orsay).

The current challenge of designing systems for information storage requires deep understanding of the thermally and light-induced electron transfer phenomenon and its driving mechanism. Therefore, advanced characterization techniques like X-ray absorption spectroscopy (XAS) and X-ray magnetic circular dichroism (XMCD) are the excellent tools to probe the change in the macroscopic magnetic properties of PBAs and can give local information about the metal centers existing in the structure. Element specific XAS and XMCD measurements at Fe and Co L_{2,3} edges were performed on the DEIMOS beamline (SOLEIL, France). XAS/XMCD at Fe and Co L_{2,3} edges were measured at 200 K and 2 K. At 2K, the sample is irradiated by a 635 nm laser that switched the diamagnetic Fe(II)-Co(III) pair to the Fe(III)-Co(II) paramagnetic one. To follow Light induced charge transfer between Fe(III)-Co(II) paramagnetic pair and Fe(II)-Co(III) diamagnetic pair, XAS/XMCD is recorded at Fe and Co L_{2,3} edges at 2 K after irradiation. In order to probe the nature of coupling between Fe and Co in photoinduced state, XMCD and magnetization curves were also recorded. Another important aspect is to check for the reversibility of the charge-transfer that has been measured by warming the sample to 200 K. XAS and XMCD coupled with Ligand Field Multiplet theory (LFM) is required to extract quantitative information and the detailed interpretation of the data [3].

REFERENCES

- O. Sato, Journal of Photochemistry and Photobiology C: Photochemistry Reviews **2004**, 5, 3, 2013-223.
- (a)A. Bleuzen et al., C. R Chimie **6**, **2003**, 343-352. (b)V. Escax et al., C. R Chimie **6**, **2003**, 1165-1173. (c) Cartier dit Moulin et al., J. Am. Chem. Soc., **122**, 2000, 6653-6658. (d) A. Bleuzen et al., Angew. Chem. Int. Ed., **43**, **2004**, 3728-3731. (e) A. Bleuzen et al., J. Am. Chem. Soc., **122**, 2000, 6648-6652. (f) V. Escax et al., J. Am. Chem. Soc., **107**, **2003**, 4763-4767. (g) V. Escax et al., Angew. Chem. Int. Ed., **44**, **2005**, 4798-4801. (h) G. Fornasieri et al., Materials. **2012**, 5, 385-403.
- B. T. Thole et al, Phys. Rev. Lett., **1992**, 68 , 1943-1946.

Investigation of Orbital Excitations in TbMnO₃

J. Feng¹, A. Juhin², R. Jarrier¹, R. Delaunay¹, A. Nicolaou³,
H. Zhou^{4,5}, J-M. Mariot¹ and G. S. Chiuzbaian^{1,3}

¹ LCPMR, CNRS and UPMC (UMR 7614), 11, Rue Pierre et Marie Curie, 75005 Paris, France

² IMPMC, CNRS and UPMC (UMR 7590), 4, place Jussieu, 75005 Paris, France

³ Synchrotron SOLEIL, Saint-Aubin, B.P. 48, F-91192 Gif-sur-Yvette, France

⁴ Department of Physics and Astronomy, University of Tennessee, Knoxville, TN 37996-1200, USA

⁵ National High Magnetic Field Laboratory, Florida State University, Tallahassee, FL 32310-3706, USA

ABSTRACT

The electronic structure of multiferroic TbMnO₃ was investigated in order to characterize the crystal field acting on the Mn sites. We performed resonant inelastic X-ray scattering (RIXS) measurements at the manganese L₃ (2*p*-3*d*) and oxygen K (1*s*-2*p*) resonances, using the AERHA spectrometer¹ installed on the SEXTANTS beamline² of Synchrotron SOLEIL. Both resonances were probed at room temperature and 25 K. We explored the presence of spectral weight at 2.9 eV transferred energy in the Mn L₃ edge spectra, as indicated in the previous RIXS study at the Mn K resonance (1*s*-3*d*)³. The RIXS spectra show that a Mn 3*d* orbital excitation is present at same transferred energy in both Mn L₃ and O K RIXS spectra. The parameters of the Mn *D*_{4h} crystal field were identified with the help of multiplet calculations (see, e.g., Ref. 4) of the spectral weight.

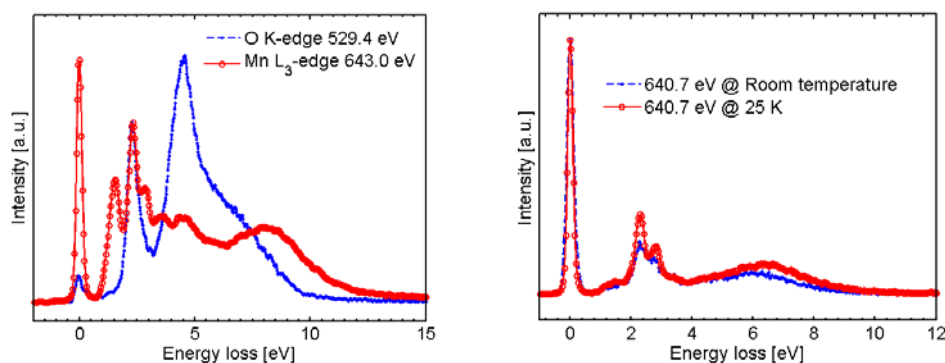


Fig. 1: RIXS spectra of TbMnO₃: (left) RIXS at Mn L₃ edge (incoming photon energy 640.7 eV) at room temperature and 25 K; (right) RIXS at Mn L₃ and O K edges (incoming photon energy 643 eV and 529.4 eV, respectively).

REFERENCES

1. S. G. Chiuzbaian *et al.*, Rev. Sci. Instrum. **85**, 043108 (2014).
2. M. Sacchi *et al.*, J. Phys. Conf. Ser. **425**, 072018 (2013).
3. J. M. Chen *et al.*, Phys. Rev. B **82**, 094442 (2010).
4. M. M. van Schooneveld *et al.*, J. Phys. Chem. C **116**, 15218 (2012).

Investigate of Interface Annealing and Switching Polarization of the $\text{Pb}_{1.1}(\text{Zr}_{0.52},\text{Ti}_{0.48})\text{O}_3/\text{Ru}/\text{Pt}$ by Operando (HAXPES) Analysis

I. Gueye¹, G. Le Rhun¹, O. Renault¹, D. Ceolin² and N. Barrett³

¹ Univ. Grenoble-Alpes, F-38000 Grenoble, France - CEA, LETI, MINATEC Campus, 17 rue des Martyrs, 38054 Grenoble Cedex 9, France

²Synchrotron-SOLEIL, L'Orme des Merisiers, St Aubin - BP 48 91192 Gif-sur-Yvette Cedex, France

³SPEC, CEA, CNRS, Université Paris Saclay, F-91191 Gif-sur-Yvette, France

ABSTRACT

$\text{Pb}(\text{Zr}_{0.52},\text{Ti}_{0.48})\text{O}_3$ (PZT) thin films are widely used for piezoelectric and ferroelectric applications such as sensors, actuators and capacitors. For all these applications, the device is based on a Metal-Insulator-Metal (MIM) structure. Optimized 200 nm sol-gel layers of PZT can have permittivity as high as 900, capacitance 40 nF/mm² and 30 V breakdown voltages [2]. The PZT/electrode interface can play a major role on the performances of capacitors [1]. The aim of our experiment was to investigate using Hard X-ray PhotoEmission Spectroscopy (HAXPES) the Pt (5nm)/Ru(5nm)/PZT interface chemistry and electronic structure as function of the applied voltage to switch the polarization state and post-etching annealing at 550°C in oxygen (fig 1.a). Switching applied voltage from $V_{dc}>0$ to $V_{dc}<0$ for the PZT (fig 1.b), gives rise to a shift of the Pb4d peak about 1.34eV toward the lower kinetic energy (from 6481.23eV to 6479.89eV) suggesting strong interaction between the polarization and the PZT/electrode interface structure. Annealing results in a shift of 1.24eV of Ru3p from 6432.28eV to 6431.04eV ($V_{dc}>0$), suggesting partial oxidation of Ru (fig 1.c). We discuss correlations between the interface chemistry and the internal field, polarization and the I-V characteristic and the effect of polarization on the Schottky barrier height.

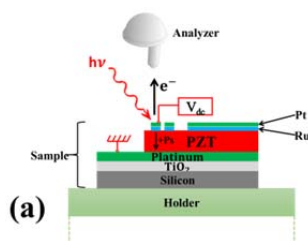


Figure 1: (a) schematic mounting of voltage generator and the connection of the sample for operando experiment (b) Pb 4d core level spectra taken at 6895 eV as a function of poling voltage for the unannealed PZT and (c) Comparison between unannealed and annealed (PZT/Ru/Pt for the positive voltage applied ($V_{dc}>0$))

REFERENCES

- [1] L. Pintilie and M. Alexe, *J. Appl. Phys.* **98**, 124103 (2005)
 [2] P. Belleville, J. Bigarre, P. Boy, Y. Montouillout, *J. Sol-Gel Sci. Technol.* **43**, 213 (2007)

Exploring the Electronic Structure along Single Bi_2Te_3 Nanowires by Nano-angle-resolved Photoemission Spectroscopy

J. Krieg^{1,2}, C. Chen³, J. Avila³, C. Trautmann^{1,2}, M-C. Asensio³,
M. E. Toimil-Molares¹

¹*Materials Research, GSI Helmholtz Center for Heavy Ion Research, Planckstr. 1,
64291 Darmstadt, Germany*

²*Institut für Materialwissenschaften, Technische Universität, Alarich-Weiss-Str. 2,
64287 Darmstadt, Germany*

³*Synchrotron SOLEIL, L'orme des Mersiers Saint-Aubin BP48, 91192 Gif-sur-Yvette CEDEX, France*

ABSTRACT

Transport measurements to address the surface states of topological insulator (TI) materials are challenging, but crucial on the way to fabricate spintronic devices. Nanowires are excellent model systems to investigate TI surface states. Due to their high surface-to-volume ratio and adjustable properties (e.g. size, composition), they enable a reduction of the large contribution of bulk charge carriers dominating the signals in a controlled manner.

Cylindrical Bi_2Te_3 nanowires were synthesized by electrochemical deposition in the channels of ion-track etched polymer membranes. Their chemical composition and crystallographic structure analyzed by high resolution scanning electron microscopy (HRSEM), energy-dispersive x-ray spectroscopy (EDX), transmission electron microscopy (TEM), and x-ray diffraction (XRD), revealed chemically homogenous and polycrystalline, highly textured Bi_2Te_3 nanowires with grain sizes of several hundreds of nm¹.

Single nanowires were investigated by nano-angle-resolved photoemission spectroscopy (nano-ARPES or k-nanoscope) at the ANTARES beamline at the SOLEIL Synchrotron, which provides an extremely high lateral resolution (~120 nm), together with a high energy and k space resolution in recording core levels and electronic bandstructure. In particular, cylindrical Bi_2Te_3 wires of 100 nm diameter and length of up to 30 μm were fabricated and randomly distributed on a p-doped silicon substrate by wet chemical dissolution of the surrounding polymer membrane and subsequent drop casting. The cleanness of the sample's surface after the transfer process was evaluated by core level spectroscopy to identify oxygen and carbon contamination which possibly originate from oxidation and polymer residues.

Core level spectra recorded along a given nanowire revealed no chemical shift of the peaks, emphasizing the chemical homogeneity on the nanometer scale confirming results from EDX measurements. By combining scanning and on-focus operation ARPES modes, individual nanowires were imaged using both Te 4d core level and top of the valence band signals. ARPES measurements were conducted on several points along several selected single wires and bundles of wires. The band structures indicate that the Fermi level of these nanowires lies within the valence band. Interestingly, different valence band structures were obtained depending on the position on a given wire.

REFERENCES

1. O. Picht et al., J. Phys. Chem. C **116**, 5367 (2012)

Electronic Structure Change Associated with Re-emergence of Superconductivity in $K_{0.8}Fe_{1.7}Se_2$ and $Tl_{0.6}Rb_{0.4}Fe_{1.67}Se_2$ under Pressure

B. Lebert¹, J-P. Rueff¹, V. Balédent², P. Toulemonde³, and L. Simonelli⁴

[1] Synchrotron SOLEIL, L'Orme des Merisiers, BP 48 Saint-Aubin,
91192 Gif-sur-Yvette Cedex, France

[2] Laboratoire de Physique des Solides, 91400 Orsay, France

[3] Institut Néel, 38042 Grenoble, France

[4] CELLS – ALBA, Carretera, BP 1413, de Cerdanyola del Vallès a Sant Cugat del Vallès, Km 3.3,
08290 Cerdanyola del Vallès, Barcelona, Spain

ABSTRACT

Since the discovery of high T_C superconductivity (SC) in iron arsenides in 2008 (with an outstanding $T_C = 55$ K, in the $LnFeAs(O_{1-x}F_x)$ 111 family with $Ln = Sm$ or Gd), superconductivity has also been reported in other analogous materials with the same tetrahedral environment for iron. In particular, a new family isostructural to the arsenides “122” was found in 2010 by intercalation of K, Rb or Cs between the FeSe layers. The new family is superconducting around 30 – 33 K [1], which is the same range of T_C obtained under high pressure for pure FeSe layers.

Recently, a surprising re-emergence of SC under pressure has been evidenced for the some specific compositions of these isostructural compounds: $K_{0.8}Fe_{1.7}Se_2$ and $Tl_{0.6}Rb_{0.4}Fe_{1.67}Se_2$, show a jump of their critical temperature under pressure up to 48 K [2] between 11 to 13 GPa. This re-emergence of superconductivity is highly unexpected since T_C progressively decreases in the 0 – 10 GPa range is totally suppressed around 10 GPa. The singularity of the re-emergence of SC in these systems is that the critical superconducting temperature observes a step-like increase to 40 K at 11 GPa, remains mostly constant until 13 GPa, and vanishes as quickly as it appeared upon. The unusual phase diagram suggests a complete and sudden reorganization of the electronic structure of the iron 3d orbitals.

A study of the electronic structure has been published on similar system ($Rb_{1-x}Fe_{2-y}Se_2$) by absorption spectroscopy on Fe and Se K edge. It reports a change of the electronic structure on both Fe and Se at 11 GPa [3]. However, this study was not conclusive as the samples are different from the series that show a re-emergence of SC temperature. Therefore, we studied the electronic structure of the substances which show re-emergence ($K_{0.8}Fe_{1.7}Se_2$ and $Tl_{0.6}Rb_{0.4}Fe_{1.67}Se_2$) on the GALAXIES beamline using Fe K-edge XAS and x-ray emission spectroscopy under pressure, at 300 K and 10 K in order to electronic change through different transitions.

REFERENCES

1. Guo et al. *Phy. Rev. B* 82, 180520(R) (2010)
2. L. Sun et al. *Nature* 483, 67-69 (2012)
3. M. Bendele et al. *PRB* 88, 180506 (2013)

Photoemission Study of Irradiation Impact on Amorphous / Crystalline (a-Si:H/ c-Si) Silicon Heterojunction

M.-I. Lee^a, A. Defresne^b, K. Ouaras^c, K. Hassouni^c, D. Ceolin^d, J.-P. Rueff^d, O. Plantevin^b, P. Roca i Cabarrocas^e, A. Tejada^a

^a LPS, CNRS, Université Paris-Saclay, Univ. Paris-Sud 91405 Orsay, France

^b CSNSM, Université Paris-Sud and CNRS/IN2P3, Bâtiments 104 et 108, 91405 Orsay, France

^c LSPM, CNRS, Université Paris 13, 93430 Villetaneuse, France

^d Synchrotron SOLEIL, L'Orme des Merisiers, St Aubin BP 48, 91192 Gif sur Yvette, France

^e LPICM, CNRS, Ecole Polytechnique, Université Paris-Saclay, 91128 Palaiseau, France

ABSTRACT

Ion irradiation of silicon heterojunction solar cells based on a-Si:H/ c-Si stacks has been demonstrated to modify their efficiency [1]. In order to relate these observations to the electronic and structural changes at the buried interface, we have performed Hard X-ray Photoelectron Spectroscopy (HAXPES) [2] at the GALAXIES beamline of SOLEIL synchrotron. We have studied a-Si:H/ c-Si silicon heterojunctions irradiated with pulsed plasma irradiation of 100 eV Ar ions under fluences upto 10^{15} ions/cm² (at this energy, the irradiation is limited to few nm). The HAXPES measurements reveal the impact of irradiation as a function of depth (using different photon energies: 3keV, 5keV and 8keV) via core-level and valence band detection. The density of states (DOS) of the valence band has been determined as a function of the depth (fig. 1b), which also provides information on the crystalline Si bands in thin heterojunctions. The DOS reveals a state of 0.3 eV of binding energy in the irradiated samples, compatible with the photoluminescence from these samples (fig. 1c) [1]. The photoemission data as a function of the photon energy allow to identify the depth where this state is localized, necessary to understand the atomistic nature of the electronic state and how it is induced.

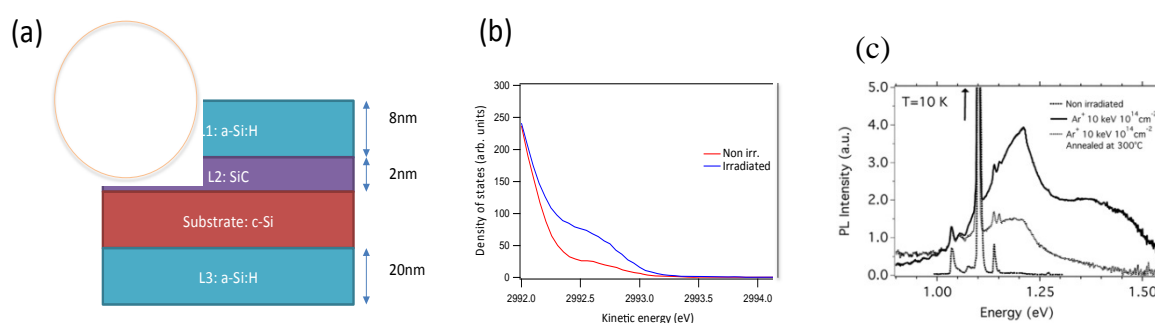


Figure 1. (a) Schematics of the studied a-Si:H/c-Si heterojunctions. Circles represent the inelastic mean free path of the emitted electrons. (b) Density of states near the Fermi level of irradiated and non-irradiated samples ($h\nu = 3$ keV) (c) Photoluminescence (PL) spectra at 10 K from crystalline silicon passivated with hydrogenated amorphous silicon layers in the as-deposited, after Ar⁺ implantation and annealed after irradiation [1].

REFERENCES

1. A. Defresne, O. Plantevin, I.P. Sobkowicz, J. Bourçois, P. Roca i Cabarrocas. Nuclear Instruments and Methods in Physics Research B (2015).
2. C. Papp et al., Nature Materials 10,759 (2011).

Two-dimensional Electron Systems at the Surface of Locally Doped Titanates Studied by ARPES

T. C. Rödel^{1,2*}, F. Fortuna¹, F. Bertran², T. Maroutian³, P. Lecoeur³,
P. Le Fèvre², A. F. Santander-Syro¹

¹CSNSM, ³Institut d'Electronique Fondamentale, Univ. Paris-Sud, CNRS,
Université Paris-Saclay, 91405 Orsay, France

²Synchrotron SOLEIL, L'Orme des Merisiers, Saint-Aubin-BP48, 91192 Gif-sur-Yvette, France

ABSTRACT

Two-dimensional electron systems (2DESs) in transition metal oxides are currently a field of intense research in the quest of novel functionalities in materials showing competing ground states. The 2DESs in SrTiO₃-based interfaces have been the cornerstone of such research.¹ The building block of SrTiO₃ and other titanates is the oxygen octahedron. Here we show, using (angle-resolved) photoemission spectroscopy in UHV that the stacking order and the rotation of those octahedra determines the order and hybridization of the t_{2g} orbitals as well as the (de)localized character of the excess electrons in 2DESs. To study different lattice configurations, we characterized the 2DESs at the surface of SrTiO₃, CaTiO₃ and TiO₂.^{2,3}

REFERENCES

1. A. Ohtomo and H.Y. Hwang, *Nature* **2004**, 427, 423.
2. A.F. Santander-Syro *et al*, *Nature* **2011**, 469, 189.
3. T.C. Rödel *et al*, *Phys. Rev. B* **2015**, 92, 041106(R).

Universal Method for the Fabrication of Two-dimensional Electron Systems in Functional Oxides

T. C. Rödel^{1,2*}, F. Fortuna¹, S. Sengupta³, E. Frantzeskakis¹,
P. Le Fèvre², F. Bertran², B. Mercey⁴, S. Matzen⁵, G. Agnus⁵,
T. Maroutian⁵, P. Lecoœur⁵, A. F. Santander-Syro¹

¹CSNSM, ³Laboratoire de Physique des Solides, ⁵Institut d'Electronique Fondamentale, Univ. Paris-Sud, CNRS, Université Paris-Saclay, 91405 Orsay, France

²Synchrotron SOLEIL, L'Orme des Merisiers, Saint-Aubin-BP48, 91192 Gif-sur-Yvette, France

⁴CRISMAT, ENSICAEN-CNRS UMR6508, 6 bd. Maréchal Juin, 14050 Caen, France

ABSTRACT

Two-dimensional electron systems (2DESs) in transition metal oxides are currently a field of intense research in the quest of novel functionalities in materials showing competing ground states. The 2DESs in SrTiO₃-based interfaces have been the cornerstone of such research.¹ To go beyond, it is essential to create new types of oxide 2DESs in a technically easy way. Here we show, using (angle-resolved) photoemission spectroscopy in UHV that the deposition of atomically-thin layers of a elementary reducing agent results in the creation of 2DESs at the interface of several functional oxides, such as the ferroelectric BaTiO₃.² This technique can be adapted for transport studies and opens the possibility to study 2DESs in strongly-correlated insulating oxides.

REFERENCES

1. A. Ohtomo and H.Y. Hwang, *Nature* **2004**, *427*, 423.
2. T.C. Rödel *et al*, *Adv. Materials* **2015**, accepted

Tailoring Electronic Properties in Long Range Ordered on Surface Synthetized Polymer

S. Xing¹, Y. Fagot-Revurat¹, G.Vasseur⁷, M. Sicot¹, B. Kierren¹, L. Moreau¹,
D.Malterre¹, G. Galeotti², J. Lipton-Duffin², L. Cardenas², F.Rosei²,
M. Di Giovannantonio³, G. Contini³, P. Le Fevre⁴, F. Bertran⁴, V. Meunier⁵,
L. Liang⁵, D. Perepichka⁶

¹Institut Jean Lamour, Université de Lorraine - CNRS, Vandoeuvre-les-Nancy, France ;

²Institut National de la Recherche Scientifique, Varennes, Canada ;

³Istituto di Struttura della Materia, CNR, Roma, Italy ;

⁴Synchrotron SOLEIL, L'Orme des Merisiers, Saint-Aubin, Gif sur Yvette, France ;

⁵Department of Physics, Applied Physics, and Astronomy, Rensselaer Polytechnic Institute, New York, United States;

⁶Department of Chemistry and Centre for Self-Assembled Chemical Structures, McGill University, Montreal, Canada;

⁷Donostia International Physics Center, San-Sebastian, Spain.

ABSTRACT

Polymerization on surfaces has been widely studied during the last two decades. The most successful method to obtain ordered polymers is based on the Ullmann reaction: noble surfaces act as catalysts and templates for polymerization [1,2]. Structural and electronic properties of 1,4 di-bromobenzene (dBB)/Cu(110) has been investigated by combining LEED, STM, HR-XPS, N-EXAFS and DFT calculations [3,4]. An intermediate organometallic phase (OM) has been clearly evidenced at room temperature transforming into a polymerized one (PPP=poly-para-phenylene) by an annealing above 200°C. More recently, we succeed to form a well ordered commensurate PPP phase for coverage close to one monolayer of dBB deposited on Cu(110) and annealed above the polymerization temperature, as shown in figure 1a [5].

In our study on the CASSIOPEE beamline, we evidenced how crucial is polymer/substrate interaction for the electronic properties. On the one hand, we studied the Br-I substitution by growing dIB/Cu(110) and obtained well-ordered PPP too (Fig1c). Nevertheless, Iodine adsorption site and PPP orientation -polymers are twisted as shown in the inset- differ in such a way that electronic properties are strongly affected. The full HOMO-LUMO gap is measured as 1.15eV for dBB/Cu(110) system whereas it is 1.7eV for dIB/Cu(110) (fig1b,1d). Finally, another physical point remains: is it possible to obtain a single long range ordering domain? Recently, we were able to synthesize infinite PPP polymers on copper vicinal surfaces as shown in figure 1e and 1f. As a consequence, a single well defined orientation (instead of the two domains), parallel to the step edges, is obtained leading to a possible contribution of 100 % of PPP polymers to the ARPES signal measured along the chains.

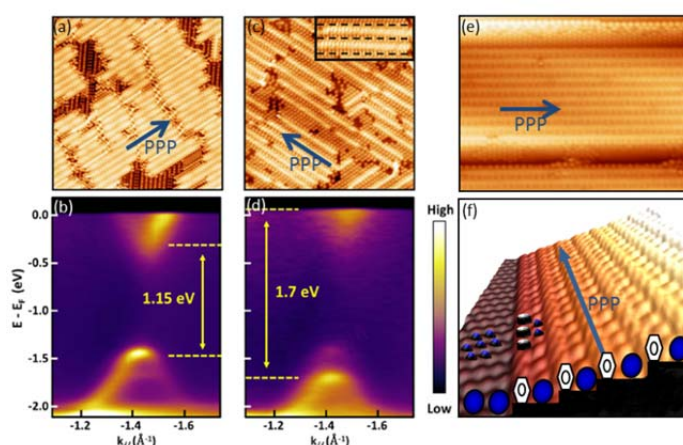


Figure 1: (a) STM image of dBB/Cu(110). (b) Homo-Lumo gap is measured as 1,15eV. (c) STM image of dIB/Cu(110). Inset shows how polymers are twisted regarding to iodine atoms that are marked by dashed lines. (d) Homo-Lumo gap measured as 1,7eV for this system. (e) STM image of dBB/Cu(775) showing infinite polymer. (f) 3D representation of image from (e), scheme is drawn and shows how steps are reconstructed and populated by one PPP line and one Bromine atom line.

REFERENCES

- [1] M. Bieri et al., Chem. Comm. 69, 19 (2009);
- [2] D. Perepichka and F. Rosei, Science 323, 216 (2009);
- [3] J.A. Lipton-Duffin et al., Small 5, 592 (2009);
- [4] M. Di Giovannantonio et al. ACS Nano 7, 8190 (2013) ;
- [5] G.Vasseur et al. accepted Nature Communication ;

Superconductivity, Pseudogap, and Stripe Correlations in High- T_c Cuprates

Z. Zhang

*Institut de Minéralogie et de Physique des Milieux Condensés (IMPMC),
Université Pierre et Marie Curie - Paris 6, case 115, 4, place Jussieu, 75252 Paris cedex 05, France*

ABSTRACT

Underdoped La-214 cuprate, are known to shows charge-modulations in the "stripes" [1], form rather than in Charge-Density-Wave one. These stripes modulation are (quasi)-static close to hole doping of 1/8, where they suppress superconductivity. In contrast to this, the pseudo-gap phase of the other cuprate compounds recently revealed rather Charge-Density-Wave [2-4] type of charge modulation, that possibly also competes with superconductivity. In this context, to better understand how the stripe phase competes with superconductivity, we use Angle Resolved Photoemission Spectroscopy on CASSIOPEE beamline, to study the electronic band structure and gap in La-214 cuprates at at 1/8 doping ($\text{La}_{2-x-y}\text{Nd}_y\text{Sr}_x\text{CuO}_4$ ($x=0.12; y=0,0.4$)) and $\text{La}_{2-x}\text{Ba}_x\text{CuO}_4$ ($x=0.12$)). A well-defined nodal quasi-particle peak is found to exist in the stripe-order state, and we study it as a function of temperature and doping, together with the gap and pseudo-gap.

REFERENCES

1. S. A. Kivelson, al., Rev. Mod. Phys., 1201 (2003).
2. Chang, J. et al., Nature Phys. 8, 871–876 (2012).
3. Comin, R. et al., Science 343, 390–392 (2014).
4. Da Silva Neto, E. H. et al. Science 343, 393–396 (2014).

Structure of Lu Phtalocyanine Thin Films Deposited on Au(111)

M. Farronato^(a); A. Jones^(b); G. Prevot^(a,c); J. Simbrunner^(c);
R. Resel^(b); N. Witkowski^(a;c)

(a) UPMC Univ. Paris 6, UMR 7588, Institut de NanoSciences de Paris 75005 Paris, France

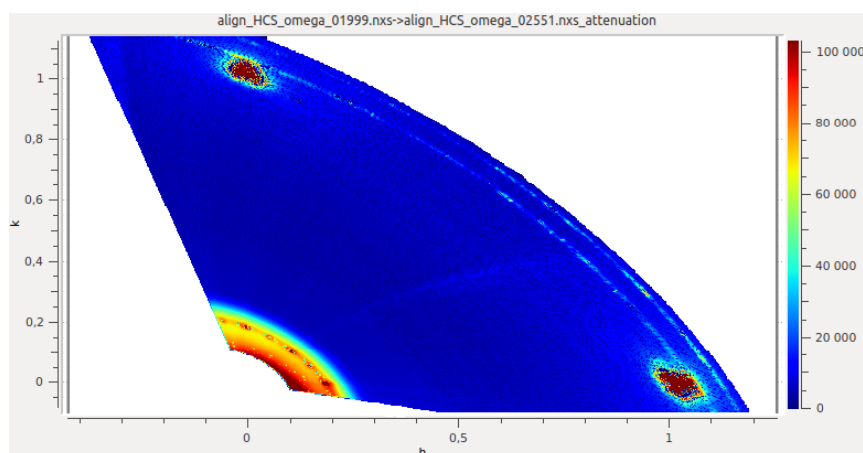
(b) Institute of Solid State Physics, Graz University of Technology, A-8010 Graz, Austria

(c) Laboratoire INSP, Universite Pierre et Marie Curie, 5 Place Jussieu, 75005 Paris, France

ABSTRACT

Lutetium bis-Phtalocyanine thin films are gaining attention as candidate for efficient gas sensing applications (1). Their peculiar electronic structure, and in particular the presence of a Single Occupied Molecular Orbital (SOMO) makes them ideal candidates for different gas sensing, as they are available for both oxidation and reduction. To better design this kind of devices more has to be understood about molecule-molecule and molecule-substrate interaction. To do this we studied the stucture and the structure of LuPc2 thin films deposited on gold. Even if this is not the ideal substrate for gas sensing, Pcs are known to lie flat on the surface (2;3), posses long range order, and self organize at room temperature, making gold an ideal substrate to better understand fundamental properties of these molecules.

In this experiment we have deposited a thin film of LuPc2 under UHV conditions over (sqrt3x22) reconstructed Au(111) and we characterized it via Grazing Incidence X-ray Diffraction (GIXRD). We show how the molecules lie flat on the surface, arranged in a square lattice (beta structure) which is stabilized by the interaction with the gold substrate. No influence of the herringbone reconstruction was seen in the orientation of the molecular layer. Also we studied the stabilizing interaction, in the form of a charge transfer from the substrate to the molecules, via the relaxation of the herringbone reconstruction of gold.



REFERENCES

- (1) M. Passard; J.P. Blanc; C. Maleysson
- (2) K. Katoh, Y. Yoshida, M. Yamashita, H. Miyasaka, B. K. Breedlove, T. Kajiwara, S. Takaishi, N. Ishikawa, H. Isshiki, Y. F. Zhang, T. Komeda, M. Yamagishi, J. Takeya, *JACS* **131** 9967-9976 (2009)
- (3) M. Toader, M. Knupfer, D. R. T. Zahn, and M. Hietschold *JACS* **133** 5538-5544 (2011)

Local Environment Analysis of High-entropy Alloys with EXAFS Measurements

L. Lilensten, K. Provost, I. Guillot

Université Paris Est, ICMPE (UMR 7182) CNRS-UPEC, 2-8 rue Henri Dunant,
F- 94320 THIAIS France

ABSTRACT

“Multi-component alloys” or “High entropy alloys” (HEA) are a new promising type of materials, which break with the classical alloy design. Instead of having one or two major components and some minor alloying elements, the community proposed recently¹ a new approach for alloy conception based on a “multicomponent” system of 5 or more elements. With an adequate combination of elements in equi- or near equi-atomic proportions, solid solutions with simple bcc or fcc structure can be obtained, without intermetallic phases. Due to the intrinsic lattice distortion – consequence of the mixing of more than 5 close but different elements – solid solution hardening is expected to be intense and more effective than in the conventional alloys. HEAs possess also very good mechanical properties (high specific strength) at high and low temperatures as recently exposed in Science with the demonstration of an incredible fracture toughness of fcc-CrMnFeCoNi at cryogenic temperatures². Two main categories of HEA can be distinguished: the first one is based on the elements Fe Co Cr Ni Cu (Al) with a fcc structure transforming in bcc structure with Al addition, and the second category concerns the refractory compositions of bcc structure, with the following elements Ti Zr Hf Nb Ta Mo V and W. Some studies mixing elements of the two aforementioned categories are also starting.

A study of the distortion and disorder of the lattice (induced by the solid solution) on the atomic scale with EXAFS measurements is proposed for the first time in the HEA TiZrHfNbTa³, in order to explain the tremendous properties of these alloys. The measurements were done at Bessy (Berlin, Germany) on the BAMline. The evolution of the number, nature and distances of nearest numbers is recorded through measurements at the K-edges of Nb and Zr of several compounds. Reference compounds Nb and Zr (pure) are measured, and the lattice deformation under elements' addition was followed with the measurements of binary, ternary, quaternary compounds and of the high entropy alloy. The first results on pure and binary compounds Zr-Hf, Zr-Ti, Nb-Ti, Nb-Ta and Nb-Hf are presented here.

REFERENCES

1. Yeh *et al.*; *Advanced Engineering Materials* **2004**, 6, 299.
2. Gludovatz *et al.*; *Science* **2014**, 345, 1153.
3. Senkov *et al.*; *Journal of Alloys and Compounds* **2011**, 509, 6043.

XANES Analyses of Low Temperature Magnetic Transition of ϵ -Fe₂O₃ Nanoparticles Embedded in SiO₂ Sol-gel Films

J. Lopez-Sanchez,^{1,2} A. Muñoz-Noval,³ A. Serrano,^{1,4} M. Abuín,^{1,5},
C. Castellanos,⁶ J. de la Figuera,^{2,7} J.F. Marco,^{2,7}
O. Rodríguez de la Fuente,^{1,2} N. Carmona^{1,2}

¹ Departamento de Física de Materiales, Universidad Complutense de Madrid, 28040 Madrid, Spain

² Unidad asociada IQFR (CSIC)-UCM, 28040 Madrid, Spain

³ ICMM-CSIC, Spanish CRG, European Synchrotron Radiation Facility (ESRF),
38000 Grenoble, France

⁴ Instituto de Cerámica y Vidrio, CSIC, 28049 Madrid, Spain

⁵ CEI Campus Moncloa, UCM-UPM, 28040 Madrid, Spain

⁶ Dipartimento di Chimica, Università degli Studi di Milano, 20133 Milano, Italy

⁷ Instituto de Química-Física "Rocasolano", CSIC, 28006 Madrid, Spain

ABSTRACT

Epsilon iron oxide is a collinear ferrimagnetic material with a Néel transition at around 500 K on the nanometric scale. Concerning its magnetic properties, epsilon nanoparticles as a single domain exhibit a coercive field of 2 T at room temperature (RT). The origin of this high value is the magnetocrystalline anisotropy ($K=10^5$ J/m³) caused by nonzero orbital component of the Fe³⁺ magnetic moment and, consequently, the occurrence of the meaningful spin-orbit coupling.¹ Apart from this feature, epsilon is a semiconductor material with a E_{gap} of 1.9 eV,² and presents coupling between the magnetic and dielectric properties at low temperatures when epsilon undergoes at around 100 K from collinear ferrimagnetic state to incommensurate magnetic order in nanoparticle form.³ Further interesting properties are found out in thin film form, as a layer of few tens of nanometers, where apart from being a ferrimagnetic material, epsilon displays a ferroelectric response at RT.⁴ In this work, a novel one-pot sol-gel route has been designed in order to obtain ϵ -Fe₂O₃ nanoparticles embedded in a SiO₂ films (see Fig. 1). Aiming at understanding the behaviour of the Fe³⁺ ions when the material undergoes towards the magnetic transition registered at low temperatures, an extensive and deep analysis has been performed by X-ray Absorption Near-Edge Spectroscopy (XANES) during this transition. Thermal expansion coefficient and Debye Waller parameter of each sub-shell are calculated from XANES results and show deviations when are represented as a function of the temperature. Further structural and morphological characterization of the samples are carried out by Confocal Raman Microscopy (CRM), Mössbauer Spectroscopy and Atomic Force Microscopy (AFM).

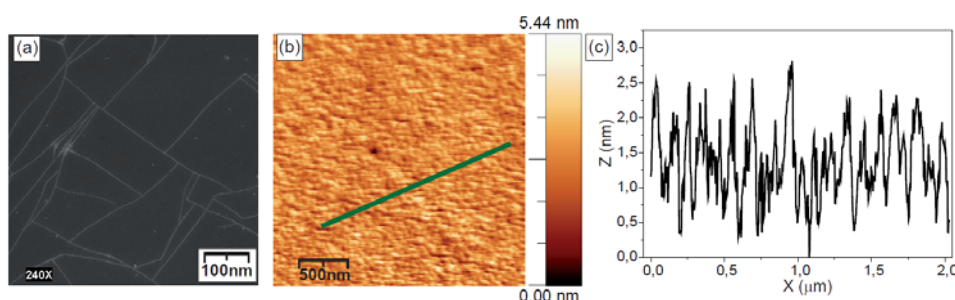


Fig. 1: (a) and (b) are respectively SEM and AFM images of the thin films of ϵ -Fe₂O₃ nanoparticles embedded in SiO₂ matrix prepared at 960 °C; (c) AFM Z-profile corresponding to the green line marked in Figure (b).

REFERENCES

- (1) MacHala, L.; Tuček, J.; Zbořil, R. *Chem. Mater.* **2011**, *23*, 3255–3272.
- (2) Korte, D.; Carraro, G.; Maccato, C.; Franko, M. *Optical Mater.* **2015**, *42*, 370–375.
- (3) Gich, M.; Frontera, C.; Roig, A.; Molins, E.; Fontcuberta, J.; Bellido, N.; Simon, C.; Fleita, C. *Nanotechlog.* **2006**, *17*, 687–691.
- (4) Gich, M.; Fina, I.; Morelli, A.; Sánchez, F.; Alexe, M.; Gàzquez, J.; Fontcuberta, J.; Roig, A. *Adv. Mater.* **2014**, *3*, 4645–4652.

Mechanical Behavior of Nanolayered Cu/W Thin Films under Cyclic and/or Monotonous Biaxial Solicitations: In-situ Study by X-ray Synchrotron Diffraction

N. Pouvreau¹, R. Guillou¹, E. Le Bourhis¹, P. Goudeau¹, P-O. Renault¹, P. Godard¹, C. Mocuta², D. Thiaudière²

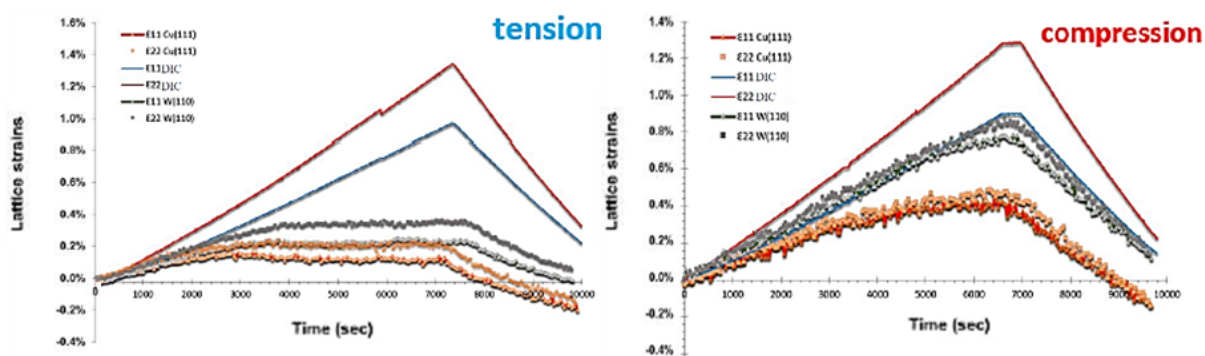
¹Institut PPRIME – CNRS/Université de Poitiers/ENSMA, Futuroscope, France

²Synchrotron SOLEIL, Gif sur Yvette, France

ABSTRACT

Mechanical properties of thin films are of utmost interest for a large variety of technological applications such as stretchable microelectronics. The mechanical behavior of thin films depends on their microstructure (grain texture, size, defects...). In order to mimic their actual in-use loading conditions, we performed controlled biaxial deformation tests on composites formed by metallic thin films deposited on polyimide substrate (Kapton®). Here, we present the results obtained for an equi-biaxial deformation test performed on two Cu/W nanocomposite thin films in order to analyze the influence of residual stresses. These thin films elaborated by ion-beam sputtering are about 150 nm thick (7 x (18 nm Cu + 6 nm W)). Film residual stresses were obtained in either **tension** or **compression** controlling the gaz pressure in the deposition chamber (the evaluated intra-granular stresses are relatively large: **+2.0 GPa** in tension and **-3.6 GPa** in compression).

To perform the mechanical experiments, we used the biaxial tensile setup of the DiffAbs beamline at synchrotron SOLEIL [1]. During mechanical testing, the applied and film in plane strains are measured simultaneously by both digital image correlation (macroscopic strains) and synchrotron X-ray diffraction (lattice strains) techniques [2].



What appears through these graphics is the significant effect of residual stresses on the mechanical behavior of Cu/W multilayers. Indeed, the presence of compressive stresses in the sample delays the plasticity event (plateau for Copper) and allows for the Copper and Tungsten sublayers to support elastic strains twice as large.

REFERENCES

- [1] G. Geandier, D. Thiaudière, et al., Rev. Sci. Instrum. 81 (2010) 103903.
 [2] S. Djaziri, P.-O. Renault, F. Hild, E. Le Bourhis, Ph. Goudeau, D. Thiaudière, D. Faurie, J. Appl. Cryst. 44 (2011) 1071-1079.

List of Other Posters

- PO-01** Photoelectron Spectroscopy on Xe⁺ and Xe⁵⁺ Ion Beams
J-M. Bizau
- PO-02** Surface Modified Mg-doped ZnO QDs for Biological Imaging
C. Bourgaux
- PO-03** Structural Studies of Double-strand Break Repair Pathway: Towards New Anti-cancer Drugs
J.B. Charbonnier
- PO-04** Drug-lipid Interaction as a Planar Model of Drug-membrane Interaction
A. Datta
- PO-05** Oscillator Strengths and Predissociation Rates for Rydberg Transitions between 92.7 and 97.5 nm in ¹³C¹⁸O . Comparaison with ¹²C¹⁶O and ¹³C¹⁶O Results
M. Eidelsberg
- PO-06** Structural Biology of Regulators of Membrane Traffic and Cell Motility
Y. Ferrandez
- PO-07** The Beamline FIP-BM30A at the ESRF: Past, Present and Future
J-L. Ferrer
- PO-08** A Chemometric Approach of the Quantitative Assessment of Ru Speciation During the Genesis of Active Phases in Co-Ru Fischer-Tropsch Catalysts
J-S. Girardon
- PO-09** High Resolution Band Structure of the Metallic Boron Doped Diamond
H. Guyot
- PO-10** Fe X-ray Spectroscopic Studies of FeMo Cofactor of Nitrogenase and Related Models
J.K. Kowalska
- PO-11** Spectroscopic Studies of GSK3b Phosphorylation of the Neuronal Tau Protein and its Interaction with the N-terminal Domain of Apolipoprotein E
A. Leroy
- PO-12** Chemometric Approach of the Quantitative Assessment of Ru Speciation During the Genesis of Active Phases in Co-Ru Fischer-Tropsch Catalysts
E. Marceau
- PO-13** Ligne de Lumière Française IF-BM32 à l'ESRF Instrumentation, Activités et Perspectives
J-S. Micha
- PO-14** A New Version of MAX-StraightNoChaser: XAFS Linear Chemometry. LSF, PCA and MCR-ALS Optimized for EXAFS and XANES
A. Michalowicz
- PO-15** Study of the Iron Oxidation States in Vitreous Phases of Ceramics by XANES Microprobe
H. Montigaud

- PO-16** CASTOR, Instrument d'Analyse Combinée XRR-GIXRF : Une Nouvelle Technique à SOLEIL
A. Novikova
- PO-17** New Perspectives for the CRG-FAME Beamline in the Framework of the ESRF - Extremely Brilliant Source : New Source for New Science ? !
O. Proux
- PO-18** Towards a New Tool Dedicated to the Normalization and Comparison of Experimental XMCD Spectra
K. Provost
- PO-19** XPEEM Microscopy at the HERMES Beamline: Commissioning and First Results
M. Rioult
- PO-20** Use of Synchrotron-radiation Infrared Microspectroscopy in Single Glioblastoma Cells to Elucidate a Specific Signature Associated with Hypoxia Levels Found in Tumours
C. Sandt
- PO-21** Fast Scanning Multi-technique Spectro-microscopy Possibilities at the Nanoscopy Beamline of Synchrotron SOLEIL
A. Somogyi
- PO-22** Polydiacetylenes Langmuir Films to Produce Biological or Environmental Sensors
S. Spagnoli
- PO-23** Projet Dichro50
M. Stora
- PO-24** Glycosylate and Move: Structural and Functional Dissection of a Glycosyltransferase Involved in Glycosylation of a Bacterial Flagellin
G. Sulzenbacher
- PO-25** STXM at the HERMES Beamline: Capabilities and the First Commissioning Results
S. Swaraj
- PO-26** Structural Determination of Metal-organic Frameworks from Single Microcrystal X-ray Diffraction
A. Tissot
- PO-27** Local Structure Around Silicon on Silicene Deposited Onto Ag(110) And Ag(111) Surfaces
N. Trcera
- PO-28** Implementation of a Multilayer Grating Monochromator on LUCIA
D. Vantelon
- PO-29** Refining the Structure of Al-substituted Ferrihydrites
D. Vantelon
- PO-30** Phase Stability, EXAFS Investigation and Correlation between Nanostructure and Extrinsic Magnetic Properties of Nanocrystalline $\text{Pr}_2(\text{Co,Fe})_7$
K. Zehani
- PO-31** XAS Spectroscopic Fingerprint of the Active Site in Non-precious Metal Electrocatalysts for PEM Fuel Cells
A. Zitolo

PO-32

Understanding the Apparent Negative Thermal Expansion in Supported Rh-based Nanoparticles
C. Zlotea

Photoelectron Spectroscopy on Xe^+ and Xe^{5+} Ion Beams

J.-M. Bizau^{*§}, D. Cubaynes^{*§}, S. Guilbaud^{*}, M.M. Al Shorman^{*},
F. Penent[†], P. Lablanquie[†], L. Andric[†], J. Palaudoux[†] and C. Blancard[°]

^{*} ISMO, CNRS, Univ. Paris-Sud, Université Paris-Saclay, F-91405 Orsay cedex, France

[§] Synchrotron SOLEIL, L'Orme des Merisiers, St Aubin, BP48, F-91192 Gif-sur-Yvette, France

[†] LCPMR, CNRS & Univ. Paris 6, 11 rue Pierre et Marie Curie, F-75231 Paris Cedex 05, France

[°] CEA-DAM-DIF, Bruyères-le-Châtel, F-91297 Arpajon cedex, France

ABSTRACT

Photoionization (PI) of free ionic species is a key process for plasmas modeling. Up to now, laboratory studies on multiply-charged ions were limited mainly to photoabsorption[1] and ionic spectrometry[2] experiments. Merged-beam setups in synchrotron radiation (SR) facilities provide absolute PI cross sections. Electron spectroscopy on ionic species is still a challenge due to the low target density. Its feasibility was demonstrated in the 90's on singly-charged atomic ions[3,4]. Since that time, only the high photon flux available at free electron lasers had allowed the observation of photoelectron spectra[5,6]. We present here the results of the first electron spectroscopy study performed on the photoionization of a multiply-charged ion. The Auger spectra emitted in the decay of the $4d^9 5p 5s^2 nf$ resonances in Xe^{5+} ion, with $n = 4$ to 6, have been recorded, as well as the photoelectron spectrum emitted in the direct PI in 4d subshell of Xe^+ ion.

The experiments were performed with the merged-beam setup of the PLEIADES beam line at SOLEIL French SR facility[7]. The Xe ions were produced in an electron cyclotron resonance ion source (ECRIS). A cylindrical mirror electron analyzer (CMA), with its axis collinear to the ions and SR counter propagating beams, analyzed the kinetic energy of the electrons emitted in coincidence with the photoions. Results of multi-configuration Dirac-Fock (MCDF) calculations are compared with the experimental spectra.

REFERENCES

1. Kennedy E T *et al* 1994 *Opt. Eng.* **33** 3984–92
2. Kjeldsen H 2006 *J. Phys. B At. Mol. Opt. Phys.* **39** R325–77
3. Bizau J M *et al* 1991 *Phys. Rev. Lett.* **67** 576–9
4. Gottwald A *et al* 1999 *Phys. Rev. Lett.* **82** 2068–70
5. Domesle C *et al* 2013 *Phys. Rev. A* **88** 043405
6. Young L *et al* 2010 *Nature* **466** 56.
7. Gharaibeh M F *et al* 2011 *J. Phys. B At. Mol. Opt. Phys.* **44** 175208

Surface Modified Mg-doped ZnO QDs for Biological Imaging

E. B. Manaia^{a,b}, B. L. Caetano^c, V. Briois^d, R. C. K. Kaminski^e,
L. A. Chivavacci^b, C. Bourgaux^a

^aFaculté de Pharmacie - Université Paris-Sud, 5, rue Jean-Baptiste Clément,
92296 Châtenay-Malabry CEDEX, France

^bFaculty of Pharmaceutical Sciences, UNESP, Araraquara, Brazil

^cInstitut of Chemistry, UNESP, Araraquara, Brazil

^dSynchrotron SOLEIL, L'Orme des Merisiers, BP48, Saint Aubin, 91192 Gif-sur Yvette, France

^eFederal University of Sergipe, Itabaiana, Brazil

ABSTRACT

ZnO quantum dots (QDs) are currently attracting great interest as potential labels for bioimaging and theranostic applications because of their biodegradability and very low toxicity in vivo. ZnO QDs doped with Mg²⁺ ions, reported to enhance the luminescence of ZnO, have been synthesized using the sol-gel method and their surface capped with oleic acid, to stabilize the nanoparticles, preventing further aggregation, and to promote their later incorporation into lipidic systems.

Briefly, ZnO colloidal suspensions were obtained by hydrolysis and condensation at 60°C of a precursor solution (Zn₄OAc₆ ethanolic solution) upon mixing with a LiOH ethanolic solution (1). Mg doping was achieved by adding a Mg(Ac)₂ ethanolic solution to the Zn precursor solution. The Mg precursor concentration was increased up to 20%. Oleic acid was then added to the Mg_(x)Zn_(1-x)O QD suspension. The influence of Mg on the growth of nanoparticles was evidenced by time-resolved synchrotron small-angle X-ray scattering (SAXS) patterns, recorded from the very beginning of the reaction on the SWING beamline. Mg²⁺ addition decreased the final size of QDs (from ~ 4 to ~ 3 nm) and inhibited their fractal aggregation at the end of the synthesis, suggesting a modification of their surface properties. Surface capped Mg-doped ZnO QDs were also characterized by elemental analysis, electronic microscopy, X-ray diffraction, Raman spectroscopy, UV-vis absorption and photoluminescence spectroscopy.

Mg-doped ZnO QDs capped by oleic acid formed stable colloidal dispersions in toluene and chloroform, with strong visible luminescence, promising for biological imaging. With increasing proportions of Mg²⁺ ions, both the absorption and emission spectra experienced a blue shift. For a 20 mol% nominal concentration of Mg²⁺ ions in the reaction medium, the quantum yield of Mg-doped QDs capped with OA was about 4 times higher than that of the ZnO QDs (2).

REFERENCES

1. Caetano, B.L.; Santilli, C.V.; Meneau, F.; Briois, V. and Pulcinelli, S.H. In situ and simultaneous UV-vis/SAXS and UV-vis/XAFS time-resolved monitoring of ZnO quantum dot formation and growth, *J. Phys. Chem. C* 115, 4404-4412 (2011).
2. Berbel Manaia E., Kaminski R., Caetano B., Briois V., Chivavacci L., Bourgaux C. Surface modified Mg-doped ZnO Quantum Dots for biological imaging, *Eur. J. Nanomed.*, 7, 109-120 (2015).

Structural Studies of Double-strand Break Repair Pathway: Towards New Anti-cancer Drugs

C. Nemoz, C. Bigot, A. Comte, C. Tellier-Lebegue, J. Yu,
M.H. Le Du, R. Guerois, P. Drevet, J.B. Charbonnier

I2BC, iBiTec-S, CEA, Bât 144, CE Saclay, 91191 Gif-s-Yvette

ABSTRACT

The double-stranded DNA breaks are the most toxic DNA lesions. Anti-cancer treatments such as radiation and drugs used in chemotherapy (cisplatin, topoisomerase inhibitors for example) create double-stranded breaks in order to bring the tumor cell apoptosis. The failures encountered in radio- and chemotherapies often come from an over-activation of the double strand breaks repair pathway called NHEJ for Non-Homologous End Joining. The main objectives of our team are (1) to understand the molecular mechanisms of the NHEJ repair pathway and (2) to design inhibitors of this pathway to make more effective therapies against resistant tumors. Our expertise is in the characterization of crystallographic structures of multi-protein complexes and analysis of interactions of the proteins involved (Ropars, 2011, PNAS, Malivert, 2006, J Biol Chem). We are also involved in the characterization of new inhibitors using small-molecules screenings and rational design of peptides from 3D structures. We will present previous and recent data obtained on this project using Proxima 1 and Swing beamlines.

REFERENCES

1. Ropars V, Drevet P, Legrand P, Baconnais S, Amram J, Faure G, Marquez JA, Pietrement O, Guerois R, Callebaut I, Le Cam E, Revy P, de Villartay JP, et al. (2011) Structural characterization of filaments formed by human Xrcc4-Cernunnos/XLF complex involved in nonhomologous DNA end-joining. *Proc Natl Acad Sci U S A* 108(31):12663-12668 .
2. Malivert L, Ropars V, Nunez M, Drevet P, Miron S, Faure G, Guerois R, Mornon JP, Revy P, Charbonnier JB, Callebaut I, & de Villartay JP (2010) Delineation of the Xrcc4-interacting region in the globular head domain of cernunnos/XLF. *J Biol Chem* 285(34):26475-26483
3. de Villartay JP, Shimazaki N, Charbonnier JB, Fischer A, Mornon JP, Lieber MR, & Callebaut I (2009) A histidine in the beta-CASP domain of Artemis is critical for its full in vitro and in vivo functions. *DNA Repair (Amst)* 8(2):202-208 .

Drug-lipid Interaction as a Planar Model of Drug-membrane Interaction

A. Datta

*Surface Physics and Materials Science Division, μ Saha Institute of Nuclear Physics
1/AF Bidhannagar, Kolkata 700 064, India*

ABSTRACT

The interaction of a drug (Piroxicam, 4-hydroxy-2-methyl-N-(2-pyridinyl)-2H-1,2-benzothiazine-3-carboxamide 1,1 dioxide) with a lipid (DMPC) monolayer has been used as a membrane-mime in terms of drug-induced changes in stability and compressibility with variation in drug-dose¹. Drug-induced fluidization is noticed in the monolayer through increase in Liquid Expanded to Liquid Condensed (LE-LC) phase-transition pressure at constant temperature. With increasing drug-lipid ratio (D/L) beyond 0.025 the fluidization is reversed and at 0.05 a rigidification of the monolayer takes place. The probable mechanism behind this reversal of behaviour is reorganization at and below the optimum dose of 0.025 where drug-molecules sitting parallel to the interface increase headgroup separations while at and above 0.05 the drug-molecules sitting roughly perpendicular to the interface bring headgroups closer. Molecular dynamics simulation shows that the ordering in the different parts of the lipid chains is changed to different extents in the presence of drugs with maximum change near the headgroups and again points to an optimum dose for maximum disorder. X-ray reflectivity measurements on the pristine monolayer in situ reveal a splay in the hydrocarbon chains to develop with time whereas the presence of the drug arrests the splay to an extent.

REFERENCES

1. U.K. Basak, A. Datta and D. Bhattacharyya, *Coll. Surf.B* **132**, 34-44 (2015).

Oscillator Strengths and Predissociation Rates for Rydberg Transitions between 92.7 and 97.5 nm in $^{13}\text{C}^{18}\text{O}$. Comparaison with $^{12}\text{C}^{16}\text{O}$ and $^{13}\text{C}^{16}\text{O}$

Results

M. Eidelsberg¹, J. L. Lemaire¹, L. Gavilan¹, S. R. Federman², G. Stark³, A. N. Heays⁴, J. Lyons⁵, N. de Oliveira⁶, and L. Nahon⁶

1 Observatoire de Paris, 92195 Meudon, France

e-mail: michele.eidelsberg@obspm.fr, jean-louis.lemaire@obspm.fr, lisseth.gavilan@obspm.fr

2 Department of Physics and Astronomy, University of Toledo, Toledo, OH, USA

e-mail: steven.federman@utoledo.edu

3 Department of Physics, Wellesley College, Wellesley, MA, USA

e-mail: gstark@wellesley.edu,

4 Leiden Observatory, Leiden University, P. O. Box 9513, 2300 RA Leiden, The Netherlands

e-mail: aheays@yahoo.com

5 School of Earth and Space Exploration, Arizona State University, 781 S. Terrace Rd,

Tempe, AZ 85281, USA

e-mail: jrlyons2@asu.edu

6 DESIRS beam line, Synchrotron SOLEIL, Saint Aubin, France

e-mail: nelson.de.oliveira@synchrotron-soleil.fr

ABSTRACT

Photodissociation plays an important role in many astrophysical environments, including photon-dominated regions in interstellar clouds. Because the photodissociation of CO is a line process, it is subject to self shielding which is an isotope selective effect. The less abundant isotopologues of CO are self-shielded to a lesser degree than $^{12}\text{C}^{16}\text{O}$, and thus have the highest photodissociation rates at most depths in a cloud. Accurate modeling requires basic quantitative spectroscopic data for CO and its isotopologues at wavelengths below the dissociation limit.

We present results of oscillator strengths and predissociation rates for Rydberg transitions involving the $W^1\Pi$, $4p\pi^1\Pi$, $5p\pi^1\Pi$, and $5p\sigma^1\Sigma$ upper states in the 92.7 and 97.5 nm wavelength range for the rare isotopologue $^{13}\text{C}^{18}\text{O}$. Comparison is also made with our recently published results on $^{12}\text{C}^{16}\text{O}$, $^{13}\text{C}^{16}\text{O}$, and $^{12}\text{C}^{18}\text{O}$ obtained with the same experimental conditions.

The experiments were performed on the DESIRS beam-line at the SOLEIL Synchrotron. A VUV Fourier Transform Spectrometer provided a resolving power of about 300,000, allowing us to analyze individual line strengths and widths in the observed transitions.

Structural Biology of Regulators of Membrane Traffic and Cell Motility

A. Nawrotek-Maalouf¹, Y. Ferrandez¹, S. Veyron¹, W. Zhang¹,
S. Fetics¹, A. Thureau², J. Perez², J. Navaza¹, S. Benabdi¹,
F. Peurois¹, M. Zeghouf¹, J. Cherfils¹

¹Laboratoire de Biologie et Pharmacologie Appliquée, CNRS-Ecole Normale Supérieure Cachan,
²SOLEIL Synchrotron

ABSTRACT

We are studying molecular reactions that govern the functions of small GTPases in cellular traffic and cytoskeleton dynamics. We will present a survey of our recent X-ray crystallography and SAXS studies of guanine nucleotide exchange factors (GEFs) that regulate Arf GTPases in endocytosis [1,2], of GEFs for Rho [3] and Rap GTPases and their inhibitors in diseases, of effectors from bacterial pathogens that hijack Rab GTPases [4,5,6], and of a new protein that regulates the nucleation of branched actin networks [7].

REFERENCES

- [1] Cherfils J. Arf GTPases and their effectors: assembling multivalent membrane-binding platforms. *Curr. Op. Struct. Biol.* 2014
- [2] Aizel K, Biou V, Navaza J, Duarte LV, Campanacci V, Cherfils J, Zeghouf M. Integrated conformational and lipid-sensing regulation of endosomal ArfGEF BRAG2. *PLoS Biol.* 2013
- [3] Vives V, Cres G, Richard C, Malaval L, Busson M, Ferrandez Y, Planson AG, Zeghouf M, Cherfils J and Blangy A. Disorganizing osteoclast podosomes through the pharmacological inhibition of Rac activation by Dock5 prevents osteolysis and preserves bone formation. *Nature Comm* (2015) (accepted 2015)
- [4] Roy C.R. & Cherfils J. Structure and function of FIC proteins. *Nature Reviews Microbiology* 2015
- [5] Campanacci V, Mukherjee S, Roy CR, Cherfils J. Structure of the Legionella effector AnkX reveals the mechanism of phosphocholine transfer by the FIC domain. *EMBO J.* 2013
- [6] Dang I, Gorelik R, Sousa-Blin C, Derivery E, Guérin C, Linkner J, Nemethova M, Dumortier JG, Giger FA, Chipysheva TA, Ermilova VD, Vacher S, Campanacci V, Herrada I, Planson AG, Fetics S, Henriot V, David V, Oguievetskaia K, Lakisic G, Pierre F, Steffen A, Boyreau A, Peyriéras N, Rottner K, Zinn-Justin S, Cherfils J, Bièche I, Alexandrova AY, David NB, Small JV, Faix J, Blanchoin L, Gautreau A. Inhibitory signalling to the Arp2/3 complex steers cell migration. *Nature.* 2013
- [7] Fetics S., Thureau A., Campanacci V., Aumont-Nicaise M., Dang I., Gautreau A., Perez J., Cherfils J. Hybrid structural analysis of the Arp2/3 regulator Arpin identifies its acidic tail as a primary binding epitope. *Structure* 2016

The Beamline FIP-BM30A at the ESRF: Past, Present and Future

J.-L. Ferrer, Y. Sallaz-Damaz, F. Borel, M. Pirocchi, C. Berzin,
D. Cobessi, P. Israel-Gouy, X. Vernede

IBS / Groupe Synchrotron, CEA, CNRS, Université Grenoble Alpes, Grenoble – France

ABSTRACT

FIP-BM30A started its operation in May 1999¹. Dedicated to protein crystallography experiment, it was specifically designed for anomalous diffraction experiments. In almost seventeen years of operation, FIP-BM30A contributed to 465 publications to date, and about the same number of structures deposited in the PDB, delivering yearly ~400 shifts of beamtime to the national (2/3) and international (1/3) MX community (respectively through the SOLEIL PRC5 “Biology/Health” comity and through the ESRF program comity).

Since 1999, FIP-BM30A evolved significantly, with a massive upgrade of the experiment from 2006 to 2011 (ADSC 315r detector, MD2 goniometer, KB optics, etc.). In parallel, efforts were made from the beginning to offer a large level of automation, with a six-axis arm based sample changer in operation since 2004² and the possibility of *in situ* experiments³, in a user friendly environment.

In the recent years several additions were made to the FIP-BM30A setup. Some of them are focused on automated room temperature (RT) data collection, opening the way to automated RT structure resolution and compound screening. Upstream, a specific bench is now available close to the beamline for crystal optimization. Efforts were also made regarding flexibility, with the possibility to host high pressure experiments, spectroscopy measurements, humidity controlled diffraction, etc. A micro-robot based system for assisted/automated crystal harvesting is also under development, and will be installed on the beamline when completed.

By 2018, FIP-BM30A will be considered for insertion into the Phase II ESRF upgrade program. Therefore it is now a critical time, and decisions will have to be taken regarding the future developments and the positioning of FIP-BM30A with respect to the other MX beamlines. The present meeting will be an opportunity to present the ongoing projects, and to collect the inputs from the users community.

REFERENCES

1. M. Roth, P. Carpentier, O. Kaikati, J. Joly, P. Charrault, M. Pirocchi, R. Kahn, E. Fanchon, L. Jacquamet, F. Borel, A. Bertoni, P. Israel-Gouy and J.-L. Ferrer, *Acta Cryst. D* **58**, pp. 805-814 (2002).
2. J. Ohana, L. Jacquamet, J. Joly, A. Bertoni, P. Taunier, L. Michel, P. Charrault, M. Pirocchi, P. Carpentier, F. Borel, R. Kahn and J.-L. Ferrer, *J. Applied Cryst.* **37**, pp. 72-77 (2004).
3. L. Jacquamet, J. Ohana, J. Joly, F. Borel, M. Pirocchi, P. Charrault, A. Bertoni, P. Israel-Gouy, P. Carpentier, F. Kozielski, D. Blot, J.-L. Ferrer, *Structure* **12**, pp. 1219-1225 (2004).

A Chemometric Approach of the Quantitative Assessment of Ru Speciation During the Genesis of Active Phases in Co-Ru Fischer-Tropsch Catalysts

J. Hong^{a,b}, E. Marceau^{a,b}, A.Y. Khodakov^a, A. Griboval-Constant^a,
J-S. Girardon^a, L. Gaberová^b, C. La Fontaine^c, V. Briois^c

^aUnité de Catalyse et de Chimie du Solide, UMR 8181 CNRS, Université Lille
 1-ENSCL-EC Lille, Villeneuve d'Ascq, France;

^bLaboratoire de Réactivité de Surface, UMR 7197 CNRS, UPMC, Paris, France
^cSynchrotron SOLEIL, Gif-sur Yvette, France

ABSTRACT

Complete reduction of the metal phase in cobalt-containing catalysts is often difficult to reach and can be promoted by a small amount of noble metals. Because these costly promoters are introduced in a very low quantity, their speciation and their chemical interaction with cobalt have seldom been studied in detail. We present here a time-resolved *in situ* X-ray absorption spectroscopy investigation of the speciation of ruthenium, used as a reduction promoter of cobalt, throughout the preparation of Co/SiO₂ catalysts.¹ Multivariate-Curve Resolution by Alternative-Least Squares (MCR-ALS) methodology, first proposed by Tauler in 1995,² was used for the quantification of chemical phases during reduction.

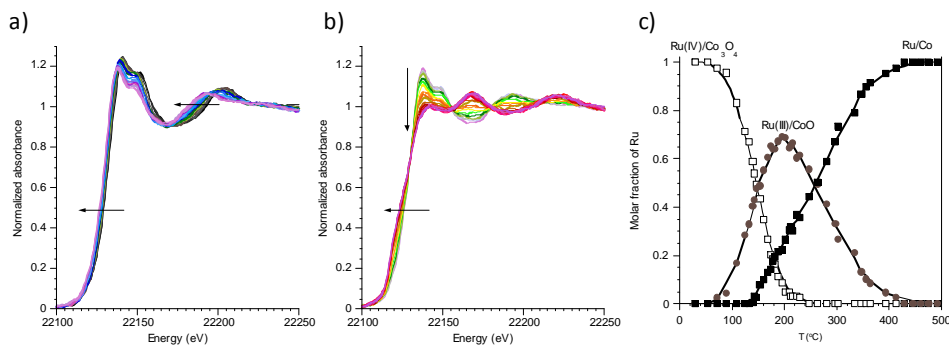


Fig. 1: Reduction of ruthenium monitored by *in situ* Ru K XANES-TPR measurements on a Co(10wt%)-Ru(0.5wt%)/SiO₂ catalyst: a) between 29 and 200°C (from black to purple); b) between 200 and 500°C (from grey to dark pink); c) Speciation as a function of temperature during reduction determined by MCR-ALS analysis.

After calcination, Ru(IV) ions appear as inserted inside Co₃O₄ nanoparticles. Reduction of the oxidic phase takes place in two distinct steps, at approximately the same temperatures whatever the ruthenium content (Fig. 1): first to Ru(III)-containing CoO nanoparticles (Ru ions modifying the electronic properties of the oxidic nanoparticles); then to bimetallic Co nanoparticles containing Ru(0) atoms, via an autocatalytic process. Ru loadings as low as 0.2 wt% are sufficient to afford complete reduction of Co. Close association between Ru and Co from the beginning of the synthesis is thus necessary for a maximum promoting effect.

REFERENCES

1. J. Hong, E. Marceau, A. Y. Khodakov, L. Gaberova, A. Griboval-Constant, J. S. Girardon, C. La Fontaine and V. Briois, *ACS Catal.* **5**, 1273-1282 (2015).
2. T.Tauler, *Chemom. Intell. Lab. Syst.* **30**, 133-146 (1995).

High Resolution Band Structure of the Metallic Boron Doped Diamond

H. Guyot^{A,B}, A. Nicolaou^C, A. Taleb^C and E. Bustarret^{A,B}

A. Université Grenoble Alpes, F-38000 Grenoble, France

B. Institut Néel, CNRS-UJF, BP 166, 38042 Grenoble Cédex 9, France

C. Synchrotron Soleil, Saint-Aubin, BP 48 91192 Gif-sur-Yvette Cédex, France

ABSTRACT

Doping pure diamond thin films with boron atoms induces a phase transition towards a metallic state. The boron doping lifts the top of the diamond valence band at the Fermi level, and makes this phase easily measurable by ARPES. The high resolution band structures measured parallel to the main direction ΓX in the first Brillouin zone are presented and compared with the hole bands previously measured in the second and third Brillouin zones [1]. These new data allow a better analysis of the band tops and a better comparison with the theoretical bands obtained using the k.p model or the DFT calculation.

REFERENCES

1. H. Guyot, P. Achatz, A. Nicolaou, P. Le Fèvre, F. Bertran, A. Taleb-Ibrahimi and E. Bustarret, *PRB* **92**, 045135 (2015)

Fe X-ray Spectroscopic Studies of FeMo Cofactor of Nitrogenase and Related Models

J.K. Kowalska, R. Bjornsson, S. Lee, T. Weyhermüller,
F. Meyer, O. Einsle and S. DeBeer

*Max Planck Institute for Chemical Energy Conversion, Stiftstrasse 34-36,
45470 Mülheim and der Ruhr, Germany*

University of Iceland, Dunhaga 3, IS-107 Reykjavik, Iceland

University of Waterloo, 200 University Avenue West, N2L 3G1, Waterloo, Ontario, Canada

Georg-August-Universität Göttingen, Tammannstraße 4, 37077 Göttingen, Germany

Albert-Ludwigs-Universität Freiburg, Albertstrasse 21, 79104 Freiburg, Germany

ABSTRACT

Nitrogenase enzyme (found in diazotrophs) catalyzes the reduction of the atmospheric nitrogen (N_2) to ammonia (NH_3), which is essential for producing fertilizers that feed the world's growing population. Presently, the cleavage of N-N bonds is achieved industrially via heterogeneous catalysts in Haber-Bosch process. Both of these processes operate highly efficiently, however at extreme thermodynamic limits (high temperature and pressure vs. ambient conditions). These different conditions arouse a large interest in understanding the mechanism of biological nitrogen fixation in order to improve future industrial catalysts.

The N_2 to NH_3 conversion occurs at the active site of nitrogenase – a Mo:7Fe:9S:C cluster (so called FeMoco, Fig. 1) which has brought out a fair amount of efforts in understanding its geometrical and electronic structure [1]. Our current goal is to determine the iron atoms' oxidation state distribution and magnetic coupling within this complex system.

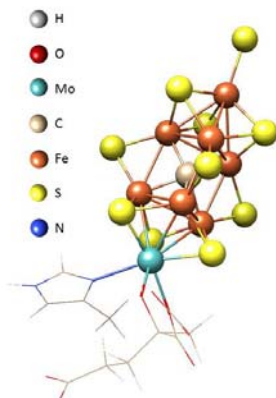


Fig. 1: FeMo cofactor of nitrogenase [2]

Recent approaches utilizing Fe K-edge High Energy Fluorescence Detected X-ray Absorption Spectroscopy (HERFD XAS), Fe L-edge XAS and Fe X-ray Magnetic Circular Dichroism (XMCD) on Fe-S, Fe-Mo-S model complexes and FeMoco will be presented. The discussed experimental data will be supported with theoretical calculations indicating possible scenarios of Fe oxidation state distribution in FeMoco.

REFERENCES

1. J. Kowalska and S. DeBeer *Biochem. Biophys. Acta Mol. Cell Res.* **1853**, 1406-1415 (2015).
2. K. Lancaster, M. Roemelt, P. Ettenhuber, Y.L. Hu, M. Ribbe, F. Neese, U. Bergmann, O. Einsle, S. DeBeer *Science* **334**, 974-977, (2011).

Spectroscopic Studies of GSK3b Phosphorylation of the Neuronal Tau Protein and its Interaction with the N-terminal Domain of Apolipoprotein E

A. Leroy^{*}, I. Huvent^{**}, D. Legrand^{**}, F. Wien[#]

**Laboratoire de biochimie appliquée (Paris XI), Tour D1 4^{ème},
5 rue J-B Clément, 92296 Châtenay-Malabry,*

***UMR 8576 UGSF USTL, 59655 Villeneuve d'Ascq,*

#Synchrotron Soleil beamline Disco l'Orme des Merisiers 91192 Gif/Yvette

ABSTRACT

Alzheimer's disease neurons are characterized by extra-neuronal plaques formed mainly by aggregated b amyloid (Ab) peptide and by intra-neuronal tangles composed of fibrillary aggregates of the microtubule associated Tau protein. This latter Tau is mostly found in a hyper-phosphorylated form in these tangles, and GSK3b is a proline directed kinase generally considered as one of the major players that (hyper) phosphorylates Tau. The kinase is proline directed Ser/Thr-Pro motifs and is believed to require a priming activity by another kinase in order to incorporate a phosphate moiety at the (i-4) position. Here, we use in vitro phosphorylation reactions and NMR spectroscopy to characterize in a qualitative and quantitative manner the phosphorylation of Tau by GSK3b. We find that three residues become phosphorylated (pSer396, pSer400, pSer404) by the action of GSK3b alone, without requiring priming by another kinase. Ser404 is essential in this process, as its mutation to an Ala prevents all activity of GSK3b in the C-terminus of Tau. However, priming does significantly enhance the catalytic efficacy of the kinase, as priming at the Ser214 position by PKA leads at least to the rapid phosphorylation of four additional sites after 6 hours of incubation. Because the regular incorporation of negative charges by GSK3b leads to a potential parallel between phospho-Tau and heparin, we investigated its interaction with the heparin-binding N-terminal LDL receptor-binding domain of human apolipoprotein E. We indeed observed an interaction between phospho-Tau and the apolipoprotein E fragment, but only when Tau was phosphorylated in a regular spaced manner by GSK3b. The absence of phosphorylation or the presence of an irregular phosphorylation pattern by the prolonged activity of PKA abolishes this interaction. Apolipoprotein E hence is able to discriminate and interact with specific phosphorylation patterns of Tau.

A Chemometric Approach of the Quantitative Assessment of Ru Speciation During the Genesis of Active Phases in Co-Ru Fischer-Tropsch Catalysts

J. Hong^{a,b}, E. Marceau^{a,b}, A.Y. Khodakov^a, A. Griboval-Constant^a,
J-S. Girardon^a, L. Gaberová^b, C. La Fontaine^c, V. Briois^c

^aUnité de Catalyse et de Chimie du Solide, UMR 8181 CNRS, Université Lille 1-ENSCL-EC Lille, Villeneuve d'Ascq, France; ^bLaboratoire de Réactivité de Surface, UMR 7197 CNRS, UPMC, Paris, France; ^cSynchrotron SOLEIL, Gif-sur Yvette, France

ABSTRACT

Complete reduction of the metal phase in cobalt-containing catalysts is often difficult to reach and can be promoted by a small amount of noble metals. Because these costly promoters are introduced in a very low quantity, their speciation and their chemical interaction with cobalt have seldom been studied in detail. We present here a time-resolved *in situ* X-ray absorption spectroscopy investigation of the speciation of ruthenium, used as a reduction promoter of cobalt, throughout the preparation of Co/SiO₂ catalysts.¹ Multivariate-Curve Resolution by Alternative-Least Squares (MCR-ALS) methodology, first proposed by Tauler in 1995,² was used for the quantification of chemical phases during reduction.

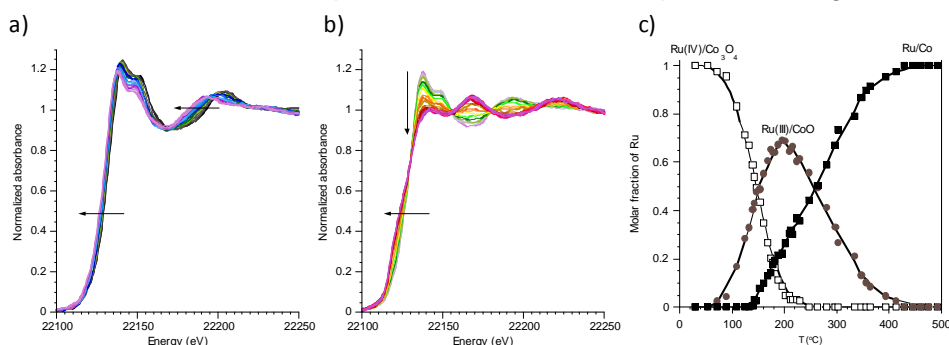


Fig. 1: Reduction of ruthenium monitored by *in situ* Ru K XANES-TPR measurements on a Co(10wt%)-Ru(0.5wt%)/SiO₂ catalyst: a) between 29 and 200°C (from black to purple); b) between 200 and 500°C (from grey to dark pink); c) Speciation as a function of temperature during reduction determined by MCR-ALS analysis.

After calcination, Ru(IV) ions appear as inserted inside Co₃O₄ nanoparticles. Reduction of the oxidic phase takes place in two distinct steps, at approximately the same temperatures whatever the ruthenium content (Fig. 1): first to Ru(III)-containing CoO nanoparticles (Ru ions modifying the electronic properties of the oxidic nanoparticles); then to bimetallic Co nanoparticles containing Ru(0) atoms, via an autocatalytic process. Ru loadings as low as 0.2 wt% are sufficient to afford complete reduction of Co. Close association between Ru and Co from the beginning of the synthesis is thus necessary for a maximum promoting effect.

REFERENCES

1. J. Hong, E. Marceau, A. Y. Khodakov, L. Gaberova, A. Griboval-Constant, J. S. Girardon, C. La Fontaine and V. Briois, *ACS Catal.* **5**, 1273-1282 (2015).
2. T.Tauler, *Chemom. Intell. Lab. Syst.* **30**, 133-146 (1995).

Ligne de Lumière Française IF-BM32 à l'ESRF- instrumentation, Activités et Perspectives

G. Renaud^{1,2}, O. Geaymond^{1,3}, J-S. Micha^{1,4}, F. Rieutord^{1,2},
O. Robach^{1,2}, M. de Santis^{1,3}, O. Ulrich^{1,2}

¹ Université Grenoble Alpes, Grenoble, France

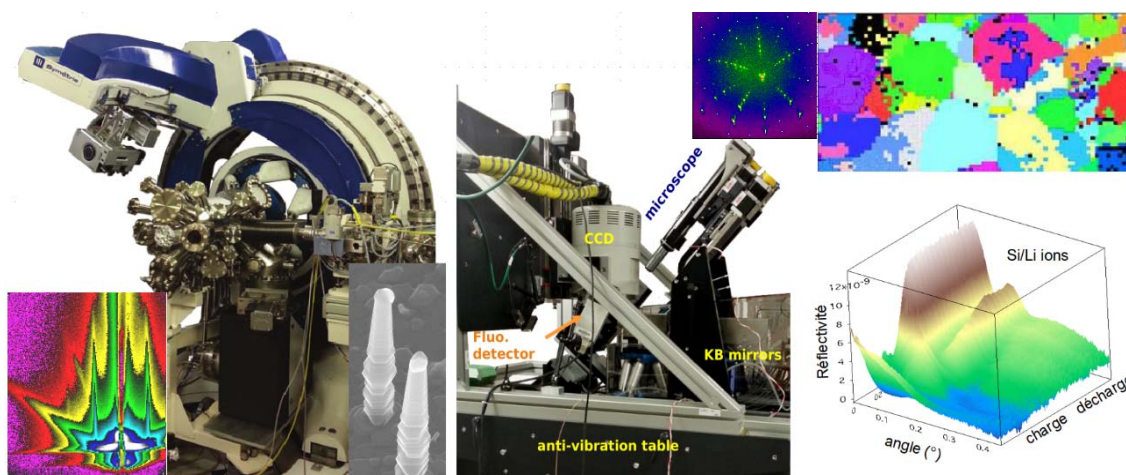
² CEA-Grenoble/INAC/SP2M, 17 Av. des Martyrs, Grenoble, France

³ Institut Néel, CNRS, 25 Av. des martyrs, Grenoble, France

⁴ UMR CNRS SprAM, CEA-Grenoble/INAC, 17 Av. des Martyrs, Grenoble, France

ABSTRACT

La ligne de lumière InterFaces (IF) mène des études structurales fondamentales et appliquées à l'aide du rayonnement synchrotron dans le domaine des nanosciences, des micro- et nanotechnologies. Les matériaux peuvent être étudiés *ex situ* ou *in situ* durant leur élaboration sous ultra-vide, en cours de fonctionnement ou sous sollicitations diverses (ex : thermique, mécanique, électrique). Elle est composée de trois instruments avec un faisceau monochromatique submillimétrique (0.3x0.5mm²) d'énergie comprise entre 5 et 30 keV ou polychromatique (de 5 à 22 keV) et de taille submicrométrique (300x300nm²).



L'instrument **In situ Nanostructures et Surfaces (INS)** sous ultra-vide permet de déterminer la structure atomique, la morphologie et la composition d'objets à l'échelle nanoscopique (îlots, nanofils, graphène, matériaux 2D) des surfaces et interfaces (alliage, hétérostructures, catalyse). Il permet d'étudier les mécanismes de croissance par épitaxie par jet moléculaire (MBE) et par dépôt chimique en phase vapeur (UHV-CVD). Le **goniomètre multitechnique (GMT)** accueille des échantillons à l'air ou avec leur environnement spécifique. Avec des photons X pénétrant (30 keV) il est particulièrement utile aux études structurales des interfaces solide/solide (adhésion, implantation) ou liquide/solide souvent *operando* (microfluidique, altération de surface, batterie Li-ions), des couches minces et les déformations dans les matériaux fonctionnels (relation propriétés-structure). L'instrument de **microdiffraction Laue (μ Laue)** permet de cartographier l'orientation et l'état de déformation des cristaux à l'échelle submicronique : mesures fines des déformations en microélectronique (intégration 3D, ingénierie du gap), de contrôle de la dispersion des contraintes internes dans des matériaux pour l'énergie. Des tests mécaniques réalisés *in situ* sur des micro- et nano-objets sont aussi effectués sur le rôle fondamental des défauts (dislocations, joints de grains) sur l'élasticité et la plasticité. Dans la perspective de l'emploi de la nouvelle source X pourvue par l'ESRF, la ligne fera appel à la communauté scientifique pour orienter les futurs développements instrumentaux répondant à ses besoins.

A New Version of MAX-StraightNoChaser: XAFS Linear Chemometry. LSF, PCA and MCR-ALS Optimized for EXAFS and XANES

A. Michalowicz, J. Moscovici, D. Muller, M. Bounif,
C. Fievez and N. Tassali

*Institut de Chime et des Materiaux Paris Est (CNRS and Universite Paris Est Creteil),
2-8 rue Henri Dunant, 92320 Thiais, France*

ABSTRACT

MAX-StraightnoChaser is the last software of the Multiplatform Applications for XAFS (MAX) data analysis suite. It is freely available either for MacOSX, Windows and Linux. StraightnoChaser is a complete set of tools for linear decomposition of mixed species XAFS spectra (either EXAFS or normalized XANES). It was already described in the XAFS15 proceedings [1] and this new presentation is essentially devoted to newly developed tools based on the Singular Value Decomposition (SVD) algorithm, PCA and MCR-ALS with new statistical tests.

1) Linear Least Squares (LSF) can be used when the series of unknown spectra can be linearly decomposed in *a priori* known models. Combinatory LSF with concentrations and errors constraints are available

2) Principal Component Analysis (PCA) was introduced in XAFS by S. Wassermann [2], and is already implemented in several other equivalent softwares [3]. Its purpose is to determine the minimum number of independent components, which can be used to decompose a series of data. Standard tests, like Malinowski's indicators [4] and Target Transformation to test PCA decomposition of model compounds are available. In addition, we have developed Score plots for the PCA analysis of time series of data.

3) Multivariate Curve Resolution-Alternating Least Squares (MCR-ALS) as been already used in several XAFS papers [5]. Its purpose is to extract the real model components by a linear transformation of a series of spectra, with unknown intermediates and/or incomplete reactions, using self-consistent LSF alternating cycles with non-negativity ($C \geq 0$), and closure ($\sum C = 1$) constrains. To our knowledge all published XAFS MCR-ALS works were performed with commercial data analysis tools [6]. MCR-ALS in StraightNoChaser is the first XAFS specific standalone routine freely available (<http://www.icmpe.cnrs.fr> > Service a la Recherche > Logiciels > Logiciels produits par l'ICMPE > Max). It was optimized for XAFS and more precisely adapted to EXAFS or XANES data, which should be treated differently, with the use of derivative spectra and normalization constrains for XANES, and a differential initial guess of the unknown species for EXAFS.

REFERENCES

- [1] A Michalowicz, J Moscovici, D Muller-Bouvet and K Provost, Journal of Physics: Conference Series, 430 (2013) 012016
 [2] a) S.R. Wasserman, Journal De Physique IV: JP 7 (1997), C2-203-C202-205
 b) S.R.Wasserman,P.G.Allen,K.Shuh,J.J.Bucher,N.M.EdelsteinJournal of Synchrotron Radiation, 6 (1999) 284–286.
 [3] a)Konstatin Klementiev, XANES dactyloscope<http://www.cells.es/old/Beamlines/CLAESS/software/xanda.html> b) Sam Webb, SIXPACK, Physica Scripta T T115 (2005) 1011–1014.
 [4] A. Manceau, M. Marcusand T.Lenoir, J. Sychrotron Rad., (2014), 21, 1140-1147
 [5] a) Arnaldo C. Faro , Jr.*, Victor de O. Rodrigues , and Jean-Guillaume Eon, *J. Phys. Chem. C*, 2011, 115 (11), pp 4749-4756
 b) Wellington H. Cassinelli, Leandro Martins, Aline R. Passos, Sandra H. Pulcinelli, Celso V. Santilli, Amélie Rochet, Valérie Briois, Catalysis Today 229 (2014) 114–122 and included references.
 [6] a) MCR-ALS Toolbox http://www.cid.csic.es/homes/rtaqam/tmp/WEB_MCR/down_mcr.html, MATLAB. CHEMOMETRICS AND INTELLIGENT LABORATORY SYSTEMS, 76(1), 101-110, MAY 2005.

Study of the Iron Oxidation States in Vitreous Phases of Ceramics by XANES Microprobe

J. Gillot¹, H. Montigaud¹, D. LeChevalier², N. Trcera³

¹ Saint-Gobain Recherche, 39 quai Lucien Lefranc, 93303 Aubervilliers, France

² Saint-Gobain Research Center NRDC, 9 Goddard Rd, Northborough, MA 01532, USA

³ Synchrotron SOLEIL, l'Ormes des Merisiers, BP 48, 91192 Gif-sur Yvette, France

ABSTRACT

In glass tank furnaces, the contact of molten glass with the refractories used in the side-wall is a key parameter for the furnace life-time and the quality of the glass produced. These ceramics are multi-phasic materials allowing vitreous phases of reduced size (several tens of microns). Oxidation/reduction reactions are suspected between these phases and the molten glass leading to changes of the oxidation states of several elements such as iron, titanium or tin. However, no data are available until now because of the small size of these vitreous domains.

The oxidation state and the coordination of the iron were studied by X-ray Absorption Near Edge Structure (XANES) spectroscopy at the Fe K-edge using LUCIA capability at SOLEIL. The reduced X-ray beam size (down to $5 \times 3 \mu\text{m}$) achieved by this beam line was well adapted to focus on the vitreous domains of the refractories¹. The two ones studied (AZS: Alumina-Zirconia-Silica (AZS) and HZ: High Zirconia Content) show a redox much lower than what could be expected from the oxidizing electrofusion processes. The $\text{Fe}^{3+}/\Sigma\text{Fe}$ ratio varies between 0.03 and 0.23 and the average coordination is around 4. After annealing of the refractories at 1100°C in air, without any contact with molten glass, the coordination does not change but the $\text{Fe}^{3+}/\Sigma\text{Fe}$ ratio increases up to 0.6. This value remains far below 0.8-0.9, the value observed for usual glass for glazing.

REFERENCES

1. A M Flank, G. Cauchon, P. Lagarde, S. Bac, M. Janousch, R. Wetter, and J.-M. Dubuisson., F. Langlois, M. Idir, T. Moreno, D. Vantelon, *LUCIA, A Microfocus soft XAS beamline*, NIM in Physics Research B, 246 p. 269-274 (2006)

CASTOR, Instrument d'Analyse Combinée XRR-GIXRF : Une Nouvelle Technique à SOLEIL

A.Novikova¹, H. Rotella², B. Boyer¹, Y. Ménesguen¹, M-C. Lépy¹

¹CEA, LIST, Laboratoire National Henri Becquerel (LNE-LNHB), Bât 602 PC 111,
91191 Gif-sur-Yvette cedex, FRANCE.

²CEA, LETI, MINATEC, 17 rue des Martyrs, 38054 Grenoble Cedex 9, France
Courriel : anastasiia.novikova@cea.fr

ABSTRACT

Caractériser de nouveaux matériaux nécessite de développer de nouvelles techniques d'analyse spécifiques. Les films minces de matériaux en couches empilées ont une importance croissante pour les développements industriels de haute technologie. Les performances de ces matériaux sont étroitement liées à la qualité des interfaces entre les différentes couches : rugosité, homogénéité. Les techniques utilisant les rayons X sous incidence rasante sont d'un intérêt majeur car elles permettent de remonter à des informations sur les propriétés des matériaux aux interfaces ou en profondeur. De plus, elles présentent l'avantage d'être sans contact et non-destructives.

Le Laboratoire National Henri Becquerel (LNHB) a réceptionné un goniomètre dédié nommé CASTOR (Chambre d'Analyse et de Spectrométrie en Transmission ou en Réflexion) sur la ligne de Métrologie au synchrotron SOLEIL [1]. CASTOR est un goniomètre expérimental basé sur un modèle développé au Physikalisch-Technische Bundesanstalt (PTB) et à l'Université Technique de Berlin [2]. Il est composé d'une chambre à vide contenant un manipulateur 7 axes. Le manipulateur comprend quatre translations et trois rotations. L'échantillon peut ainsi se mouvoir dans les multiples orientations requises par les méthodes d'analyse : Grazing Incidence X-Ray Fluorescence (GIXRF), réflectométrie (XRR), etc. La chambre sera équipée de plusieurs photodiodes, qui peuvent être étalonnées en rendement absolu par le LNHB en utilisant un radiomètre cryogénique à substitution électrique, BOLUX [3, 4].

Nous présentons une étude systématique par analyse combinée XRR-GIXRF, utilisant le rayonnement synchrotron comme source de photons X, d'une série de couches minces de ZnO dopé Ga présentant une variabilité d'épaisseur et soumises à différents budgets thermiques. Cette étude, corrélée à une analyse des propriétés optiques des couches permet de caractériser de façon précise non seulement l'épaisseur, la densité et la rugosité des couches mais aussi de comparer de façon qualitative le profil chimique de dopant au sein des couches ayant subi ou non un recuit. Ceci est effectué par la modélisation des données de XRR-GIXRF à l'aide d'un modèle commun en utilisant le logiciel Jgixa [5]. De plus, le développement de cette métrologie, ici réalisée avec un rayonnement synchrotron est prometteuse et en bonne voie pour être étendue en laboratoire pour un suivi « in-fab ».

REFERENCES

- [1] Y. Ménesguen, M.-C. Lépy, X-Ray Spectrometry, 40(6), 2011, 411-416.
- [2] J. Lubeck, B. Beckhoff, R. Fliegau, P. Hönicke, M. Müller, B. Pollakowski, F. Reinhardt, and J. Weser, Rev. Sci. Instrum. 84, 2013, 045106.
- [3] P. Troussel, N. Coron, Nuclear Instruments and Methods in Physics Research A, 61, 2010, 260-270.
- [4] Y. Ménesguen, M. Rodrigues, B. Boyer, M.-C. Lépy, G. Lidove, P. Troussel, 2014, XRM.
- [5] D. Ingerle, F. Meirer, G. Pepponi, E. Demenev, D. Giubertoni, P. Wobruschek and C. Strelti (2014). Spectrochimica Acta Part B. 99(100):121-128.

New Perspectives for the CRG-FAME Beamline in the Framework of the ESRF - Extremely Brilliant Source : New Source for New Science ? !

W. Del Net^{1,2}, I. Kieffer^{1,2}, E. Lahera^{1,2}, O. Proux^{1,2},
D. Testemale^{1,3}, J.-L. Hazemann^{1,3*}

¹ CRG-FAME @ ESRF, Grenoble ;

² OSUG, UMS 832 CNRS - Univ. J. Fourier, Grenoble ;

³ Institut Néel UPR 2940 CNRS, Grenoble.

* jean-louis.hazemann@neel.cnrs.fr

ABSTRACT

The CRG-FAME beamline uses X-ray absorption spectroscopy (XAS) for structural investigation of (very) diluted systems of environmental, chemical and biological interest. FAME is opened to users since 2002.¹ The main set-up consists of a 30-element Ge solid-state detector with a large beam (300 x 100 μm^2), was progressively completed by a microfocus station (the beam size is then around 10x10 μm^2) and a high spectral resolution station^{2,3} (the energy resolution of the crystal analyzer spectrometer, CAS, is around 1-2eV). The CAS station will be installed on a dedicated beamline in 2016, CRG-FAME/UHD. Both beamlines will be located on 0.85T bending magnets (BM30B & BM16) until the end of 2018.

The ESRF is entering into the final phase of its upgrade programme called ESRF - EBS, Extremely Brilliant Source, which aims at delivering a low emittance electron beam in a new storage ring in 2020. In the new configuration the "BM" beamlines will be equipped with a 2-poles wiggler, instead of the current dipole. The main consequences for FAME will be

- an increase of the flux by a factor 2-3,
- a decrease of the source size by a factor ~3 in both vertical and horizontal directions,
- the necessity to have a dedicated port, separated from BM30A.

With this new source, new scientific opportunities may arise that take advantage of the higher flux, the smaller beam-size and the larger space available around the sample. The establishment of a Conceptual Design Report (by the end of 2016) for FAME reviewed by the Science Advisory Committee of the ESRF during 2017, offers a great opportunity for beamline staff and users to ponder the beamline's future, its scientific perspectives and technical orientations.

Preliminary ideas are 1) the optimization of the micro-focus system to the new source design, in order to maximize the photons flux in a spot-size adapted to small samples and 2) the continuation of the automation of the set-up towards more efficient measurements (more samples in less time) and more user-friendliness.

All these objectives will be complementary with the resources available at SOLEIL and the national portfolio of the existing XAS beamlines.

The science done on FAME is yours, we look forward to hearing from you⁴ !

REFERENCES

1. Proux O., Biquard X., Lahera E., Menthonnex J.-J., Prat A. et al., *Phys. Scr.* **115**, 970-973 (2005).
2. Hazemann J.-L., Proux O., Nassif V., Palancher H., Lahera E. et al., *J. Synchrotron Radiat.* **16**, 283-292 (2009).
3. Llorens I., Lahera E., Delnet W., Proux O., Brillard A. et al., *Rev. Sci. Instrum.* **83**, 063104 (2012).
4. You can for example give your opinions at <http://www.esrf.fr/fame-user-requests>

Towards a New Tool Dedicated to the Normalization an Comparison of Experimental XMCD Spectra

K. Provost¹, F. Baudalet², L. Nataf², V. Paul-Boncour¹,
A. Polian³ and A. Michalowicz¹

¹ICMPE, UMR 7182 CNRS UPEC, 2-8 rue Henri Dunant, Thiais, France;

²SOLEIL, L'Orme des Merisiers, Saint-Aubin – BP48, Gif/Yvette, France;

³IMPMC, UPMC, Paris, France

ABSTRACT

Normalization of XMCD spectra proceeds in different steps including the definition of a baseline and normalization based on the XAS edge jump. To our knowledge, no tool is available for XMCD data analysis, and these steps are made by hand, eventually using tools provided for general data analysis. When working on spectra with poor baselines, what may occur for 3d metals K-edge, with homogeneity troubles in powder samples, these steps may be quite time consuming and rather subjective in the definition of a set of points for the baseline definition. Comparison of spectra may then be difficult.

Some of us have developed recognized efficient tools for XAS data treatment¹. Preliminary tests done on spectra recorded on powder samples under high pressure conditions showed that some of the numeric tools used for EXAFS extraction might be of great interest for XMCD spectra data analysis, and strongly speed up the baseline definition. Furthermore, EXAFS and XMCD share the question of a normalization based on the XAS edge jump.

This is why we propose a new tool dedicated to XMCD spectra. It provides in a unique tool, the treatment of both XAS and XMCD spectra. XANES normalization is based on a linear pre-edge, atomic absorption determined by polynomial regression, and normalization similar to normalization applied for XANES and EXAFS normalization. XMCD baseline definition is based on polynomial regression and the same normalization as for XANES. Comparison of spectra recorded on Fe foil and Fe powder shows that these tools are efficient to extract a large part of the XMCD signal, even in case of poor quality data [Fig.1]. Tools for spectra analysis are provided.

This new tool is written with the scripting compiled language Livecode², and soon available for users.

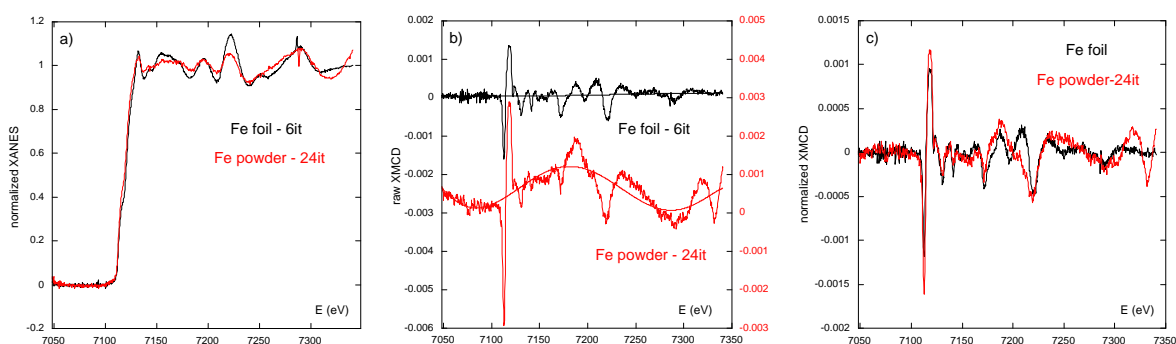


Fig. 1: Comparison of spectra recorded on a Fe foil (6 iterations) and on Fe powder (24 iterations) at the Fe K-edge: a) normalized XANES; b) raw XMCD spectra and polynomial baseline; c) normalized XMCD.

REFERENCES

1. A. Michalowicz, J. Moscovici, D. Muller-Bouvet and K. Provost, *J. Phys. Conf. Ser.* **190**, 012034 (2009).
2. Livecode.com

XPEEM Microscopy at the HERMES Beamline: Commissioning and First Results

M. Rioult, S. Stanescu, S. Swaraj, A. Besson, and R. Belkhou

Synchrotron SOLEIL, L'Orme des Merisiers, Saint-Aubin - BP 48,
F-91192 Gif-sur-Yvette cedex, France

ABSTRACT

We present here the first results obtained using the X-ray PhotoEmitted Electron Microscope (XPEEM) installed at the HERMES beamline at synchrotron SOLEIL [1]. The originality of the HERMES beamline is to combine two complementary microscopy methods (XPEEM and STXM) within the same beamline to allow the users to adequately choose the most appropriate instrument for their specific scientific case. Each microscope is installed on a dedicated branch and can operate alternatively and independently.

The XPEEM is based on photon-in/electron-out interactions and is therefore intrinsically a surface-interface microscopy method (probing depth <10nm), operating in an ultra-high vacuum environment. After few years of functioning at the Nanospectroscopy beamline [2] at the ELETTRA synchrotron (Trieste, Italy), the XPEEM instrument was upgraded prior to its final installation at the HERMES beamline (new cooling stage, motorized/encoded (X,Y, θ) manipulator...). The most important upgrade was the installation of a new prototype of hemispherical energy analyzer that opens up the way to perform high-resolution local XPS and ARPES measurements.

The commissioning results of the XPEEM branch will be presented together with the specifications of the X-ray beam in term of flux, size and energy resolution. The beamline allows to achieve very high photon flux (up to 10^{13} photons/s), micro-sized beamspot (< 25 μ m), high resolving power (> 10,000 within the 70 eV – 2.5 keV range) and hence a high-energy resolution (e. g. < 40meV at 400 eV photon energy). The XPEEM microscope performances will also be presented, both in the imaging and local spectroscopy modes. In the LEEM mode, the microscope reaches 6 nm spatial resolution. With the X-ray, spatial resolutions well below 35 nm are routinely achieved.

Finally, some examples of the first user experiments results will be given, together with new additional available capabilities (*in-situ* growth, current injection...).

REFERENCES

- [1] R. Belkhou et al., J. Synchrotron Rad., 22, 968-979 (2015)
[2] <https://www.elettra.trieste.it/elettra-beamlines/nanospectroscopy.html>

Use of Synchrotron-radiation Infrared Microspectroscopy in Single Glioblastoma Cells to Elucidate a Specific Signature Associated with Hypoxia Levels Found in Tumours

C. Sandt^a, C. Nadaradjane^a, R. Richards^b, P. Dumas^a, V. Sée^b

^a*Synchrotron SOLEIL, L'Orme des Merisiers, 91192 Gif sur Yvette, France*

^b*Department of Biochemistry, Institute of Integrative Biology, University of Liverpool, Liverpool, UK*

ABSTRACT

Hypoxia is a common feature of solid tumours and is associated with poor prognosis, resistance to radio- and chemotherapy, and tumour aggressiveness. It is necessary to have direct and specific diagnostic tools for measuring the extent of tumour hypoxia in order to predict tumour response, improve therapeutic treatment, and provide personalized medicine.

We have investigated the potential of Fourier Transform Infrared (FTIR) microspectroscopy, at cellular and subcellular resolution, for detecting hypoxia-induced metabolic changes in brain tumour (glioblastoma) cells in various cell lines and in short term primary cultures derived from patient samples. The most prominent and common changes observed were the increase in lipids (all cell lines studied) and in glycogen (specifically in the U87MG cell line). Additionally, each cell line presented specific individual metabolic fingerprints. The metabolic changes were harder to detect under chronic hypoxic conditions, which suggests cellular adaptation occurring upon long term changes in the microenvironment. The metabolic signature was similar regardless of the severity of the hypoxic insult and was replicated by the hypoxia mimetic drug dimethyloxallylglycine. To investigate any specific changes at subcellular levels and to improve the sensitivity of the detection method, spectra were recorded separately in the cytoplasm and in the nucleus of D566 glioblastoma cells, thanks to the use of SOLEIL synchrotron source. A different hypoxic signature was detected in both compartments and this improved the detection of hypoxic cells especially in chronic hypoxia conditions.

Whilst there was a high spectral variability between cell lines, we show that FTIR microspectroscopy allowed the detection of the common metabolic changes triggered by hypoxia regardless of cell type, providing a potential new approach for the detection of hypoxic tumours.

REFERENCES

- 1 Sandt et al., *Analyst* (2015).

Fast Scanning Multi-technique Spectro-microscopy Possibilities at the Nanoscopium Beamline of Synchrotron SOLEIL

A. Somogyi, K. Medjoubi, G. Baranton, V. Le Roux, M. Ribbens,
F. Polack, M. Ribbens, J.P. Samama

Synchrotron Soleil, BP 48, Saint-Aubin, Gif sur Yvette, 91192, France

ABSTRACT

The Nanoscopium 155 m long beamline of Synchrotron Soleil is dedicated to scanning hard X-ray nanoprobe techniques in the 5-20 keV energy range. For the first user experiments Nanoscopium offers hierarchical length-scale X-ray Fluorescence Imaging with down to ~200 nm spatial resolution. The proof of principle fast scanning experiments showed the possibility of high resolution 2D imaging of some hundred μm^2 sample areas in some minutes. As next step multi-technique scanning imaging and tomography including X-ray fluorescence spectrometry and spectro-microscopy, absorption, differential phase and dark field contrasts is being implemented at the beamline in order to provide simultaneous information on the elemental distribution, speciation and sample morphology.

This poster presents the first measured performance of the Nanoscopium beamline followed by the proof of principle multi-technique fast scanning imaging and tomography experiments performed with ms dwell time per pixel.

REFERENCES

1. Somogyi A., Polack F., Moreno T., (2010). Nanoscopium: a Scanning Hard X-ray Nanoprobe Beamline at Synchrotron Soleil, SRI 2009, 10th International Conference on Radiation Instrumentation. AIP Conference Proceedings, Volume 1234. p.395-398.
2. Medjoubi K., Leclercq N., Langlois F., Buteau A., Lé S., Poirier S., Mercère P., Sforza M.C., Kewish C.M., Somogyi A. (2013). Development of Fast, Simultaneous and Multi-Technique Scanning Hard X-Ray Microscopy at Synchrotron Soleil. *Journal of Synchrotron Radiation*, 20(2), 293–299.
3. Somogyi A., Medjoubi K., Baranton G., Le Roux V., Ribbens M., Polack F., Philippot P., Samama J.P. 2015. "Optical Design and Multi-Length-Scale Scanning Spectro-Microscopy Possibilities at the Nanoscopium Beamline of Synchrotron Soleil." *Journal of Synchrotron Radiation* 22 (4): 1118–29. doi:10.1107/S1600577515009364.

Polydiacetylenes Langmuir Films to Produce Biological or Environmental Sensors

S. Spagnoli¹, M.-C. Fauré^{2,3}, M. Goldman^{2,3,5}, M. Schott², C. Allain⁴.

¹LIPhy : 140 avenue de la physique, BP 87, 38402 Saint Martin d'Hères France ,

²INSP : 4 place Jussieu 75252 Paris cedex 05 France.

³Faculté des Sciences Fondamentales et Biomédicales, 45 rue des Saints-Pères 75006 Paris France.

⁴PFSM : 61 avenue du Président Wilson 94235 Cachan France

⁵Synchrotron SOLEIL L'Orme des Merisiers Saint-Aubin - BP48 91192 Gif/Yvette cedex France

ABSTRACT

Polydiacetylenes (PDA): $=(CR-C\equiv C-CR')_n=$ are conjugated polymers, generally obtained by UV irradiation, that present a color transition, blue-red, when they are stimulated (Fig.1). This transition corresponds to a conformational and electronic structure change of the chain. If an appropriate group is attached at the end of R' , the color transition can be selectively triggered by reaction of this group with a suitable target (molecule, protein, ion etc.). These compounds present therefore suitable properties to be used as sensors. Our objective is to use the versatility of the molecules forming a Langmuir film to study and control the basic mechanism of this transition which is still not understood and implement such kinds of sensors.

The structure of PCDA ($CH_3(CH_2)_{11}-C\equiv C-C\equiv C-(CH_2)_8COOH$) and 13-4OH ($CH_3(CH_2)_{12}-C\equiv C-C\equiv C-(CH_2)_3-CH_2OH$) Langmuir films have been studied at the SIRIUS beamline by GIXD on pure water surface in: non-irradiated monolayer and trilayer cases (monomer case) and in-situ irradiated monolayer (polymerized case). Results of a first series of experiments will be discussed. PCDA, which has been the material of choice in previous studies, suffers from the instability of the monolayer with respect to the trilayer structure. 13-4OH is a newly synthesized molecule which should remain more stable at the air/water interface. The compression isotherms indicate a liquid expanded (LE) phase followed by a (LC) phase and then the monolayer-trilayer transition. However, expansion recompression cycles shows that, contrary to PCDA, the molecule respreads in a monolayer state, even after being compressed up to a pure trilayer state. The 13-4OH molecule appears then as a good candidate for obtaining a functional polymerized sensor which require a single layer structure.

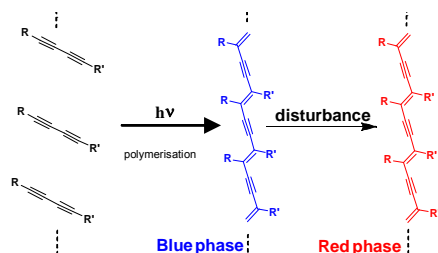


Fig. 1: Schematic representation of the blue-red transition in polydiacetylene polymers

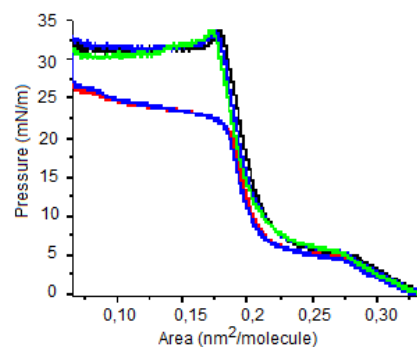


Fig.2: Compression, expansion and recompression isotherms on water surface of a) PCDA b) 13_4OH molecules

Projet Dichro50

M. Stora¹, J-P. Kappler¹, O. Guia², P. Ohresser¹, P. Bonnet²

(1) Ligne DEIMOS, Synchrotron Soleil, L'Orme des Merisiers, 91190 Saint-Aubin

(2) Société Cryoconcept, 4 Avenue des Andes, 91940 Courtaboeuf

ABSTRACT

DICHROISME MAGNETIQUE A 50mK SOUS ULTRA VIDE ET CHAMP MAGNETIQUE INTENSE

Les mesures d'absorption x reposent sur plusieurs méthodes de détection, parmi lesquelles le rendement total d'électrons (TEY, pour *Total Electron Yield*) qui est la méthode privilégiée aux basses températures. Elle s'obtient grâce à la mesure du courant échantillon, ce qui suppose que celui-ci est isolé électriquement de la masse. Ce photo-courant est directement relié à l'absorption de l'échantillon.

Les propriétés magnétiques de la matière dépendent essentiellement de la température. Les molécules-aimants présentent des propriétés exceptionnelles à très basses températures. Pour atteindre leur caractérisation magnétique il faut un dispositif permettant de refroidir la molécule tout en garantissant une isolation électrique parfaite, pour des mesures, en particulier, de dichroïsme magnétique.

L'objectif du **Projet Dichro50**, regroupant la ligne **DEIMOS** du Synchrotron Soleil et l'entreprise **Cryoconcept**, est de créer un outil de mesure original avec comme caractéristiques essentielles :

- une très bonne isolation électrique (de l'ordre de 200GΩ).
- des températures avoisinant les 50mK.
- Un champ magnétique pouvant atteindre 7T.

Glycosylate and Move: Structural and Functional Dissection of a Glycosyltransferase Involved in Glycosylation of a Bacterial Flagellin

G. Sulzenbacher,¹ D. Murat,^{3,4} V. Zamboni,¹ R. Vincentelli,¹,
L.F. Wu,^{2,3} and F. Alberto,^{2,3}

¹Architecture et Fonction des Macromolécules Biologiques, UMR 7257 CNRS, Aix-Marseille Université, Case 932, 163 Avenue de Luminy, F-13288 Marseille Cedex 9;

²Laboratoire de Chimie Bactérienne, UMR 7283 CNRS, Aix-Marseille Université, 31 Chemin Joseph Aiguier, F-13402 Marseille Cedex 20;

³Laboratoire International Associé de la Bio-Minéralisation et Nano-Structures (LIA-BioMNSL), CNRS, 31 Chemin Joseph Aiguier F-13402 Marseille Cedex 20;

⁴Laboratoire Information Génomique et Structurale, UMR 7256 CNRS, Aix-Marseille Université, Case 934, 163 Avenue de Luminy, F-13288 Marseille Cedex 9

ABSTRACT

Bacterial motility is governed by motor rotation of a filament that is assembled via polymerization of flagellins after secretion via a dedicated Type III secretion system (1). Many bacteria modify their flagellins through attachment of carbohydrate groups (2), shown to be essential for the formation and functionality of an intact flagellum (3). The flagellin of our model organism *Magnetospirillum magneticum* AMB-1 (AMB-1) is glycosylated and deletion of the gene *amb0685* produced non-glycosylated flagellin and a non-flagellated phenotype. A functional flagellar filament and bacterial motility could be restored by complementation of the deletion mutant. Proteomic analysis revealed that the flagellin of AMB-1 is O-glycosylated with pseudoaminic acid, a sugar related to sialic acid. We solved the crystal structure of the product of *amb0685*, which is organised into three domains: a N-terminal Rossman-like domain of unknown function, a central $\beta/\alpha/\beta$ domain exhibiting striking structural similarity with sialyltransferases and a C-terminal α -helical bundle with intriguing structural reminiscence of flagellar chaperons. By mutation studies we could identify residues crucial for the glycosyltransferases activity of AMB0685.

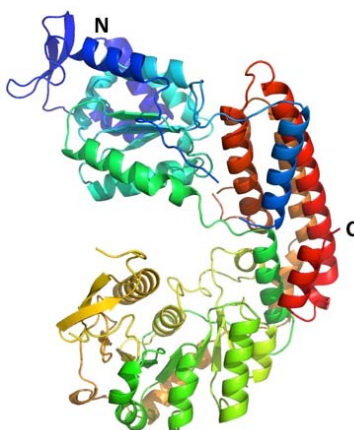


Fig. 1: Cartoon representation of the overall structure of Amb0685.

REFERENCES

1. M. Erhardt, K. Namba and K.T. Hughes, Cold Spring Harb Perspect Biol 2, a000299 (2010).
2. H. Nothaft and C.M. Szymanski, Nat Rev Microbiol 8, 765–778 (2010).
3. D.J. McNally, J.P. Hui, A.J. Aubry, K.K. Mui, O. Guerry, J.R. Brisson, S.M. Logan and E.C. Soo. J Biol Chem 281, 18489–18498 (2006).

STXM at the HERMES Beamline: Capabilities and the First Commissioning Results

S. Swaraj^a, R. Belkhou^a, S. Stanescu^a, A. Besson^a,
M. Rioult^a, C. Pampfer^b

^a Synchrotron SOLEIL, L'Orme des Merisiers, Saint-Aubin - BP 48,
F-91192 Gif-sur-Yvette cedex, France

^b RI Research Instruments GmbH, Friedrich-Ebert-Str. 1, 51429 Bergisch Gladbach, Germany

ABSTRACT

The capabilities and the first commissioning results of the new interferometrically controlled Scanning Transmission X-ray Microscopy (STXM) installed at the HERMES beamline at SOLEIL are presented. The STXM instrument is designed to perform with high stability and to achieve high spatial resolutions in the soft x-ray regime with a multitude of different detection techniques and different sample environments. A photomultiplier tube (PMT), a quadrant diode detector and a channeltron are currently installed for bulk and surface sensitive measurements. Various spectro-microscopic techniques and detection modes such as XANES, XAS, XMCD and XMLD are already implemented. The different sample mounts available include a temperature controlled sample mount (-150°C to 80°C), a magnetic system (vectorially variable ± 200 mT) and a rotatable sample mount. The design of the instrument could additionally allow for many different sample environments such as sealed and flow cells and different detection techniques such as a ptychography, tomography etc. In addition, photon detection technique, such as using the PMT, allows the investigation of samples at atmospheric pressures. Special attention has been taken during the designing of the beamline to minimize the carbon contamination of the beamline optics [1]. Thus the STXM instrument is also capable of measuring organic samples.

We present the very first commissioning results in this presentation. We have demonstrated a spatial resolution of <40 nm using a zone plate of 30 nm outer zone. We have performed magnetic imaging of CoPt thin films (Co thickness=15 nm) where the worm domains of 200 nm width are easily visible at circular left and right polarizations (Fig. 1). Reference polystyrene thin film and polystyrene nanospheres (70 nm diameter) were also investigated in the initial tests to demonstrate that measurements at the Carbon K-edge are possible.

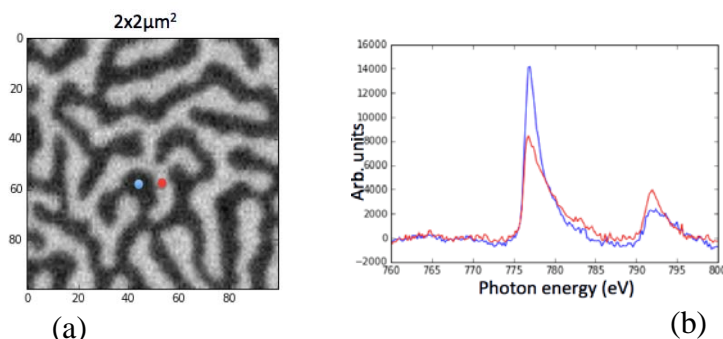


Fig 1: (a) Image at 777 eV and (b) point scans of a CoPt sample (Co thickness 15 nm)

REFERENCES

1. R. Belkhou et al., J. Synchrotron Rad., 22, 968-979 (2015)

Structural Determination of Metal-organic Frameworks from Single Microcrystal X-ray Diffraction

A. Tissot,^a J. Marrot,^a M. Benzaqui,^a W. Shepard,^b C. Serre^a

^a CNRS, Institut Lavoisier de Versailles, Université de Versailles Saint-Quentin

^b Synchrotron SOLEIL, ligne PROXIMA 2

ABSTRACT

Crystalline porous hybrid solids, known as Metal Organic Frameworks (MOFs), are one of the most recent classes of porous solids.¹ They are built up from inorganic subunits and organic polycomplexing linkers and offer an unprecedented structural and chemical diversity leading to architectures with various pore sizes (from micro- to mesopores), shapes and chemical functionalities. Most of the work on applications of MOFs during the past decade has focused on domains like energy, environment, medicine, etc. For example, Al carboxylate based MOFs, such as MIL-96 are promising candidates for gas separation². MIL-100(Fe) is an example of highly porous biocompatible MOF used for biomedical applications.³

Laboratory X-Ray powder diffraction data allows to obtain the unit-cells and space groups of Metal-Organic Frameworks, but determining their structures is not straightforward due to the large unit-cells and/or low scattering factors. Therefore, the collection of high-resolution data on few μm sized single crystals is a keypoint for determining the structure of such materials. In this contribution, we will present the structure of MIL-96 and MIL-100(Fe) solved on 10 μm large single crystals on PROXIMA 2 beamline.

REFERENCES

- [1] Themed issue: Metal–Organic Frameworks, *Chem Soc. Rev.* **2014**, *16*, 5403.
- [2] T. Loiseau, L. Lecroq, C. Volkringer, J. Marrot, G. Férey, M. Haouas, F. Taulelle, S. Bourrelly, P.L. Llewellyn, M. Latroche, *J. Am. Chem. Soc.*, **2006**, *128*, 10223-10230
- [3] P. Horcajada, S. Surblé, C. Serre, D.-Y. Hong, Y.-K. Seo, J.-S. Chang, J.-M. Grenèche, I. Margiolaki, G. Férey, *Chem. Comm.*, **2007**, 2820-2822

Local Structure Around Silicon on Silicene Deposited Onto Ag(110) And Ag(111) Surfaces

N. Trcera, P. Lagarde, M. Chorro and D. Roy

Synchrotron SOLEIL, l'Orme des Merisiers, Saint Aubin, Gif sur Yvette CEDEX, France

ABSTRACT

Over the last decade, silicene, a two-dimensional material consisting of Si atoms, has attracted much attention because of potentially very interesting electronic properties for a wide range of applications; it is a particularly promising for nano-electronics because it is a silicon-based material. Since the discovery of these new systems in 2010, several techniques aimed to describe the structure of these deposits have been used: scanning tunneling microscopy, low energy electron diffraction, grazing incidence x-ray diffraction and density functional theory calculations. All give the honeycomb structure for Si/Ag(111) and the nanoribbon one for Si/Ag(110) but the results are widely scattered as far as the local order around the silicon atoms (interatomic distances, bonding angles, buckling, distance with the substrate) is concerned. We then have conducted x-ray absorption spectroscopy at the Si K-edge on the LUCIA beamline in order to gain advantage of this technique for the precise description of the local order.

The study of the local structure around the silicon atoms of silicene deposited onto Ag(110) and Ag(111) has been investigated by Extended X-ray Absorption Fine Structure (EXAFS) spectroscopy at the silicon K-edge. The results show that this structure is identical to that of the double Si(111)-plane isolated from crystalline silicon with the same first and second interatomic distances (2.35 and 3.83 Å). Moreover the results allow us to determine the distance between the silicene sheet and the substrate planes as well as they show that silver ad-atoms probably sit on top of the silicene layer.

Implementation of a Multilayer Grating Monochromator on LUCIA

D. Vantelon^a, T. Moreno^a, N. Trcera^a, B. Lassalle-Kaiser^a, D. Roy^a,
E. Meltchakov^b, F. Delmotte^b, S. Guilet^c, D. Mailly^c,
P. Lagarde^a, A.M. Flank^a

^a*Synchrotron SOLEIL, Gif sur Yvette, France,*

^b*Institut d'Optique Graduate School, Orsay, France,*

^c*Laboratoire de Photonique et de Nanostructures, CNRS-UPR20, Marcoussis, France*

ABSTRACT

The LUCIA beamline of SOLEIL is dedicated to experiments of μ XAS and μ XRF in the tender X-ray domain (previously from 0.8 to 8.0 keV) using a beamsize of $2.5 \times 2.5 \mu\text{m}$ [1]. This energy domain allows determining the speciation of elements, performing XAS experiments at the K-edge of Na to Co, the L-edges of Ni to Gd, and the M-edges of rare earths and actinides.

The spectral range of the beamline is now extended to 600 eV. Among others, it allows reaching the L-edges of additional transition elements such as Co, Fe and Mn. Knowing that the $L_{2,3}$ -edges of the transition elements are more sensitive to the oxidation states than the K-edges, LUCIA offers now the opportunity to collect, with the same spot size, on the same sample, XANES measurements at the $L_{2,3}$ -edges of Mn to Co in addition to the XANES and EXAFS spectra at the K-edge.

This extension is allowed thanks to the implementation of a Multilayer Grating Monochromator (MGM). Combining the performances of the grating diffraction with the Bragg diffraction of the multilayer, it provides a high flux and a reasonable resolution. The focus properties are retained. Additionally, it advantageously replaces crystals with large cell (KTP, Beryl) which suffer of beam damages. The originality of this installation is to use the existing mechanics of the DCM.

In this poster, a description of the set up will be given as well as its actual performances. The scientific interest of this implementation will be described using examples in material and geosciences.

REFERENCES

- [1] Flank et al. (2006) LUCIA : a microfocus soft XAS beamline. *NIM B*, **246**, 1, 269-274
- [2] Vantelon et al. (2016) The LUCIA beamline at SOLEIL. *JSR* accepted

Refining the Structure of Al-substituted Ferrihydrites

I. Kaddouri^a, R. Pichon^b, V. Peyre^c, K. Chaouchi^a, S. Blanchandin^a,
E. Montarges-Pelletier^d, A. Adra^e, G. Morin^e and D. Vantelon^a

^aSynchrotron SOLEIL, Gif sur Yvette, France,

^bGEOPS, UMR 8148 CNRS, UPSud, Orsay, France

^cLaboratoire PHENIX, UMR 8234 CNRS, UPMC, Paris, France

^dLIEC, UMR 7360 CNRS, Université de Lorraine, Vandœuvre lès Nancy, France,

^eIMPMC, UMR 7590 CNRS, UPMC, Paris, France

ABSTRACT

In soils and surface waters, poorly ordered Fe oxy-hydroxides such as ferrihydrite (Fh) play a crucial role on the cycle of elements and on the behavior of trace metal elements. In natural systems, Al for Fe substitution was shown to occur in the structure of Fh (1). This substitution was found to increase the stability of the Fh by retarding its transformation to more crystalline phases (2), and to influence its surface properties and its ability to trap pollutants, such as arsenic (3). However the reported modifications of the surface reactivity are variable (4,5). The Al contents measured in natural Al-Fh ranges from 15 to 30 mol %, with EXAFS evidence of Al for Fe substitution to up to 30 mol% Al (1). The proposed mechanisms for the Al association with Fh are however variable in synthetic phases. Al for Fe substitution has been demonstrated using recent PDF (7) and EXAFS (1) analyses, but it has been shown not to exceed 15-20 mol% (1) or 20-30 mol% (7). For higher Al contents, i.e. higher than 30 mol%, gibbsite was formed and the formation of small amounts of an Al-hydroxide phase for Al concentration over 20 mol% is suspected. In the same way, Al K-XANES and FTIR study have suggested surface precipitation of aluminous phases (6). The formation of individual Al-phases was found enhanced by the slowness of the precipitation rate (7). In order to study the local environment of substituted Al in the Fh structure and its impact on the Fh properties, we have optimized the synthesis protocol of Al-substituted ferrihydrites using rapid precipitation rate with Al/Fe ratios ranging from 0 to 40 mol%.

In agreement with literature (1,7), the highest Al content that could be incorporated in the Fh structure is 30 mol%. XRD patterns revealed that the presence of Al modified slightly the Fh structure and that no crystalline aluminum hydroxide was formed. According to calculations proposed by Ducher et al. (8), XANES spectra collected at the Al K-edge revealed that Al atoms form clusters for Al contents higher than 20% while Al atoms remain rather isolated for lower contents. Those results are in agreement with EXAFS data collected at the Al and Fe K-edges as well as with measurements of surface charge, showing that the point of zero charge increased from 7.5 to 8.5 when Al content reached 20%.

REFERENCES

- (1) Adra A., et al. (2013) *ES&T*, 47, 12784-12792
- (2) Cornell, R. M., Schwertmann, U. *The iron oxides: Structure, properties, reactions, occurrences and uses*; Wiley-VCH: 2003.
- (3) Adra A., et al. (2015) *Applied Geochemistry* (in press) doi:10.1016/j.apgeochem.2015.09.015
- (4) Masue Y., et al. (2007) *ES&T*, 41, 837-842
- (5) Cismasu A.C., et al. (2013) *GCA*, 119, 46-60
- (6) Hofmann A., et al. (2013). *J. Colloid Interface Sci.*, 407, 76-88
- (7) Cismasu A.C., et al. (2012) *GCA*, 92, 275-291
- (8) Ducher M., et al. accepted in *Phys. Chem. Min.*

Phase Stability, EXAFS Investigation and Correlation between Nanostructure and Extrinsic Magnetic Properties of Nanocrystalline $\text{Pr}_2(\text{Co,Fe})_7$

K. Zehani^{a*}, R. Bez^{a,b}, R. Fersi^b, J. Moscovici^a,
L. Bessais^a, N. Mliki^b, A. Michalowicz^a, E. Fonda^c

^aCMTR, ICMPE, UMR7182, CNRS, Universit Paris Est, 2-8 rue Henri Dunant F-94320 Thiais, France

^bLMOP, Faculté des Sciences de Tunis, Université de Tunis El Manar, 2092 Tunis, Tunisia

^cSynchrotron SOLEIL, L'Orme des Merisiers, Saint-Aubin, BP48, F-91192 Gif-sur-Yvette Cedex, France

*Email of corresponding author: zehani@icmpe.cnrs.fr

ABSTRACT

Nanocrystalline $\text{Pr}_2\text{Co}_{7-x}\text{Fe}_x$ ($x = \leq 3.5$) powder was synthesized by high energy milling and was subsequently annealed at 973 K for 30 min. Their crystalline structures were investigated by means of X-ray diffraction (XRD), X-ray absorption spectroscopy (XAS) and transmission electron microscopy (TEM). Magnetic properties were also studied at room temperature and 10 K as a function of the iron composition. This compounds structure depends on the iron content; for $x \leq 1$ they crystallize in the Ce_2Ni_7 -type hexagonal structure (space group: $\text{P6}_3/\text{mmc}$). For $1 < x \leq 3$, we observe a mixture of three phases, $\text{Pr}_2(\text{Co,Fe})_7$, $\text{Pr}(\text{Co,Fe})_3$ and $\text{Pr}_2(\text{Co,Fe})_{17}$ while for larger values of x the $\text{Pr}_2(\text{Co,Fe})_7$ phase disappears completely. Since the substitution of cobalt by iron in a pure $\text{Pr}_2\text{Co}_{7-x}\text{Fe}_x$ phase is limited to $x \leq 1$, a site preference can be suggested. Unfortunately standard XRD cannot be used unambiguously because Co and Fe have too close normal X-ray atomic scattering factors. Among the local and Fe selective available experimental methods, we have chosen to explore the $\text{P6}_3/\text{mmc}$ space group Wyckoff positions for iron by EXAFS at the Fe edge. This study shows that the local iron radial distribution function is much larger than expected for all the specific sites, at least two Fe-Pr distances, except for 12k which gives the best fit. A preferential substitution of cobalt by iron in 12k site is coherent with (i) the EXAFS result (ii) the substitution rate $x < 1$ (iii) the anisotropic increase of the crystal cell parameters. A mixture of 12k, 6h and 2a cannot be excluded. However, if we assume a unique preferential site, 12k is the only solution.

For $x \leq 1$, the magnetocrystalline anisotropy is observed in $\text{Pr}_2\text{Co}_{7-x}\text{Fe}_x$ alloys with fairly strong anisotropy fields at room temperature in range from 123 to 136 kOe for $x = 0$ and $x = 1$, respectively. For $x > 1$, the magnetocrystalline anisotropy field of the 2:17 phase is lower than that of the 2:7 phase, which causes a further reduction in anisotropy and coercivity.

Keywords: Phase stability, EXAFS study, Magnetic properties

XAS Spectroscopic Fingerprint of the Active Site in Non-precious Metal Electrocatalysts for PEM Fuel Cells

A. Zitolo^a, V. Goellner^b, V. Armel^b, M-T. Sougrati^b, T. Mineva^b,
L. Stievano^b, E. Fonda^a and F. Jaouen^b

a. Synchrotron SOLEIL, L'Orme des Merisiers, BP 48 Saint Aubin, 91192 Gif-sur-Yvette, France

b. Institut Charles Gerhardt Montpellier, UMR 5253, 34095 Montpellier, France

ABSTRACT

Heat-treated Me-N-C (Me=Fe,Co) catalysts are promising non-precious substitutes to traditional platinum-based catalysts for the cathodic oxygen reduction reaction (ORR) in fuel cells. While recent advances lead to greatly improved activity and durability of Me-N-C catalysts both in alkali media and in the proton exchange membrane fuel cells, the exact structure of the active site has remained elusive due to the presence of nanoparticles (metal, metal carbides, nitrides or oxides) in the final synthesized compounds, leading to a complex and not clear identification of the ORR active site. Several advanced techniques have provided structural information on the metal-centred active sites, such as extended X-ray absorption fine structure (EXAFS) and ⁵⁷Fe Mössbauer spectroscopy,¹ X-ray photoelectron spectroscopy,² and time-of-flight secondary ion mass spectroscopy.³ On the basis of those investigations, several active-site structures with different levels of completeness have been proposed, including FeN₄ and FeN₂₊₂ species embedded in a graphene matrix.

In this study the synthesis was carefully designed to prevent the formation of inactive crystalline metal species. This allowed us to carry out a clear and accurate structural characterization of the catalytic active sites by studying both the EXAFS and the X-ray absorption near-edge structure (XANES) regions at the Fe and Co K-edge, revealing the existence of active sites based on a porphyrinic MeN₄C₁₂ architecture.⁴

REFERENCES

1. U. I. Kramm et al. *Physical Chemistry Chemical Physics* **14**, 11673-11688 (2012).
2. F. Jaouen et al. *ACS Applied Materials & Interfaces* **1**, 1623-1639 (2009).
3. M. Lefèvre et al. *Journal of Physical Chemistry B* **106**, 8705-8713 (2002).
4. A. Zitolo et al. *Nature Materials* **14**, 937-942 (2015).

Understanding the Apparent Negative Thermal Expansion in Supported Rh-based Nanoparticles

C. Zlotea, Y. Oumellal and K. Provost

Institut de Chimie et des Matériaux Paris-Est CNRS UPEC
2-8 rue Henri Dunant 94320 Thiais France

ABSTRACT

As compared to bulk state, supported nanoparticles offer larger surface to volume ratios, faster transport properties, altered physical properties and interesting confinement effects that are consequences of combination of their nanoscale dimensions and interaction with the supports. Due to these exciting properties, these materials are currently studied for solid state H₂ storage. In this context, we have recently shown that nanosizing of supported Rh-based nanoparticles can drastically change the H₂ sorption properties. Bulk Rh can absorb H₂ at 20 °C only under severe conditions (4 GPa) and form the hydride RhH. However at nanoscale, Rh hydride can be formed easily under low H₂ pressure if the particle sizes decrease below 2 nm.¹ Moreover, this nano-hydride is stable at 20 °C and only desorbs H₂ at around 180 °C, as demonstrated by thermo-desorption-spectroscopy. We report here *in situ* EXAFS study during the H₂ desorption from 1,3 nm Rh-based nanoparticles supported on carbon. This experiment was carried out by the help of the catalysis cell available on the ROCK beam line.² The evolutions of the 1st neighbor distance (R) and the Debye-Waller factor (σ^2) during constant heating under N₂ atmosphere are plotted in Fig. 1. Data processing and XAS refinements have been performed by the help of the MAX platform.³ The thermal variation of the bulk Rh *fcc* lattice parameters obeys a linear increase with temperature with a known thermal expansion coefficient ($\alpha=8.2 \cdot 10^{-6} \text{ K}^{-1}$). On the contrary, the thermal variation of the R in 1.3 nm particles is showing a decrease while σ^2 is increasing with temperature. These results can be understood in terms of both hydrogen desorption that contracts the interatomic distances and negative thermal expansion already reported for supported Pt nanoparticles.⁴

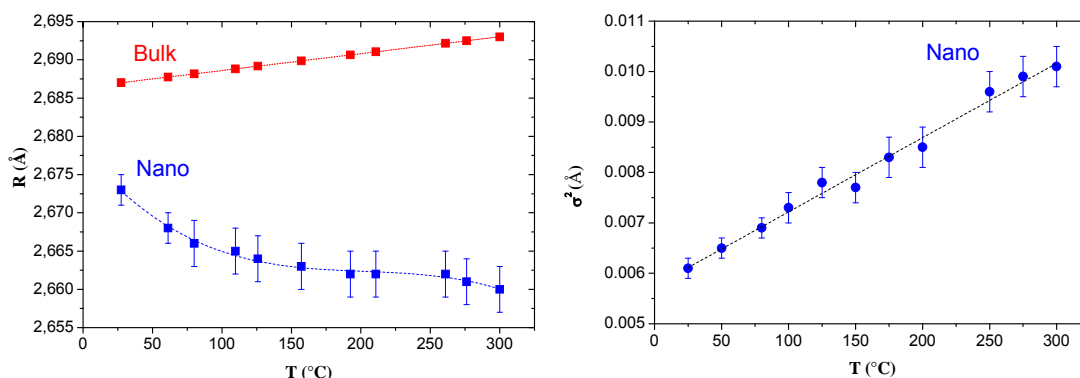


Fig. 1: Left: thermal evolution of the 1st neighbor distance for Rh bulk (red) and Rh-based nanoparticles (blue). Right: thermal evolution of the Debye-Waller factor for Rh-based nanoparticles.

REFERENCES

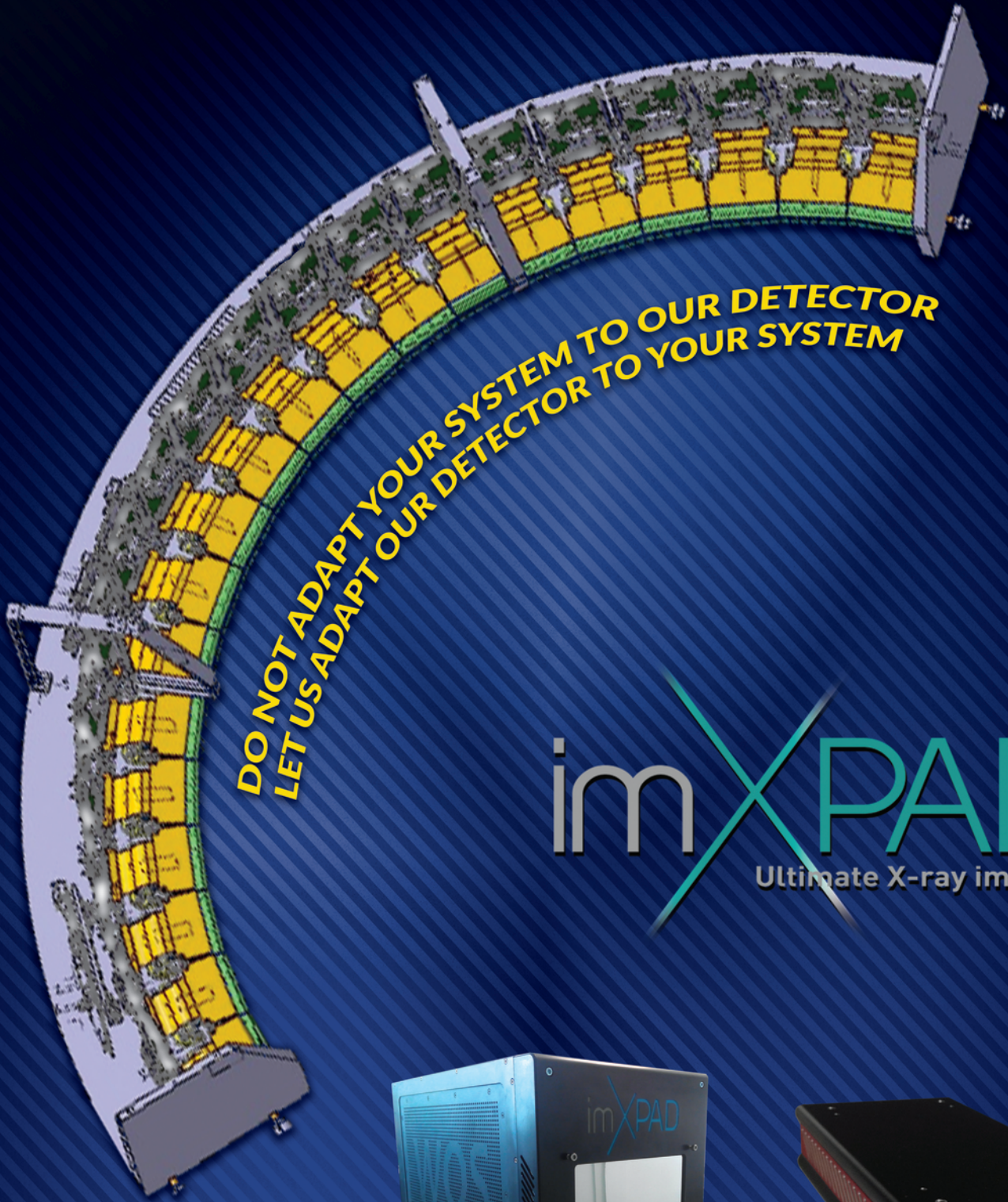
1. C. Zlotea, Y. Oumellal, M. Msakni, J. Bourgon, S. Bastide, C. Cachet-Vivier, and M. Latroche, *Nano Letters* 2015, 15, 4752
2. C. La Fontaine, L. Barthe, A. Rochet, and V. Briois, *Operando IV 4th Int. Congr. Operando Spectrosc.*, 2013, 205, 148
3. A. Michalowicz, J. Moscovicci, D. Bouvet-Muller and K. Provost *J. of Physics*, 2009, 190, 12034
4. S. I. Sanchez, L. D. Menard, A. Bram, J. H. Kang, M. W. Small, R. G. Nuzzo, and A. I. Frenkel, *JACS* 2009, 131, 7040

LIST OF COMMERCIAL EXHIBITORS

List of Commercial Exhibitors

Company	Contacts	Phone numbers	Email	Web site
ALECTRA 	Béatrice WILLIS Mario PELLI	02 97 27 23 07	bwillis@allectra.com mario@allectra.com	http://allectra.com/index.php/en/
IMXPAD 	Franck AZOULAY Frédéric BOMPARD	06 88 81 32 73 06 07 62 24 49	franck.azoulay@imxpad.com frederic.bompard@imxpad.com	http://www.imxpad.com/
FLEX-EQUIPEMENTS - MEWASA 	Jean-Luc DIAT	01 60 88 24 81	jl.diat@wanadoo.fr	http://www.mewasa.ch
MDC VACUUM PRODUCTS SARL 	Anne-Sophie JAUBERT	33 9 75 77 62 81	asiaubert@mdcvacuum.fr	http://www.mdcvacuum.com/
NEWPORT 	Dalila AIT AMIR Jean VILAIN	01 60 91 68 68 02 38 40 50 00	dalila.aitamir@newport.com jean.vilain@newport.com	http://www.newport.com
PHYSICAL INSTRUMENTS 	Ludovic RUSE	09 50 13 94 03	ludovic.ruse@physical-instruments.fr	http://www.physical-instruments.fr
PI France SAS 	Emmanuel PASCAL Stéphane BUSSA	01 55 22 60 00 01 55 22 60 00	e.pascal@pi.ws s.bussa@pi.ws	http://www.pi-france.fr
PREVAC / SCIENTEC 	Iwona Falbikowska Didier Pellerin	48666829786 01 64 53 2700	i.falbikowska@prevac.pl d.pellerin@scientec.fr	https://www.prevac.pl/
QUEENSGATE INSTRUMENTS (ELEKTRON TECHNOLOGY GROUP) 	David GOLDWIN	447 833 093 059	David.godwin@elektron-technology.com	http://www.elektron-technology.com
SMARACT GmbH 	Matthieu NICOUL	49-441 800879/36	nicoul@smaract.de	http://www.smaract.de
SPECS 	Michael MEYER Bjoern MUENZING	493 04 67 82 40 493 04 67 82 40	bjoern.muenzing@specs.com michael.meyer@specs.com	http://www.specs.de
SUMITOMO CRYOGENICS 	Carlos de AZEVEDO	06 22 87 23 01	cdeazevedo@shicryogenics.fr	http://www.shicryogenics.com
SYMETRIE 	Olivier LAPIERRE Anne DUGET	06 10 20 10 53 04 66 28 87 24	info@symetrie.fr anne.duget@symetrie.fr	http://www.symetrie.fr/
TRIOPTICS France 	Gwendal GIRAD-SUARD Lambert TISSOT	04 37 47 89 62 04 37 47 89 67	gwendal.girard@trioptics.fr lambert.tissot@trioptics.fr	http://www.trioptics.fr/

COMPANIES ADVERTISEMENTS



**DO NOT ADAPT YOUR SYSTEM TO OUR DETECTOR
LET US ADAPT OUR DETECTOR TO YOUR SYSTEM**

imXPAD
Ultimate X-ray imaging



**Visualisez vos recherches dans un temps record
avec le meilleur des contrastes**
Watch your searches in record time with the best of contrasts



- | | |
|--|---------------------------------------|
| NIM 150T | 5U, 5 slots - power 150 W - Portable |
| NIM 150C | 5U, 10 slots - power 150 W - Compact |
| NIMpactI23, I24, I26, I27 | 5U, 12 slots - power 300 W - Low Cost |
| NIMpactI23, I24, I26, I27 | 7U, 12 slots - power 300 W - Low Cost |
| NIM300 & NIM300S CERN Spec. | 5U, 12 slots - power 300 W - Standard |
| NIM600 & NIM600S CERN Spec. | 5U, 12 slots - power 600 W - Standard |
| NIM300L & NIM300LS CERN Spec. | 7U, 12 slots - power 300 W - Fan Tray |
| NIM600L & NIM600LS CERN Spec. | 7U, 12 slots - power 600 W - Fan Tray |
| NIM1920L & NIM6000 | 7U, 12 slots - power 2700 W |
| NIM N-C 2010 | 5U, 6 slots - power 90 W - Portable |
| NIM N-C 2020 | 5U, 12 slots - power 200 W - Standard |
| NIM N-C 2030 | 5U, 12 slots - power 300 W - Standard |
| NIM N-C 2040 | 5U, 12 slots - power 400 W - Standard |

NHQ 1 kV to 10 kV - 12 W to 30 W, NIM unit, 1 or 2 channels
NHS 100 V to 6 kV - 9 W, NIM unit, 6 channels

- Standard and High Precision versions
- Fixed, mixed or switchable polarity depending on model
- Very high overall stability and accuracy
- Low temperature & time drift
- 2 mV, 5 mV, 50 mV, 200 mV ripple & noise depending on model
- 50 pA to 1 µA resolution depending on model
- Manual front panel operation with LCD or TFT display
- Remote control: analog, CANbus, RS232, USB
- Compact size, 1 slot width
- To be integrated into NIM Crates



We offer unshielded and shielded coaxial cables for voltages up to 150 kV. The standardized offer contains Silicone and PE dielectrics, but miscellaneous dielectrics with good AC ratings are available too.

- | | |
|-----------------|--|
| SILICONE | Silicone rubber |
| PE | Polyethylene |
| XLPE | Cross-linked Polyethylene |
| LDHMW PE | Low density high molecular weight Polyethylene |
| EPR | Ethylene Propylene copolymer rubber |
| EPDM | Ethylene Propylene Diene Monomer rubber |

Beamline Instrumentation

SOPHISTICATED COMPONENTS AND SYSTEM SOLUTIONS



Optics alignment

- Nanometer resolution with mm stroke
- Radiation resistant
- Self-locking
- Minimum dimensions, high forces



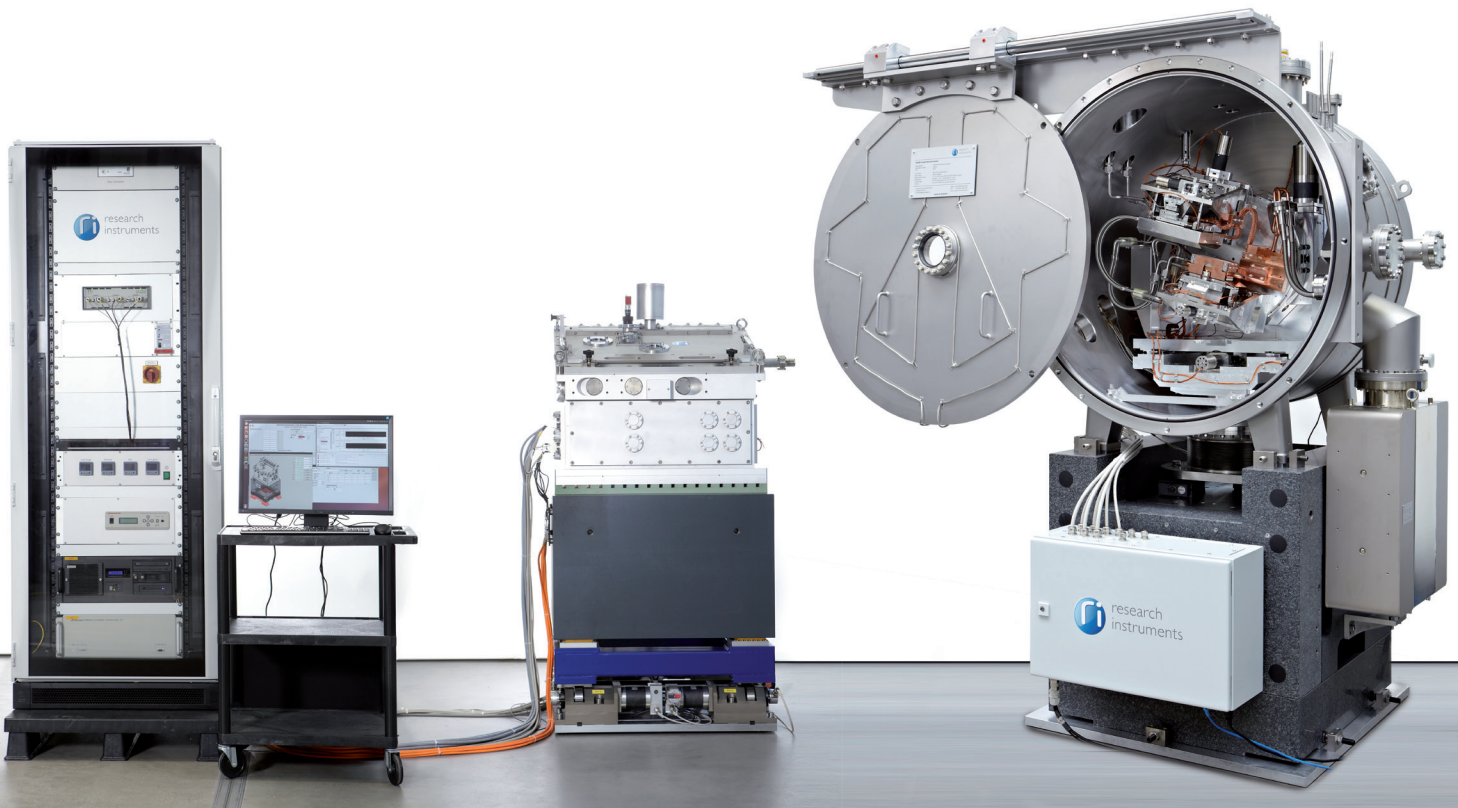
Tomography stages

- 6DOF sample alignment
- Unmatched excentricity
- Air bearings & torque motor
- Direct metrology



End stations

- From customized multi-axis solutions to complete turn-key solutions
- UHV-compatible equipment



Experience, solutions, performance

From Accel to RI Research Instruments.

Our name stands for innovative solutions and high performance through many years of experience.

Photon Instrumentation from RI

- Beamline systems
- Monochromators (step and fast scanning)
- Scanning Transmission X-ray Microscopes (STXM)
- Endstations
- Insertion Devices
- Front end components
- LN2 cryocooler
- XUV/EUV systems and solutions

Our mission

We develop, design, manufacture and test high performance accelerator and photon instrumentation components and systems to the requirements of our customers in research and industry.

With decades of experience within the market, we have taken the latest technologies to the ultimate level of performance.

For the most advanced of your applications.